USC
UNIVERSIDADE
DE SANTIAGO
DE COMPOSTELA

ESCOLA DE DOUTORAMENTO
INTERNACIONAL

Inés
Fernández Piñeiro

Tese de doutoramento

Polysaccharide functionalised span nanoparticles as gene delivery systems. Application in the treatment of colorectal liver metastasis

Santiago de Compostela 2017

PD en Investigación e Desenvolvemento de Medicamentos

USC
UNIVERSIDADE
DE SANTIAGO
DE COMPOSTELA

CENTRO INTERNACIONAL DE ESTUDOS
DE DOUTORAMENTO E AVANZADOS
DA USC (CIEDUS)

TESE DE DOUTORAMENTO

POLYSACCHARIDE FUNCTIONALISED SPAN NANOPARTICLES AS GENE DELIVERY SYSTEMS. APPLICATION IN THE TREATMENT OF COLORECTAL LIVER METASTASIS

Inés Fernández Piñeiro

ESCOLA DE DOUTORAMENTO INTERNACIONAL

PROGRAMA DE DOUTORAMENTO EN INVESTIGACIÓN E DESENVOLVEMENTO DE MEDICAMENTOS

SANTIAGO DE COMPOSTELA

2017

USC
UNIVERSIDADE
DE SANTIAGO
DE COMPOSTELA

CENTRO INTERNACIONAL DE ESTUDOS DE DOUTORAMENTO E AVANZADOS DA USC (CIEDUS)

DECLARACIÓN DO AUTOR/A DA TESE

POLYSACCHARIDE FUNCTIONALISED SPAN NANOPARTICLES AS GENE DELIVERY SYSTEMS. APPLICATION IN THE TREATMENT OF COLORECTAL LIVER METASTASIS

D./Dna. Inés Fernández Piñeiro

Presento a miña tese, seguindo o procedemento axeitado ao Regulamento, e declaro que:

1) A tese abarca os resultados da elaboración do meu traballo.
2) De selo caso, na tese faise referencia ás colaboracións que tivo este traballo.
3) A tese é a versión definitiva presentada para a súa defensa e coincide coa versión enviada en formato electrónico.
4) Confirmo que a tese non incorre en ningún tipo de plaxio doutros autores nin de traballos presentados por min para a obtención doutros títulos.

En Santiago de Compostela, 15 de Decembro de 2017

Asdo.

USC
UNIVERSIDADE
DE SANTIAGO
DE COMPOSTELA

CENTRO INTERNACIONAL DE ESTUDOS DE DOUTORAMENTO E AVANZADOS DA USC (CIEDUS)

AUTORIZACIÓN DOS DIRECTORES DA TESE

POLYSACCHARIDE FUNCTIONALISED SPAN NANOPARTICLES AS GENE DELIVERY SYSTEMS. APPLICATION IN THE TREATMENT OF COLORECTAL LIVER METASTASIS

D. Alejandro Sánchez Barreiro
D. Iker Badiola Etxaburu

INFORMA/N:

Que a presente tese, correspóndese co traballo realizado por Dna. ***Inés Fernández Piñeiro****, baixo a miña dirección, e autorizo a súa presentación, considerando que reúne os requisitos esixidos no Regulamento de Estudos de Doutoramento da USC, e que como director desta non incorre nas causas de abstención establecidas na Lei 40/2015.*

En Santiago de Compostela, 15 de Decembro de 2017

Asdo. Asdo.

USC
UNIVERSIDADE
DE SANTIAGO
DE COMPOSTELA

En memoria de Begoña Seijo

USC
UNIVERSIDADE
DE SANTIAGO
DE COMPOSTELA

Agradecimientos / Acknowledgements

Hay muchas personas a las que me gustaría agradecer el haber llegado hasta aquí. Son tanto personas que ya formaban parte de mi vida, y han seguido apoyándome a lo largo de estos cuatro años, como otras que he ido sumando a lo largo del camino. Porque, sin lugar a dudas, lo mejor que me llevo después de estos cuatro años son ellos.

En primer lugar, dedico este trabajo a la que siempre será mi directora de tesis, Begoña Seijo. Gracias por, con el entusiasmo que te caracterizaba, haber despertado en mí esa curiosidad por el mundo de la investigación que me llevó a donde estoy ahora. Gracias por todas las horas que me dedicaste en tu despacho, por haber confiado en mí desde un principio y por tu apoyo constante. Estarás siempre en mi memoria.

A mis directores de tesis, Alejandro Sánchez e Iker Badiola, por vuestra dedicación y consejos. A Alejandro por aportarme una perspectiva diferente y por la libertad que siempre me has dado a la hora de tomar decisiones. A Iker por todo lo que me has aportado: tu visión, tu permanente apoyo, tu total dedicación, tus horas de trabajo, tus ideas, tu confianza, tu comprensión… Gracias por, sin lugar a dudas, haber hecho posible esta tesis. Gracias por ayudarme a ver las cosas con perspectiva y por todo lo que me has enseñado sin esperar nada a cambio.

A Andrea, por ser casi una directora de tesis más, pero sobre todo una amiga. Gracias por todo lo que me has enseñado y por tu apoyo aún desde la distancia. Gracias por entender mis neuras y darme esperanza cuando más lo necesitaba. A Delia, por acompañarme en mis comienzos en el laboratorio y en mi aventura finlandesa, y por haber sido una amiga desde entonces. A todas las personas con las que he coincidido en el laboratorio de Santiago, especialmente a Rafa, Jesús, Diana, Joaquín y Marta por vuestro apoyo y por el tiempo compartido.

A todos los profesores del Departamento de Farmacia y Tecnología Farmacéutica, especialmente a Dolores Torres y a Francisco Otero. A todos mis compañeros de doctorado y de departamento, tanto en la facultad como en el Cimus, por vuestro apoyo y ayuda siempre que lo he necesitado.

A Fernando Unda y a todos los profesores de su grupo por abrirme las puertas de vuestro grupo de par en par. Gracias por la confianza depositada en mí, por vuestro trato y por vuestros

consejos. A mis compañeros de grupo, y ahora amigos, Patri, Igor, Lutxu y Vero por hacerme sentir una más desde el principio y por todos los momentos compartidos tanto dentro como fuera del laboratorio. Gracias a Patri por su apoyo permanente, sus consejos y su energía. Gracias a Igor por su ayuda y por aportarme la tranquilidad que tantas veces me hace falta. Gracias a Lutxu por su entusiasmo y por aportarme su visión positiva de las cosas. Gracias a Vero por su comprensión y su apoyo.

A Xandra por muchas cosas, pero sobre todo por ser una gran amiga. Gracias por abrirme las puertas de tu casa y de tu vida desde el principio, por entenderme y apoyarme cuando más lo necesitaba y por todas las experiencias compartidas. Gracias a sus padres, Lourdes y Pepe, por ser mi familia en Bilbao y por toda su ayuda.

A todos y cada uno de mis compañeros de *BioCell*, por ser un grupo de gente tan maravilloso, por su buen ambiente y por todos los momentos compartidos. A todas los profesores y técnicos del Departamento de Biología Celular e Histología de la UPV que me han ayudado.

I would like to thank Professor Cameron Alexander for giving me the opportunity to work as part of his research group at The University of Nottingham. Thank you for trusting in me and for your words of encouragement and guidance. I have learned a lot from you and your group. I wish to thank all my colleagues and friends in B28 and B15, especially Lucy, Shelly, Ruggero, Akosua, Nora, Alejandro, Rosa, Claudia, Vincenzo, Giovanna and Tatiana, for their help and support. I would like to particularly thank Patrícia, Rebeca and Alessandra for being such generous, kind and big-hearted friends. I also wish to thank Arsalan, Valentina, Dara, Francesco and Lisa for all the wonderful moments we have shared.

A todos mis amigos no relacionados con el mundo de la investigación por mantenerme conectada a la realidad, por vuestra comprensión y apoyo y por vuestra amistad. Aunque son muchos, y seguramente me olvide de alguien, quiero nombrar especialmente a Lorena, Nuria, Cris, Carla, Miriam, Lili, Alba, Grisel y Gian Paolo.

E por último, á miña familia e, sobre todo, aos meus pais polo seu apoio incondicional. Gracias por darme os valores que rexen a miña vida. Gracias por estar aí para levantarme cada vez que caio. Gracias por permitirme chegar ata aquí.

"*Si quieres ir rápido camina solo, pero si quieres llegar lejos ve acompañado*"

USC
UNIVERSIDADE
DE SANTIAGO
DE COMPOSTELA

USC
UNIVERSIDADE
DE SANTIAGO
DE COMPOSTELA

Table of contents

USC
UNIVERSIDADE
DE SANTIAGO
DE COMPOSTELA

Abstract

Resumen

USC
UNIVERSIDADE
DE SANTIAGO
DE COMPOSTELA

Abstract

The main objective of this work has been the design of a new polysaccharide functionalised nanosystem as a non-viral microRNA vector for the treatment of liver metastasis from colorectal cancer. For this purpose, we modified our previously developed span nanoparticles using polysaccharides with endothelial targeting properties. Thus, we have developed a xanthan gum-functionalised nanosystem able to associate, protect from degradation and deliver *in vitro* a model plasmid without compromising cell viability. Moreover, these nanoparticles showed a remarkable short- and long-term stability at different temperatures, both in suspension and as a lyophilised product. The xanthan gum cover targeted the nanoparticles, and therefore, the plasmid delivery to endothelial cells of liver, kidney and lung *in vivo.* In addition, span nanoparticles were functionalised with the glycosaminoglycans chondroitin sulfate and hyaluronic acid. The resulting systems were efficiently loaded with a model plasmid and characterised in terms of physicochemical, stability, DNA protection, cytotoxicity and transfection properties. Once selected the chondroitin sulfate-functionalised nanoparticles for further studies, we evaluated their clinical potential associating microRNA in the treatment of a murine model of colorectal cancer liver metastasis. First, these nanoparticles demonstrated to successfully target liver sinusoidal endothelial cells (LSECs) and deliver miR-20a, which has been found to be downregulated in tumour-activated LSECs. Finally, the administration of these miR-20a loaded nanoparticles demonstrated to reduce the tumour volume by 80% and the LSECs infiltration into tumour foci by 70% in a murine model of colorectal liver metastasis. Therefore, these results provide an *in vivo* proof-of-concept of the clinical potential of the developed nanoparticles as a novel microRNA-based therapeutic strategy for cancer treatment.

Keywords: nanoparticles, polysaccharides, microRNA, gene therapy, cancer

Resumen

El principal objetivo de este trabajo ha sido el diseño de un nuevo nanosistema funcionalizado con polisacáridos como vector no viral de microRNA para el tratamiento de metástasis hepáticas de cáncer colorrectal. Con tal finalidad se han modificado las nanopartículas de span previamente desarrolladas utilizando polisacáridos con propiedades de direccionamiento al endotelio vascular. Así, se ha desarrollado un nanosistema funcionalizado con goma xantana que es capaz de asociar, proteger de la degradación y liberar *in vitro* un plásmido modelo, sin comprometer la viabilidad celular. Asimismo, estas nanopartículas mostraron una notable estabilidad a corto y largo plazo durante su almacenamiento a diferentes temperaturas, tanto en suspensión como en su forma liofilizada. La cubierta de goma xantana direccionó las nanopartículas y, por lo tanto, la entrega del plásmido a las células endoteliales de hígado, riñón y pulmón *in vivo*. Además, las nanopartículas de span se funcionalizaron con los glucosaminoglicanos condroitín sulfato y ácido hialurónico. Un plásmido modelo fue asociado eficazmente a estas nanopartículas y los sistemas resultantes se caracterizaron en términos de propiedades fisicoquímicas, de estabilidad, de protección del DNA, de citotoxicidad y de transfección. Una vez seleccionadas las nanopartículas funcionalizadas con condroitín sulfato para la evaluación de su potencial clínico, se emplearon las mismas asociando microRNA en el tratamiento de un modelo murino de metástasis hepática de cáncer colorrectal. En un primer paso, estas nanopartículas demostraron direccionar la entrega de miR-20a -cuya expresión se encuentra disminuida en este tipo de procesos-, a las células endoteliales del sinusoide hepático. Finalmente, la administración de estas nanopartículas asociando miR-20a demostró reducir el volumen de las metástasis en un 80% y la infiltración de células endoteliales en los focos metastáticos en un 70% en un modelo animal de metástasis hepática de cáncer colorrectal. Por lo tanto, estos resultados proporcionan una prueba de concepto *in vivo* del potencial clínico de las nanopartículas desarrolladas como estrategia terapéutica a base de microRNA para el tratamiento del cáncer.

Palabras clave: nanopartículas, polisacáridos, microRNA, terapia génica, cáncer

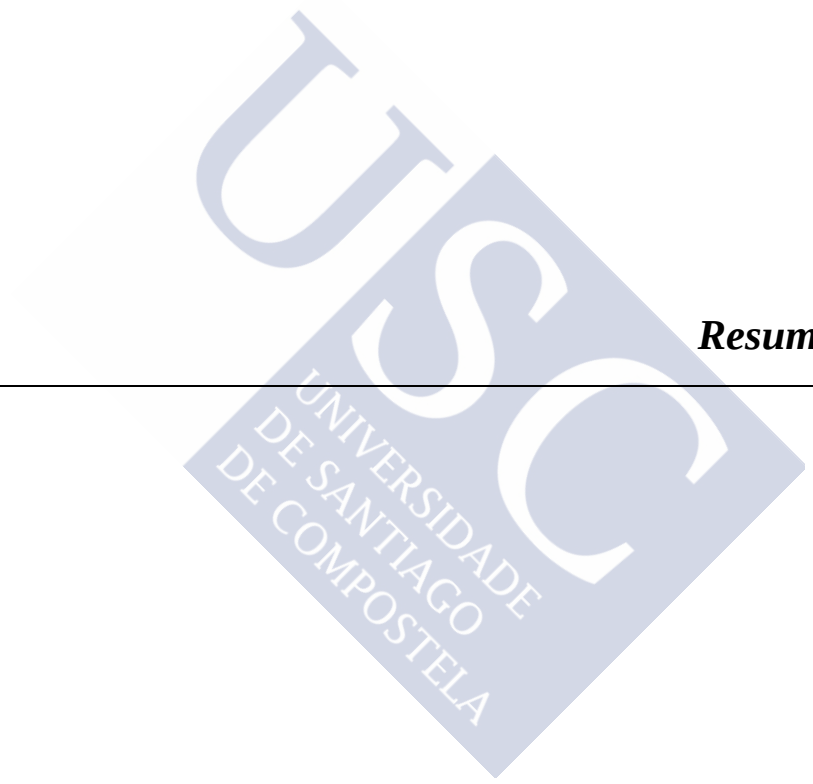

Resumen in extenso

USC
UNIVERSIDADE
DE SANTIAGO
DE COMPOSTELA

Introducción

1. Terapia génica

La terapia génica consiste en la transferencia de ácidos nucleicos a células específicas para evitar los efectos indeseados causados por genes aberrantes o disfuncionales y con el objetivo final de tratar o aliviar una patología. El material genético empleado puede ser tanto un plásmido de ácido desoxirribonucleico (DNA), empleado para compensar un déficit de producción causado por un gen defectuoso o ausente, como reguladores post-transcripcionales en forma de pequeñas secuencias de ácido ribonucleico (RNA) o DNA (oligonucleótidos antisentido), utilizados para suprimir o alterar la expresión de un gen a nivel post-transcripcional.

Las estrategias actualmente utilizadas en terapia génica pueden ser clasificadas en términos generales en terapias de reemplazo génico y de adición génica, aplicables a enfermedades causadas por uno o diversos defectos genéticos respectivamente, así como en terapia de modificación del RNA. Dentro de esta última se incluyen el silenciamiento genético mediado por una molécula de RNA (RNA interferente pequeño, siRNA, o microRNA) que se une a un RNA mensajero complementario, inhibiendo su traducción o provocando su degradación; así como la reprogramación del splicing del RNA, es decir la inclusión o exclusión de un exón durante la maduración del RNA mensajero (mRNA) para producir una proteína funcional, mediante el uso de oligonucleótidos antisentido.

Aunque la terapia génica supone una alternativa terapéutica para numerosas enfermedades, la mayoría de los ensayos clínicos y estudios realizados actualmente están dirigidos al tratamiento del cáncer. No obstante, debe tenerse en cuenta que el cáncer engloba un conjunto de enfermedades multifactoriales que implica alteraciones genéticas tanto en las propias células cancerígenas como en las células adyacentes, es decir, en el conocido como microambiente tumoral. Por lo tanto, están surgiendo numerosas dianas terapéuticas dentro de este microambiente, como es el caso de las células endoteliales, como alternativa al tratamiento exclusivo de las células cancerosas

Los ácidos nucleicos son moléculas hidrofílicas, cargadas negativamente y de alto peso molecular; características que dificultan su paso a través de barreras biológicas y membranas celulares. Además, son moléculas lábiles susceptibles de degradación enzimática por

endonucleasas una vez administradas al organismo. Por lo tanto, se hace necesaria la incorporación del material genético a vehículos que aseguren el transporte a su lugar de acción, el traspaso de barreras biológicas y la protección frente a la degradación enzimática. Estos vehículos se pueden clasificar en vectores virales y vectores no virales. Los vectores virales se unen a las células diana e introducen su material genético como parte de su proceso de replicación, presentando una alta eficacia de transfección. Con respecto a los vectores no virales se caracterizan por ser más seguros y fáciles de escalar, así como por poseer una mayor capacidad de carga génica, que los vectores virales. Entre los vectores no virales destacan los nanosistemas para el transporte de material genético.

2. Polímeros naturales para la administración de moléculas bioactivas en general y material genético en particular

Los polímeros naturales han despertado mucho interés en el ámbito de la administración de material genético debido a la idoneidad de sus propiedades, puesto que son sustancias biocompatibles, renovables y fácilmente modificables. Dentro de los polímeros naturales, los polisacáridos son unos de los más empleados en el diseño de sistemas transportadores de moléculas activas. Entre los motivos de esta gran aplicación destacan la capacidad de algunos polisacáridos para actuar como moléculas de direccionamiento a receptores o tejidos específicos, así como para aportar protección estérica a los sistemas transportadores reduciendo el reconocimiento de los mismos por parte del sistema reticuloendotelial y, por lo tanto, prolongando su tiempo de circulación en sangre.

Los polisacáridos son polímeros formados por más de 10 monosacáridos unidos mediante enlaces glucosídicos. Son heterogéneos en estructura y composición química, pudiendo ser obtenidos de diversas fuentes naturales, como algas (p. ej. alginato), plantas (p. ej. pectinas, celulosa y ciclodextrinas) y animales (p. ej. quitosano, ácido hialurónico y condroitín sulfato).

3. Endotelio vascular

El endotelio forma el revestimiento celular interno de los vasos sanguíneos. Sin embargo, las células endoteliales (CEs) tienen funciones muy diversas más allá de simplemente aportar un revestimiento a las paredes de los vasos sanguíneos. Estas CEs muestran una enorme heterogeneidad estructural, funcional y genética, que difiere a lo largo del árbol vascular y de los diferentes órganos y tejidos para adaptarse a requisitos específicos.

El papel del endotelio vascular en la progresión de diversas enfermedades, como es el caso del cáncer, es cada vez más evidente. Se ha descubierto que, en el microambiente tumoral, el endotelio muestra características específicas. Así, aunque las CEs están en estado quiescente durante la mayor parte de su vida adulta, pueden pasar a un estado proliferativo y migratorio en respuesta a estímulos angiogénicos procedentes de las células del microambiente tumoral. Así, la progresión del cáncer está regulada por una comunicación cruzada entre las células cancerosas y células no cancerosas del microambiente tumoral. Además de participar en la comunicación cruzada con las células tumorales, estas células no cancerosas son genéticamente más estables que las células cancerígenas. Por lo tanto, orientar las terapias antineoplásicas hacia estas células presenta un especial atractivo como estrategia alternativa para vencer al cáncer.

Se han desarrollado diferentes aproximaciones terapéuticas dirigidas a tratar el potencial angiogénico de las CEs, pero sin embargo, el desarrollo de terapias antiangiogénicas sigue siendo limitado debido al escaso entendimiento que se tiene de sus beneficios, así como de los efectos secundarios y de las resistencias causadas por esta estrategia terapéutica. Sin embargo, teniendo en cuenta las diferencias moleculares y de expresión génica entre las CEs quiescentes y las activadas por el tumor, el direccionamiento de las terapias hacia el tratamiento de las CEs a un nivel transcripcional surge como una alternativa terapéutica de gran interés. Así, unas de las estrategias terapéuticas que están siendo actualmente exploradas para el tratamiento del cáncer son las dirigidas a regular la expresión de microRNAs en las CEs del microambiente tumoral.

4. Metástasis hepáticas

El hígado es el órgano más frecuentemente afectado por metástasis en la mayoría de las neoplasias prevalentes, siendo las metástasis hepáticas mucho más comunes que los tumores hepáticos primarios. Esta gran susceptibilidad del hígado a las metástasis se debe, por una parte, a sus características estructurales y hemodinámicas que favorecen la interacción y retención de células tumorales, y por otra parte, a su capacidad regenerativa y de supresión inmune que propician un ambiente favorable para el crecimiento tumoral. El hígado tiene un suministro dual de sangre constituido por la artería hepática y la vena porta, drenando ambas en los sinusoides hepáticos, los cuales representan la red capilar en el hígado. Las células endoteliales del sinusoide hepático, o LSECs de “liver sinusoidal endothelial cells”, suponen el 50% de las

células no parenquimatosas del hígado y forman un endotelio discontinuo y fenestrado que funciona como un tamiz selectivo para fluidos, solutos y partículas desde la sangre hacia los hepatocitos. Entre sus diversas funciones, las LSECs eliminan macromoléculas de desecho de la sangre a través de endocitosis mediada por receptor.

El proceso metastático al hígado implica cuatro fases interrelacionadas:

1. Fase microvascular infiltrante del tumor, en la cual las células tumorales son retenidas por las LSECs.
2. Fase de micrometástasis pre-angiogénica interlobular, en la cual células estromales hepáticas son reclutadas en micrometástasis avasculares.
3. Fase de micrometástasis angiogénicas, en la cual los tumores se vuelven vascularizados.
4. Fase de crecimiento que lleva al establecimiento de macrometástasis.

Objetivos

En línea con lo anteriormente expuesto, los principales objetivos de este trabajo pueden resumirse en:

1. Funcionalización y caracterización de nanopartículas de span con diferentes polímeros naturales para aportar una orientación específica de las nanopartículas a las células endoteliales del sinusoide hepático (LSECs).
2. Evaluación de la capacidad de las nanopartículas desarrolladas para actuar como vehículos transportadores de material genético *in vitro.*
3. Evaluación de la toxicidad *in vitro* e *in vivo* de las nanopartículas desarrolladas y su biodistribución *in vivo*.
4. Aplicación del sistema más adecuado en el tratamiento de un modelo animal de metástasis hepática de cáncer colorrectal, usando microRNA-20a como molécula terapéutica.

Materiales y métodos

-Elaboración de las nanopartículas y asociación del material genético

Para la elaboración de las nanopartículas de span, los componentes lipofílicos del sistema, es decir, span 80 (monooleato de sorbitán) y oleilamina, se añadieron a la fase etanólica a una concentración de 6.6 y 0.33 mg/ml respectivamente. En la fase acuosa se solubilizaron los polisacáridos (goma xantana o XG, condroitín sulfato o CS y ácido hialurónico o HA) y el material genético (el plásmido pEGFP o los microRNAs). Las concentraciones de los polisacáridos en la fase acuosa fueron de 0.26 mg/ml para XG y 0.125 mg/ml para CS y HA. Las nanopartículas se formaron espontáneamente al añadir la fase etanólica sobre la acuosa bajo agitación magnética constante en una proporción 1:2 en volumen de etanol:agua. Una vez formadas las nanopartículas, se eliminó la totalidad de la fase etanólica y parte de la fase acuosa hasta reducir 9 veces el volumen de las nanopartículas.

El tamaño medio de las nanopartículas y el potencial zeta se determinaron mediante espectroscopía de correlación fotónica y anemometría de dispersión láser, respectivamente. La morfología de las nanopartículas se evaluó mediante microscopía electrónica de transmisión tras teñir las muestras con ácido fosfotúngstico al 2%.

La eficacia de asociación del material genético, así como los estudios de protección frente a DNasa, se valoraron mediante electroforesis en gel de agarosa al 1% para las muestras de plásmido y al 2% para las muestras conteniendo microRNA.

-Estudios de estabilidad y de liofilización

Para llevar a cabo los estudios de liofilización, las nanopartículas se liofilizaron en presencia de azúcares lioprotectores: trehalosa al 15% para XG, glucosa al 10% para CS y sacarosa al 10% para HA. Tanto las muestras liofilizadas como las nanopartículas en suspensión se almacenaron a 4°C, a temperatura ambiente (TA) y a 37°C y su tamaño y potencial zeta se midieron inicialmente y tras 3 y 12 meses de almacenamiento.

-Estudios in vitro

Los estudios *in vitro* se realizaron en células endoteliales humanas derivadas de la vena umbilical HUVEC y en la línea celular A549 de carcinoma de pulmón. Para evaluar el efecto de las nanopartículas en la viabilidad celular se empleó el ensayo XTT, incubando las células

con concentraciones crecientes de nanopartículas y siguiendo las instrucciones del fabricante. Los mismos tiempos de incubación fueron utilizados en los estudios de transfección con las nanopartículas conteniendo el plásmido pEGFP, que codifica una proteína verde fluorescente o GFP. La expresión de GFP en las células se evaluó 24 horas después de la transfección mediante microscopía de fluorescencia.

-Estudios in vivo: toxicidad y biodistribución

Para evaluar la toxicidad *in vivo* de los sistemas desarrollados, 200 µl de las nanopartículas asociando pEGFP y en presencia de glucosa al 5% se inyectaron por vía intravenosa a ratones. Los animales se sacrificaron 24 horas después, y se extrajeron los órganos principales y muestras de sangre para realizar un análisis histológico de los mismos y medir los niveles serológicos de aspartato aminotransferasa, respectivamente. El mismo procedimiento se siguió para los estudios de biodistribución, tratando los cortes histológicos con anticuerpo contra GFP para determinar la expresión de GFP, y por lo tanto la distribución de las nanopartículas.

-Estudio de eficacia terapéutica en un modelo animal

Para el estudio de eficacia terapéutica, se escogieron las nanopartículas funcionalizadas con CS y se desarrolló un modelo murino de metástasis hepática de cáncer colorrectal mediante inoculación intraesplénica de células C26 de carcinoma de colon. Los animales se dividieron en 5 grupos según los tratamientos recibidos, que se administraron cada 3 días: glucosa al 5%, microRNA-20a libre, nanopartículas asociando microRNA-20a, nanopartículas asociando microRNA control y nanopartículas blancas o vacías. A los 21 días se sacrificaron los animales y, después de fijar y procesar los hígados, se realizaron tinciones histológicas con hematoxilina y eosina y se cuantificaron los focos tumorales. Para analizar las LSECs infiltradas y potencialmente activadas en el área metastatizada, los cortes histológicos se marcaron con el anticuerpo contra CD31 o receptor de manosa, y la fluorescencia se cuantificó por técnicas de imagen.

Resultados

1. Nanopartículas de span funcionalizadas con goma xantana para el direccionamiento de material genético a células endoteliales

La incorporación del polisacárido goma xantana (XG) a nanopartículas de span dio lugar a un nanosistema con un tamaño medio de 147 nm y un potencial zeta de -48 mV (Capítulo I, Tabla 1). La morfología del sistema se confirmó por microscopía electrónica de transmisión, observándose partículas de tamaño nanométrico en las que se aprecia una cubierta externa y un núcleo central (Cap. I, Figura 2). Para evaluar la capacidad del sistema desarrollado para actuar como vehículo transportador de material genético, se incorporó al mismo el plásmido modelo pEGFP, que codifica la proteína verde fluorescente ("*Green Fluorescent Protein*", GFP). Además de asociar eficazmente el plásmido, las nanopartículas demostraron su capacidad para proteger al mismo frente a la degradación por la enzima DNasa I (Cap. I, Fig. 3). En cuanto a la estabilidad del sistema, el tamaño medio de partícula se mantuvo estable tras el almacenamiento de las nanopartículas en suspensión a 4°C y a temperatura ambiente (TA) durante 3 y 12 meses, con excepción de las muestras almacenadas a 37°C, en las que se observaron mayores incrementos en el tamaño de las nanopartículas. Por otra parte, las nanopartículas se mostraron resistentes al proceso de liofilización, manteniendo sus propiedades fisicoquímicas y con incrementos mínimos de tamaño tras un almacenamiento de 12 meses en comparación con las muestras en suspensión. Además, tras estos 12 meses las nanopartículas, tanto en suspensión como liofilizadas, mantuvieron la asociación del plásmido (Cap. I, Fig. 4 y 6).

Cuando la toxicidad del sistema fue evaluada *in vitro* en HUVEC, mediante el ensayo XTT, se observó un descenso en la viabilidad celular a la concentración testada más alta de 768 μg/ml (Cap. I, Fig. 7). También se demostró que cuando las nanopartículas se incuban con estas células a una concentración de 384 μg/ml, la expresión del marcador celular de proliferación ki-67 no se ve afectada (Cap. I, Fig. 8). Asimismo, se consiguió transfectar el plásmido pEGFP eficazmente en estas células empleando una concentración de las nanopartículas de 223.6 μg/ml (Cap. I, Fig. 9).

Tras la administración sistémica de las nanopartículas a ratones, los niveles plasmáticos de aspartato aminotransferasa permanecieron estables, lo que indica que las mismas no produjeron un daño hepático significativo. Sin embargo, en los exámenes histológicos de los principales

órganos se encontraron algunos infiltrados de células inflamatorias en el hígado, indicativo de una respuesta inflamatoria leve. Finalmente, se determinó la biodistribución del sistema mediante la expresión de GFP en los principales órganos tras la administración sistémica de este sistema asociando el plásmido pEGFP. Así, se observó expresión de GFP en las células endoteliales de los vasos sanguíneos del riñón, hígado y pulmón, así como en las LSECs del hígado. Adicionalmente, se demostró que este direccionamiento de las nanopartículas es específico a las células endoteliales, evitando la fagocitosis por parte de las células de Kupffer del hígado.

2. ***Desarrollo y caracterización de nanopartículas de span funcionalizadas con condroitín sulfato y ácido hialurónico como sistemas transportadores de material genético***

Se elaboraron nanosistemas híbridos a base de nanopartículas de span decoradas con condroitín sulfato (CS) o ácido hialurónico (HA) mediante un método de nanoprecipitación y autoensamblaje. En este método, el ensamblaje espontáneo de las nanopartículas se produce tras añadir una fase orgánica, que contiene span (SP) y oleilamina (OA), sobre una fase acuosa, en la que se encuentra los glucosaminoglicanos CS o HA, debido tanto a la insolubilidad de SP y OA en agua como a la aparición de interacciones electrostáticas entre las cargas positivas de OA y las cargas negativas de CS y HA. Esta misma interacción puede ser aprovechada para incorporar ácidos nucleicos cargados negativamente como es el caso del plásmido pEGFP. Las nanopartículas resultantes de este proceso mostraron un tamaño nanométrico de entre 120 y 140 nm, con una carga superficial negativa y una morfología esférica (Cap. II, Tabla 1 y Fig. 2). Ambas formulaciones desarrolladas demostraron además ser capaces de asociar eficazmente el plásmido pEGFP, protegerlo frente a la degradación enzimática por DNasa I, así como liberarlo *in vitro*, transfectando eficazmente la línea celular de carcinoma pulmonar A549 (Cap. II, Fig. 3, 8 y 10). Adicionalmente, ambos nanosistemas mostraron una excelente estabilidad en suspensión, exceptuando los incrementos de tamaño de partícula observados cuando las formulaciones fueron almacenadas a 37°C. Sin embargo, estos incrementos fueron mucho menores cuando las nanopartículas se almacenaron liofilizadas, demostrando la utilidad del proceso de liofilización en la conservación de las nanopartículas.

El efecto de ambas formulaciones en la viabilidad celular se evaluó *in vitro* en la línea celular A549 mediante el ensayo XTT. Así, no se observó un descenso de la viabilidad celular hasta la concentración de nanopartículas de 768 μg/ml, concentración con la cual la viabilidad

se vio reducida al 59% con las nanopartículas de CS y al 84% con las nanopartículas de HA. Sin embargo, no se observó ningún efecto inflamatorio o de toxicidad tras la administración sistémica de ambas formulaciones a ratones. De este modo, los niveles plasmáticos de aspartato aminotransferasa permanecieron estables y no se observó ningún daño evidente en los órganos principales, lo que indica que las nanopartículas de CS y de HA pueden ser consideradas como sistemas transportadores de material genético bien tolerados y no inmunogénicos.

3. Nanopartículas de span cargadas con microRNA-20a reducen la metástasis murina de cáncer colorrectal en el hígado

Un modelo murino de metástasis hepática de cáncer colorrectal fue desarrollado mediante la inoculación intraesplénica de células de cáncer colorrectal C26 a ratones. A continuación, 15 días después de la inoculación se aislaron las LSECs de estos ratones y se compararon los niveles de expresión de miRNAs de estas células con LSECs de ratones sanos. De esta forma, se descubrió que en las LSECs activadas por los tumores la expresión de miR-20a se encuentra disminuida, mientras que la expresión de sus proteínas diana E2F1 y ARHGAP1 está aumentada. Posteriormente, se demostró que la restauración *in vitro* de los niveles de miR-20a en LSECs activadas por el tumor es suficiente para reducir la capacidad de migracion de las mismas. Por lo tanto, se decidió incorporar este miRNA a las nanopartículas de span funcionalizadas con CS previamente desarrolladas, con la finalidad de proteger y transportar esta molécula a LSECs *in vivo*. La incorporación de miR-20a a las nanopartículas dio lugar a un sistema con un tamaño medio de partícula de 143 nm y una carga superficial de -33 mV (Cap. III, Tabla 1 y Fig. 5). Asimismo, la capacidad de esta formulación para dirigirse a las LSECs se demostró tras la administración intravenosa de este sistema asociando el plásmido pEGFP a ratones. De esta forma, se observó expresión de GFP únicamente en las LSECs, mientras que esta no se apreció en las células de Kupffer (Cap. III, Fig. 6). Este mismo resultado se observó tras la administración sistémica de miR-20a marcado fluorescentemente, cuando éste se administra asociado a las nanopartículas. Sin embargo, cuando miR-20a se administró en su forma libre, la señal fluorescente de la misma se detectó en menor medida y no delimitada a LSECs (Cap. III, Fig. 7).

Una vez demostrado el potencial de las nanopartículas para transportar la molécula terapéutica a las células diana, el citado sistema con el miR-20a incorporado se administró a un modelo murino de metástasis hepática de cáncer colorrectal. Tras 21 días de tratamiento, el área ocupada por los tumores se redujo en un 80% cuando miR-20a fue administrado en asociación

con las nanopartículas, en contraposición con la reducción del 20% observada cuando esta molécula fue administrada en su forma libre. Asimismo, se consiguió reducir en un 70% la presencia de LSECs infiltradas en el tumor en comparación con los controles, demostrando el potencial terapéutico de las nanopartículas desarrolladas (Cap. III, Fig. 8, 9 y 10).

Discusión

1. Funcionalización de nanopartículas de span con polímeros naturales

En este trabajo nos hemos centrado en la funcionalización con polímeros naturales de nanopartículas lipídicas a base de monooleato de sorbitán, también conocido como span 80 (SP). Además de SP, un surfactante no iónico, estos nanosistemas incluyen en su composición la amina grasa oleilamina (OA), la cual fue incorporada para facilitar la asociación de los ácidos nucleicos a través de interacciones electrostáticas con las cargas negativas del material genético. Los polímeros naturales escogidos para funcionalizar estas nanopartículas se han seleccionado teniendo en cuenta el objetivo final de esta tesis, el cual ha sido el desarrollo de un nanosistema transportador de microRNA capaz de dirigirse a las células endoteliales del sinusoide hepático (LSECs) como nueva terapia en el tratamiento de metástasis hepática de cáncer colorrectal. Así, los polisacáridos goma xantana (XG), condrotín sulfato (CS) y ácido hialurónico (HA) se incorporaron al sistema buscando modular sus propiedades fisicoquímicas y su comportamiento biológico.

De acuerdo con las propiedades fisicoquímicas de las nanopartículas resultantes de la funcionalización, podemos suponer que los grupos aniónicos de XG, CS y HA se disponen en la superficie de las nanopartículas. Esta cubierta externa cargada negativamente resulta de gran interés a la hora de evitar interacciones inespecíficas con componentes biológicos, así como para incrementar la estabilidad del sistema y para direccionar el mismo a células o regiones específicas del organismo. Adicionalmente, la disminución observada en el tamaño de las nanopartículas tras la funcionalización con los polisacáridos podría ser explicada por un incremento en el empaquetamiento de los diferentes componentes debido a interacciones electrostáticas y a la subsiguiente reticulación física de los mismos. Además, esta cubierta polisacarídica ha demostrado proteger eficazmente el plásmido pEGFP frente a la degradación enzimática por DNasas, que son enzimas presentes en los tejidos y fluídos biológicos,

prerrequisito para asegurar la entrega intacta de los ácidos nucleicos asociados a las nanopartículas en su lugar de acción.

Por otra parte, estas nanopartículas solucionan otro aspecto crítico en el desarrollo y escalado a la industria farmacéutica de las nanomedicinas, como es la baja estabilidad de los nanosistemas y su tendencia a perder sus propiedades fisicoquímicas durante el almacenamiento. De este modo, hemos desarrollado sistemas lipídicos funcionalizados con polisacáridos que destacan por su estabilidad a corto y largo plazo, tanto en suspensión como en forma liofilizada. Este comportamiento podría explicarse por diferencias estructurales con otros nanosistemas lipídicos conocidos por su baja estabilidad, como los liposomas, puesto que los sistemas desarrollados en este trabajo muestran una estructura sólida no vesicular.

2. Evaluación de la toxicidad, capacidad de transfección y biodistribución de las nanopartículas desarrolladas

Los estudios de viabilidad celular realizados *in vitro* con las tres formulaciones desarrolladas, mostraron una disminución en la viabilidad a las concentraciones más altas ensayadas de las nanopartículas. Sin embargo, este efecto no puede ser explicado por la toxicidad de los polímeros en sí, puesto que diversos estudios han descrito la biocompatibilidad y seguridad de XG, CS y HA. En consecuencia, esta toxicidad podría atribuirse a una mayor internalización celular de las nanopartículas mediada por la cubierta polisacarídica. Asimismo, no se observaron signos de toxicidad sistémica después de la administración intravenosa de las nanopartículas a ratones, exceptuando los infiltrados leucocitarios observados en el hígado de los animales tratados con nanopartículas de XG. Esta reacción inflamatoria leve podría ser debida tanto a la actividad inmunomoduladora de XG como a una respuesta inmune a la sobreexpresión a que dan lugar las nanopartículas de GFP, efectos que se encuentran descritos en la literatura.

Igualmente, el efecto protector y estabilizador de la cubierta de polisacáridos quedó demostrado una vez que se pudo verificar la elevada capacidad de las nanopartículas de XG para transfectar la línea celular A549 en presencia de suero, el cual es una de las principales barreras a superar por los sistemas transportadores de material genético en el organismo. Por otra parte, se confirmó que tanto las nanopartículas funcionalizadas con XG como con CS pueden escapar de la captura por parte de las células de Kupffer y, por lo tanto, estos resultados

apoyarían la teoría de que la funcionalización polisacarídica de las nanopartículas de span puede ayudar al sistema a evitar la eliminación por parte del sistema reticuloendotelial.

Tras la administración sistémica de las nanopartículas de XG a ratones, la expresión de GFP se observó tanto en las LSECs como en las células endoteliales de los vasos sanguíneos de hígado, pulmón y riñón. La internalización de las nanopartículas por parte de las LSECs puede estar mediada por receptores de manosa, teniendo en cuenta la presencia de residuos manosa en la estructura de XG y la sobreexpresión de estos receptores en las LSECs. Sin embargo, este receptor no está presente en las células endoteliales de los vasos sanguíneos, por lo que consideramos que el direccionamiento de las nanopartículas a estas células podría ser explicado por una interacción con los dominios lipídicos caveola o mediante una unión no específica a sitios catiónicos de la membrana celular, sin la necesidad de la intervención específica de un receptor.

En el caso de las nanopartículas funcionalizadas con CS y HA, la expresión de GFP se encuentra más delimitada a las LSECs después de su administración sistémica. De esta forma, se aprovechó la afinidad de ambos polisacáridos por el receptor de hialuronano (HARE), así como la afinidad del CS por el receptor de manosa, siendo ambos receptores expresados por las LSECs. Debido a la mayor expresión de GFP observada en los hígados tratados con nanopartículas de CS, se decidió continuar la investigación con esta formulación.

3. Aplicación de las nanopartículas de condroitín sulfato cargadas con microRNA en el tratamiento de la metástasis hepática de cáncer colorrectal

El hígado es uno de los órganos más frecuentemente metastatizados debido a su posición anatómica y su arquitectura histológica. La transformación fenotípica de las LSECs es una de las etapas más importantes de la progresión de la metástasis hepática. Por lo tanto, tras demostrar la desregulación en la expresión de miR-20a en LSECs activadas tumoralmente, y debido a la inestabilidad de las moléculas de miRNA y a su incapacidad para cruzar barreras biológicas, se decidió incorporar esta molécula bioactiva a las nanopartículas de span funcionalizadas con CS para que ésta sea transportada específicamente a las LSECs en un modelo murino de metátasis hepática de cáncer colorrectal y, así, explorar su potencial terapéutico en el tratamiento de esta patología.

En un primer paso, hemos demostrado la capacidad de las nanopartículas de span funcionalizadas con CS para asociar la molécula activa miR-20a, evidenciando la versatilidad

del sistema desarrollado para incorporar ácidos nucleicos de diverso tamaño. Asimismo, la capacidad de proteger y transportar específicamente esta molécula a las LSECs *in vivo* ha quedado demostrada tras la administración sistémica de estas nanopartículas asociando miR-20a marcado fluorescentemente.

La estrategia para restaurar el fenotipo normal de LSECs sanas mediante la entrega de miR-20a utilizando nanopartículas de span funcionalizadas con CS demostró ser un éxito, puesto que se consiguió reducir la presencia de LSECs infiltradas en los focos tumorales en un 70%. Esto es indicativo de que las nanopartículas consiguieron transportar y restaurar los niveles de miR-20a en LSECs, disminuyendo la neoangiogénesis y el soporte vascular a los tumores. Otro resultado que supone el espaldarazo o la confirmación de la eficacia de la estrategia terapéutica diseñada es la reducción del 80% en el área ocupada por las metástasis que se consiguió con las nanopartículas en comparación con el 20% de reducción observado cuando el miR-20a se administró en su forma libre.

Conclusiones

Por lo tanto, las siguientes conclusiones pueden ser extraídas de este trabajo:

1. Es posible modular las propiedades fisicoquímicas de las nanopartículas de span mediante la incorporación a su composición de diversos polisacáridos naturales.
2. Los nanosistemas desarrollados muestran una destacable estabilidad tanto en suspensión como en su forma liofilizada.
3. Las nanopartículas desarrolladas han demostrado su capacidad para actuar como sistemas transportadores del plásmido pEGFP.
4. La cubierta polisacarídica permite modular la biodistribución del sistema.
5. Las nanopartículas funcionalizadas con condroitín sulfato y asociando miR-20a han permitido obtener una prueba de concepto *in vivo* que confirma el gran potencial terapéutico de la estrategia diseñada en el tratamiento de la metástasis hepática de cáncer colorrectal.

USC
UNIVERSIDADE
DE SANTIAGO
DE COMPOSTELA

Introduction

USC
UNIVERSIDADE
DE SANTIAGO
DE COMPOSTELA

1. Gene therapy

Gene therapy consists of the transference of nucleic acids to specific cells to avoid the undesirable effects caused by aberrant or malfunctioning genes with the aim to treat or alleviate a pathological condition. The genetic material can be genes encoded in deoxyribonucleic acids (DNA) molecules, or post-transcriptional regulators such as ribonucleic acids (RNA), including small interfering RNA (siRNA) and microRNA, and small DNA sequences, known as antisense oligonucleotides. Thus, DNA is used to compensate a production deficit caused by a defective or absent gene; while RNA and antisense oligonucleotides are used for gene suppression or alteration at a post-transcriptional level. Both siRNA, miRNA and antisense oligonucleotides consist of small strands of DNA or RNA that can hybridize with specific pre-mRNA or mature mRNA sequences and suppress or regulate gene expression (1, 2).

Gene therapy offers new treatment possibilities for both acquired and hereditary diseases where conventional therapies are less effective, such as cancer, AIDS, cystic fibrosis, arthritis, peripheral vascular diseases and neurodegenerative disorders (3). Thus, more than 64% of all gene therapy trials worldwide are aiming at the treatment of cancer, and cancer gene therapy represents the predominant field of basic research, as it is a major global health problem accounting, annually, for more than eight million deaths worldwide. Although gene therapy was quickly adapted for cancer therapy (4) it should be taken into account that cancer is not caused by just a single alteration, but a complex, multifactorial disease involving changes in the genome, both in cancer cells and in the surrounding tissue. Recently, tumour microenvironment and, specially, tumour endothelial cells have emerged as alternative therapeutic targets for gene therapy. To fully understand the basis of this novel therapeutic approach, more specific aspects of endothelium physiology, functions and its role in cancer progress are described in further detail in section 3 and 4 of this introduction.

1.1. Gene therapy strategies

Gene manipulation strategies employed in current human gene therapy can be broadly classified into gene replacement, gene addition and gene expression alteration therapies (5).

-Gene replacement therapy: therapeutic approach for treating monogenic diseases which are caused by a single gene defect. Most of clinical gene therapy developments focus on this strategy, due to its simplicity and, also, to the ease of obtaining animal models for monogenic

human diseases. The first gene therapy product to reach the market, called Glybera (Table 1), belongs to this category. It consists of a recombinant adeno-associated virus for treating lipoprotein lipase deficiency by replacing with a functional lipoprotein lipase gene.

-Gene addition: therapeutic approach for complex disorders such as cancer and heart diseases which involve multiple genes deregulation and environmental factors. Thus, a deep understanding of these diseases mechanisms and the use of gene addition to supplement a therapeutic agent is required, since gene replacement is not feasible for these disorders.

-Gene expression alteration targeting RNA: RNA can be an intermediate (mRNA) or final (microRNA) gene product with diverse functions in controlling gene expression. Two commonly utilized gene therapy strategies based on RNA biology are gene silencing and reprogramming mRNA splicing.

-*Gene silencing by RNA interference*: gain-of-toxicity mutations lead to the production of toxic gene products which require a gene silencing strategy by RNA interference (RNAi). RNAi is a RNA-based gene silencing process which was discovered in 1998 by Fire and Mello (6), consisting in the binding of a molecule of RNA to a complementary mRNA and the consequent mRNA degradation or protein synthesis inhibition. The triggering RNA molecule can be a small interfering RNA (siRNA), which can also be used as the precursor short hairpin RNA (shRNA), or a microRNA. MicroRNAs seem to be safer, causing less cellular toxicity, and can target more than one mRNA and, therefore, modify the expression of different proteins.

-*Reprogramming messenger RNA splicing by antisense oligonucleotides (AONs)*: Many diseases are caused by mutations in genes that lead to disrupt in reading frame of pre-mRNAs. Thus, when this pre-mRNAs undergo splicing to form mature mRNAs composed of exons to be translated into proteins, the disruption in the reading frame of pre-mRNA produce an altered mRNA and, therefore, an abnormal protein. AONs are designed to induce exon skipping or inclusion to modify this RNA splicing and produce a functional protein.

1.2. Gene delivery systems

Nucleic acid delivery must overcome numerous barriers and obstacles before its therapeutic effect can be exerted. Naked nucleic acids are quickly degraded by nucleases in the

body and cleared via renal excretion. In addition to their instability, their hydrophilic nature, negative charge and high molecular weight prevent nucleic acids from penetrating biological barriers (7-9). These properties make necessary the development and inclusion of nucleic acids into gene delivery systems.

There are two main approaches for gene delivery into target cells: viral and non-viral vectors. Viral vectors bind to target cells and introduce their genetic materials into the host cell as part of their replication process, referred as "transduction". As non-viral vectors, physical and chemical approaches, among others, have been used for genetic transfer, which is referred as "transfection". Non-viral vectors are safer and easier to be modified and scaled-up, as well as amenable to carry larger gene payloads, compared with viral vectors. However, they have a lower transfection efficiency (2, 10).

-Non-viral vectors: the non-viral strategies for nucleic acid delivery can be divided in physical and chemical methods.

-*Physical mediated gene transfer*: nucleic acids are delivered by compressed air or fluid (gene gun), or using ultrasound, which can force the genetic material into the target cell. Another approach is based in electroporation, consisting of membrane disruption with high-voltage electrical pulses. These techniques consist of applying a physical force that creates transient membrane holes and facilitate nucleic acid transfer to the cell nucleus (3).

-*Chemical mediated gene transfer*: several chemicals have been used to protect and help nucleic acids to cross cell membranes, mainly condensing nucleic acids into nanocarriers. These nanocarriers can be grouped into inorganic, polymer-based and lipid-based systems, depending on the chemical used to condense the genetic material. Potential benefits of nanocarriers for gene delivery are their reduced toxicity, efficient packing and stabilization of high contents of genetic material, simple manufacturing, low cost and high versatility (11).

-Viral vectors: viruses consist of ribonucleic acid (RNA) or deoxyribonucleic acid (DNA) surrounded by a protective protein coat (viral capsid) which helps the virus to–attach to specific host cell receptors. Some viruses may also have a lipid bilayer envelope derived from the host cell's membrane, and an outer layer of viral envelope made of glycoprotein. Vectors based on gammaretroviruses, adenoviruses, adeno-associated virus, herpes simplex virus and lentivirus are among the most widely used viral vectors. Although viral vectors are thought to

have superior transfection efficiencies over non-viral vectors, safety concerns, such as insertional mutagenesis, as well as induction of an immune response, have limited their use. In addition, they are associated with limitation of the inserted DNA size and difficulty for affordable large-scale pharmaceutical production (11).

1.3. Gene therapies on the market

Currently there are a few products involving gene therapy approved for their clinical use (Table 1). However, despite promising new treatment options for serious diseases, nucleic-based therapies have barely reached clinical drug development and sales. One theory holds that this is due to a lack of profitability of "personalized" gene-based medication for rare disorders compared with the broad spectrum of disorders treatable with a single drug. In addition, if we take into account that most of the vectors investigated in clinical trials are viral vectors, safety concerns do not help, as patients do not look favourably the European Medicines Agency (EMA) safety warnings such as that for Strimvelis ("Because Strimvelis is produced using a retrovirus, there could be a potential risk of cancer caused by unintended changes in the genetic material, although no such cases have been seen so far") (12). However, safety is not the only explanation of the difficulty to reach the market. Worryingly, the aforementioned limitations of these vectors have led to high final prices generating substantial controversy (1). Within such scenario and although gene therapy seems likely to continue to grow in academia and in smaller biotech companies, it seems unlikely that they will obtain a strong back up from big pharmaceutical companies (13). Following we cover products involving gene therapy that are currently in the market and have been approved by European Medicines Agency (EMA) and/or U.S. Food and Drug Administration (FDA).

Product name	Mechanism of action	Gene therapy strategy	Application	Approval
Glybera or Alipogene tiparvovec	Adeno-associated virus containing a functional lipoprotein lipase gene (16, 17)	Gene replacement	Lipoprotein lipase deficiency	2012 by EMA (withdrawal in October 2017 due to excessive cost)
Imlygic or Talimogene laherparepvec (T-VEC)	Genetically modified herpes virus which invades tumour cells, replicates itself and induces tumour cell lysis. It also incorporates the human cytokine granulocyte macrophage colony stimulating factor to induce tumour-specific immune response (18)	Gene addition	Unresectable recurrent melanoma	2015 by EMA and FDA
Strimvelis	Gammaretrovirus containing adenosine deaminase gene to transduce CD34-expressing hematopoietic stem cells extracted from and later transfected to patients (19)	Ex-vivo gene replacement and cell therapy	Severe Combined Immunodeficiency due to Adenosine Deaminase Deficiency	2016 by EMA
Zalmoxis	Allogeneic T cells genetically modified with a retroviral vector encoding for a truncated form of the human low affinity nerve growth factor receptor (ΔLNGFR) and the herpes simplex I virus thymidine kinase (HSV-TK Mut2).	Ex-vivo gene addition and cell therapy	Haploidentical haematopoietic stem cell transplant for various types of blood cancer to aid immune reconstitution and reduce the risk of graft-versus-host disease	2016 by EMA

Table 1. Gene therapy products on the market.

2. Natural polymers for gene and drug delivery

Natural polymers have attracted much interest in the field of drug delivery, especially polysaccharides, due to their superior properties. Thus, natural polymers have been incorporated to drug delivery systems to improve the solubility of poorly water-soluble drugs, to achieve a targeted drug delivery and to protect drugs from degradation and control their release, among others. For this purpose, both synthetic and natural biodegradable polymers have been extensively adopted. However, natural polymers have certain advantages over synthetic ones as drug carriers, such as biocompatibility, having the intrinsic property of environmental responsiveness via degradation and remodelling by cell-secreted enzymes. In addition, they are generally non-toxic and therefore can readily be incorporated into oral and systemic delivery systems (14, 15).

Natural polymers have been incorporated to diverse gene therapeutics, from nano- and microparticles to three-dimensional scaffolds, to address the limitations of current gene delivery systems. As derivatives of extracellular matrix components, natural polymers can function as not only DNA complexing agents but also structural scaffolds for tissue engineering applications. Thus, cationic polymers such as collagen, gelatine, chitosan and alginate can function as complexing agents for nucleic acids forming polymeric complexes. On the other hand, they can form three-dimensional polymeric matrices, enabling to control the environment in which gene transfer occurs and to achieve a localized delivery and retention at the site of implantation. For this purpose, collagen, fibrin, chitosan, hyaluronic acid or alginate have been used to construct polymeric matrices. Nucleic acids can be included as naked molecules or associated to viral or non-viral vectors (15).

2.1. Polysaccharides

Among natural polymers, polysaccharides are the most commonly used in drug and gene delivery due to their advantageous properties. Polysaccharides are renewable, biocompatible, biodegradable, and relatively cheap naturally occurring polymers. Moreover, polysaccharides posse functional groups such as hydroxyl, amino, and carboxylic acid groups that can be utilized to easily modify or tailor them to a range of clinical applications. These properties make them attractive polymers for developing drug and gene delivery carriers (20). Carbohydrates and their derivatives can also act as polyelectrolytes, since they have positive (chitosan) and negative charges (hyaluronic acid, alginate, chondroitin sulfate, heparin, etc.), or as targeting moieties,

inasmuch some of them are substrates for cell surface receptors. In addition, the presence of hydrophilic groups favours the interaction with and bioadhesion to biological tissues via noncovalent bonds (21). Alternatively, their presence on nanocarriers surface may also lengthen their circulation time in the bloodstream by reducing mononuclear phagocyte system recognition, due to steric shielding and mitigated complement activation.

Polysaccharides comprise more than 10 monosaccharide units interlinked via a glycosidic bond. They are heterogeneous in structure and chemical composition, distinguishing neutral or charged, linear or branched and low or high molecular weight polymers with varying hydrophilicity. Homopolysaccharides are composed of the same repeating monosaccharide and they include polymers such as cellulose and chitin, which function as structural elements in plant cell walls and in arthropods exoskeleton. On the other hand, heteropolysaccharides are formed by at least two different monosaccharide units. This group includes polymers such as hyaluronic acid, keratan sulfate and chondroitin sulfate, which provide protection, support and shape to cells, tissues and organs. In addition, polysaccharides can be obtained from various natural resources, such as algae (e.g. alginate), plants (e.g. pectins, cellulose, cyclodextrins), microorganisms (e.g. dextran, pullulan, xanthan gum) and animals (e.g. chitosan, hyaluronic acid, chondroitin sulfate) (21).

Here we describe the main polysaccharides used in gene and drug delivery systems (22, 23):

-Dextran: highly water-soluble polysaccharide of bacterial origin, produced by *Lactobacillus*, *Leuconostoc* and *Streptococcus* species. It is composed predominantly of α-1,6-linked glucopyranose with a high molecular weight and polydispersity, that can be tailored by controlled hydrolysis. It has been widely used as a plasma volume expander for controlling wounds shock since 1953. It is widely used as coating of different nanocarriers, as well as part of polyelectrolyte complexes for drug and gene delivery (24).

-Xanthan: microbial branched anionic exopolysaccharide composed of five repeated sugar units, two β-D-glucose units on its main chain, and two mannoses and one glucuronic acid on its side chain; as well as different amounts of acetate and pyruvate. It was approved by FDA for its application in food and pharmaceutical industries in 1968. Its properties as a thickener and suspension stabilizer make it suitable for creams and suspensions and, recently, it has been used in drug controlled release carriers (25).

-Gellan: bacterial anionic exopolysaccharide, with a repeating unit of α-rhamnose, two residues of β-D-glucose and β-D-glucuronate. It was FDA approved as a stabilizer and thickener in food since 1990. It forms *in situ* strong gels and it has been used in solid dosage formulations, as a disintegration agent in immediate release tablets, or, in higher concentrations, as a matrix-forming excipient in sustained release, based on its swelling behaviour (23, 25).

-Chitosan: obtained by partial deacetylation of chitin, which is the natural main structural component of the crustacean exoskeleton and the cell wall of fungi. It is a linear and positively charged polysaccharide composed of repeating D-glucosamine and N-acetyl-D-glucosamine units. It shows mucoadhesive and permeation-enhancing properties, favouring its use in mucosal drug delivery and tissue engineering. It is the most significant polymer for use in gene delivery because of its low toxicity, low immunogenicity and excellent biocompatibility (11).

-Hyaluronic acid: glycosaminoglycan composed of alternating disaccharide units of N-acetyl-D-glucosamine and D-glucuronic acid. In its native form in mammalian organisms, hyaluronic acid is usually found as a high molecular weight linear polymer and it is one of the main components of extracellular matrix. It has a mechanical and structural role in the synovial fluid, the vitreous humour of the eye and in connective tissues. One of the most promising advantages of hyaluronic acid is based on the polymer interactions with specific receptors such as CD44, which allows its use as targeting moiety to specific tissues. Originally obtained by animal tissue extraction, especially from rooster coombs, it is now produced by recombinant bacteria (22, 23).

-Chondroitin sulfate: is a linear glycosaminoglycan composed of repeating disaccharide units of β-1,3-linked N-acetyl galactosamine and β-1,4-linked D-glucuronic acid with sulfate groups at certain positions. It is a polysaccharide found in mammals particularly abundant in bone, cartilage, skin, extracellular matrix, nerve tissue and blood vessels. Chondroitin has been used in the therapy of osteoarthritis and other cartilage damage diseases. It has been extensively used as a component of drug and gene delivery systems. Chondroitin can be degraded by colonic micro flora, so it has been investigated as a component for colon-specific drug delivery systems. As well as hyaluronic acid, chondroitin sulfate has also the ability of targeting tumours by binding with CD44 which is overexpressed on the surfaces of various tumour cells (26, 27).

-Cyclodextrin: naturally occurring cyclic oligosaccharides, consisting of α-1,4 linked D-glucopyranose units, that are produced by enzymatic conversion of starch. These polysaccharides show an amphiphilic topology, with a hydrophilic exterior and an inner hydrophobic cavity. They have been traditionally used for the formulation of poorly water-soluble drugs, to improve drug stability or to enhance drug permeability across biological membranes (28).

-β-Glucans: heterogeneous group of polysaccharides composed of repeating D-glucose units linked via β-glycosidic bonds, varying in chain length as well as in number and position of branches. They are part of the cell wall of fungi and bacteria and hence have innate immunomodulatory properties. This group of polysaccharides include cellulose, shizophyllan, curdlan or lentinan. They can be cationic modified to enable electrostatic complexation of nucleic acids, although some of them, such as curdlan, lentinan and shizophyllan, also have the intrinsic ability to form macromolecular complexes with nucleotides based on hydrogen bonding. β-Glucans have been used in drug delivery for the elaboration of hydrogels, micro- and nanoparticles (22, 29).

-Alginate: linear block copolymer composed of regions with consecutive β-1,4-D-mannuronic acid, α-L-guluronic acid residues and alternating mannuronic acid and guluronic acid residues. It can form hydrogels via ionic gelation induced by divalent cations. Originally obtained by extraction from seaweeds, it was discovered as a bacterial product in 1964. This anionic polysaccharide is a good disintegrating agent in tablets, a thickening and stabilizing agent in pharmaceutical suspensions and emulsions, as well as an antiacid stomach protector in capsules. It has also been employed in cell microencapsulation and as microsphere vectors for drug delivery (22, 25).

-Pullulan: neutral and non-toxic exopolysaccharide of fungi composed of α-1,6-linked maltotriose units. It is produced from starch by the fungus *Aureobasidum pullulans*. It has the ability to form fibres and biodegradable films. Additionally, it has intrinsic liver targeting properties due to its interaction with the asialoglycoprotein receptor present on hepatocytes. It can be cationic modified to complex nucleic acids (22, 23).

2.2. Methods of preparation of polysaccharide nanoparticles

Different methods have been utilized in the preparation of polysaccharide nanoparticles and selection of the method is greatly dependent on the nature of the therapeutic molecule (21, 22, 30-36). Briefly, techniques used in the preparation of nanoparticles loaded with thermosensitive or less stable substances such nucleic acids may be broadly classified as described below.

-Emulsion cross-linking: An aqueous polysaccharide solution is emulsified with an oil phase that contains an appropriate concentration of surfactant. A cross-linker is added to the emulsion leading to the gelation of the emulsion droplets where the polymer is dissolved. This method has been used for the preparation of chitosan, alginate and dextran nanoparticles, among others.

-Desolvation technique: polysaccharides aggregate forming nanoparticles by desolvation through the addition of desolvating agents like alcohols or salts, inducing a coacervation effect. This effect is observed because water-salt or alcohol interactions are more favourable than those occurring between the water and the polysaccharide.

-Polyelectrolyte complexation: this is a method based on mixing aqueous solutions of two polymers carrying opposite charges. It has been extensively used to prepare natural polysaccharides-based particles and hydrogels. It is a good method to prepare nanoparticles for its mild preparation conditions and simple procedures, and it can avoid destroying the structure and property of the bioactive molecules.

-Ionic cross-linking or ionic gelation: involves electrostatic interactions between charged polysaccharides and small ions of opposite charges in an aqueous environment, under mild conditions.

-Self-assembly: polysaccharides grafted with lipid moieties of amphiphilic character, spontaneously form self-aggregates in aqueous solution. Consequently, polymeric micelles with core-shell structure are formed.

-Nanoprecipitation: diffusion of an aqueous polymer solution in a water-miscible nonsolvent, resulting in the instantaneous formation of nanoparticles. This technique has been applied for chitosan, cyclodextrins and dextrin nanoparticles, among others.

3. Vascular endothelium

3.1. Endothelial cells heterogeneity

The endothelium forms the inner cellular lining of blood vessels. Endothelial cells (ECs) have very distinct and unique functions besides merely providing a lining for vessel walls. Moreover, ECs show a huge heterogeneity, differing among the vascular tree and different organs and tissues to adapt to specific requirements. This heterogeneity can be explained by the enormous variety of tissue microenvironments to which ECs are exposed, although some properties are epigenetically fixed and not dependent on the surrounding environment. Vascular heterogeneity comprises morphologic, functional and molecular differences.

Arterial and venous vessels possess distinct morphological and physiological characteristics. Arterial vessels present a layer of muscle cells and they deliver oxygen and nutrients from the heart to various tissues, where they branch into capillaries. Then, capillaries converge to form venous vessels that deliver deoxygenated blood back to the heart. ECs of capillaries acquire specific characteristics and functions regarding the surrounding tissue. For example, endothelium of the central nervous system forms the blood-brain barrier characterised by tight junctions, while endothelium of endocrine glands, pancreas, intestine and kidney are highly permeable due to the presence of pore-like fenestrations. Moreover, the molecular profile of ECs is often organ-specific due to the tissue-specific signal specializing them.

Traditionally, three types of endothelial cells are recognised: continuous, discontinuous and fenestrated cells (Figure 1) (37, 38).

-Continuous endothelium shows a basement membrane and lack of fenestrations which make it almost impermeable. It is found in arteries, veins, and capillaries of the brain, skin, heart and lung.

-Discontinuous endothelium is present in the liver and bone marrow and it is characterised by the presence of large fenestrations without diaphragms and basement membrane. This endothelium also contains large circular pores within individual cells.

-Fenestrated endothelium is observed in locations that are characterised by increased filtration or transendothelial transport such as exo- and endocrine glands, gastric and intestinal mucosa and kidney glomeruli. It is characterised by the presence of fenestrations, which consist of transcellular pores with diaphragm and a basement membrane.

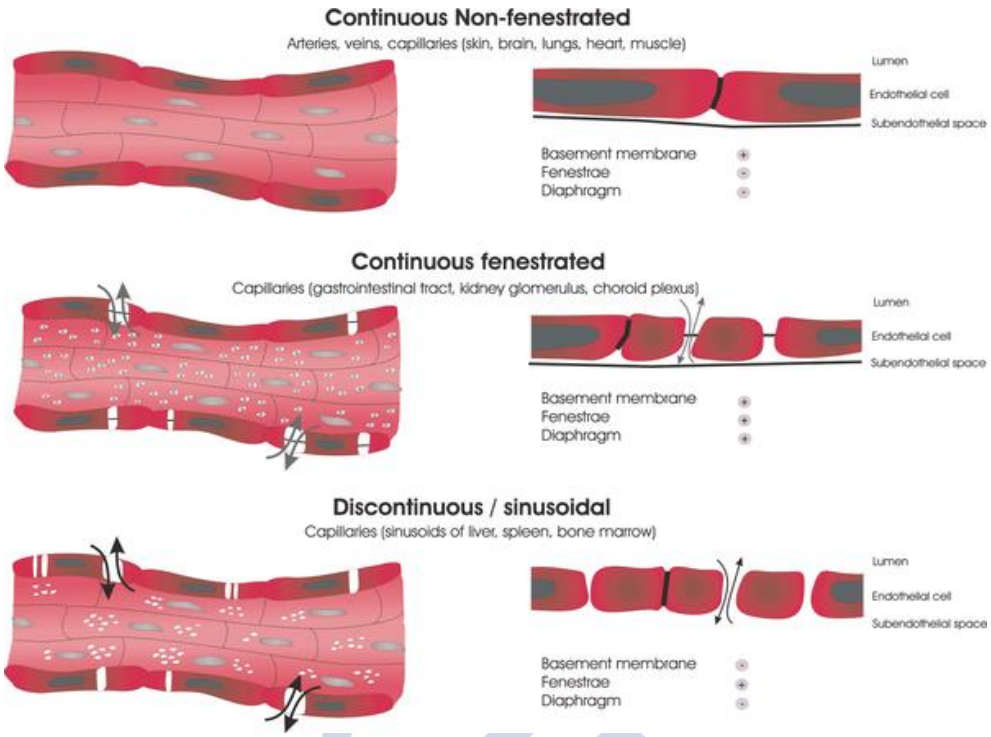

Figure 1. Types of vascular endothelium (37).

3.2. Endothelium functions

Vascular ECs have very distinct and unique functions, including a wide range of homeostatic functions (37-41). The main vascular endothelium functions are summarised below.

-Blood haemostasis: the endothelium has an important role in maintaining blood haemostasis. ECs prevent thrombosis and maintain blood fluidity by means of different anticoagulant and procoagulant factors which are differentially expressed across the vascular tree. They can also regulate coagulation by regulating the expression of binding sites for anticoagulant and procoagulant factors on the cell surface.

-Platelet and leukocyte interaction: platelet adhesion to and leukocyte rolling on the endothelium represent the initial stage of a multistep process leading to extravasation of white blood cells to sites of inflammation or infection, to platelet-leukocyte interaction and aggregation on a thrombogenic surface, and finally to vascular occlusion. Trafficking of leukocytes from blood to underlying tissue involves a multistep adhesion cascade that includes initial attachment, rolling, arrest and transmigration. This transmigration can occur between

ECs (paracellular pathway) or through ECs (transcellular pathway), and it takes place primarily in postcapillary venules.

-Regulation of vascular tone and growth: endothelium secretes a variety of regulatory substances such as vasoactive substances, growth inhibitors, contraction-inducing factors. Deregulation of this endothelial-dependent system is involved in many cardiovascular diseases, such as hypertension and atherosclerosis.

-Cell proliferation and angiogenesis: the endothelium is also involved in blood vessel formation, which is dependent upon signals exchanged between ECs and surrounding cells. Mature ECs are normally in a quiescent state, and neovascularization occurs predominantly by angiogenesis from pre-existing vessels or, to a lesser extent, by vasculogenesis or blood vessels formation by endothelial progenitor cells.

-Permeability: the endothelium regulates the transport of fluids and solutes into and out of the blood. Such transport takes place primarily in the capillaries, the major exchange vessels of the circulation. Fluids and small solutes move passively across the endothelium via the paracellular route, whereas macromolecules use a transcellular route. This transcellular transport takes place by two different mechanisms: endocytosis and transcytosis. The endocytic pathway can occur via a nonspecific process or through a receptor-mediated endocytosis. The later, also called clathrin-mediated endocytosis, is performed by scavenger receptors which are particularly expressed in liver sinusoidal ECs. Clathrin-mediated endocytosis is responsible for uptake of macromolecules such as low density lipoprotein (LDL), transferrin, albumin and advanced glycosylation end products. In addition to endocytosis, macromolecules move across the endothelium through transcytosis, which is mediated by caveolae and vesiculo-vacuolar organelles (VVOs). Caveolae are membrane-bound vesicles that, with exception of liver sinusoids, are present in ECs to a greater extent than clathrin-coated pits, mainly in capillary endothelium. VVOs are focal collections of membrane-bound vesicles and vacuoles, and they are most commonly observed in venular endothelium than in capillaries.

ECs were until recently considered to be just a lining for vessel walls, but it is now realised that ECs have important functions and perturbations of these functions are involved in many pathological conditions. Endothelial dysfunction is characterised by reduced vasodilation, a proinflammatory state and prothrombotic properties. It is associated with most forms of

cardiovascular disease, such as hypertension, coronary artery disease, chronic heart failure, peripheral vascular disease, diabetes, chronic kidney failure, cancer and severe viral infections.

3.3. Role of endothelium in cancer

Endothelial cells are in a quiescent state most of their adult life, but they can turn to a proliferative and migrative state after angiogenic stimuli from cancer cells. Diverse works suggest that angiogenesis is not only determined by cytokines and growth factors, but also endothelial cells metabolism interfere in this process. Thus, targeting endothelial metabolism is possible to target cancer progress (42).

Cancer progression and metastasis is regulated by cross-talk between cancer cells and non-cancer cells of tumour microenvironment. Tumour microenvironment is composed by non-malignant cells which supports and promote tumour progression, including macrophages, fibroblasts, endothelial cells, infiltrating immune cells and extracellular matrix (43). These cell-communication promotes tumour growth, angiogenesis, drug resistance, invasion and provides cancer cells with stem cell-like properties and epithelial-to-mesenchymal transition phenotypes. Moreover, these non-cancer cells are genetically more stable than cancer cells, thus targeting these cells can serve as an effective strategy to defeat cancer. Among non-cancer cells involved in tumour microenvironment, blood vessels endothelial cells play an important role.

3.3.1. Abnormalities in tumour endothelium

Endothelium in tumour microenvironment differs from normal endothelium in respect of morphological, functional and genetic characteristics (44). There is evidence that these abnormalities in the tumour endothelium contribute to tumour growth and metastasis and, therefore, determining the biological basis underlying these abnormalities will facilitate the development of new antineoplasic therapies.

Tumour ECs are more dilated and tortuous than normal ECs, with excessive branching, chaotic flow patterns and increased permeability to macromolecules through increased fenestrations and widened intercellular gaps, along with a high proliferative rate. These tumour ECs phenotypic heterogeneity is determined by diverse factors. The first factor to considered is the vascular bed of origin and the tumour microenvironment where ECs are exposed to abnormal conditions such as low pH, hypoxia, variable blood flow, hypoglycaemia, and growth factor and cytokines release by tumour cells and stromal cells. Moreover, epigenetic factors

play an important role in phenotypic heterogeneity. Thus, some site-specific epigenetic treads will be retained by ECs regardless of tumour microenvironment. In addition, there is some evidence that genetic alterations of tumour ECs may also influence phenotype heterogeneity. Thus, the presence of bone marrow-derived cells, such as endothelial progenitor cells, or the genetically instability of some tumour ECs may also have an impact on phenotype (41, 44). Some of these tumour endothelium abnormalities are summarised below.

-Defective endothelial monolayer: tumour endothelial cells have an irregular shape and size, with fragile cytoplasmatic projections which may penetrate the vessel lumen creating small intercellular gaps in the vessel wall.

-Large intercellular openings and holes*:* transcellular holes, fenestrations, channels and larger openings in the tumour blood vessels are probably for haemorrhage and plasma leakage observed in most tumours.

-Abnormal sprouts*:* tumour vessels have thin cytoplasmic projections extending across the vessel lumen. The origin of these sprouts may be the oxygen seeking tip cells in hypoxic regions of the tumour microenvironment.

-Altered gene expression*:* showing diverse patterns from different tumour types and stages of progression. For example, miRNAs are deregulated in many types of cancer and they have been demonstrated to influence the progression of the disease through alteration of the tumour microenvironment. Through miRNA manipulation in tumour endothelial cells, cancer cells are able to promote their angiogenic potential. Moreover, miRNAs have been demonstrated to be direct transferred between cancer cells and tumour microenvironment cells in exosomes or through direct cell contact.

3.3.2. Targeting endothelial cells in cancer therapy

Diverse therapeutic approaches that target ECs angiogenic potential have been developed and reached the market. For example, anti-VEGF monoclonal antibody bevacizumab was the first commercially available angiogenesis inhibitor. It was approved to be used alone for glioblastoma that has not improved with other treatments and to be used in combination with other drugs to treat metastatic colorectal cancer, some non-small cell lung cancers, and metastatic renal cell cancer. Since then, other antiangiogenic drugs have been approved,

including receptor tyrosine kinase inhibitors such as sorafenib, sunitinib, pazopanib, regorafenib and axitinib, or the VEGF-trap fusion protein aflibercept (45).

However, the use of antiangiogenic therapy is still limited due to poor understanding of the benefit, as well as the side effects and drug resistances caused by this therapeutic (41, 46). More than 100 clinical trials have been conducted worldwide with antiangiogenic drugs, but the survival benefits of antiangiogenic drugs have been modest so far in the clinic. Surprisingly, the majority of patients stop responding to this therapy or do not respond at all, and this controversy has been highlighted lately by some preclinical studies suggesting that antiangiogenic drugs may lead to a more aggressive and invasive tumour phenotype (47).

Nevertheless, targeting ECs at a transcriptional level has arisen as a therapeutic alternative. Considering that tumour ECs differ from normal ECs also at molecular level, this provides the scientific rationale for transcriptional targeting strategies. The distinct characteristics of tumour ECs make them an excellent target for gene therapy. As previously mentioned, one way ECs promote cancer progression is by altering the expression of microRNAs. Thus, therapeutic strategies aimed to regulate microRNA expression are being explored in preclinical studies (48).

4. Liver metastasis

4.1. Liver endothelium

The liver receives 15 to 20% of the cardiac output and it has a dual blood supply: the hepatic artery, which delivers well oxygenated blood, and the portal vein, which delivers poorly oxygenated, nutrient-rich blood. As shown in Figure 2, both drain into the hepatic sinusoids, which represent the capillary network in the liver. After circulating in the sinusoids, blood empties into hepatic venules and ultimately in the hepatic vena cava.

Liver endothelium is characterised by its heterogeneity. From portal vein to portal venules, the endothelial cells become spindle shaped, nonfenestrated, and possess short microvilli. At the transition point between the terminal portal venule and hepatic sinusoid, the ECs are smooth and large and contain many actin fibres, and together with Ito cells, they can control blood flow. In the case of the blood delivered by hepatic artery, the blood flow is regulated by a precapillary

sphincter consisting of tall ECs and smooth muscle cells at the junction between the hepatic artery and sinusoid (49).

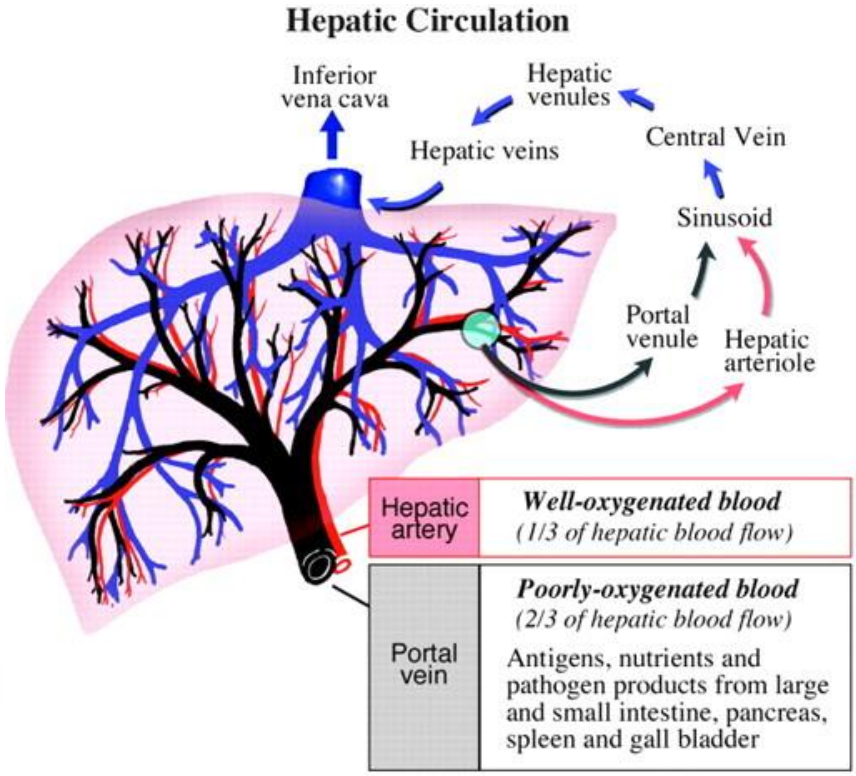

Figure 2. Liver blood circulation (49).

4.1.1. Liver sinusoidal endothelial cells

Liver sinusoidal endothelial cells (LSECs) comprise 50% of the non-parenchymal cells of the liver. They form a discontinuous and fenestrated endothelium which functions as a selective sieve for fluids, solutes and particles from blood to hepatocytes via the space of Disse (Figure 3). The fenestrations have approximate diameters of 100 to 150 nm and provide open channels between the sinusoidal blood and the subendothelial space of Disse. Sieving plays an important role in lipoprotein metabolism, which finally occurs in the hepatocytes. LSECs also contribute to vasomotor tone, organogenesis and liver regeneration (50).

In addition, LSECs also function as scavengers, eliminating soluble waste macromolecules from portal venous blood by receptor-mediated endocytosis, such as hyaluronan, acetylated low-density lipoprotein (LDL), denatured albumin, glycation end products and ovalbumin. Some of the receptors involve in this scavenger function are the mannose receptor, the hyaluronan receptors HARE and stabilin-2.

Another function of LSECs is related to immunity, since they take up antigens through scavenger and mannose receptor and present them to lymphocytes via major histocompatibility complex molecules. In contrast with professional antigen presenting cells, LSECs antigen presentation to immune system results in immune tolerance rather than enhanced immunity. Thus, this tolerance prevents response to innocuous oral antigens.

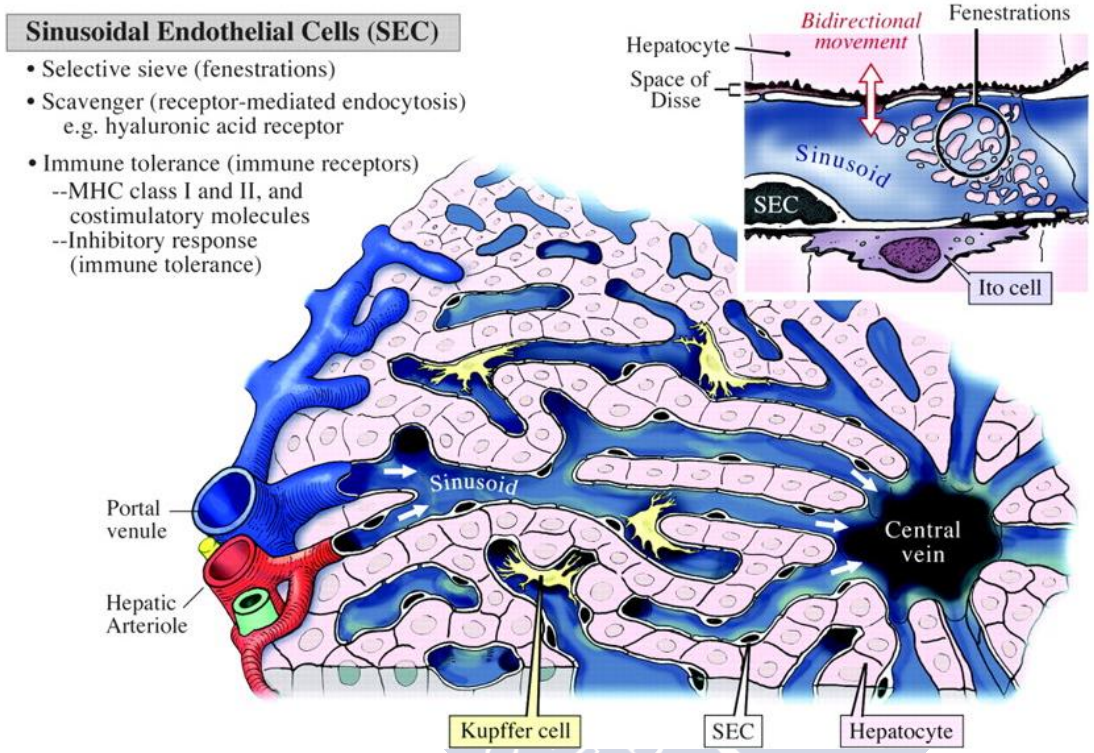

Figure 3. Liver sinusoidal endothelial cells characteristics and functions (50).

The liver is one of the greatest leukocyte margination sites in the body. This leukocyte trafficking is mainly mediated by the sinusoids, and the migration mechanisms differs from those of other vascular beds. Thus, leukocyte accumulation and adhesion are not preceded by rolling and PECAM-1/CD-31 is not necessary.

4.2. Metastasizing to the liver

The liver is the most frequently afflicted organ by metastasis for the majority of prevalent malignancies, and liver metastases are much more common than primary hepatic tumours (51). The liver is the main site of metastatic disease and a major cause of death from gastrointestinal malignancies such as colon, gastric and pancreatic carcinomas, as well as melanoma, breast

cancer and sarcomas (52). The main factors related to the great susceptibility of liver to metastases are:

-Architectural and hemodynamic features: dual, slow and tortuous liver-specific microcirculation, along with the expression by non-parenchymal cells of surface molecules that facilitate attachment of circulating tumour cells, promote tumour cells hepatic retention. Moreover, LSECs fenestrations allow direct access of tumour cells to the basement membrane.

-Regenerative capabilities: self-renewal and reconstruction capability of the liver can create a favourable environment for tumour growth.

-Regional immune suppression: tolerant microenvironment permissive to foreign tumour cell survival and growth due to its constant exposure to inflammatory stimuli from the gut.

4.3. Liver metastatic tumour microenvironment

The metastatic process to the liver involves four interrelated phases (51):

5. Tumour-infiltrating microvascular phase, which involves tumour cell arrest by LSECs that leads to tumour cell death or extravasation.
6. Interlobular pre-angiogenic micrometastasis phase, during which host stromal cells are recruited into avascular micrometastases.
7. Angiogenic micrometastasis phase, in which tumours become vascularised through several possible interactions with the microenvironment.
8. Growth phase that leads to the establishment of the macrometastasis.

The hepatic metastatic tumour microenvironment is highly dynamic and is regulated by interactions between cellular and non-cellular components of the environment. These interactions are bidirectional, and communication occurs through soluble signalling factors, such as cytokines, chemokines and growth factor; receptor-mediated cell-cell and cell-extracellular matrix contacts, and proteolytic enzymes. Each hepatic cell type is involved in different metastases phases and capable of playing tumouricidal and tumour promoting roles.

-LSECs: the tumour-endothelial cell interaction determines the progression of the process. LSECs can play tumoricidal and tumour progression-promoting activities, and this role is determined indirectly by cytokines produced by Kupffer cells or directly by interactions with

the invading tumour cells. Tumour cells activate KCs which produce proinflammatory cytokines, which in turn stimulate LSECs to express high levels of adhesion molecules that enable tumour cells attachment and extravasation.

-Kupffer cells (KCs): involved in the microvascular and intralobular micrometastasis phases. Similar to LSECs, they play a bimodal role during metastatic process, which can involve cytotoxic activity towards tumour cells or tumour promoting activity. The switch from one role to the other is determined predominantly by tumour cell burden. Thus, when KCs phagocytic capacity is overwhelmed due to excessive numbers of tumour cells invading the liver, KCs switch to promote liver colonization and metastic progression. KCs are capable of directly stimulating metastatic proliferation through the release of growth factors as well as cytokines and indirectly via extracellular matrix modifications.

-Hepatic stellate cells (HSCs) or Ito cells: they generate a pro-metastatic liver microenvironment. After micrometastases development, quiescent HSCs are triggered to transdifferentiate into myofibroblasts, highly proliferative and mobile cells, by factors released by tumour and Kupffer cells. Thus, activated HSCs promote metastatic progression via multiple mechanisms, including growth factors and cytokines, extracellular matrix degradation, angiogenesis and immunosuppression.

-Hepatocytes: they are involved in intralobular phase and play a critical role in metastatic seeding, colonization and survival. Upon seeding in the liver, cancer cells can interact with hepatocytes through the fenestrated endothelium into the space of Disse.

References

1. Naldini L. Gene therapy returns to centre stage. Nature. 2015 Oct 15;526(7573):351-60.

2. Amer MH. Gene therapy for cancer: present status and future perspective. Mol Cell Ther. 2014 Sep 10;2:27,8426-2-27. eCollection 2014.

3. Silva AC, Lopes CM, Sousa Lobo JM, Amaral MH. Nucleic Acids Delivery Systems: A Challenge for Pharmaceutical Technologists. Curr Drug Metab. 2015;16(1):3-16.

4. Walther W, Schlag PM. Current status of gene therapy for cancer. Curr Opin Oncol. 2013 Nov;25(6):659-64.

5. Wang D, Gao G. State-of-the-art human gene therapy: part I. Gene delivery technologies. Discov Med. 2014 Jul-Aug;18(97):67-77.

6. Fire A, Xu S, Montgomery MK, Kostas SA, Driver SE, Mello CC. Potent and specific genetic interference by double-stranded RNA in Caenorhabditis elegans. Nature. 1998 Feb 19;391(6669):806-11.

7. Whitehead KA, Langer R, Anderson DG. Knocking down barriers: advances in siRNA delivery. Nat Rev Drug Discov. 2009 Feb;8(2):129-38.

8. Chen Y, Gao DY, Huang L. In vivo delivery of miRNAs for cancer therapy: challenges and strategies. Adv Drug Deliv Rev. 2015 Jan;81:128-41.

9. Singh MS, Peer D. RNA nanomedicines: the next generation drugs? Curr Opin Biotechnol. 2016 Jan 8;39:28-34.

10. Wang D, Gao G. State-of-the-art human gene therapy: part II. Gene therapy strategies and clinical applications. Discov Med. 2014 Sep;18(98):151-61.

11. Gupta M, Tiwari S, Vyas S. Structuring polymers for delivery of DNA-based therapeutics: updated insights. Crit Rev Ther Drug Carrier Syst. 2012;29(6):447-85.

12. European Medicines Agency [Internet].; 2017 [updated 17/08/2017;]. Available from: http://www.ema.europa.eu/ema/index.jsp?curl=pages/medicines/human/medicines/003854/human_med_001985.jsp&mid=WC0b01ac058001d124.

13. Espiritu MJ, Collier AC, Bingham JP. A 21st-century approach to age-old problems: the ascension of biologics in clinical therapeutics. Drug Discov Today. 2014 Aug;19(8):1109-13.

14. Fan Q, Ma J, Xu Q, Zhang J, Simion D, Carmen G, et al. Animal-derived natural products review: focus on novel modifications and applications. Colloids Surf B Biointerfaces. 2015 Apr 1;128:181-90.

15. Dang JM, Leong KW. Natural polymers for gene delivery and tissue engineering. Adv Drug Deliv Rev. 2006 Jul 7;58(4):487-99.

16. Bryant LM, Christopher DM, Giles AR, Hinderer C, Rodriguez JL, Smith JB, et al. Lessons learned from the clinical development and market authorization of Glybera. Hum Gene Ther Clin Dev. 2013 Jun;24(2):55-64.

17. Senior M. After Glybera's withdrawal, what's next for gene therapy? Nat Biotechnol. 2017 Jun 7;35(6):491-2.

18. Rehman H, Silk AW, Kane MP, Kaufman HL. Into the clinic: Talimogene laherparepvec (T-VEC), a first-in-class intratumoral oncolytic viral therapy. J Immunother Cancer. 2016 Sep 20;4:53,016-0158-5. eCollection 2016.

19. Schimmer J, Breazzano S. Investor Outlook: Rising from the Ashes; GSK's European Approval of Strimvelis for ADA-SCID. Hum Gene Ther Clin Dev. 2016 Jun;27(2):57-61.

20. Wen Y, Oh JK. Recent strategies to develop polysaccharide-based nanomaterials for biomedical applications. Macromol Rapid Commun. 2014 Nov;35(21):1819-32.

21. Lalatsa A, Barbu E. Carbohydrate Nanoparticles for Brain Delivery. Int Rev Neurobiol. 2016;130:115-53.

22. Raemdonck K, Martens TF, Braeckmans K, Demeester J, De Smedt SC. Polysaccharide-based nucleic acid nanoformulations. Adv Drug Deliv Rev. 2013 Aug;65(9):1123-47.

23. Moscovici M. Present and future medical applications of microbial exopolysaccharides. Front Microbiol. 2015 Sep 29;6:1012.

24. Kim JK, Kim HJ, Chung JY, Lee JH, Young SB, Kim YH. Natural and synthetic biomaterials for controlled drug delivery. Arch Pharm Res. 2014 Jan;37(1):60-8.

25. Luo Y, Wang Q. Recent development of chitosan-based polyelectrolyte complexes with natural polysaccharides for drug delivery. Int J Biol Macromol. 2014 Mar;64:353-67.

26. Alvarez-Lorenzo C, Blanco-Fernandez B, Puga AM, Concheiro A. Crosslinked ionic polysaccharides for stimuli-sensitive drug delivery. Adv Drug Deliv Rev. 2013 Aug;65(9):1148-71.

27. Zhao L, Liu M, Wang J, Zhai G. Chondroitin sulfate-based nanocarriers for drug/gene delivery. Carbohydr Polym. 2015 Nov 20;133:391-9.

28. Raemdonck K, Martens TF, Braeckmans K, Demeester J, De Smedt SC. Polysaccharide-based nucleic acid nanoformulations. Adv Drug Deliv Rev. 2013 Aug;65(9):1123-47.

29. Verma MS, Gu FX. 1,3-Beta-Glucans: Drug Delivery and Pharmacology. In: Karunaratne DN, editor. The Complex World of Polysaccharides. Rijeka: InTech; 2012. p. Ch. 21.

30. Yang J, Han S, Zheng H, Dong H, Liu J. Preparation and application of micro/nanoparticles based on natural polysaccharides. Carbohydrate Polymers. 2015 5 June 2015;123(Supplement C):53-66.

31. Krishnamoorthy K, Mahalingam M. Selection of a suitable method for the preparation of polymeric nanoparticles: multi-criteria decision making approach. Adv Pharm Bull. 2015 Mar;5(1):57-67.

32. Vauthier C, Bouchemal K. Methods for the preparation and manufacture of polymeric nanoparticles. Pharm Res. 2009 May;26(5):1025-58.

33. Rao JP, Geckeler KE. Polymer nanoparticles: Preparation techniques and size-control parameters. Progress in Polymer Science. 2011 July 2011;36(7):887-913.

34. Ahmed TA, Aljaeid BM. Preparation, characterization, and potential application of chitosan, chitosan derivatives, and chitosan metal nanoparticles in pharmaceutical drug delivery. Drug Des Devel Ther. 2016 Jan 28;10:483-507.

35. Namazi H, Fathi F, Heydari A. Nanoparticles Based on Modified Polysaccharides. In: Hashim AA, editor. The Delivery of Nanoparticles. InTech; 2012. p. 149-84.

36. Grenha A. Chitosan nanoparticles: a survey of preparation methods. J Drug Target. 2012 May;20(4):291-300.

37. Nikitenko LL. Vascular endothelium in cancer. Cell Tissue Res. 2009 01/01;335(1):223-40.

38. Aird WC. Phenotypic heterogeneity of the endothelium: I. Structure, function, and mechanisms. Circ Res. 2007 Feb 2;100(2):158-73.

39. Rajendran P, Rengarajan TF, Thangavel JF, Nishigaki YF, Sakthisekaran DF, Sethi GF, et al. The vascular endothelium and human diseases. International journal of biological sciences JID - 101235568. 0714.

40. Geraud C, Koch PS, Goerdt S. Vascular niches: endothelial cells as tissue- and site-specific multifunctional team players in health and disease. J Dtsch Dermatol Ges. 2014 Aug;12(8):685-9.

41. Aird WC. Endothelial Cell Heterogeneity. Cold Spring Harbor Perspectives in Medicine. 2012 01;2(1):a006429.

42. Zecchin A, Borgers G, Carmeliet P. Endothelial cells and cancer cells: metabolic partners in crime? Curr Opin Hematol. 2015 May;22(3):234-42.

43. Lee E, Pandey NB, Popel AS. Crosstalk between cancer cells and blood endothelial and lymphatic endothelial cells in tumour and organ microenvironment. Expert Rev Mol Med. 2015 Jan 30;17:e3.

44. Dudley AC. Tumor Endothelial Cells. Cold Spring Harbor Perspectives in Medicine. 2012 03;2(3):a006536.

45. Wang Z, Dabrosin C, Yin X, Fuster MM, Arreola A, Rathmell WK, et al. Broad targeting of angiogenesis for cancer prevention and therapy. Semin Cancer Biol. 2015 Dec;35 Suppl:S224-43.

46. Hida K, Ohga N, Akiyama K, Maishi N, Hida Y. Heterogeneity of tumor endothelial cells. Cancer Sci. 2013 Nov;104(11):1391-5.

47. Sounni NE, Noel A. Targeting the tumor microenvironment for cancer therapy. Clin Chem. 2013 Jan;59(1):85-93.

48. Dong Z, Nör J,E. Transcriptional targeting of tumor endothelial cells for gene therapy. Adv Drug Deliv Rev. 2009 04/23;61(7-8):542-53.

49. Aird WC. Phenotypic heterogeneity of the endothelium: II. Representative vascular beds. Circ Res. 2007 Feb 2;100(2):174-90.

50. Sorensen KK, Simon-Santamaria J, McCuskey RS, Smedsrod B. Liver Sinusoidal Endothelial Cells. Compr Physiol. 2015 Sep 20;5(4):1751-74.

51. Clark AM, Ma B, Taylor DL, Griffith L, Wells A. Liver metastases: Microenvironments and ex-vivo models. Exp Biol Med (Maywood). 2016 Sep;241(15):1639-52.

52. Brodt P. Role of the Microenvironment in Liver Metastasis: From Pre- to Prometastatic Niches. Clin Cancer Res. 2016 Dec 15;22(24):5971-82.

USC
UNIVERSIDADE
DE SANTIAGO
DE COMPOSTELA

Annex I

Nanocarriers for microRNA delivery in cancer medicine

USC
UNIVERSIDADE
DE SANTIAGO
DE COMPOSTELA

Abstract

The number of deaths caused by cancer is expected to increase partly due to the lack of selectivity and undesirable systemic effects of current treatments. Advances in the understanding of microRNA (miRNA) functions and the ideal properties of nanosystems have brought increasing attention to the application of nanomedicine to cancer therapy. This review covers the different miRNA therapeutic strategies and delivery challenges for its application in cancer medicine. Current trends in inorganic, polymeric and lipid nanocarrier development for miRNA replacement or inhibition are summarized. To achieve clinical success, in-depth knowledge of the effects of the promotion or inhibition of specific miRNAs is required. To establish the dose and the length of treatment, it will be necessary to study the duration of gene silencing. Additionally, efforts should be made to develop specifically targeted delivery systems to cancer cells to reduce doses and unwanted effects. In the near future, the combination of miRNAs with other therapeutic approaches is likely to play an important role in addressing the heterogeneity of cancer.

Keywords: cancer therapy, gene silencing, microRNA, nanocarriers, RNA interference

1. Introduction

1.1. Limitations of current cancer therapies

Cancer consists of a group of diseases characterized by uncontrolled division of abnormal cells that can invade and spread to other organs to form metastases. Neoplastic diseases exhibit distinctive capabilities such as proliferative signalling, evading growth suppressors, resisting cell death, enabling replicative immortality, inducing angiogenesis, and activating invasion and metastasis (1). Cancer is the second cause of death in developed countries and is associated with aging of the population and lifestyle (2). The number of deaths caused by cancer was estimated to be 8.2 million in 2012, corresponding to 13% of all deaths. Although approximately two-thirds of cancer cases are cured due to advances in diagnosis, health care and treatment, the number of deaths is expected to increase. The lack of selective delivery of current treatments and the consequent systemic toxicity are among the major reasons for this trend (3).

Radiotherapy and surgery are the most effective treatments for local and non-metastatic tumours, whereas chemotherapy, hormone and biological therapies are currently used for the treatment of metastatic cancers (4). However, despite significant progress in cancer treatments, the low selectivity, undesirable systemic effects and dose-limiting toxicity of current treatments make them nonspecific and non-ideal therapeutic approaches (5).

1.2. Nanomedicine in cancer treatment

Recent advances in nanomedicine applied to cancer therapeutics may help to overcome the existing limitations of antineoplastic drugs. Nanomedicine includes the design and development of nanoscopic delivery vehicles and diagnostic agents. These delivery systems can improve drug stability, increase the circulation time and selectively accumulate at the tumour site (6, 7). Their nanometric size facilitates accumulation preferably at the tumour site due to the enhanced permeability and retention effect (EPR). The EPR effect is based on the presence of fenestrated blood vessels in the tumour, leading to extravasation of nanocarriers through a passive mechanism. Additionally, active targeting can be achieved through functionalization of the nanosystems with specific ligands for receptors on target cells.

Furthermore, current progress in understanding the molecular pathways and functions of cancer have enabled the identification of new targets and the development of novel therapeutic

strategies. Hence, the finding of specifically altered signalling networks in cancer cells and the ideal properties of nanosystems have brought increasing attention to the application of nanomedicine to cancer treatment. A wide range of materials has been employed in the synthesis of nanocarriers and can be grouped into inorganic, polymer and lipid-based materials. In this review, we will cover nanosystems for microRNA (miRNA) delivery developed to date for cancer therapy.

2. MicroRNA

2.1. MicroRNA mechanism

RNA interference (RNAi) is an evolutionarily conserved method of gene expression regulation. RNAi is based on a post-transcriptional pathway triggered by a double-stranded RNA (dsRNA) that leads to sequence-specific silencing of a messenger RNA (mRNA) (8). RNAi was discovered by Fire and Mello in 1998 (9) and included endogenous (miRNA) or exogenous (siRNA and shRNA) RNAs. Gene silencing occurs when the double-stranded RNA molecules incorporate into the RNA-induced silencing complex (RISC). Then, the guide strand or anti-sense strand guides RISC to the complementary or near-complementary region of the target mRNA (10). miRNAs are only partially complementary to their target mRNAs and result in their degradation or translational inhibition, whereas siRNAs and shRNAs bind completely to and cleave the complementary strand (11-13). Toxicity associated with siRNA and shRNA overexpression is being debated; however, miRNA therapeutics seem to be safer and do not compromise the gene knockdown efficacy (14-16).

Functional miRNAs are produced from the cleavage of pre-miRNAs in the cytoplasm. Mature miRNAs are 20-23 base pair double-stranded molecules comprised of a guide and a passenger strand that is released after loading into RISC, as shown in Figure 1. Due to the ability of the miRNA to inhibit gene expression by partial complementarity to the mRNA, one miRNA can bind to different mRNAs and thus affect the expression of multiple genes.

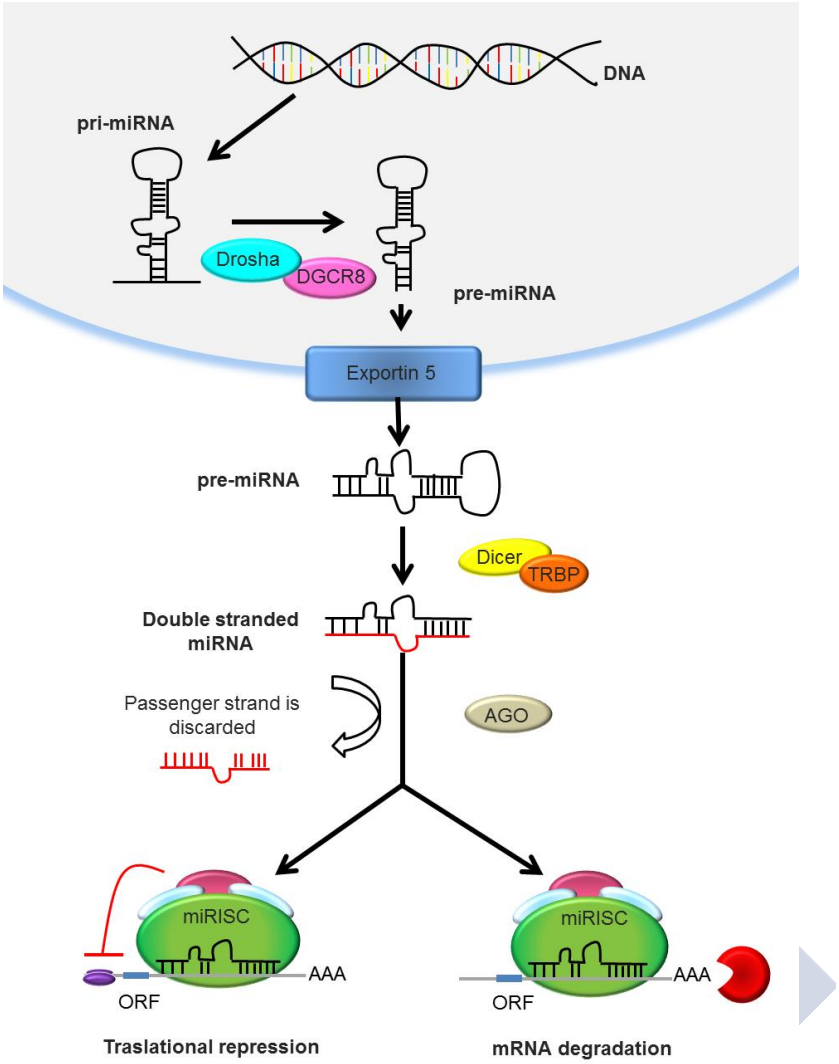

Figure 1. Gene silencing mechanism of miRNAs. The long primary miRNA transcripts (pri-miRNAs) obtained from the transcription of miRNA genes are cleaved by the Drosha-DGCR8 complex in the nucleus to form pre-miRNA hairpins. These pre-miRNAs are exported by Exportin 5 into the cytoplasm and cleaved by the Dicer-TRBP complex into miRNA duplexes, which are incorporated into the miRNA-induced silencing complex (miRISC). AGO, which is a component of the RISC, releases and degrades the passenger strand while RISC is guided by the guide strand to the target mRNA, resulting in translation repression or mRNA degradation.

2.2. MicroRNAs and cancer

The use of miRNAs for cancer therapy is based in the finding that miRNA expression is deregulated in cancer tissues and the ability of miRNAs to target multiple genes and alter cancer phenotypes (17, 18). Cancers are complex diseases involving deregulated expression of

multiple genes, whereas miRNAs can modulate different disease pathways and increase the chances of eliminating the cancer. Moreover, distinctive miRNA expression profiles have been associated with specific cancer types, allowing for the discrimination and identification of poorly differentiated tumours (19, 20). Thus, miRNAs have shown relevant clinical utility for cancer therapeutics and diagnosis.

2.3. MicroRNA therapeutic strategies: sense and antisense microRNAs

In neoplastic diseases, miRNAs can be downregulated when they function as tumour suppressors or overexpressed when they function as oncogenes. Hence, two therapeutic approaches are currently being used to modulate miRNA functions: restoring miRNA activity using a synthetic miRNA and inhibiting the function of a miRNA through anti-miRNA oligonucleotides.

In situations where miRNAs are down-regulated, replacement therapy with miRNA mimics is used to restore miRNA levels and their tumour suppressive properties. Because the objective of this replacement therapy is to accomplish biological functions that are identical to the endogenous miRNAs, miRNA mimics should be loaded onto RISC to silence their target mRNAs. For this reason, double-stranded miRNA mimics are preferred over single-stranded mimics because the duplex structure has been found to facilitate RISC loading and thereby enhance the gene silencing efficacy (21).

In the case of overexpressed oncogenic miRNAs, the most widely used strategy is based on the use of miRNA antagonists to inhibit miRNA expression. The most common antisense approach is the use of single-stranded oligonucleotides that are partially or completely complementary to the target miRNA. The complementary binding of the antagonist to the endogenous miRNA prevents its processing by RISC. These antisense oligonucleotides (known as anti-miRNAs) are chemically modified to increase their binding affinity for the miRNA (22). Accordingly, miRNAs could act as therapeutic agents or as therapeutic targets (23).

2.4. Challenges in microRNA delivery

Similar to other therapeutic oligonucleotides, miRNA delivery is a major challenge because naked miRNAs are quickly degraded by nucleases and cleared via renal excretion. Moreover, RNA administration may induce innate immune responses, leading to unwanted toxicities. In addition to their instability and toxicity, their hydrophilic nature, negative charge

and high molecular weight prevent nucleic acids from crossing cell membranes. Once inside cells, miRNA should achieve endosomal escape and compete with endogenous RNAi pathways (23-25). Because miRNAs are designed to target multiple pathways, they may cause off-target gene silencing that can induce toxic effects. Finally, insufficiency or saturation of the enzymes involved in miRNA processing may lead to inefficient gene silencing efficacy. In this case, the use of mature miRNAs can avoid saturation of the processing enzymes (23). To overcome these hurdles, diverse strategies and delivery systems are currently being studied. Traditionally, delivery systems for nucleic acids are classified as viral and non-viral vectors, but this review will be limited to non-viral vectors for miRNA therapy with a focus on nanocarriers.

3. MicroRNA Delivery

3.1. Chemical modifications and oligonucleotide conjugates

One of the approaches used to overcome the poor stability and immune responses of miRNAs is based on chemical modifications. These can reduce the off-target effects associated with miRNAs. The principal strategies are based on i) ribose 2'-OH group modification, ii) locked nucleic acids (LNA), iii) backbone modifications and iv) peptide nucleic acids (PNA) (26).

i. The ribose 2'-OH group is easily attacked by nucleases. Substitution of the ribose 2'-OH group for 2'-O-methyl, 2'-O-fluoro or 2'-methoxyethyl has been shown to increase the binding affinity, stability and gene silencing activity of anti-miRNAs (27).
ii. LNAs are antisense oligonucleotides based on ribose-modified RNA nucleotides with an extra bridge connecting the 2' oxygen and 4' carbon to create a stable "locked ring conformation". LNAs exhibit increase stability and a reduced immune response but may lead to a reduction in activity (17).
iii. The most widely used strategy among backbone modifications is phosphorotioate modifications in which one of the non-bridging phosphate oxygen atoms is replaced with a sulphur atom. This modification has been demonstrated to increase nuclease resistance but shows a short circulation life and low binding affinity (28)
iv. PNA consists of uncharged oligonucleotide analogs in which the sugar-phosphodiester backbone has been replaced by N-(2-aminoethyl)-glycine units. The lack of charge of

PNA eliminates the need for transfection reagents and enhances oligonucleotide stability with low toxicity (29).

Another strategy consists of conjugation with small transport domains, such as aptamers and cell-penetrating peptides. Aptamers are small single-stranded oligonucleotides with a particular three-dimensional structure that can bind to specific surface receptors and act as drug delivery agents. Conjugation of miRNAs to aptamers has been used to specifically target the nucleic acid to cells expressing the ligands recognized by the aptamer (30). For example, Rohde *et al.* used the ubiquitously expressed transferrin receptor as an aptamer for miR-126 delivery (31).

Conjugation to cell-penetrating peptides is intended to enable crossing of cell and endosomal membranes (32). For example, Fabani et al. conjugated a PNA anti-miR-122 to the cell-penetrating peptide penetratin to deliver the oligonucleotide *in vitro* (33).

Although these modifications and strategies improve miRNA stability and the pharmacokinetic profile and reduce the immune response, increased toxicity and reduced activity have been observed. Consequently, the high doses of modified miRNAs required result in off target effects and saturation of the silencing machinery. Hence, the lack of efficient and specific delivery of miRNAs to tumour cells remains a significant challenge.

3.2. Nanocarriers

Nanocarriers have recently become popular for miRNA delivery in an attempt to enhance cellular uptake and pharmacological effectiveness and reduce toxicity. Non-viral vectors have the advantage of being highly versatile; thus, it is possible to modify the systems with targeting ligands or polyethylene glycol (PEG) molecules to achieve site-specific delivery or prolong the circulation time of the system. Nanocarriers are safe and require simple manufacturing; moreover, they are characterized by their low immunogenicity, low cost and versatility. Table 1 summarizes miRNA nanocarries that, to the best of our knowledge, have been tested *in vivo*, while Table 2 lists some of the functions of the miRNAs here presented.

3.2.1. Inorganic systems

Inorganic materials have been used to develop nanocarriers with a controlled size and morphology. The unique properties of inorganic systems make them vehicles that are biocompatible, non-immunogenic, nontoxic and easy to scale up.

Gold nanoparticles have received attention as nucleic acid delivery carriers due to their suitable physico-chemical properties, such as shape, surface area, amphiphilicity, biocompatibility and easy surface functionalization. However, these nanosystems also have drawbacks, such as low encapsulation efficiency, poor storage stability and slow endosomal escape.

Hao *et al*. synthetized gold nanoparticles functionalized with a monolayer of double-stranded alkylthiol-modified miRNA molecules (34). Briefly, the gold nanoparticles associated with miR-205, which was found to be markedly down-regulated in the human prostate cancer cell line PC-3, inhibited cancer cell proliferation and migration. Additionally, nanoparticles functionalized with miR-20a, which played an oncogenic role in PC-3 carcinogenesis, protected the cells from doxorubicin-induced apoptosis.

Cysteamine-functionalized gold nanoparticles bound to unmodified miRNAs were utilized by Ghosh e*t al.* (35). The tumour suppressor miR-31 and cell proliferator miR-1323 were successfully delivered at levels up to 10-20-fold higher than conventional liposome-mediated transfection in neuroblastoma cell lines and ovarian cell lines with low toxicity.

Ekin *et al.* also used gold nanoparticles chemically modified with thiolated RNAs. Subsequently, the proliferation inhibitor miR-145 was hybridized to the covalently attached RNAs (36). These nanoparticles were successfully transfected into the human prostate cancer cell line PC3 and the human breast cancer cell line MCF7.

Silica has also been used for miRNA delivery because it is a biodegradable, safe, stable, inert and easily functionalizable delivery system. Tivnan *et al.* demonstrated targeted delivery of miR-34a, which is a tumour suppressor downregulated in several cancer types, associated with porous silica nanoparticles conjugated with a disialoganglioside GD2 (GD_2) antibody to neuroblastoma tumours (37). GD_2 is a glycolipid that is highly expressed on the cell surface of neuroblastomas and other cancers. The anti-GD_2-coated nanoparticles resulted in inhibition of

neuroblastoma tumour growth in a murine orthotopic disease model with increased apoptosis and inhibition of vascularization.

Bertucci et al. used mesoporous silica nanoparticles (MSNPs) for the co-delivery of the PNA anti-miR-221-octaarginine conjugate and temozolomide to drug-resistant glioma cells (38). MSNPs, which are characterized by their large surface area and their controllable porous structure for loading active molecules, associated with the PNA anti-miR-221 on the surface and temozolomide in the pore system. Upregulation of miR-221 has been shown to promote cell cycle progression and chemoresistance in glioma cells. The co-delivery of both drugs showed the most effective induction of apoptosis in the temozolomide-resistant T98G human glioma cell line.

The use of magnetic materials has shown added value for the synthesis of nanoparticles for miRNA delivery. Yin *et al.* designed magnetic zinc-doped iron oxide nanoparticles for the delivery of the tumour suppressor lethal-7a miRNA. The authors induced magnetic hyperthermia to enhance the treatment of glioblastoma multiforme brain cancer cells (39). The nucleic acid was loaded onto the system through an external layer of polyethylenimine (PEI) and together with the magnetic hyperthermia therapy enhanced apoptosis *in vitro*.

Lellouche *et al.* used maghemite nanoparticles surface-doped with lanthanide $Ce^{3/4+}$ cations and covered with oxidized PEI for the delivery of an antisense miR-486 and anti-miR-99a, which have been found overexpressed by the authors, to hard-to-transfect human CMK leukaemia cells and anti-miR-21, which is one of the most common miRNAs involved in the genesis and progression of human cancers, to BxPC-3 human pancreatic adenocarcinoma cells (40). Moreover, intravenous injection of the system in mice was not lethal at a therapeutic dose.

Inorganic nanoparticles that can be monitored by magnetic resonance imaging (MRI) have also been studied. Yang *et al.* functionalized nanoscale graphene oxide (NGO) with polyethylene glycol, low molecular weight poly-amidoamine (PAMAM) and gadolinium (Gd) to enhance the transfection efficiency of miRNAs and maintain low cytotoxicity (41). This delivery system consists of a PAMAM-dendrimer associated with the let-7g miRNA and Gd-functionalized NGO loading of the chemotherapeutic epirubicin. The Gd-NGO carrier was capable of knocking down the expression of Ras family proteins in glioma U87 cells by efficient simultaneous delivery of the let-7g miRNA and epirubicin.

Finally, Yoo *et al.* reported the synthesis of layered gadolinium hydroxychloride nanoparticles for the *in vitro* delivery of anti-miR-10b to breast cancer cell lines, since overexpression of miR-10b has been found to promote metastasis in this type of cancer. The traceability of the system by MRI was demonstrated *in vivo* (42).

3.2.2. Polymer-based systems

Polymeric carriers are the most extensively used delivery systems for miRNAs. Amine groups of cationic polymers interact with the phosphate groups of nucleic acids to form polyplexes. Traditionally, these cationic polymers are classified into natural and synthetic polymers. Natural polymers include polysaccharides, peptides and proteins, whereas synthetic polymers principally comprise polyethylenimines, poly(lactic-co-glycolic acid) and dendrimers.

3.2.2.1. Synthetic polymers

i. Polyethylenimines (PEIs)

PEI is the most widely used cationic polymer for nucleic acid delivery and is considered the gold standard of non-viral vectors due to its high transfection efficacy. Its pH buffering capacity promotes endosome destabilization and the release of nucleic acids into the cytoplasm. The high charge density of PEIs allows them to form polyplexes with miRNAs but is also associated with high toxicity, thereby limiting their clinical use. To overcome this problem, modified PEI molecules have been developed.

Some studies have successfully used PEIs and PEI-derived systems for miRNA delivery. Jung *et al*. entrapped a combination of miRNA-34a and a long chain miRNA-34a conjugate (lc-miRNA) in PEI-coated calcium phosphate nanoparticles (43). The authors demonstrated that the chemically cross-linked miRNA (lc-miRNA) inhibited the proliferation and migration of the prostate cancer cell line PC-3 to a greater extent than common miRNA-loaded nanoparticles.

Ibrahim *et al.* delivered tumour suppressors miR-145 and miR-33a to form polyplexes with the low molecular weight branched PEI *in vitro* and *in vivo* (44). Intraperitoneal and intratumoural injections of PEI-complexed miR-145 in mouse models of colon carcinoma significantly decreased tumour growth. Similar results were obtained when miR-33a-

polyplexes were administered systemically, establishing for the first time the relevance of miR-33a in cancer therapy.

Che *et al.* synthesized miR-145-loaded disulphide cross-linked PEI nanoparticles immobilized in paclitaxel-loaded poly(β-caprolactone) nanofibers (45). The system demonstrated the ability to promote apoptosis and reduce tumour invasion in a hepatocellular cancer cell line *in vitro*.

Modified PEIs have been synthetized and studied with the aim of enhancing polymer biocompatibility. Zhang *et al.* evaluated polyarginine-disulphide-linked polyethyleneimine polyplexes for the delivery of miR-145 to prostate cancer (46). The disulphide linkage was introduced in PEIs to overcome their high cytotoxicity and increase their cell biocompatibility. The peptide polyarginine was added to the system to harness its prostate-specific uptake properties. Thus, PEG chain was used as a linker to enhance biocompatibility and extend the circulation time of the nanocarrier. The authors demonstrated greater accumulation of miR-145 in the prostate tumour region using the polyarginine nanocarrier *in vivo*. Thus, the miR-145 polyplexes showed effectiveness in reducing peritoneal tumour growth and increasing the animal survival rate**.**

Chiou *et al*. assessed the utility of polyurethane-short branch PEI as a vehicle for miR-145 delivery to lung adenocarcinoma *in vitro* and *in vivo* (47). The authors demonstrated that intratumoural delivery of the polyplexes associated with miR-145 reduced tumour growth, enhanced the therapeutic efficacy of chemoradiotreatment and prolonged the survival time of xenograft tumour-bearing mice.

As another example of a modified PEI, Gao *et al.* synthesized the cationic poly(L-lysine)-modified polyethylenimine copolymer and successfully delivered two types of anti-miR-21 to breast cancer MCF-7 cells (48).

ii. Poly(lactic-co-glycolic acid) (PLGA)

Poly(lactic-co-glycolic acid) is a well-known and widely studied safe, biocompatible and biodegradable polymer. PLGA delivery systems are capable of sustained release of the therapeutic molecule and allow multiple surface modifications. Here, we present the PLGA systems currently used for miRNA delivery.

Wang *et al.* tested FDA-approved pegylated PLGA nanoparticles as carriers for the delivery of miR-122, which are involved in apoptosis and tumourigenesis inhibition, into human colon cancer xenografts facilitated by sonoporation. This technique is based on an interaction between ultrasound and microbubbles to increase nanoparticle permeability across natural barriers (49). The system showed higher tumour penetration and miRNA silencing when this mechanical adjuvant technique was used.

In another study, Devulapally *et al.* synthesized biodegradable polymer nanoparticles based on pegylated PLGA for the co-delivery of anti-miR-21 and 4-hydroxytamoxifen (50). The system showed antiproliferative effects in different human breast cancer cells and mouse mammary carcinoma *cells in vitro*. The same system was modified with the uPA peptide to target the breast cancer-specific urokinase plasminogen activator receptor (uPAR) (51). This targeted carrier was able to simultaneously deliver anti-miR-21 and anti-miR-10b *in vitro* and to reduce tumour growth after implantation of pre-treated cells into mice.

Another example of PLGA surface functionalization is the vehicle utilized by Babar *et al.* These authors synthesized PLGA nanoparticles surface-coated with the cell-penetrating peptide penetratin for the delivery of the antisense PNA miR-155 to pre-B cell tumours. MiR-155 has been shown to be overexpressed in several lymphomas and involved in myeloproliferative pathology induction. The authors combined the effectiveness of chemically modified anti-miRNAs with the flexibility of nanosystems to support surface modifications. The use of neutral-charged PNAs has the advantage of not requiring the use of a cationic substance to associate the nucleic acids. The work demonstrated that the systemic administration of the system slowed tumour growth *in vivo* (52).

Cheng et al. developed PLGA nanoparticles coated with the cell-penetrating peptide nona-arginine for the delivery of chemically modified oligonucleotide analogs to human KB oral carcinoma cells (53). The system showed efficient delivery of antisense phosphorodiamidate morpholino oligomers (PMO) and peptide nucleic acids (PNA) to silence miR-155 and avoided the use of cationic substances due to the neutral charge density of the analogs.

Likewise, Ananta et al. demonstrated the effectiveness of PLGA nanoparticles for the delivery of anti-miR-21 and enhanced the sensitivity of glioblastoma U87 MG cells to temozolomide (54).

It is always a challenge to obtain high loading efficiencies and cellular uptake due to the hydrophobic and neutral nature of PLGA. For this reason, copolymers containing PEI and PLGA have been synthetized. For instance, the PLGA-PEI copolymer synthesized by Wang *et al.* formed a micelle-like structure in which doxorubicin and miR-542-3p, a known regulator of cell cycle and angiogenesis, could be loaded in the core and onto the surface, respectively (55). These polyplexes were coated with hyaluronic acid and showed effectiveness in promoting cancer cell apoptosis and cytotoxicity in breast cancer cells.

iii. Dendrimers

Dendrimers are highly branched polymers with a defined structure. Similar to PEI, the buffering amines inside dendrimers can act as a proton sponge, thereby enabling endosomal escape and miRNA delivery into the cytoplasm. The most widely used dendrimer is poly-amidoamine (PAMAM), although modified polymers have been explored to address toxicity issues. Studies that applied miRNA dendriplexes are presented below.

Conde *et al.* designed a novel RNA triple-helix structure containing miR-205 and antagomiR-221, showing both functions in cell proliferation, conjugated to the PAMAM G5 dendrimer (56). These triplex nanoparticles were embedded in a dextran hydrogel for local administration in a triple-negative breast cancer mouse model, leading to a noticeable decrease in the tumour size and increased animal survival.

The influence of the dendrimer structure on the delivery efficiency was studied by Qian *et al.* Their work proved the utility of the amphiphilic hyperbranched star polymers synthesized from polylactic acid (PLA) and polymethylaminoethyl methacrylate (PDMAEMA) as a drug and gene co-carrier for glioma treatment (57). The authors synthetized three types of molecular architecture by conjugating different numbers of hydrophilic PDMAEMA arms into the hydrophobic PLA core and demonstrated higher transfection efficiency of the more highly branched system. Therefore, a miR-21 inhibitor and the hydrophobic drug doxorubicin were successfully associated with the system and synergistically co-delivered both into LN229 glioma cells *in vitro* and subcutaneously in a nude mouse model.

iv. Other polymers

Other synthetic polymeric systems, such as the nanocapsules prepared by *in situ* polymerization of the positively charged monomer N-(3-aminopropyl) methacrylamide (APM),

the crosslinker ethylene glycol dimethacrylate (EGDMA) and the neutral monomer acrylamide (AAM), have also been used. Liu *et al.* synthesized anti-miR-21-loaded nanocapsules in which anti-miR-21 molecules were encapsulated within a thin network of polymer shells (58). The crosslinker molecules were degradable under the acidic conditions of the endosomes, leading to miRNA release. The system was able to suppress tumour growth after intratumoural administration in mice bearing glioma U87 subcutaneous tumours.

Functionalized polycarbonates have also been used as polymers for miRNA delivery systems. Mittal *et al*. developed gemcitabine-conjugated cationic copolymers complexed with miR-205 to form micelle-like polyplexes. miR-205 is a tumour suppressor miRNA that was shown to chemosensitize gemcitabine-resistant MIA PaCa-2R pancreatic cancer cells (59). The micelles were formed from an amphiphilic copolymer containing a PEG hydrophilic segment and a polypropylene carbonate hydrophobic chain with different cationic pendent groups. These micelleplexes were demonstrated to be effective in reverting the chemo-resistance, invasion and metastasis of gemcitabine-resistant pancreatic cancer cells *in vitro. In vivo* studies showed a reduction in the tumour growth rate and tumour weight in a pancreatic cancer xenograft model treated with the miR-205-gemcitabine complexes.

Choi et al. developed an engineered nanocarrier for RNA delivery composed of a hydrophilic shell of the CD44-targeting ligand hyaluronan, a hydrophobic core of 5β-cholanic acid as a drug reservoir, a RNA binding site of the artificial phosphate receptor Zn(II)-dipicolylamine (DPA/Zn) and a calcium phosphate layer that increased the protection and pH-dependent RNA release. The system demonstrated the ability to efficiently deliver miR-34a to a colon carcinoma cell line and tumour mouse model after intravenous administration (60). This nanosystem does not contain a cationic substance to bind the nucleic acids and thus achieves higher specific accumulation and lower toxicity than conventional gene transfection systems.

Liu et al. synthesized gelatinases-stimuli nanoparticles by polymerization of poly(Ɛ-caprolactone) (PCL) as a hydrophobic core and PEG as a hydrophilic corona connected by a tumour-specific gelatinases-cleavable peptide (61). This system demonstrated the ability to synergistically deliver docetaxel and miR-200c, which is known to improve sensitivity of cancer cells to chemotherapy, *in vitro* and *in vivo,* thereby suppressing tumour growth in a xenograft gastric cancer mouse model.

3.2.2.2. Natural polymers

i. Chitosan

Chitosan is one of the most studied natural polymers for gene delivery. It is a biocompatible, biodegradable and safe polysaccharide that has been explored as a miRNA delivery system. Deng *et al.* co-encapsulated miR-34a and doxorubicin into nanocomplexes composed of hyaluronic acid and chitosan (62). The authors reported efficient co-delivery of miR-34a and doxorubicin into the breast cancer cell line MDA-MB-231, thereby achieving synergistic effects on tumour suppression.

Santos-Carballal *et al.* studied the effect of the degree of acetylation and the molecular weight of chitosan on miRNA delivery. The authors showed that polyplexes formed of chitosan and miR-145 were efficiently transfected into MCF-7 breast cancer cells *in vitro* (63).

ii. Peptides and proteins

Peptide and protein-based carriers have been widely explored for nucleic acid delivery because they can condense nucleotides through electrostatic interactions with the positive charges of the amino acids. Moreover, amino acids contribute to endosomal escape, targeted delivery and bioreversible polyplex stabilization of the system. Nanosystems containing peptides and proteins are presented below.

Wang *et al.* prepared miR-34a self-assembled nanocomplexes composed of cationic protamine sulphate and negatively charged hyaluronic acid (HA) (64). HA was used due to its specific binding ability for the overexpressed CD44 receptors of tumours. miR-34a was efficiently delivered into both triple-negative breast cancer cells and a xenograft mouse breast cancer model in vivo.

Hao *et al.* constructed a nanosystem for tumour suppressors miR-15a and miR-16-1 delivery based on an aptamer-conjugated atelocollagen (65).The RNA aptamer A10-3.2 was used to target prostate-specific membrane antigen (PSMA) on the cell surface of prostate cancer cells. Atelocollagen is a type I collagen, which is a fibrous protein involved in maintaining the morphology of tissues and organs. This system effectively delivered both miRNAs to PSMA-overexpressing pancreatic cancer cells *in vitro* and *in vivo*.

Song *et al.* studied the efficacy of the antimiR-21/R3V6 peptide complex in the induction of apoptosis in C6 and A172 glioblastoma cells (66). The system was demonstrated to be more efficient than PEI and Lipofectamine and exhibited less cytotoxicity.

3.2.3. Lipid-based systems

Lipids are among the most widely studied materials for nucleic acid delivery. They can be grouped into cationic lipids, ionisable lipids and helper lipids.

3.2.3.1. Cationic lipids

Cationic lipids can interact with miRNAs to form lipoplexes. Generally, cationic lipids are formed by a hydrophilic head and a hydrophobic chain that will determine the transfection efficacy and toxicity of the system. Among the lipid-based systems, the most widely used cationic lipids for RNA delivery are 1,2-di-O-octadecenyl-3-trimethylammonium propane (DOTMA) and 1,2-dioleoyloxy-3-trimethylammonium propane (DOTAP).

Wang *et al*. used the cationic lipid DOTMA to complex miR-122, which is a liver-specific miRNA associated with cancer and other hepatic diseases, and the unsaturated fatty acid oleic acid as a helper lipid in liposomal nanoparticles (67). DOTMA-oleic acid lipid nanoparticles demonstrated hepatic delivery of miR-122 when the system was administered intravenously.

Wu *et al*. condensed miR-133b, a potential tumour suppressor, with DOTMA to form lipoplexes for the treatment of non-small cell lung cancer. This system achieved much higher lung accumulation and induction of miR-133b expression than standard transfection agent siPORT NeoFX complexes (68). The same authors successfully tested the delivery efficiency of miR-29b, which has been found to be involved in cell proliferation and apoptosis, by the lipoplexes in a xenograft mouse model of non-small cell lung cancer and achieved significant inhibition of tumour growth (69). Lee *et al.* engineered liposomes composed of the cationic lipids DOTAP and pegylated 1,2-distearoyl-sn-glycero-3-phosphoethanolamine (DSPE-PEG) containing cyanuric groups to chemically conjugate the protein ephrin-A1 for delivery of the let-7a miR to lung cancer cells (70). The ephrin-A1 protein is a well-known ligand of the overly expressed EphA2 receptor of lung cancer cells. This carrier inhibited effective cell proliferation, migration and tumour growth of malignant pleural mesothelioma and non-small cell lung cancer cell lines.

Zhang *et al.* associated a histidine-rich antimicrobial peptide ([D]-H6L9) to the surface of DOTAP-soybean phospatidylcholine-DSPE-PEG_{2000} liposomes (71). The liposomes successfully associated and delivered anti-miR-10b and paclitaxel *in vitro* and *in vivo*, thereby delaying tumour growth and reducing lung metastases in a murine metastatic mammary tumour model. The histidines of [D]-H6L9 helped the system escape endosomes/lysosomes due to their protonation under acidic pH and their consequent membrane lytic effect

Biocompatible and biodegradable ethylphosphocoline lipids have also been studied as cationic substances (72). Passadouro *et al.* developed 1-palmitoyl-2-oleoyl-sn-glycero-3-ethylphosphocholine (EPOC)-cholesterol cationic liposomes associated with albumin and demonstrated their ability to inhibit miR-21, miR-221, miR-10b and miR-222 in pancreatic cancer cells and their synergistic antitumour effect when co-administered with sunitinib (73).

Shi *et al.* utilized the cationic lipid dimethyldioctadecylammonium bromide (DDAB) to associate miR-34a in solid lipid nanoparticles. The solid lipid nanoparticles were composed of glycerol monostearate, cholesterol, soy phosphatidylcholine and DDAB and were able to deliver miR-34a alone (74) and simultaneously with paclitaxel *in vivo* (75). These nanoparticles demonstrated passive targetability to lung metastasis of the murine B16F10-CD44+ melanoma model and higher inhibition of tumour growth than the single drug-loaded solid lipid nanoparticles.

3.2.3.2. Ionizable lipids and helper lipids

Early cationic lipids, such as DOTMA and DODAC, contain a permanently positive quaternary amine, whereas ionizable cationic lipids, such as 1,2-dioleoyl-3-dimethylammonium propane (DODAP) and 1,2-dioleyloxy-N,N-dimethyl-3-aminopropane (DODMA), have tertiary amine positive charges at acidic pH but neutral charges at physiological pH (76). Moreover, the incorporation of helper and neutral lipids, such as cholesterol and saturated phosphatidylcholines (PC), has been used to increase system stability and transfection efficiency.

Daige *et al.* used liposomes to deliver miR-34a into mice with orthotopic Hep3B and HuH7 liver cancer xenografts, causing tumour regression in both models (77). These registered liposomes (known as SMARTICLES®) are formed of the lipids 1-palmitoyl-2-oleoyl-snglycero-3-phosphocholine (POPC), 1,2-dioleoyl-snglycero-3-phosphoethanolamine

(DOPE), cholesteryl hemisuccinate (CHEMS), and cholesteryl-4-([2-(4-morpholinyl)ethyl]amino)-4-oxoburanoate (MOCHOL) (78). The outstanding property of this system is its amphoteric behaviour because the particles are cationic during elaboration and anionic at physiological pH to facilitate movement across physiological membranes.

Costa *et al.* developed glioblastoma-targeted stable nucleic acid lipid particles (SNALPs) consisting of liposomes coupled with chlorotoxin (CTX), which is a peptide that acts as a specific marker for gliomas. The liposomes formed of DODAP, 1,2-distearoyl-sn-glycero-3-phosphocholine (DSPC), C16 Ceramide PEG2000 and 1,2-distearoyl-sn-glycero-3-phosphatidylethanolamine (DSPE)-PEG-Maleimide were loaded with locked nucleic acid-modified anti-miR-21. The authors demonstrated tumour accumulation of the system after systemic injection and enhanced anti-tumoural activity after combination with orally administered sunitinib (79).

Liu *et al*. studied the effect of co-treatment of miR-506, which is known to regulate proliferation and therapy response of cancer cells, loaded into 1,2-dioleoyl-sn-glycero-3-phosphocholine (DOPC) liposomes and the antineoplastics cisplatin and olaparib in an orthotopic ovarian cancer model (80). The intraperitoneal administration of this therapy resulted in the reduction of tumour growth through miR-506 inhibition of the epithelial-to-mesenchymal transition.

Moreover, PEG lipids are incorporated into liposomes to prolong the circulation time, stabilize the system and reduce immunostimulation (17). However, pegylation can reduce cellular uptake of the system. To overcome this problem, D-α-tocopheryl polyethylene glycol succinate (TPGS) formed by vitamin E and PEG combines the advantages of PEG but promotes cellular uptake. Dai *et al.* reported the systemic delivery of paclitaxel and the let-7b miRNA loaded in micelles composed of an amphiphilic copolymer made from PEG 5000, D-α-tocopherol (vitamin E) and the cationic moiety diethylentriamine (81). The system demonstrated marked potentiation due to the antiproliferative activity of paclitaxel and the let-7b miRNA both *in vitro* and *in vivo* in mice bearing KRAS mutant tumour xenografts.

3.2.3.3. Lipopolyplexes

Lipopolyplexes are systems composed of both lipids and polymers to address the limitations and combine the advantages of lipid-based and polymer-based systems. Chen *et al.*

developed DOTAP liposome-polycation-hialuronic acid nanoparticles modified with the monoclonal antibody GC4 single chain variable fragment (scFv) for the delivery of miR-34a and siRNA to B16F10 melanoma lung metastasis in a murine model (82). The GC4 scFv-targeted system consists of a cationic liposome of DOTAP and cholesterol encapsulating a complex composed of HA, siRNA or miRNA and protamine. The intravenous injection of the system resulted in the inhibition of the tumour load in the lungs, particularly when antibody-targeted nanoparticles containing miRNA and siRNA were applied simultaneously. Moreover, the presence of the pegylated-targeting scFv reduced the toxicity of the system.

Wang *et al.* developed near-infrared (NIR) laser-activated nanoparticles containing ammonium bicarbonate that could escape endosomes/lysosomes when heated due to conversion of encapsulated ammonium bicarbonate to gases (83). The nanoparticles consisted of a water-in-oil-in-water structure where indocyanine green (with a NIR laser-activated photothermal effect), miR-34a and ammonium bicarbonate were encapsulated in the hydrophilic core dispersed in the hydrophobic layer formed by PLGA, pluronic F127 and the phospholipid dipalmitoyl phosphatidylcoline (DPPC). Moreover, a more external hydrophilic layer contained hyaluronic acid and chitosan-pluronic F127. This thermal responsive system demonstrated cytosolic delivery of miR-34a both *in vitro* and *in vivo* in prostate cancer stem cells.

3.2.4. Clinical trials

Despite the huge attention received by this field, most of the current miRNA non-viral delivery systems for cancer treatment are still in preclinical studies. The first miRNA vector to enter the clinic (MRX34) was a miR-34-loaded liposome for the treatment of solid tumours and hematologic malignancies in a multicentre (84) phase I clinical trial (https://www.clinicaltrials.gov/ct2/show/NCT01829971). A novel delivery system based on non-living nano-sized cells (85) known as EDV^{TM} nanocells has recently entered phase I clinical trials for malignant pleural mesothelioma and non-small cell lung cancer treatment. These nanoparticles contain miR-16 and miR-15 and are targeted with an anti-epidermal growth factor receptor monoclonal antibody (https://clinicaltrials.gov/ct2/show/NCT02369198).

4. Future directions

The advances achieved in understanding miRNA functions and their roles in cancer have generated great expectations for miRNA therapeutics. The awarding of the Nobel Prize to Andrew Fire and Craig Mello in 2006 for the discovery of double-stranded RNA interference described in 1998 (9) attracted considerable attention and investment in the field. However, *in vivo* miRNA delivery has been challenging due to the physicochemical properties of miRNAs and biological barriers. The lack of rapid RNAi-based therapeutic development has limited the enthusiasm of pharmaceutical companies. Nevertheless, the development of non-viral systems for miRNA delivery has undergone a considerable boost in recent years, providing solutions for many of the challenges hindering miRNA therapeutic success. New opportunities and solutions for miRNA therapeutics have been created from progress in nanotechnology, which should reawaken the interest of pharmaceutical companies in the field (86).

The ultimate goal of miRNA delivery research is to achieve an efficient delivery system that enables the translation of RNAi therapeutics into the clinic. Although there is evidence of a miRNA antineoplastic effect in several *in vitro* and *in vivo* preclinical studies, only two miRNA delivery systems for cancer treatment are currently undergoing clinical trials. To achieve clinical success, in-depth knowledge of miRNA biology is required. Because one miRNA can regulate the expression of multiple genes through different signalling pathways, all effects that promote or inhibit specific miRNAs should be completely recognized and characterized. To establish the dose and the length of treatment, it will also be necessary to study the duration of gene silencing.

Efforts should also be made to develop targeted delivery systems. Delivery systems should be able to target specific cancer cells. Targeted therapies may reduce therapeutic doses and prevent possible toxic effects in other cells. For this reason, novel findings concerning cancer cells and the tumour microenvironment will play crucial roles in the emergence of new targets and targeting moieties for nanosystem functionalization. In addition to targeted delivery systems, new non-invasive imaging techniques should be developed. Monitorization of the *in vivo* distribution of the therapeutic nanocarrier may help optimize and predict treatment efficacy.

Although the field has come a long way since the discovery of RNAi over a decade ago, miRNA therapy is still in its infancy. Cancer is a heterogeneous disease in which many pathways are simultaneously altered. Thus, the delivery of multiple miRNAs at the same time may be a more effective way to fight cancer in the near future. In addition to its potential as single therapy, the combination of miRNAs with other therapeutic approaches is likely to focus researchers' attention as a means to address the heterogeneity of cancer.

Table 1. Recent miRNA nanocarriers that have been tested in vivo

Delivery system	Targeted miRNA	Therapeutic strategy	Cancer type	Route	Ref.
Inorganic systems					
Anti-GD_2-conjugated silica nanoparticles	miR-34a	Replacement	Neuroblastoma	Intravenous	(37)
Polymer-based systems					
PEI polyplexes	miR-145 and miR-33a	Replacement	Colon carcinoma	Intravenous and intratumoural	(44)
Polyarginine-modified PEI polyplexes	miR-145	Replacement	Prostate cancer	Intravenous	(46)
Polyurethane-short branch PEI polyplexes	miR-145	Replacement	Lung adenocarcinoma	Intratumoural	(47)
PLGA-PEG nanoparticles	MiR-122	Replacement	Colon carcinoma	Intravenous	(49)
Penetratin-coated PLGA nanoparticles	MiR-155	Inhibition	Lymphoma	Intratumoural	(52)
PAMAM dendrimers embedded in a dextran hydrogel	MiR-205 and miR-221	Replacement and inhibition	Breast cancer	Intratumoural	(56)
PLA-b-PDMAEMA dendrimers	MiR-21	Inhibition	Glioma	Intratumoural	(57)
Methacrylamide/Ethylene glycol dimethacrylate/Acrylamide nanocapsules	MiR-21	Inhibition	Glioma	Intratumoural	(58)
Polypropylene carbonate-PEG micelles	MiR-205	Replacement	Prostate cancer	Intratumoural	(59)
Hyaluronan/Cholanic acid/Zn-dipicolylamine nanoparticles	MiR-34a	Replacement	Colon carcinoma	Intravenous	(60)
Polycaprolactone-PEG nanoparticles	MiR-200c	Replacement	Gastric cancer	Intravenous	(61)
Hyaluronic acid/Chitosan nanoparticles	MiR-34a	Replacement	Breast cancer	Intravenous	(62)
Hyaluronic acid/Protamine sulphate nanocapsules	MiR-34a	Replacement	Breast cancer	Intravenous	(64)

Aptamer-conjugated atelocollagen nanoparticles	MiR-15a and miR-16-1	Replacement	Breast cancer	Intravenous	(65)
Lipid-based nanosystems					
DOTMA/Cholesterol/TPGS lipoplexes	MiR-29b	Replacement	Non-small cell lung cancer	Intravenous	(69)
DOTAP/SPC/DSPE-PEG lipoplexes	MiR-10b	Inhibition	Breast cancer	Intravenous	(71)
DDAB nanoparticles	MiR-34a	Replacement	Melanoma lung metastasis	Intravenous	(74, 75)
MOCHOL/CHEMS/DOPE/POPC lipoplexes	MiR-34a	Replacement	Liver cancer	Intravenous	(77)
Chlorotoxin-targeted stable nucleic acid lipid particles	MiR-21	Inhibition	Glioma	Intravenous	(79)
DOPC lipoplexes	MiR-206	Replacement	Ovarian cancer	Intraperitoneal	(80)
PEG 5000-D-α-tocopherol-diethylenetriamine micelles	Let-7b	Replacement	Non-small cell lung cancer	Intravenous	(81)
GC4-ScFv-modified DOTAP liposomes-polycation-hialuronic acid nanoparticles	MiR-34a	Replacement	Melanoma lung metastasis	Intravenous	(82)
Hyaluronic-DPPC-PLGA-Pluronic F127 nanoparticles	MiR-34a	Replacement	Prostate cancer	Intravenous	(83)

This table provides examples of some of the most recent miRNA delivery systems that have demonstrated therapeutic efficacy in animal models of cancer. Anti-GD2: disialoganglioside GD2-antibody; PEI: polyethylenimine; PLGA: poly(lactic-co-glycolic acid); PEG: polyethylene glycol; PMAM: poly(amidoamine); PLA-b-PDMAEMA: polylactic acid polymethylaminoethyl methacrylate copolymer; DOTMA: 1,2-di-O-octadecenyl-3-trimethylammonium propane; TPGS: D-α-Tocopheryl polyethylene glycol succinate; DOTAP: 1,2-dioleoyloxy-3-trimethylammonium propane; SPC: soybean phosphatidylcholine; DSPE-PEG: 1,2-Distearoyl-sn-glycero-3-phosphoethanolamine; DDAB: dimethyldioctadecylammonium bromide; MOCHOL: cholesteryl-4-([2-(4-morpholinyl)ethyl]amino)-4-oxoburanoate; CHEMS: cholesteryl hemisuccinate; DOPE: 1,2-dioleoyl-snglycero-3-phosphoethanolamine; POPC: 1-palmitoyl-2-oleoyl-snglycero-3-phosphocholine; DOPC: 1,2-Dioleoyl-sn-glycero-3-phosphocholine; GC4-scFv: monoclonal antibody GC4 single-chain variable fragment; DPPC: dipalmitoyl phosphatidylcoline.

Table 2. Functions of miRNAs that have been associated to nanocarriers for cancer treatment

MiRNA	Functions	References
MiR-205	Downregulated in several types of cancers such as prostate cancer, lung cancer, breast cancer, pancreatic cancer and melanoma. Role in cell proliferation, migration and metastasis.	(34, 56, 59)
MiR-20a	Oncogenic role in prostate cancer carcinogenesis by reducing the expression of transcription factors E2F1 and the phosphatase and tensin homolog (PTEN).	(34)
MiR-31	Downregulated in ovarian and other cancer cell lines. Role in cell proliferation and apoptosis.	(35)
MiR-1323	Cell proliferation enhancer in neuroblastoma cell lines.	(35)
MiR-145	Downregulated in several cancer types, including colon, prostate, breast and hepatocellular carcinoma. Pro-apoptotic and antiproliferative role, inhibiting invasion and migration in cancer cells.	(36, 44-47, 63)
MiR-34a	Downregulated in a variety of cancers, including breast cancers, non-small-cell lung carcinoma, osteosarcoma, hepatocellular carcinoma, and colon cancer. Its expression induces cell apoptosis and inhibits cell proliferation, migration and cancer stem cell development. Anti-angiogenic effect and implication in chemo-drug sensitivity.	(37, 43, 60, 62, 64, 74, 75, 77, 82, 83)
MiR-221 and miR-222	Upregulated in several tumour forms, especially in gliomas. Proliferative role.	(38, 56, 73)
Let-7 miRNAs family	Downregulated in cancers such as lung cancer, colon cancer, brain cancer, prostate cancer, gastric cancer and melanoma. Tumour suppressors implicated in cell proliferation.	(39, 41, 70, 81)
MiR-99a and miR-486	Overexpressed in CMK leukemia cells.	(40)
MiR-21	Overexpressed in cancers such as glioma or breast cancer cells. Proliferative, antiapoptotic and invasive role.	(40, 48, 50, 51, 54, 57, 58, 66, 73, 79)
MiR-10b	Overexpression promotes early stage metastasis in breast cancer. Inhibition reduces metastatic spread to the lungs of human breast cancer.	(42, 51, 71, 73)
MiR-33a	Antiproliferative role inhibiting cell-cycle progression in various cancers including lymphoma and colon carcinoma.	(44)

MiR-122	Key role in liver function, down-regulation results in inflammation, fibrosis and cancer. Overexpression induces apoptosis, cell cycle arrest, inhibition of tumourigenesis and angiogenesis, and re-sensitizes various types of cancers to chemotherapy.	(33, 49, 67)
MiR-155	Overexpressed in several lymphomas. Inducer of myeloproliferative pathology in hematopoietic cells.	(52, 53)
MiR-542-3p	Downregulated in a variety of cancers. Role in cell proliferation, cell cycle arrest, apoptosis and tumour angiogenesis.	(55)
MiR-221	Upregulated in various types of cancer, including breast cancers. Role in cell proliferation and drug resistance mechanisms.	(56, 73)
MiR-200c	Can reverse epitelial to mesenchymal transition (EMT) program by depriving epithelial cells of the invasive ability and increasing E-cadherin expression. It can improve sensitivity of cancer cells to microtubule-targeting chemotherapeutic drugs.	(61)
MiR-15a and miR-16-1	Tumour suppressor genes, promoting survival, proliferation and invasion.	(65)
MiR-133b	Downregulated in lung cancer. It reduces the expression of MCL-1 protein, which reduces the sensitivity of lung cancer cells to apoptotic stimuli.	(68)
MiR-29b	Downregulated in several types of cancer, such as leukemia, melanoma, liver, colon, cervical, and lung cancer. Role in cell proliferation, differentiation, apoptosis, migration, and invasion.	(69)
MiR-506	Down-regulated in different types of cancer. Inhibitor of the epithelial-to-mesenchymal transition (EMT), associated with chemoresistance. Role in cell proliferation and therapy response.	(80)

References

1. Hanahan D, Weinberg R. Hallmarks of Cancer: The Next Generation. Cell. 2011 3/4;144(5):646-74.

2. World Health Organization [Internet].; 2016. Available from: http://www.who.int/en/.

3. Wicki A, Witzigmann D, Balasubramanian V, Huwyler J. Nanomedicine in cancer therapy: challenges, opportunities, and clinical applications. J Control Release. 2015 Feb 28;200:138-57.

4. Perez-Herrero E, Fernandez-Medarde A. Advanced targeted therapies in cancer: Drug nanocarriers, the future of chemotherapy. Eur J Pharm Biopharm. 2015 Jun;93:52-79.

5. Chabner BA, Roberts TG,Jr. Timeline: Chemotherapy and the war on cancer. Nat Rev Cancer. 2005 Jan;5(1):65-72.

6. Xu X, Ho W, Zhang X, Bertrand N, Farokhzad O. Cancer nanomedicine: from targeted delivery to combination therapy. Trends Mol Med. 2015 Apr;21(4):223-32.

7. Dawidczyk CM, Russell LM, Searson PC. Nanomedicines for cancer therapy: state-of-the-art and limitations to pre-clinical studies that hinder future developments. Front Chem. 2014 Aug 25;2:69.

8. Olson KE, Keene KM, Blair CD. Interfering RNAs. In: Regenmortel BWJMHVV, editor. Encyclopedia of Virology (Third Edition). Oxford: Academic Press; 2008. p. 148-55.

9. Fire A, Xu S, Montgomery MK, Kostas SA, Driver SE, Mello CC. Potent and specific genetic interference by double-stranded RNA in Caenorhabditis elegans. Nature. 1998 Feb 19;391(6669):806-11.

10. Wang Z, Rao DD, Senzer N, Nemunaitis J. RNA interference and cancer therapy. Pharm Res. 2011 Dec;28(12):2983-95.

11. Davidson BL, McCray PB,Jr. Current prospects for RNA interference-based therapies. Nat Rev Genet. 2011 May;12(5):329-40.

12. Rao DD, Vorhies JS, Senzer N, Nemunaitis J. siRNA vs. shRNA: Similarities and differences. Adv Drug Deliv Rev. 2009 7/25;61(9):746-59.

13. Deng Y, Wang CC, Choy KW, Du Q, Chen J, Wang Q, et al. Therapeutic potentials of gene silencing by RNA interference: principles, challenges, and new strategies. Gene. 2014 Apr 1;538(2):217-27.

14. Wang D, Gao G. State-of-the-art human gene therapy: part II. Gene therapy strategies and clinical applications. Discov Med. 2014 Sep;18(98):151-61.

15. Fellmann C, Lowe SW. Stable RNA interference rules for silencing. Nat Cell Biol. 2014 Jan;16(1):10-8.

16. Boudreau RL, Martins I, Davidson BL. Artificial microRNAs as siRNA shuttles: improved safety as compared to shRNAs in vitro and in vivo. Mol Ther. 2009 Jan;17(1):169-75.

17. Lam JK, Chow MY, Zhang Y, Leung SW. siRNA Versus miRNA as Therapeutics for Gene Silencing. Mol Ther Nucleic Acids. 2015 Sep 15;4:e252.

18. Garzon R, Marcucci G, Croce CM. Targeting microRNAs in cancer: rationale, strategies and challenges. Nat Rev Drug Discov. 2010 Oct;9(10):775-89.

19. Lu J, Getz G, Miska EA, Alvarez-Saavedra E, Lamb J, Peck D, et al. MicroRNA expression profiles classify human cancers. Nature. 2005 06/09;435(7043):834-8.

20. Volinia S, Calin GA, Liu CG, Ambs S, Cimmino A, Petrocca F, et al. A microRNA expression signature of human solid tumors defines cancer gene targets. Proc Natl Acad Sci U S A. 2006 Feb 14;103(7):2257-61.

21. Bader AG, Brown D, Stoudemire J, Lammers P. Developing therapeutic microRNAs for cancer. Gene Ther. 2011 Dec;18(12):1121-6.

22. van Rooij E, Kauppinen S. Development of microRNA therapeutics is coming of age. EMBO Mol Med. 2014 Jun 16;6(7):851-64.

23. Chen Y, Gao DY, Huang L. In vivo delivery of miRNAs for cancer therapy: challenges and strategies. Adv Drug Deliv Rev. 2015 Jan;81:128-41.

24. Singh MS, Peer D. RNA nanomedicines: the next generation drugs? Curr Opin Biotechnol. 2016 Jan 8;39:28-34.

25. Whitehead KA, Langer R, Anderson DG. Knocking down barriers: advances in siRNA delivery. Nat Rev Drug Discov. 2009 Feb;8(2):129-38.

26. Lennox KA, Behlke MA. Chemical modification and design of anti-miRNA oligonucleotides. Gene Ther. 2011 Dec;18(12):1111-20.

27. Davis S, Lollo B, Freier S, Esau C. Improved targeting of miRNA with antisense oligonucleotides. Nucleic Acids Res. 2006 May 11;34(8):2294-304.

28. Prakash TP, Kawasaki AM, Wancewicz EV, Shen L, Monia BP, Ross BS, et al. Comparing in vitro and in vivo activity of 2'-O-[2-(methylamino)-2-oxoethyl]- and 2'-O-methoxyethyl-modified antisense oligonucleotides. J Med Chem. 2008 May 8;51(9):2766-76.

29. Zhang Y, Wang Z, Gemeinhart RA. Progress in microRNA delivery. J Control Release. 2013 Dec 28;172(3):962-74.

30. Xiang D, Shigdar S, Qiao G, Zhou SF, Li Y, Wei MQ, et al. Aptamer-mediated cancer gene therapy. Curr Gene Ther. 2015;15(2):109-19.

31. Rohde JH, Weigand JE, Suess B, Dimmeler S. A Universal Aptamer Chimera for the Delivery of Functional microRNA-126. Nucleic Acid Ther. 2015 Jun;25(3):141-51.

32. Wagner E. Tumor-targeted Delivery of Anti-microRNA for Cancer Therapy: pHLIP is Key. Angew Chem Int Ed Engl. 2015 May 11;54(20):5824-6.

33. Fabani MM, Gait MJ. miR-122 targeting with LNA/2'-O-methyl oligonucleotide mixmers, peptide nucleic acids (PNA), and PNA-peptide conjugates. RNA. 2008 Feb;14(2):336-46.

34. Hao L, Patel PC, Alhasan AH, Giljohann DA, Mirkin CA. Nucleic acid-gold nanoparticle conjugates as mimics of microRNA. Small. 2011 Nov 18;7(22):3158-62.

35. Ghosh R, Singh LC, Shohet JM, Gunaratne PH. A gold nanoparticle platform for the delivery of functional microRNAs into cancer cells. Biomaterials. 2013 1;34(3):807-16.

36. Ekin A, Karatas OF, Culha M, Ozen M. Designing a gold nanoparticle-based nanocarrier for microRNA transfection into the prostate and breast cancer cells. J Gene Med. 2014 Nov-Dec;16(11-12):331-5.

37. Tivnan A, Orr WS, Gubala V, Nooney R, Williams DE, McDonagh C, et al. Inhibition of neuroblastoma tumor growth by targeted delivery of microRNA-34a using anti-disialoganglioside GD2 coated nanoparticles. PLoS One. 2012;7(5):e38129.

38. Bertucci A, Prasetyanto EA, Septiadi D, Manicardi A, Brognara E, Gambari R, et al. Combined Delivery of Temozolomide and Anti-miR221 PNA Using Mesoporous Silica Nanoparticles Induces Apoptosis in Resistant Glioma Cells. Small. 2015 Nov;11(42):5687-95.

39. Yin PT, Shah BP, Lee KB. Combined magnetic nanoparticle-based microRNA and hyperthermia therapy to enhance apoptosis in brain cancer cells. Small. 2014 Oct 29;10(20):4106-12.

40. Lellouche E, Israel LL, Bechor M, Attal S, Kurlander E, Asher VA, et al. MagRET Nanoparticles: An Iron Oxide Nanocomposite Platform for Gene Silencing from MicroRNAs to Long Noncoding RNAs. Bioconjug Chem. 2015 Aug 19;26(8):1692-701.

41. Yang HW, Huang CY, Lin CW, Liu HL, Huang CW, Liao SS, et al. Gadolinium-functionalized nanographene oxide for combined drug and microRNA delivery and magnetic resonance imaging. Biomaterials. 2014 Aug;35(24):6534-42.

42. Yoo SS, Razzak R, Bedard E, Guo L, Shaw AR, Moore RB, et al. Layered gadolinium-based nanoparticle as a novel delivery platform for microRNA therapeutics. Nanotechnology. 2014 Oct 24;25(42):425102,4484/25/42/425102. Epub 2014 Oct 3.

43. Jung H, Kim SA, Yang YG, Yoo H, Lim SJ, Mok H. Long chain microRNA conjugates in calcium phosphate nanoparticles for efficient formulation and delivery. Arch Pharm Res. 2015;38(5):705-15.

44. Ibrahim AF, Weirauch U, Thomas M, Grunweller A, Hartmann RK, Aigner A. MicroRNA replacement therapy for miR-145 and miR-33a is efficacious in a model of colon carcinoma. Cancer Res. 2011 Aug 1;71(15):5214-24.

45. Che HL, Lee HJ, Uto K, Ebara M, Kim WJ, Aoyagi T, et al. Simultaneous Drug and Gene Delivery from the Biodegradable Poly(epsilon-caprolactone) Nanofibers for the Treatment of Liver Cancer. J Nanosci Nanotechnol. 2015 Oct;15(10):7971-5.

46. Zhang T, Xue X, He D, Hsieh JT. A prostate cancer-targeted polyarginine-disulfide linked PEI nanocarrier for delivery of microRNA. Cancer Lett. 2015 Sep 1;365(2):156-65.

47. Chiou GY, Cherng JY, Hsu HS, Wang ML, Tsai CM, Lu KH, et al. Cationic polyurethanes-short branch PEI-mediated delivery of Mir145 inhibited epithelial-mesenchymal transdifferentiation and cancer stem-like properties and in lung adenocarcinoma. J Control Release. 2012 Apr 30;159(2):240-50.

48. Gao S, Tian H, Guo Y, Li Y, Guo Z, Zhu X, et al. miRNA oligonucleotide and sponge for miRNA-21 inhibition mediated by PEI-PLL in breast cancer therapy. Acta Biomater. 2015 Oct;25:184-93.

49. Wang TY, Choe JW, Pu K, Devulapally R, Bachawal S, Machtaler S, et al. Ultrasound-guided delivery of microRNA loaded nanoparticles into cancer. J Control Release. 2015 Apr 10;203:99-108.

50. Devulapally R, Sekar TV, Paulmurugan R. Formulation of Anti-miR-21 and 4-Hydroxytamoxifen Co-loaded Biodegradable Polymer Nanoparticles and Their Antiproliferative Effect on Breast Cancer Cells. Mol Pharm. 2015 Jun 1;12(6):2080-92.

51. Devulapally R, Sekar NM, Sekar TV, Foygel K, Massoud TF, Willmann JK, et al. Polymer nanoparticles mediated codelivery of antimiR-10b and antimiR-21 for achieving triple negative breast cancer therapy. ACS Nano. 2015 Mar 24;9(3):2290-302.

52. Babar IA, Cheng CJ, Booth CJ, Liang X, Weidhaas JB, Saltzman WM, et al. Nanoparticle-based therapy in an in vivo microRNA-155 (miR-155)-dependent mouse model of lymphoma. Proc Natl Acad Sci U S A. 2012 Jun 26;109(26):E1695-704.

53. Cheng CJ, Saltzman WM. Polymer nanoparticle-mediated delivery of microRNA inhibition and alternative splicing. Mol Pharm. 2012 May 7;9(5):1481-8.

54. Ananta JS, Paulmurugan R, Massoud TF. Nanoparticle-Delivered Antisense MicroRNA-21 Enhances the Effects of Temozolomide on Glioblastoma Cells. Mol Pharm. 2015 Dec 7;12(12):4509-17.

55. Wang S, Zhang J, Wang Y, Chen M. Hyaluronic acid-coated PEI-PLGA nanoparticles mediated co-delivery of doxorubicin and miR-542-3p for triple negative breast cancer therapy. Nanomedicine. 2015 Dec 19;12:411-20.

56. Conde J, Oliva N, Atilano M, Song HS, Artzi N. Self-assembled RNA-triple-helix hydrogel scaffold for microRNA modulation in the tumour microenvironment. Nat Mater. 2015 Dec 7;15:353-63.

57. Qian X, Long L, Shi Z, Liu C, Qiu M, Sheng J, et al. Star-branched amphiphilic PLA-b-PDMAEMA copolymers for co-delivery of miR-21 inhibitor and doxorubicin to treat glioma. Biomaterials. 2014 Feb;35(7):2322-35.

58. Liu C, Wen J, Meng Y, Zhang K, Zhu J, Ren Y, et al. Efficient delivery of therapeutic miRNA nanocapsules for tumor suppression. Adv Mater. 2015 Jan 14;27(2):292-7.

59. Mittal A, Chitkara D, Behrman SW, Mahato RI. Efficacy of gemcitabine conjugated and miRNA-205 complexed micelles for treatment of advanced pancreatic cancer. Biomaterials. 2014 Aug;35(25):7077-87.

60. Choi KY, Silvestre OF, Huang X, Min KH, Howard GP, Hida N, et al. Versatile RNA interference nanoplatform for systemic delivery of RNAs. ACS Nano. 2014 May 27;8(5):4559-70.

61. Liu Q, Li RT, Qian HQ, Wei J, Xie L, Shen J, et al. Targeted delivery of miR-200c/DOC to inhibit cancer stem cells and cancer cells by the gelatinases-stimuli nanoparticles. Biomaterials. 2013 Sep;34(29):7191-203.

62. Deng X, Cao M, Zhang J, Hu K, Yin Z, Zhou Z, et al. Hyaluronic acid-chitosan nanoparticles for co-delivery of MiR-34a and doxorubicin in therapy against triple negative breast cancer. Biomaterials. 2014 May;35(14):4333-44.

63. Santos-Carballal B, Aaldering LJ, Ritzefeld M, Pereira S, Sewald N, Moerschbacher BM, et al. Physicochemical and biological characterization of chitosan-microRNA nanocomplexes for gene delivery to MCF-7 breast cancer cells. Sci Rep. 2015 Sep 1;5:13567.

64. Wang S, Cao M, Deng X, Xiao X, Yin Z, Hu Q, et al. Degradable hyaluronic acid/protamine sulfate interpolyelectrolyte complexes as miRNA-delivery nanocapsules for triple-negative breast cancer therapy. Adv Healthc Mater. 2015 Jan 28;4(2):281-90.

65. Hao Z, Fan W, Hao J, Wu X, Zeng GQ, Zhang LJ, et al. Efficient delivery of micro RNA to bone-metastatic prostate tumors by using aptamer-conjugated atelocollagen in vitro and in vivo. Drug Deliv. 2015 Jul 17:1-8.

66. Song H, Oh B, Choi M, Oh J, Lee M. Delivery of anti-microRNA-21 antisense-oligodeoxynucleotide using amphiphilic peptides for glioblastoma gene therapy. J Drug Target. 2015 May;23(4):360-70.

67. Wang X, Yu B, Ren W, Mo X, Zhou C, He H, et al. Enhanced hepatic delivery of siRNA and microRNA using oleic acid based lipid nanoparticle formulations. J Controlled Release. 2013 12/28;172(3):690-8.

68. Wu Y, Crawford M, Yu B, Mao Y, Nana-Sinkam SP, Lee LJ. MicroRNA delivery by cationic lipoplexes for lung cancer therapy. Mol Pharm. 2011 Aug 1;8(4):1381-9.

69. Wu Y, Crawford M, Mao Y, Lee RJ, Davis IC, Elton TS, et al. Therapeutic Delivery of MicroRNA-29b by Cationic Lipoplexes for Lung Cancer. Mol Ther Nucleic Acids. 2013 Apr 16;2:e84.

70. Lee HY, Mohammed KA, Kaye F, Sharma P, Moudgil BM, Clapp WL, et al. Targeted delivery of let-7a microRNA encapsulated ephrin-A1 conjugated liposomal nanoparticles inhibit tumor growth in lung cancer. Int J Nanomedicine. 2013;8:4481-94.

71. Zhang Q, Ran R, Zhang L, Liu Y, Mei L, Zhang Z, et al. Simultaneous delivery of therapeutic antagomirs with paclitaxel for the management of metastatic tumors by a pH-responsive anti-microbial peptide-mediated liposomal delivery system. J Control Release. 2015 Jan 10;197:208-18.

72. Montis C, Sostegni S, Milani S, Baglioni P, Berti D. Biocompatible cationic lipids for the formulation of liposomal DNA vectors. Soft Matter. 2014 Jun 28;10(24):4287-97.

73. Passadouro M, Pedroso de Lima MC, Faneca H. MicroRNA modulation combined with sunitinib as a novel therapeutic strategy for pancreatic cancer. Int J Nanomedicine. 2014 Jul 3;9:3203-17.

74. Shi S, Han L, Gong T, Zhang Z, Sun X. Systemic delivery of microRNA-34a for cancer stem cell therapy. Angew Chem Int Ed Engl. 2013 Apr 2;52(14):3901-5.

75. Shi S, Han L, Deng L, Zhang Y, Shen H, Gong T, et al. Dual drugs (microRNA-34a and paclitaxel)-loaded functional solid lipid nanoparticles for synergistic cancer cell suppression. J Control Release. 2014 Nov 28;194:228-37.

76. Leung AK, Tam YY, Cullis PR. Lipid nanoparticles for short interfering RNA delivery. Adv Genet. 2014;88:71-110.

77. Daige CL, Wiggins JF, Priddy L, Nelligan-Davis T, Zhao J, Brown D. Systemic delivery of a miR34a mimic as a potential therapeutic for liver cancer. Mol Cancer Ther. 2014 Oct;13(10):2352-60.

78. Tolcher AW, Rodrigueza WV, Rasco DW, Patnaik A, Papadopoulos KP, Amaya A, et al. A phase 1 study of the BCL2-targeted deoxyribonucleic acid inhibitor (DNAi) PNT2258 in patients with advanced solid tumors. Cancer Chemother Pharmacol. 2014 Feb;73(2):363-71.

79. Costa PM, Cardoso AL, Custodia C, Cunha P, Pereira de Almeida L, Pedroso de Lima MC. MiRNA-21 silencing mediated by tumor-targeted nanoparticles combined with sunitinib: A new multimodal gene therapy approach for glioblastoma. J Control Release. 2015 Jun 10;207:31-9.

80. Liu G, Yang D, Rupaimoole R, Pecot CV, Sun Y, Mangala LS, et al. Augmentation of response to chemotherapy by microRNA-506 through regulation of RAD51 in serous ovarian cancers. J Natl Cancer Inst. 2015 May 20;107(7):10.1093/jnci/djv108. Print 2015 Jul.

81. Dai X, Fan W, Wang Y, Huang L, Jiang Y, Shi L, et al. Combined Delivery of Let-7b MicroRNA and Paclitaxel via Biodegradable Nanoassemblies for the Treatment of KRAS Mutant Cancer. Mol Pharm. 2015 Dec 23;13:520-33.

82. Chen Y, Zhu X, Zhang X, Liu B, Huang L. Nanoparticles modified with tumor-targeting scFv deliver siRNA and miRNA for cancer therapy. Mol Ther. 2010 Sep;18(9):1650-6.

83. Wang H, Agarwal P, Zhao S, Yu J, Lu X, He X. A Near-Infrared Laser-Activated "Nanobomb" for Breaking the Barriers to MicroRNA Delivery. Adv Mater. 2016 Jan;28(2):347-55.

84. Bouchie A. First microRNA mimic enters clinic. Nat Biotechnol. 2013 Jul;31(7):577.

85. MacDiarmid JA, Brahmbhatt H. Minicells: versatile vectors for targeted drug or si/shRNA cancer therapy. Curr Opin Biotechnol. 2011 Dec;22(6):909-16.

86. Conde J, Artzi N. Are RNAi and miRNA therapeutics truly dead? Trends Biotechnol. 2015 Mar;33(3):141-4.

Objectives

USC
UNIVERSIDADE
DE SANTIAGO
DE COMPOSTELA

Objectives

The main objective of this work has been the design of polysaccharide functionalised span nanoparticles as gene delivery systems and, more specifically, the design of nanoparticles based on sorbitan monooleate functionalised with natural polymers as non-viral microRNA vectors to treat colorectal liver metastasis.

This main objective can be articulated into the following specific objectives:

1. Functionalisation of span nanoparticles with different natural polymers to provide specific targeting properties to liver sinusoidal endothelial cells.

2. Characterisation of the developed nanoparticles in terms of physicochemical properties and stability.

3. Evaluation of the *in vitro* ability of the developed nanoparticles to act as non-viral gene delivery systems able to associate, protect from degradation and effectively deliver into cells a model plasmid DNA.

4. Evaluation of the *in vitro* and *in vivo* toxicity of the developed nanoparticles and their *in vivo* biodistribution.

5. Evaluation of the potential of the most suitable nanosystem in the treatment of colorectal cancer metastasis to the liver in an animal model, using microRNA-20a as a therapeutic molecule.

USC
UNIVERSIDADE
DE SANTIAGO
DE COMPOSTELA

Chapter I

Xanthan gum-functionalised span nanoparticles for gene targeting to endothelial cells

USC
UNIVERSIDADE
DE SANTIAGO
DE COMPOSTELA

Abstract

Endothelial cells play a critical role in many physiological processes; therefore, endothelium deregulation is involved in numerous diseases. There is increasing evidence that the future of many treatments for pathologies depends on the development of endothelium-targeting systems. The purpose of this work was to incorporate the natural polysaccharide xanthan gum (XG) into our previously developed sorbitan monooleate nanoparticles to provide them with a hydrophilic and negatively charged surface shell with stabilising properties and an inherent ability to target endothelial cells. Enhanced Green Fluorescent Protein plasmid (pEGFP) was incorporated into the nanosystem, and the DNase I protection ability of this system was confirmed. XG stabilisation of the system both in suspension and as a lyophilised product was also confirmed at short- and long-term time scales. XG-functionalised nanoparticles were successfully tested in Human Umbilical Vein Endothelial Cells (HUVECs) to characterise nanoparticle cytotoxicity and transfection capacity *in vitro* as a preliminary step to study them further *in vivo*. Then, nanoparticle biocompatibility and safety *in vivo* were confirmed. Finally, biodistribution studies after EGFP-XG nanoparticle systemic administration to mice evidenced GFP expression in the vascular endothelium of lung, liver and kidney, thus confirming the potential of xanthan gum-functionalised span nanoparticles for gene targeting to endothelial cells.

1. Introduction

Xanthan gum (XG) is an extracellular polysaccharide produced by the bacteria X*anthomonas campestris* (1). It is composed of (1, 4)-β-D- glucan with trisaccharide side chains composed of mannose-(1, 4)- β-glucuronic acid-(1, 2)- β-mannose attached to alternating glucose residues in the backbone. It is a non-toxic and biodegradable polymer of natural origin that is widely used in the food, cosmetic and pharmaceutical industries and has been approved by FDA for its application in food and pharmaceutical industry since 1968 (2). It is used as a functionalising, thickening and suspending agent and as an emulsion stabilizer. Its use has been described in the preparation and stabilisation of inorganic nanoparticles (1, 3, 4) and the formation of polyelectrolytes complexes, mainly with chitosan, to form hydrogels, hydrogels beads, cryogels and tablets (2, 5-7). In addition, it has shown antitumour effects by inducing IL-12 and TNF α production *in vitro* and increasing Natural Killer and CD8 T cells activity *in vivo* due to its ability to stimulate Toll-like receptors (TLRs) (8).

Endothelial cells are the inner cellular lining of blood vessels and play a critical role in many physiological processes, such as the trafficking of blood cells between blood and tissues, maintenance of blood fluidity, blood vessel tone, permeability, angiogenesis and immunity. Since these functions are all related to physiology, endothelium deregulation promotes numerous diseases (9, 10). There is increasing evidence that the future of many pathology treatments, including cardiovascular diseases, stroke, chronic kidney failure, diabetes, infectious diseases and cancer, depends on the development of endothelium targeting systems (10). Although it is also involved in almost all disease states, there is still a huge bench-to-bedside gap in endothelial biomedicine, in part due to the non-accessible nature of the endothelium and its heterogeneity. Endothelial cells are heterogeneous and vary in their function, morphology and gene expression among different organs or even among different regions of the same organ (11, 12). Advances in the proteomic profiling of endothelial cells has allowed the targeting of biologically active molecules to specific vascular beds, taking advantage of endothelium phenotype heterogeneity (13). This heterogeneity is regulated partially by the extracellular matrix because endothelial cells are exposed to a huge variety of tissue microenviroments and by site-specific properties that are epigenetically fixed and, thus, mitotically stable and impervious to changes in the extracellular environment. Thus, expanding our knowledge of endothelial function and physiology may allow the development of new

therapeutic approaches for many human life-threatening diseases. For instance, it is widely accepted that endothelial cells show abnormal properties in tumour environments (13). High-throughput expression profiling has shown altered gene and protein expression in tumour endothelia. Therefore, targeting endothelial cells rather than tumour cells may be advantageous and easy to achieve because these cells are more accessible to systemically delivered agents, are less likely to develop drug resistance and can amplify the inhibitory effect to numerous tumour cells. There are some examples in the literature of nanosystems targeting endothelial cells in tumour environments as an alternative cancer therapy approach (9, 14) or as treatment for other vascular-related diseases (15-17).

The purpose of this work was to incorporate XG into our previously developed sorbitan monooleate nanoparticles (NPs) to take advantage of the polysaccharide composition to target liver sinusoidal endothelial cells (LSECs). Given the presence of mannose residues in XG composition, we initially theorized that these residues could be used to target mannose receptors, which are known to be overexpressed in LSECs. Mannose receptor acts as a scavenger receptor, recognizing and facilitating the uptake of diverse glycoconjugate ligands (18). Thus, we here describe the design and characterisation of XG-functionalised nanoparticles with endothelium targeting purposes in terms of their physicochemical characteristics, stability properties and toxicity *in vitro* and *in vivo*. For this purpose, Enhanced Green Fluorescent Protein plasmid (pEGFP) was associated with nanoparticles to evaluate the system potential to protect, stabilise and deliver DNA both *in vitro*, using Human Umbilical Vein Endothelial Cells (HUVEC), and *in vivo* and to track the system biodistribution after systemic administration to mice.

2. Materials and methods

2.1. Materials

Sorbitan monooleate (Span® 80) (SP), oleylamine (OA) (purity ≥70%), xanthan gum, trehalose, and sodium dodecyl sulfate (SDS) were purchased from Sigma (Spain). The pEGFP-C3 plasmid was obtained from Elim Biopharmaceutics (United States). SYBR Safe DNA Gel Stain, SYBR® Gold post-electrophoresis and agarose were provided by Life Technologies (Spain). DNase I, Lipofectamine 2000, Opti-MEM I Reduced Serum Media and normal goat serum (10%) were acquired from ThermoFisher (Spain). Endothelial Cell Medium (ECM),

Foetal Goat Serum (FGS), Endothelial Cell Growth Supplement (ECGS) and Penicillin/Streptomycin (P/S) were acquired from ScienCell (United States). XTT viability reagent was provided by Roche (Spain). An aspartate aminotransferase colorimetric kit was purchased from Randox (Spain). DAPI stain, ki-67 and GFP antibodies were obtained from Abcam (United Kingdom).

2.2. Preparation and characterisation of XG nanoparticles

For construction of nanoparticles, a solution of sorbitan monooleate (Span 80, SP) and oleylamine (OA) was prepared in ethanol at a concentration of 6.6 and 0.33 mg/ml, respectively. This organic phase was added under magnetic stirring to an aqueous phase containing xanthan gum (XG) at a concentration of 0.26 mg/ml at a volume ratio of 1:2 of ethanol:water. A stock solution of XG at 2 mg/ml was previously prepared and moist heat sterilized. Ethanol was removed under reduced pressure on a rotary evaporator. For encapsulation of Enhanced Green Fluorescent Protein plasmid (pEGFP), the plasmid was incorporated in the aqueous phase. The final formulations obtained were 200 μg/ml pEGFP-loaded NPs.

The mean particle size and size distribution of the nanoparticles was determined using photon correlation spectroscopy (PCS). Samples were suitably diluted in Milli-Q water. Each analysis was performed at 25°C, with an angle of detection of 173°. The zeta potential of the nanoparticles was determined using laser scattering anemometry (LDA). The samples were suitably diluted in a millimolar KCl solution. PCS and the LDA analysis were performed with a Zetasizer® 3000HS (Malvern Instruments, UK).

The morphology of the nanoparticles was examined with transmission electron microscopy (CM 12 Philips, Eindhoven, The Netherlands) after staining with 2% w/v phosphotungstic acid solution. For this purpose, samples were placed on copper grids (400 mesh) coated with a Formvar® film.

2.3. Plasmid association and DNase protection assay

The efficiency of the association of pEGFP with nanoparticles was determined using agarose gel electrophoresis. Gels with 1% of agarose were prepared in TAE (Tris-Acetate-EDTA, 40 mM Tris, 1% acetic acid, 1 mM EDTA). SYBR® Gold Nucleic Acid Gel Stain and SYBR® SAFE DNA Gel Stain as stains and glycerol as a loading substance were used. A potential difference of 100 mV was applied for 30 minutes, and free pEGFP was used as control.

To confirm the ability of XG nanoparticles to protect pEGFP from endonucleases, DNase I protection assay was performed. Nanoparticles containing 5 µg of pEGFP were incubated with 1 unit of DNase I at 37°C for 1 h. A 5-µg sample of naked pEGFP treated with DNase I served as a positive control. The DNase I reaction was terminated by adding 0.5 M EDTA solution. The plasmid was dissociated from the nanoparticles by incubation with a 2% solution of SDSfor 30 minutes at 37°C. DNA integrity was assessed by 1% agarose gel electrophoresis (100 V, 30 min).

2.4. Lyophilisation and stability studies

The nanoparticles were lyophilised using an aqueous solution of cryoprotectant in a 1:1 (v/v) ratio of nanoparticles:cryoprotectant to a final concentration of 15% (w/v) of trehalose, using freeze-drying equipment (VirTis Genesis 25 ES, S.P. Industries, USA). Then, each sample was completely sealed to inhibit humidification, and these lyophilised samples, as well as samples in suspension, were stored at various temperatures (Room Temperature (RT), 4°C and 37°C). After three and twelve months of storage, the lyophilised samples were rehydrated with RNase-free water, and their physicochemical characteristics were analysed.

2.5. Cell culture

In vitro assays were performed using Human Umbilical Vein Endothelial Cells (HUVEC), provided by ScienCell (United States). Cells were maintained in ECM supplemented with 2% FGS, 1% of Penicillin-Streptomycin and 1% of ECGS at 37°C with a 5% CO_2 humidified atmosphere. Cell culture surfaces were pre-treated with a solution of collagen in Phosphate Buffered Saline (PBS) 1:100 (v:v) for 1 hour at 37°C to enhance cell adhesion.

2.6. Cell viability

The effect of nanoparticles on cell viability was evaluated using the XTT assay. HUVECs were seeded at $7.5x10^3$ cells per well in a 96-well plate and incubated overnight. Then, different concentrations of nanoparticles in Opti-MEM reduced serum medium were incubated with the cells. After 2 hours, the treatment was removed, and the cells were incubated with fresh culture medium for 24 hours. Then, XTT reagents were added to the wells and incubated with the cells, following the manufacturer's instructions.

2.7. Proliferation assay

The influence of XG nanoparticles on cell proliferation was evaluated by ki-67 expression. Coverslips were placed in a 24 well-plate. HUVECs were seeded over the coverslips at a density of $4x10^4$ cells per well and incubated overnight. Then, XG nanoparticles were incubated with the cells at a concentration of 384 μg/ml for 3 hours. Cells were fixed with paraformaldehyde 4% and blocked with 10% goat serum. The coverslips were incubated with mouse antihuman Ki-67 primary antibody at a concentration of 10 μg/ml overnight at 4°C. The coverslips were incubated with antimouse secondary antibody and DAPI for 1 hour at room temperature. Finally, the coverslips were mounted on glass slides, and ki-67 expression was detected by fluorescence microscopy. The images were analysed through image processing software ImageJ, and the percentage of ki-67 positive cells was calculated from the images.

2.8. Transfection of HUVECs

For transfection experiments, HUVECs were seeded in a 24-well plate at a density of $4x10^4$ cells per well and incubated overnight. The medium was replaced with Opti-MEM and plasmid-loaded NPs were added at a dose of 1 μg of plasmid per well and incubated with the cells for 2 hours. Lipofectamine 2000 was used as a positive control according to the manufacturer's instructions. After 2 hours, the medium was replaced for serum supplemented medium. The expression of GFP was detected 24 hours post-transfection using an inverted microscope (AxioObserver.Z1 Inverted Microscope, Zeiss, Germany).

2.9. Animals

Balb/c mice (6- to 8-week-old males) were obtained from Charles River Laboratories Spain S.A. (Barcelona, Spain). All procedures were approved by the Ethical Committee for Animal Experimentation (CEEA) of the University of the Basque Country (EHU/UPV) in accordance with institutional, national and international guidelines regarding the protection and care of animals used for scientific purposes (CEBA/237/2012/BADIOLA ETXABURU). Mice were kept in the animal facility of EHU/UPV and had access to standard chow and water ad libitum.

2.10. *In vivo* toxicity and biodistribution

For *in vivo* toxicity and biodistribution studies, 200 μl of pEGFP-loaded nanoparticles in 5% glucose was administered intravenously to mice. For this purpose, 4 mice were used per

condition and a 5% solution of glucose was injected into control mice. After 24 hours, the animals were sacrificed, blood samples were collected by cardiac puncture and major organs were fixed in paraformaldehyde and embedded in paraffin. For biochemical analysis, serum was isolated from blood samples, and the hepatic function was analysed using the aspartate aminotransferase (AST) levels using an AST colorimetric assay. For histopathological examination, sections (4 μm) of liver, spleen, lung and kidney were cut and stained with Haematoxylin and Eosin (H&E). Representative sections were observed and examined using an optical microscope (Nikon Eclipse E-100).

To study the biodistribution of the nanoparticles after systemic administration, GFP expression was evaluated in major organs. For this purpose, sections of paraffin-embedded liver, spleen, lung and kidney were cut into 4-μm slices and deparaffinized and rehydrated through xylenes and graded ethanol solutions to water. After deparaffinisation and rehydration, the sections were placed in a citrate buffer solution for antigen retrieval. The sections were blocked with 10% normal goat serum for 10 minutes at room temperature and incubated overnight at 4°C with mouse antihuman GFP primary antibody at 1:100 dilution. The slides were incubated with antimouse secondary antibody at 1:1000 dilution and DAPI for 1 hour at room temperature. Finally, the slides were sealed with coverslips, and GFP expression was detected by fluorescence microscopy.

2.11. Statistical analysis

All experimental measurements were collected in triplicate. The values are expressed as the mean ± standard deviation (SD). Statistically significant differences between the treatments were evaluated by analysis of variance (ANOVA) and Fisher's least significant difference (LSD) using GraphPad Prism, with alpha < 0.05 as the probability of error.

3. Results

3.1. Nanoparticles characterisation and DNase I protection ability

As shown in Table 1, XG-functionalised NPs showed an average size of 146.8 nm and a negative zeta potential of -48 mV. Incorporating pEGFP into the system did not significantly change the NP size. However, the Z potential increased slightly to -40.6 mV. The nanometric size and population homogeneity of the system was confirmed by TEM images (Figure 2).

These images show NP morphology characterised by a central core and an external shell. In addition, the efficacy of plasmid association by the NPs was corroborated by agarose gel electrophoresis (Figure 3A) because no free DNA band was observed. Moreover, XG nanoparticles successfully protected pEGFP from DNase I degradation, as shown in Figure 3B, as the pEGFP band appears intact after incubation of XG-pEGFP with DNase I and subsequent plasmid release with SDS.

Table 1. Size and Z potential of blank and pEGFP-loaded nanoparticles.

Formulation	Size (nm)	PdI	ζ Potential (mV)
SP-OA-XG	146.8 ± 7.4	0,150 ± 0.036	-48.0 ± 1.5
SP-OA-XG (200 µg/ml pEGFP)	153.5 ± 17.8	0.102 ± 0.036	-40.6 ± 4.6

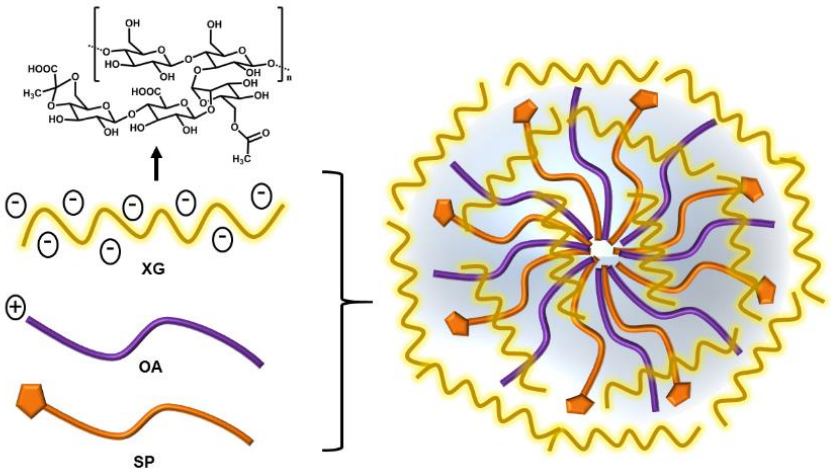

Figure 1. XG nanoparticle schematic representation,

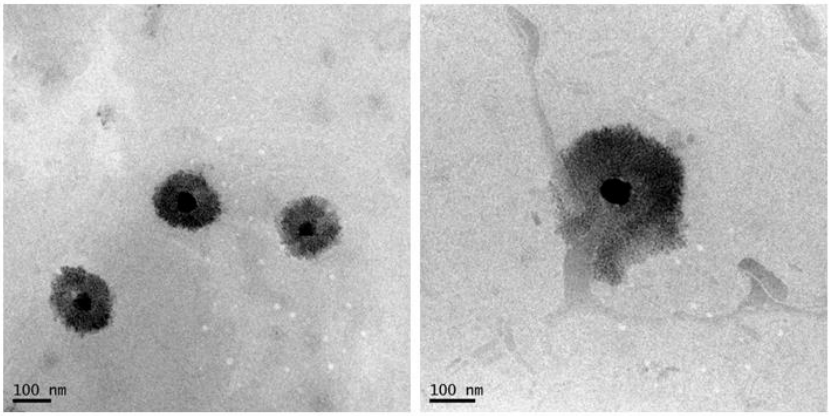

Figure 2. TEM images of blank XG nanoparticles.

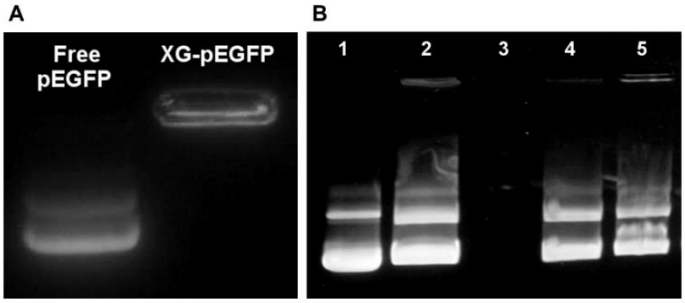

Figure 3. (A) Agarose gel electrophoresis showing efficacy of pEGFP association with XG nanoparticles. (B) Agarose gel electrophoresis after DNase protection assay: (1) free pEGFP, (2) free pEGFP + SDS, (3) free pEGFP + DNase I + SDS, (4) XG-pEGFP + SDS, and (5) XG-pEGFP + DNase I + SDS.

3.2. Stability of suspended and lyophilised nanoparticles

XG nanoparticles showed remarkable stability in suspension, with minor size increments after 3 months of storage at 4°C, RT and 37°C (Figure 4A). However, a 3-fold size increase was observed for samples stored for 12 months at 37°C, from 145.7 nm to 441.8 nm. Z potential showed a slight tendency to increase in samples kept at RT and at 4°C and RT after 3 and 12 months of storage, respectively (Figure 4B). In contrast, the Z potential was stable for samples stored at 37°C. In addition to stability in suspension, XG nanoparticles were able to maintain plasmid association during 12 months at all temperatures assayed (Figure 4C).

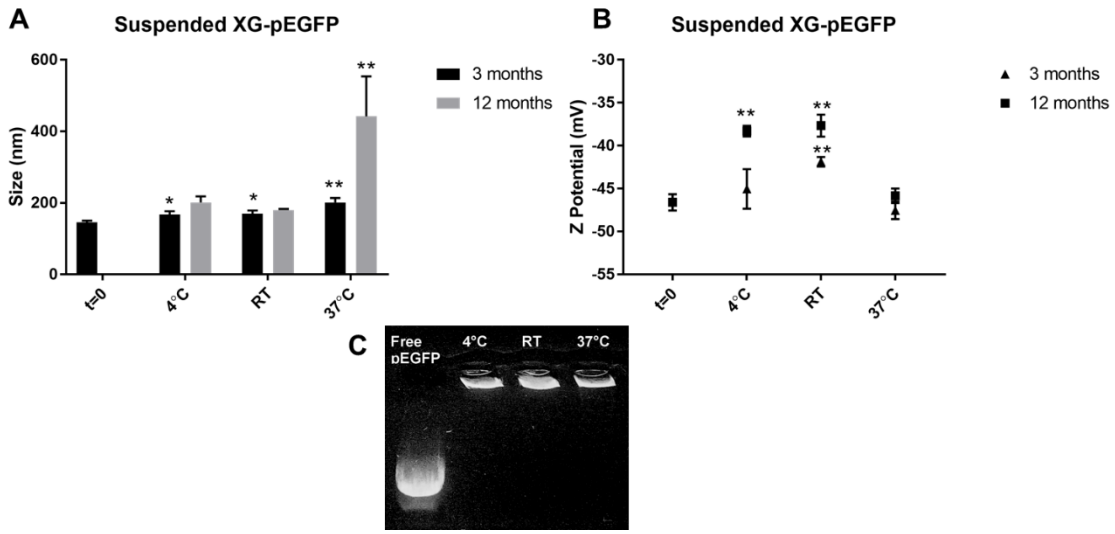

Figure 4. Stability of XG nanoparticles stored in suspension at 4°C, room temperature,(RT) and 37°C. After 3 and 12 months, size (A) and Z potential (B) were

measured. *p<0.05 and **p<0.01 vs. samples at initial time (t=0). Plasmid association was corroborated by agarose gel electrophoresis after 12 months of storage (C).

The system was subjected to lyophilisation, and its stability in the absence of water was studied. After a preliminary study, XG nanoparticles were lyophilised using trehalose as a lyoprotectant. Samples were resuspended in water, and NP physicochemical properties were compared to their properties before lyophilisation. As shown in Figure 5A, the system displayed resistance to lyophilisation, with a small size increase and Z potential decrease. Moreover, the nanoparticles successfully maintained plasmid binding (Figure 5B). Although some size increases were observed after the resuspension of samples kept at RT and 37°C, especially after 12 months, the sizes obtained were only 1.5 times bigger than the initial size. No statistically significant differences were seen for Z potential. Additionally, lyophilised NPs conserved plasmid association after 12 months of storage (Figure 6C).

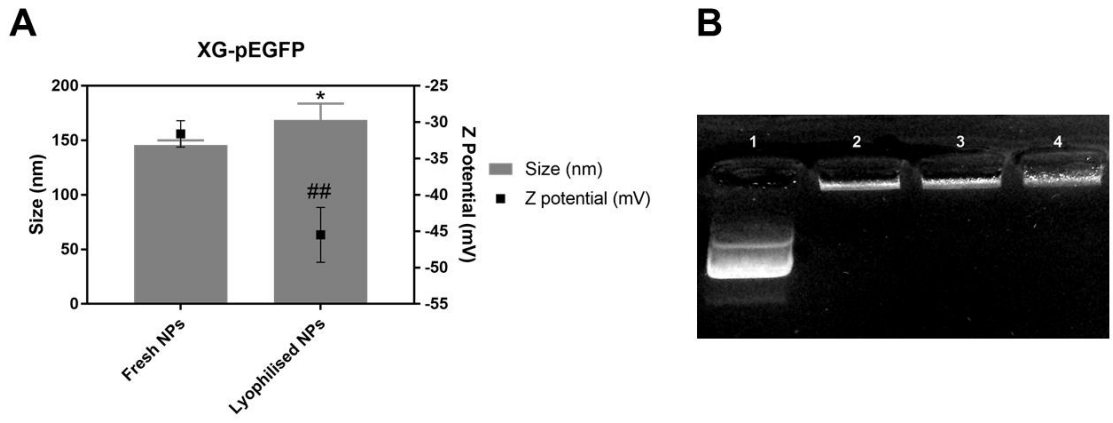

Figure 5. (A) Size and Zeta potential of fresh and lyophilised XG nanoparticles. *p<0.05 vs. size at t=0. ##p<0.01 vs. Z potential at t=0. (B) Agarose gel electrophoresis demonstrates XG nanoparticles maintain plasmid association after electrophoresis (lanes 2, 3 and 4). Free pEGFP was used as control (lane 1).

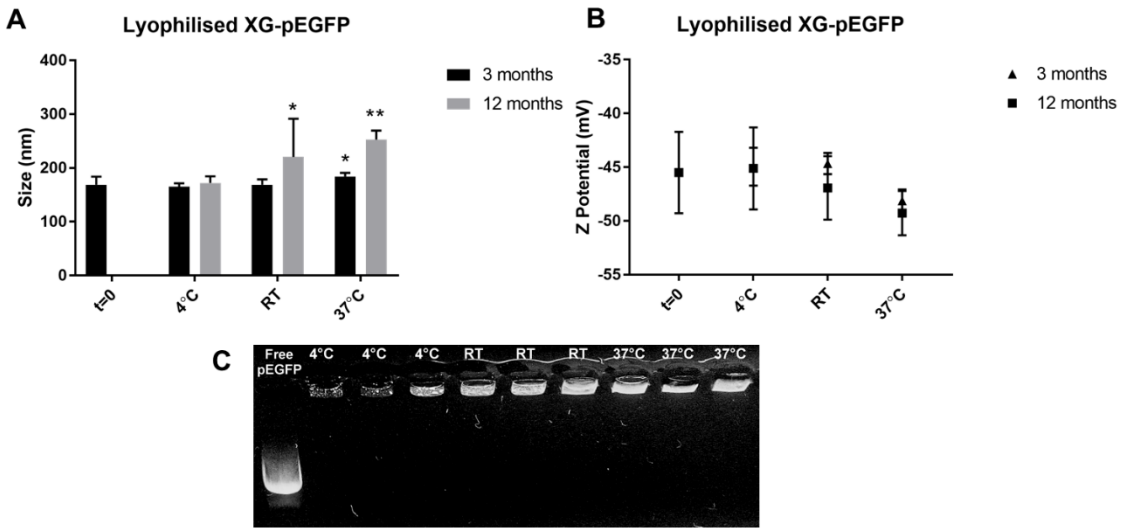

Figure 6. Stability of lyophilised XG nanoparticles stored at 4°C, room temperature (RT) and 37°C. After 3 and 12 months, NPs were resuspended and size (A) and Z potential (B) were measured. *p<0.05 and **p<0.01 vs. samples at initial time (t=0). Plasmid association was corroborated by agarose gel electrophoresis after 12 months of storage (C).

3.3. Cell viability and proliferation

The effect of XG nanoparticles on HUVEC cell viability was studied by XTT assay, considering the metabolic activity of the cells. HUVECs were exposed to increasing concentrations of XG nanoparticles for 2 hours. Cell viability was determined and, as shown in Figure 7, remained unchanged until the highest nanoparticle concentration of 768 µg/ml. Although cell viability decreased to 30%, this concentration is much higher than the one required to effectively transfect cells *in vitro*.

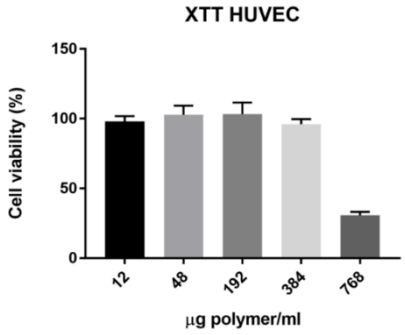

Figure 7. Cell viability of HUVECs measured by XTT after 2 hours of incubation with XG nanoparticles.

XG nanoparticles cytotoxicity was further studied in HUVECs using the ki-67 assay to analyse cell proliferation. For this purpose, cells were exposed to 384 μg/ml of XG nanoparticles for 3 hours. This concentration was higher than that required to effectively transfect the cells *in vitro*. Then, a ki-67 immunocytochemistry assay was performed on control and XG-treated cells and images were obtained by fluorescence microscopy. The images obtained were processed through ImageJ, and ki-67 positive XG-treated cells were calculated and compared to the control cells (Figure 8B). As shown in Figure 8, there was no significant difference in ki-67 expression between control cells and XG-treated cells, indicating that the nanoparticles do not induce growth arrest.

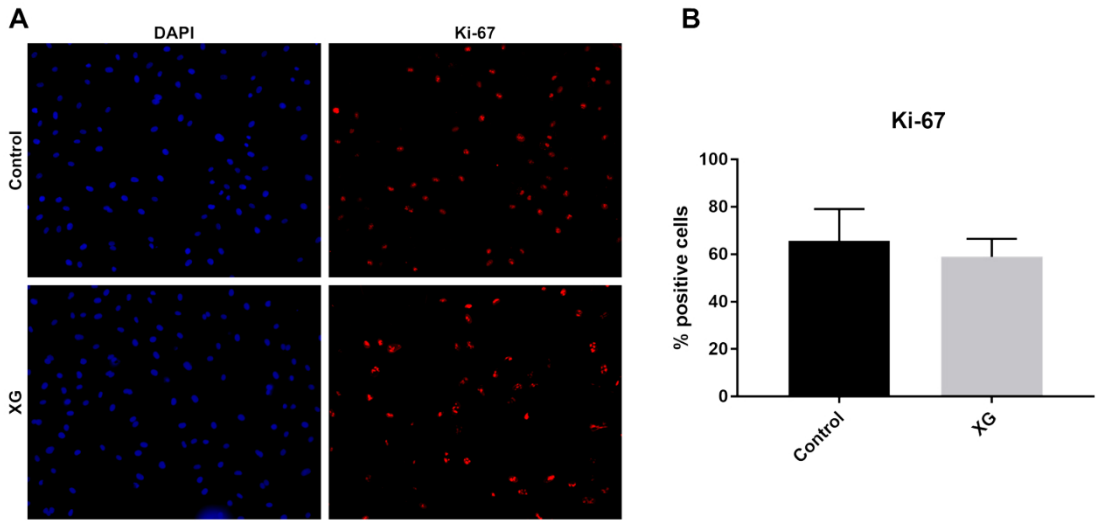

Figure 8. Images (A) and graph (B) showing ki-67 expression in control and XG-treated cells.

3.4. *In vitro* transfection

The ability of XG nanoparticles to transfect pEGFP was evaluated in HUVEC. Cells were incubated with pEGFP-XG nanoparticles for 2 hours, and GFP expression was evaluated by fluorescence microscopy after 24 hours. As shown in Figure 9, the system efficiently transfected the primary cell line at a dose of 1 μg of plasmid, corresponding to a nanoparticle concentration of 223.6 μg/ml.

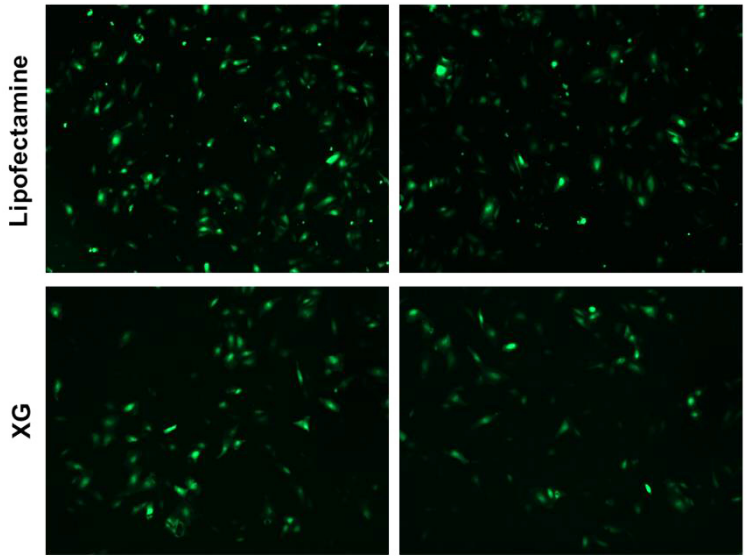

Figure 9. HUVEC were efficiently transfected with pEGFP-loaded NPs using doses of 1 μg of plasmid per well. Lipofectamine was used as positive control, with doses of 0.5 μg of plasmid per well.

3.5. *In vivo* toxicity

To assess the safety profile of systemically administered XG functionalised nanoparticles associated with pEGFP, the aspartate aminotransferase (AST) serum levels were analysed. For this purpose, 200 μl of pEGFP-XG nanoparticles (4.03 mg/ml) was intravenously injected in a 5% solution of glucose, and this same solution without nanoparticles was injected into the control mice. As shown in Figure 10A, no significant differences were observed in AST levels of control and XG-treated mice, indicating that there was no significant liver damage caused by the nanoparticles.

Moreover, the toxicity of the nanoparticles to the major mouse organs including kidney, liver, lung and spleen, was evaluated by haematoxylin and eosin (H&E) staining (Figure 10B). Some inflammatory cell infiltration was observed in the liver and surrounding blood vessels, indicating that the XG nanoparticles may induce a mild inflammatory response in the liver. No significant pathology was observed in the other organs compared to controls.

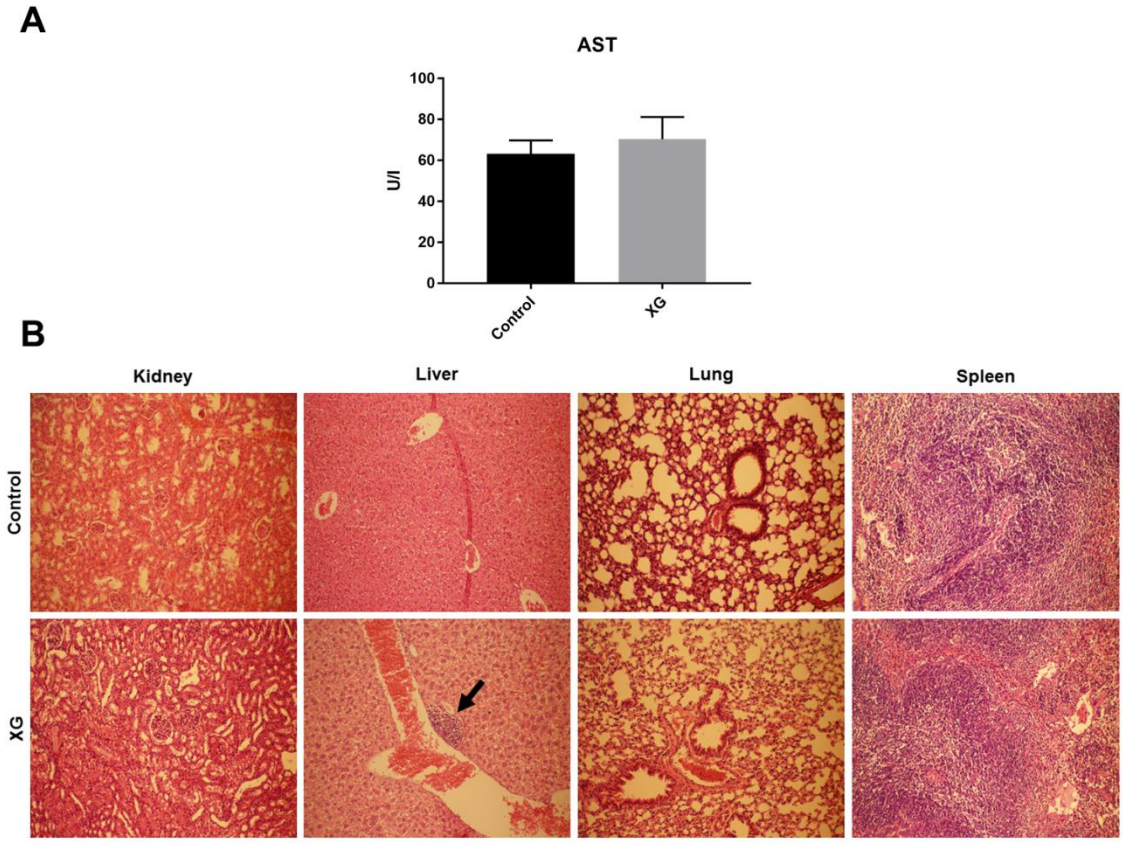

Figure 10. *In vivo* XG nanoparticle toxicity was evaluated by aspartate aminotransferase (AST) serum levels (A) and histopathological examination of major organs sections stained with haematoxylin and eosin (B), after intravenous administration of the nanoparticles to mice. The black arrow shows a small lymphocyte aggregate in the liver of an animal treated with XG nanoparticles.

3.6. Biodistribution

The biodistribution of XG nanoparticles was evaluated after an intravenous tail injection of pEGFP-loaded nanoparticles to mice. Mice were sacrificed 24 hours after administration, and GFP expression was evaluated in major organs. First, endothelium targeting specificity was evaluated in the liver. As shown in Figure 11, after immunostaining of Kupffer cells, no colocalization was observed between Kupffer cells and GFP staining. This indicates that the nanoparticles specifically target endothelial cells and escape the phagocytic functions of Kupffer cells as part of the reticuloendothelial system (RES). The biodistribution of XG nanoparticles in other organs was evaluated. As shown in Figure 12, GFP expression was found in the endothelial cells of blood vessels in the kidney, liver and lung and in LSECs.

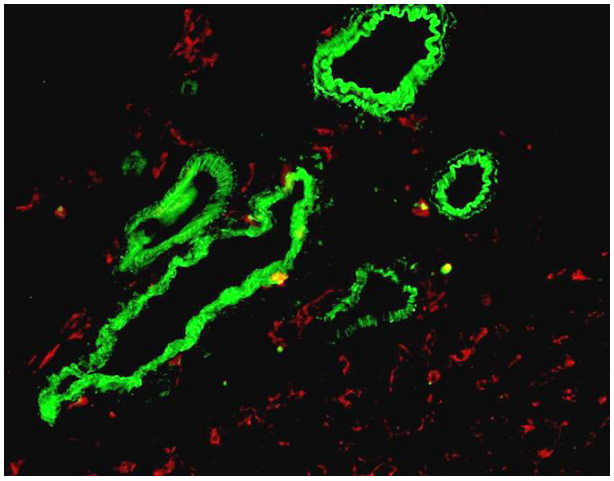

Figure 11. Liver sections showing GFP expression in green and Kupffer cells labelled with F4/80 antibody in red.

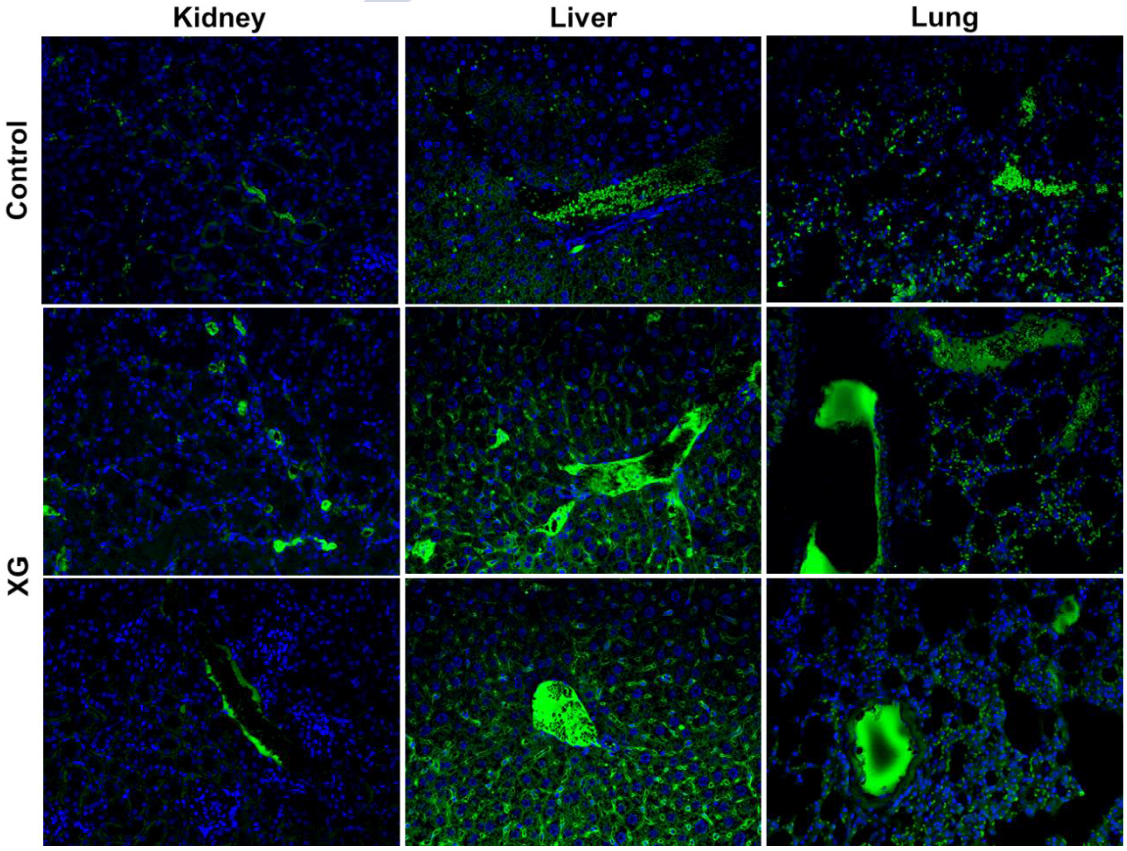

Figure 12. Immunohistochemistry of major organs sections showing GFP expression (green) in endothelial cells 24 hours after XG-pEGFP intravenous administration to mice. Mice injected with 5% glucose solutions were used as controls (red blood cells autofluorescence in green). Cell nuclei are stained in blue with DAPI.

4. Discussion

Here, we studied the versatility of span nanoparticles to be functionalised with a natural polysaccharide enabling the modulation of the nanoparticles' physicochemical properties, biodistribution and, hence, clinical potential. For this purpose, we selected the exopolysaccharide XG due to its mannose residues, which provided specific delivery of the associated bioactive molecule (pDNA) not only to LSECs but also to vascular endothelial cells of different organs. Accordingly, we decided to exploit this specificity to develop a new targeting strategy with potential application in the development of therapies against a wide range of diseases involving endothelium dysfunctions, such as cardiovascular diseases, diabetes, cancer and chronic kidney failure (10).

Specifically, using XG, we were able to provide a hydrophilic, negatively charged surface shell for our recently developed sorbitan monooleate-based nanoparticles (Table 1, Figure 1 and Figure 2), which may help prevent unspecific interactions of these nanoparticles with serum components and cell membranes. According to these results, we can assume that the carboxylic groups of XG are exposed on the nanoparticle surface, as evidenced by the negative zeta potential of the resulting nanosystems. Such a negatively charged external shell created around the nanoparticles is an interesting feature to avoid undesirable interactions with biological entities after systemic administration. The ability of such a shell to protect associated DNA from DNase degradation (Figure 3) has been demonstrated, which is a prerequisite for ensuring intact delivery of the associated molecule in its bioactive form to its site of action. In this respect, we should consider that when naked nucleic acids are systemically administered, they are quickly degraded by DNases, which are enzymes naturally present in tissues and biological fluids. However, we have demonstrated that incorporating plasmid DNA into XG nanoparticles prevents its enzymatic degradation, thus ensuring its intact delivery to its site of action.

Another critical issue in the development of nanomedicines is their low stability or tendency to lose their physicochemical properties after storage, which precludes their scalability to the pharmaceutical industry. Although numerous lipid gene delivery carriers have been developed and studied, none have made it to the market. Nevertheless, we have developed a lipid system functionalised with XG that is notable for its short- and long-term stability both in suspension and as a lyophilised product (Figure 4 and 6). When nanoparticles were stored in suspension, they resisted even high temperatures (37°C) for at least 3 months without major

changes in size and Z potential. Moreover, lyophilisation enhanced the system's long-term stability.

Once we found that the developed nanosystem possesses adequate physicochemical properties, we initiated cell viability studies to determine their toxicological profile. Cell viability is determined from the number of healthy cells in a sample and it is quantified by measuring the metabolic activity of cells, whereas cell proliferation is determined from the number of dividing cells or growth rate. In this work, we evaluated the metabolic activity of cells and the expression of ki-67 protein to determine the viability and proliferation of the cells, respectively, after exposure to XG-decorated nanoparticles. Ki-67 is a cellular marker of proliferation that is present during all active phases of the cell cycle and absent from resting cells (19). Here, we have shown that the developed systems decrease metabolic activity at the higher tested concentration, but no effect on cell proliferation was observed at the tested concentration. The effect of nanoparticles on cell viability cannot be explained by the toxicity of their components. Diverse studies have described XG biocompatibility and safety. For example, a study showed that XG-stabilised gold nanoparticles did not decrease A549 cell viability but that the cytotoxicity of doxorubicin increased when it was loaded into the nanoparticles, attributing this effect to enhanced cellular uptake. The authors theorized that the high cellular uptake could be attributed to the presence of mannose sugars in XG, which can interact with A549-overexpressed mannose receptors (1). Another study demonstrated that high XG concentrations were not toxic to a NIH/3T3 mouse fibroblasts cell line (20). Accordingly, the cytotoxicity observed for XG nanoparticles in HUVEC may be related to significant nanoparticle uptake due to XG functionalisation rather than to the toxicity of the polymer itself. Notably, HUVECs are primary cells isolated directly from tissues and, in contrast with cell lines, are especially sensitive. They are more representative of *in vivo* responsiveness and environment. Accordingly, the ability of the system to transfect HUVEC *in vitro* should be determined because primary cells' resistance to transfection is widely known.

Once determined that the developed nanosystem displays an appropriate cytotoxicity profile, we decided to evaluate its *in vivo* toxicity. Inflammatory cell infiltrates were observed in the liver after the systemic administration of XG-functionalised nanoparticles, which we consider a mild inflammatory reaction (Figure 10). We have considered two different possibilities to explain this reaction. Diverse studies have described XG's role in immunomodulation. Thus, XG has been described to activate polyclonal lymphocytes B in the

absence of T-cells (21) and to induce a humoral response mediated by IgG1 when they are subcutaneously administered as an adjuvant associated with ovalbumin (20). In addition, XG antitumoural activity has been described in mice by induction of inflammatory cytokine production, such as TNF- and IL-12, through toll-like receptor- (TLR-) 4 recognition (8). Thus, XG could be responsible for lymphocyte activation and extravasation. However, we should consider that the nanoparticles are loaded with pEGFP and that GFP expression is associated with inflammatory and immune responses (22). Furthermore, GFP expression has been reported to cause toxicity and side effects such as ubiquitination, prostaglandin production, apoptosis and enhanced sensitivity to cytotoxic drugs (23-26). Accordingly, the mild inflammation observed in the liver could be explained by both the XG immunomodulation activity and/or an immune response to GFP expression or even the synergistic effect of both factors. However, it should be emphasized that the AST levels remained unchanged after nanoparticle administration, indicating no major liver toxicity caused by the nanoparticles.

After the systemic administration of pEGFP-XG nanoparticles and immunostaining of Kupffer cells in the liver, no colocalization was observed between Kupffer cells and GFP staining (Figure 11), which indicates that the nanoparticles specifically target endothelial cells and escape the reticuloendothelial system (RES). Kupffer cells have an important role in the removal of nanoparticles from the organism, as one of main causes of low stability and efficacy of these systems *in vivo* (27, 28). Negative surface charge of particles is related to a greater RES uptake (29). Contrary to the literature, we have developed a negatively charged nanosystem that evades non-specific uptake by RES, thus achieving the specific targeting of endothelial cells. In addition, GFP expression was observed in LSECs, in the endothelial cells of liver blood vessels, and in the blood vessels of lung and kidney, but it was not observed in the spleen (Figure 12). These results suggest that XG-functionalised nanoparticles have a targeting ability to the endothelial cell populations at the aforementioned levels. In the case of LSECs, this ability can be mediated by mannose receptors, considering XG mannose residues and expression of this receptor in LSECs. Moreover, the ability of negatively charged molecules to act as ligands for scavenger receptors in LSECs has been described and exploited for LSECs targeting in numerous works (30-32). However, considering vascular endothelium heterogeneity, as exemplified by the absence of mannose receptors in endothelial cells of blood vessels, a further hypothesis should be considered to explain the nanoparticles' ability to also target endothelium of blood vessels. Diverse works cover the targeting of vascular endothelium

and some aspects to consider (33-35). Interaction of nanoparticles with the microvasculature, i.e., arterioles, capillaries and venules, is favoured by an extended luminal surface area, small vessel calibre and low flow rate. However, the arterial endothelium is less favourable for nanoparticle interactions than the venous endothelium is due to the hydrodynamic conditions of arteries, which include high shear stress and pulsative flow (35). Some studies have even discussed the relation between nanoparticle composition and physicochemical properties and endothelium targeting. Thus, it is reported that lipid nanoparticles with surfaces that are rich in negatively charged polyelectrolytes are preferentially taken up by endothelial cells compared to epithelial cells, without the need for cell-specific targeting ligands (36). The authors of this study suggest that nanoparticles enter the cell through hydrophobic interactions promoted by electrostatic repulses with the cell membrane negative charge. On the other hand, they demonstrate that NP-containing polymers with high affinity for cell membrane lipids and highly negative charges can specifically target caveolae lipid rafts that are overexpressed in endothelial cells, avoiding nonspecific charge-charge interactions with the cell membrane. In addition, polysaccharides, such as glycosaminoglycans and fucoidans, are extensively used as endothelium-targeting moieties (37, 38). In particular, fucoidan has shown high affinity for the P-selectin adhesion molecule on the endothelium surface (39). Thus, we conjecture that sorbitan monooleate nanoparticles can specifically target endothelial cells via the particular surface shell created by the polysaccharide XG, without the need for receptor-ligand-type targeting strategies. Thus, we consider that endothelial uptake occurs through the NP interactions with caveolae lipid rafts or through nonspecific binding and clustering of the particles at cationic sites on the plasma membrane and subsequent endocytosis (40).

5. Conclusions

We have demonstrated that the characteristics of sorbitan monooleate-based nanoparticles can be easily modulated with the incorporation of the polysaccharide XG. Such a strategy allows the development of nanosystems that are characterised by a hydrophilic, negatively charged surface shell. The main features of the resulting nanosystems are their long-term stability and the protection of associated plasmid DNA against enzymatic degradation. These features are translated into an appropriate cell transfection (i.e., in primary HUVECs) while achieving a compromise between transfection and cytotoxicity. This capability allows *in vivo*

plasmid DNA delivery to the vascular endothelium of lung, liver and kidney by avoiding RES uptake without inducing major toxicity. Therefore, we conclude that sorbitan monooleate-based nanoparticles can be specifically tailored to fulfil specific delivery requirements, creating functionalised sorbitan ester-based nanosystems that are promising gene delivery carriers to specifically target the vascular endothelium. On the basis of these results, we envisage the great potential of the aforementioned nanosystems in the management of many vascular-related diseases.

References

1. Pooja D, Panyaram S, Kulhari H, Rachamalla SS, Sistla R. Xanthan gum stabilized gold nanoparticles: characterization, biocompatibility, stability and cytotoxicity. Carbohydr Polym. 2014 Sep 22;110:1-9.

2. Luo Y, Wang Q. Recent development of chitosan-based polyelectrolyte complexes with natural polysaccharides for drug delivery. Int J Biol Macromol. 2014 Mar;64:353-67.

3. Xu W, Jin W, Lin L, Zhang C, Li Z, Li Y, et al. Green synthesis of xanthan conformation-based silver nanoparticles: antibacterial and catalytic application. Carbohydr Polym. 2014 Jan 30;101:961-7.

4. Bueno VB, Bentini R, Catalani LH, Barbosa LR, Petri DF. Synthesis and characterization of xanthan-hydroxyapatite nanocomposites for cellular uptake. Mater Sci Eng C Mater Biol Appl. 2014 Apr 1;37:195-203.

5. Chellat F, Tabrizian M, Dumitriu S, Chornet E, Magny P, Rivard CH, et al. In vitro and in vivo biocompatibility of chitosan-xanthan polyionic complex. J Biomed Mater Res. 2000 Jul;51(1):107-16.

6. Fukuda M, Peppas NA, McGinity JW. Properties of sustained release hot-melt extruded tablets containing chitosan and xanthan gum. Int J Pharm. 2006 Mar 9;310(1-2):90-100.

7. Phaechamud T, Ritthidej GC. Sustained-release from layered matrix system comprising chitosan and xanthan gum. Drug Dev Ind Pharm. 2007 Jun;33(6):595-605.

8. Takeuchi A, Kamiryou Y, Yamada H, Eto M, Shibata K, Haruna K, et al. Oral administration of xanthan gum enhances antitumor activity through Toll-like receptor 4. Int Immunopharmacol. 2009 Dec;9(13-14):1562-7.

9. Dahlman JE, Barnes C, Khan O, Thiriot A, Jhunjunwala S, Shaw TE, et al. In vivo endothelial siRNA delivery using polymeric nanoparticles with low molecular weight. Nat Nanotechnol. 2014 Aug;9(8):648-55.

10. Rajendran P, Rengarajan T, Thangavel J, Nishigaki Y, Sakthisekaran D, Sethi G, et al. The Vascular Endothelium and Human Diseases. International Journal of Biological Sciences. 2013 10/07;9(10):1057-69.

11. Aird WC. Phenotypic heterogeneity of the endothelium: I. Structure, function, and mechanisms. Circ Res. 2007 Feb 2;100(2):158-73.

12. Aird WC. Phenotypic heterogeneity of the endothelium: II. Representative vascular beds. Circ Res. 2007 Feb 2;100(2):174-90.

13. Aird WC. Endothelial Cell Heterogeneity. Cold Spring Harbor Perspectives in Medicine. 2012 01;2(1):a006429.

14. Hood JD, Bednarski M, Frausto R, Guccione S, Reisfeld RA, Xiang R, et al. Tumor regression by targeted gene delivery to the neovasculature. Science. 2002 Jun 28;296(5577):2404-7.

15. Ma Z, Zhang J, Alber S, Dileo J, Negishi Y, Stolz D, et al. Lipid-mediated delivery of oligonucleotide to pulmonary endothelium. Am J Respir Cell Mol Biol. 2002 Aug;27(2):151-9.

16. Cicha I. Strategies to enhance nanoparticle-endothelial interactions under flow. Journal of Cellular Biotechnology. 2016 12/05/2016;1(2):191-208.

17. Lin A, Sabnis A, Kona S, Nattama S, Patel H, Dong JF, et al. Shear-regulated uptake of nanoparticles by endothelial cells and development of endothelial-targeting nanoparticles. J Biomed Mater Res A. 2010 Jun 1;93(3):833-42.

18. Gupta A, Gupta RK, Gupta GS. Targeting cells for drug and gene delivery: Emerging applicationsof mannans and mannan binding lectins. Journal of Scientific and Industrial Research. 2009 03/03/2009;68(6):465-83.

19. Scholzen T, Gerdes J. The Ki-67 protein: from the known and the unknown. J Cell Physiol. 2000 Mar;182(3):311-22.

20. Schuch RA, Oliveira TL, Collares TF, Monte LG, Inda GR, Dellagostin OA, et al. The Use of Xanthan Gum as Vaccine Adjuvant: An Evaluation of Immunostimulatory Potential in BALB/c Mice and Cytotoxicity In Vitro. Biomed Res Int. 2017;2017:3925024.

21. Ishizaka S, Sugawara I, Hasuma T, Morisawa S, Moller G. Immune responses to xanthan gum. I. The characteristics of lymphocyte activation by xanthan gum. Eur J Immunol. 1983 Mar;13(3):225-31.

22. Yang C, Hao F, He J, Lu T, Klein RL, Zhao LR, et al. Sequential Adeno-Associated Viral Vector Serotype 9-Green Fluorescent Protein Gene Transfer Causes Massive Inflammation and Intense Immune Response in Rat Striatum. Hum Gene Ther. 2016 Jul;27(7):528-43.

23. Baens M, Noels H, Broeckx V, Hagens S, Fevery S, Billiau AD, et al. The dark side of EGFP: defective polyubiquitination. PLoS One. 2006 Dec 20;1:e54.

24. Zhang F, Hackett NR, Lam G, Cheng J, Pergolizzi R, Luo L, et al. Green fluorescent protein selectively induces HSP70-mediated up-regulation of COX-2 expression in endothelial cells. Blood. 2003 Sep 15;102(6):2115-21.

25. Liu HS, Jan MS, Chou CK, Chen PH, Ke NJ. Is green fluorescent protein toxic to the living cells? Biochem Biophys Res Commun. 1999 Jul 14;260(3):712-7.

26. Goto H, Yang B, Petersen D, Pepper KA, Alfaro PA, Kohn DB, et al. Transduction of green fluorescent protein increased oxidative stress and enhanced sensitivity to cytotoxic drugs in neuroblastoma cell lines. Mol Cancer Ther. 2003 Sep;2(9):911-7.

27. Sadauskas E, Wallin H, Stoltenberg M, Vogel U, Doering P, Larsen A, et al. Kupffer cells are central in the removal of nanoparticles from the organism. Part Fibre Toxicol. 2007 Oct 19;4:10.

28. Rinkenauer AC, Press AT, Raasch M, Pietsch C, Schweizer S, Schworer S, et al. Comparison of the uptake of methacrylate-based nanoparticles in static and dynamic in vitro systems as well as in vivo. J Control Release. 2015 Oct 28;216:158-68.

29. Frohlich E. The role of surface charge in cellular uptake and cytotoxicity of medical nanoparticles. Int J Nanomedicine. 2012;7:5577-91.

30. Poelstra K, Prakash J, Beljaars L. Drug targeting to the diseased liver. J Control Release. 2012 Jul 20;161(2):188-97.

31. Melgert BN, Olinga P, Jack VK, Molema G, Meijer DK, Poelstra K. Dexamethasone coupled to albumin is selectively taken up by rat nonparenchymal liver cells and attenuates LPS-induced activation of hepatic cells. J Hepatol. 2000 Apr;32(4):603-11.

32. Kamps JA, Morselt HW, Swart PJ, Meijer DK, Scherphof GL. Massive targeting of liposomes, surface-modified with anionized albumins, to hepatic endothelial cells. Proc Natl Acad Sci U S A. 1997 Oct 14;94(21):11681-5.

33. Lee R, Channon KM, Antoniades C. Therapeutic strategies targeting endothelial function in humans: clinical implications. Curr Vasc Pharmacol. 2012 Jan;10(1):77-93.

34. Sun X, Rossin R, Turner JL, Becker ML, Joralemon MJ, Welch MJ, et al. An assessment of the effects of shell cross-linked nanoparticle size, core composition, and surface PEGylation on in vivo biodistribution. Biomacromolecules. 2005 Sep-Oct;6(5):2541-54.

35. Howard M, Zern BJ, Anselmo AC, Shuvaev VV, Mitragotri S, Muzykantov V. Vascular targeting of nanocarriers: perplexing aspects of the seemingly straightforward paradigm. ACS Nano. 2014 May 27;8(5):4100-32.

36. Voigt J, Christensen J, Shastri VP. Differential uptake of nanoparticles by endothelial cells through polyelectrolytes with affinity for caveolae. Proc Natl Acad Sci U S A. 2014 Feb 25;111(8):2942-7.

37. Rasente RY, Imperiale JC, Lazaro-Martinez JM, Gualco L, Oberkersch R, Sosnik A, et al. Dermatan sulfate/chitosan polyelectrolyte complex with potential application in the treatment and diagnosis of vascular disease. Carbohydr Polym. 2016 Jun 25;144:362-70.

38. Lamichhane SP, Arya N, Ojha N, Kohler E, Shastri VP. Glycosaminoglycan-functionalized poly-lactide-co-glycolide nanoparticles: synthesis, characterization, cytocompatibility, and cellular uptake. Int J Nanomedicine. 2015 Jan 19;10:775-89.

39. Rouzet F, Bachelet-Violette L, Alsac JM, Suzuki M, Meulemans A, Louedec L, et al. Radiolabeled fucoidan as a p-selectin targeting agent for in vivo imaging of platelet-rich thrombus and endothelial activation. J Nucl Med. 2011 Sep;52(9):1433-40.

40. Verma A, Stellacci F. Effect of surface properties on nanoparticle-cell interactions. Small. 2010 Jan;6(1):12-21.

USC
UNIVERSIDADE
DE SANTIAGO
DE COMPOSTELA

Chapter II

Development and characterisation of chondroitin sulfate- and hyaluronic acid-incorporated sorbitan ester nanoparticles as gene delivery systems

USC
UNIVERSIDADE
DE SANTIAGO
DE COMPOSTELA

Abstract

Glycosaminoglycans (GAGs) are natural polymers that are broadly used in gene delivery systems to increase stability as well as decrease toxicity and nonspecific interactions, thereby increasing transfection efficiency. In this work, we propose sorbitan ester-based lipid nanoparticles functionalised with the GAGs chondroitin sulfate (CS) and hyaluronic acid (HA) as gene delivery systems. For this purpose, we describe the design and evaluation of these nanosystems loaded with plasmid DNA, including an evaluation of their physicochemical characteristics, stability properties, ability to protect and efficiently transfect cells with Enhanced Green Fluorescent Protein plasmid (pEGFP) *in vitro*, and biocompatibility both *in vitro* and *in vivo*. We confirm that molecules with high biological value and targeting potential, such as HA and CS, can be successfully incorporated into our recently developed sorbitan ester-based nanoparticles and that this incorporation leads to effective stabilisation of both nanosystems as well as protects plasmid DNA. We demonstrated that the aforementioned incorporation of HA and CS enables long-term stability of the nanosystems in both liquid and lyophilised states, which is a remarkable property that can aid in their transfer to industry. The ability of these functionalised nanosystems to transfect the A549 cell line without compromising cell viability was also shown, as well as their innocuous safety profile *in vivo*. Thus, we provide valuable evidence of the suitable properties and potential of these hybrid nanoparticles as gene delivery systems.

1. Introduction

Gene therapy consists of the delivery of nucleic acids to specific cells to replace or silence malfunctioning genes with the aim of curing or favourably altering pathological progression (1). Deregulation of gene expression is associated with the origin of multiple diseases. Thus, recent advances in identification of the molecular basis of numerous inherited genetic disorders have made them susceptible to gene therapy treatment. Although gene therapy can be applied to treatment and prevention of multiple pathologies, such as infectious diseases, Parkinson's disease or cystic fibrosis, most efforts and clinical trials have been focused on cancer therapy (2). Cancer comprises a group of diseases with multifactorial origin. Despite considerable advances in the field of cancer therapy, chemical-based therapeutics, radiotherapy and surgery have been insufficient in addressing the diverse cancer aetiologies, leading to a high rate of treatment failure. Gene-based therapies could solve this problem by targeting specific pathways that are altered in cancer while avoiding most of the side effects associated with conventional therapies (3, 4).

However, gene delivery to cancer cells remains a major challenge. Nucleic acid delivery must overcome numerous barriers and obstacles before its therapeutic effect can be exerted. Nucleic acids are negatively charged macromolecules with a hydrophilic nature, characteristics that explain their poor ability to penetrate biological barriers and their susceptibility to degradation by enzymes in the body. These properties make necessary the development and inclusion of nucleic acids into gene delivery systems. Non-viral delivery systems have been extensively studied due to their safety, low cost and scalability in comparison with viral vectors (4-6).

The most common traditional non-viral systems can be classified as lipidic, polymeric or polymer-lipid hybrid systems (3). Among them, cationic lipids have been broadly used for gene delivery due to their high efficacy in transfecting a variety of cell types with different types of nucleic acids and their reproducibility and ease of use (7). However, their positive charge is related to high cytotoxicity, nonspecific uptake and short blood circulation time due to interaction with negatively charged serum proteins and eventual phagocytosis by the reticuloendothelial system (RES). Diverse strategies have been applied in an attempt to shield the positive surface charge and avoid these side effects. Pegylation is known to reduce non-specific interactions of nanosystems; however, this strategy might decrease cellular uptake and

gene release (8-10). Alternatively, surface modification of nanocarriers with anionic macromolecules, such as glycosaminoglycans (GAGs), may lengthen their circulation time by reducing complement activation and thus recognition by the RES (11, 12). Therefore, it has been demonstrated that incorporation of GAGs into gene delivery systems increases the stability of the carriers and decreases toxicity and nonspecific interactions, thereby increasing their transfection efficiency *in vivo* (13-18). GAGs have also been shown to influence intracellular routing of nanosystems by improving endosomal escape and localisation at the nuclear periphery (19). In our study, the natural anionic polymers chondroitin sulfate (CS) and hyaluronic acid (HA) were employed to stabilise and functionalise the system by taking advantage of their suitable properties for gene delivery. They are the main components of the extracellular matrix and are considered biocompatible and biodegradable polymers, and thus, they are widely used in the biomedical field (20-23). CS and HA are mucopolysaccharides naturally present in the body, and they are composed of glucuronic acid and N-acetylglucosamine repeats connected via a β-1-4 linkage. A sulfate group in at least one of the CS side groups is the primary structural difference between them. HA is present in connective tissue, vitreous humour and synovial joint fluid, while CS has a role in wound healing and chondrogenesis (24).

Despite the large number of lipid-based nanosystems described in the literature, only a few have reached the market (25). One of the limitations of lipid nanosystems is their low stability in aqueous suspensions, which compromises their transfection efficiency (26). Thus, more stable systems are necessary to scale production from basic research to the pharmaceutical industry. In addition, advances in characterisation and manufacturing of the vectors are needed for successful therapy.

In this work, we propose sorbitan ester-based lipid nanoparticles functionalised with the natural polymers CS or HA as gene delivery systems. For this purpose, we describe the design and evaluation of these nanosystems loaded with plasmid DNA, including their physicochemical characterisation, their stability properties upon storage at different temperatures in both a suspension and as a lyophilised product, their ability to protect the delicate bioactive molecule associated with them, their transfection properties and their biocompatibility both *in vitro* and *in vivo*.

1. Materials and Methods

1.1. Materials

Sorbitan monooleate (Span® 80) (SP), oleylamine (OA) (purity ≥70%), glucose, sucrose, and sodium dodecyl sulfate (SDS) were purchased from Sigma (Spain). Chondroitin sulfate (CS) and hyaluronic acid (HA) were provided by Merck (Spain) and Bioiberica (Spain), respectively. The pEGFP-C3 plasmid was obtained from Elim Biopharmaceutics (United States). SYBR Safe DNA Gel Stain and SYBR® Gold post-electrophoresis and agarose were provided by Life Technologies (Spain). Dulbecco's modified Eagle's medium (DMEM), foetal bovine serum (FBS), penicillin-streptomycin, L-glutamine, DNase I and Lipofectamine 2000 were acquired from Thermo Fisher (Spain). XTT cell viability reagent was provided by Roche (Spain). The aspartate aminotransferase colorimetric kit was purchased from Randox (Spain).

1.2. Nanoparticle preparation and characterisation

For construction of the nanoparticles (NPs), a solution of sorbitan monooleate (Span 80, SP) and oleylamine (OA) was prepared in ethanol at a concentration of 6.6 and 0.33 mg/ml, respectively. Then, this organic phase was added under magnetic stirring to an aqueous phase containing either chondroitin sulfate (CS) or hyaluronic acid (HA) at a concentration of 0.125 mg/ml in a volume ratio of 1:2. Ethanol was removed under reduced pressure on a rotary evaporator. For encapsulation of Enhanced Green Fluorescent Protein plasmid (pEGFP), the plasmid was incorporated into the aqueous phase. The final formulations obtained were 200 μg/ml pEGFP-loaded NPs.

The mean particle size and the size distribution of the nanoparticles were determined using photon correlation spectroscopy (PCS). Samples were suitably diluted in Milli-Q water. Each analysis was performed at 25°C with an angle of detection of 173°. The zeta potential of the nanoparticles was determined with laser scattering anemometry (LDA). To that end, the samples were suitably diluted in a millimolar KCl solution. The PCS and LDA analyses were performed with a Zetasizer® 3000HS (Malvern Instruments, UK).

The morphology of the nanoparticles was examined with transmission electron microscopy (CM 12 Philips, Eindhoven, The Netherlands) after staining with 2% w/v phosphotungstic acid solution. For this purpose, the samples were placed on copper grids (400 mesh) coated with a Formvar® film.

1.3. Gel electrophoresis

The efficiency of the association of pEGFP with the nanoparticles was determined using agarose gel electrophoresis. Gels with 1% agarose were prepared in TAE (Tris-Acetate-EDTA, 40 mM Tris, 1% acetic acid, 1 mM EDTA). SYBR® Gold Nucleic Acid Gel Stain and SYBR® SAFE DNA Gel Stain were employed as stains, and glycerol was used to aid in loading the gel. A potential difference of 100 mV was applied for 30 minutes, and free pEGFP was used as the control.

1.4. Lyophilisation and stability studies

The nanoparticles were lyophilised in an aqueous solution of cryoprotectant in a 1:1 (v/v) ratio of nanoparticles:cryoprotectant (10% glucose for CS NPs, and 10% sucrose for HA NPs) using freeze-drying equipment (VirTis Genesis 25 ES, S.P. Industries, USA). Afterwards, each sample was completely sealed to inhibit humidification, and these lyophilised samples, as well as the nanoparticles in suspension, were stored under various temperature conditions (Room Temperature (RT), 4°C and 37°C). After three and twelve months of storage, the lyophilised samples were rehydrated with RNase-free water, and their physicochemical characteristics were analysed.

1.5. DNase protection assay

To confirm the ability of CS and HA nanoparticles to protect pEGFP from endonucleases, a DNase I protection assay was performed. Both formulations containing 5 μg of pEGFP were incubated with 1 unit of DNase I at 37°C for 1 h. Naked pEGFP treated with DNase I served as a positive control. The DNase I reaction was terminated by adding 0.5 M EDTA solution. The plasmid was then dissociated from the nanoparticles by incubation with a 2% solution of sodium dodecyl sulfate (SDS) for 30 minutes at 37°C. The DNA integrity was assessed via 1% agarose gel electrophoresis (100 V, 30 min).

1.6. Cell culture

In vitro assays were performed using a human lung adenocarcinoma cell line (A549) obtained from the American Type Culture Collection (ATCC). Cells were maintained in DMEM supplemented with 10% FBS, 1% penicillin-streptomycin and 1% L-glutamine at 37°C with a 5% CO_2 humidified atmosphere.

1.7. Cell viability

The effect of CS and HA nanoparticles on cell viability was evaluated in the A549 cell line using an XTT assay. Cells were seeded at $1x10^4$ cells per well in a 96-well plate and incubated overnight. Then, different concentrations of the NPs in Opti-MEM reduced-serum medium were incubated with the cells. After 4 hours, the treatment was removed, and the cells were incubated with fresh culture medium for 24 hours. Then, XTT reagents were added to the wells and incubated with the cells following the manufacturer's instructions.

1.8. In vitro transfection

For transfection experiments, A549 cells were seeded in a 24-well plate at a density of $6x10^4$ cells per well and incubated overnight. Then, the medium was replaced with Opti-MEM, and plasmid-loaded NPs were added at doses from 1 to 2 μg of the plasmid per well and incubated with the cells for 4 hours. Lipofectamine 2000 was used as a positive control according to the manufacturer's instructions. After 4 hours, the medium was replaced with serum-supplemented medium. The expression of GFP was detected 24 hours post-transfection using an inverted microscope (AxioObserver.Z1 Inverted Microscope, Zeiss, Germany).

1.9. Animals

Balb/c mice (6- to 8-week-old males) were obtained from Charles River Laboratories Spain S.A. (Barcelona, Spain). All the procedures were approved by the Ethical Committee for Animal Experimentation (CEEA) of the University of the Basque Country (EHU/UPV) in accordance with institutional, national and international guidelines regarding the protection and care of animals used for scientific purposes (CEBA/237/2012/BADIOLA ETXABURU). Mice were maintained in the animal facility of EHU/UPV and had access to standard chow and water ad libitum.

1.10. *In vivo* toxicity: blood biochemical assays and histopathological examination

For *in vivo* toxicity studies, 200 μl of pEGFP-loaded NPs in 5% glucose were administered intravenously to mice. For this purpose, 4 mice were used per condition, and a 5% solution of glucose was injected into the control mice. After 24 hours, the animals were sacrificed, blood samples were collected by cardiac puncture, and major organs were fixed in paraformaldehyde and embedded in paraffin. Serum was isolated from the blood samples, and hepatic function was analysed by examining aspartate aminotransferase (AST) levels using an AST colorimetric assay. For histopathological examination, sections (4 μm) of the liver, spleen, lung and kidney

were cut and stained with Haematoxylin and Eosin (H&E). Representative sections were observed and examined using an optical microscope (Nikon Eclipse E-100).

1.11. Statistical analysis

All experimental measurements were collected in triplicate. The values are expressed as the mean ± standard deviation (SD). Statistically significant differences between the treatments were evaluated with analysis of variance (ANOVA) and Fisher's least significant difference (LSD) using GraphPad Prism, with alpha<0.05 being the probability of error.

2. Results

2.1. Nanoparticle preparation and characterisation

Hybrid nanosystems consisting of sorbitan ester-based nanoparticles decorated with chondroitin sulfate (CS) or hyaluronic acid (HA) were produced through a nanoprecipitation-self-assembly method. For this purpose, the lipophilic substances OA and SP were dissolved in an organic phase, and the hydrophilic polymers CS and HA were solubilised in an aqueous phase. The spontaneous nanoparticle assembly after the addition of the aqueous phase over the organic phase occurs due to the insolubility of SP and OA in water and as a result of the simultaneous occurrence of electrostatic interactions between the positive charges of OA and the negative charges of the hydrophilic CS and HA components. This procedure also allows electrostatic association of charged bioactive molecules, such as plasmid DNA, with the nanosystems. The structure of the resulting hybrid nanosystems is schematised in Figure 1. Table 1 shows the size and zeta potential of both formulations. Incorporation of plasmid DNA did not significantly modify nanoparticle size or zeta potential ($p>0.05$). TEM images show spherical nanoparticles of nanometric size, corroborating the results obtained with DLS (Figure 2).

Table 1. Physicochemical characterisation of blank and pEGFP-loaded nanosystems.

Formulation	Size (nm)	PdI	ζ Potential (mV)
SP-OA-CS	122.8 ± 11.9	0.079 ± 0.019	-37.7 ± 2.1
SP-OA-CS-pEGFP	137.3 ± 13.7	0.091 ± 0.022	-37.1 ± 6.9
SP-OA-HA	137.0 ± 10.4	0.114 ± 0.024	-28.6 ± 8.4
SP-OA-HA-pEGFP	134.5 ± 11.4	0.083 ± 0.026	-32.4 ± 2.8

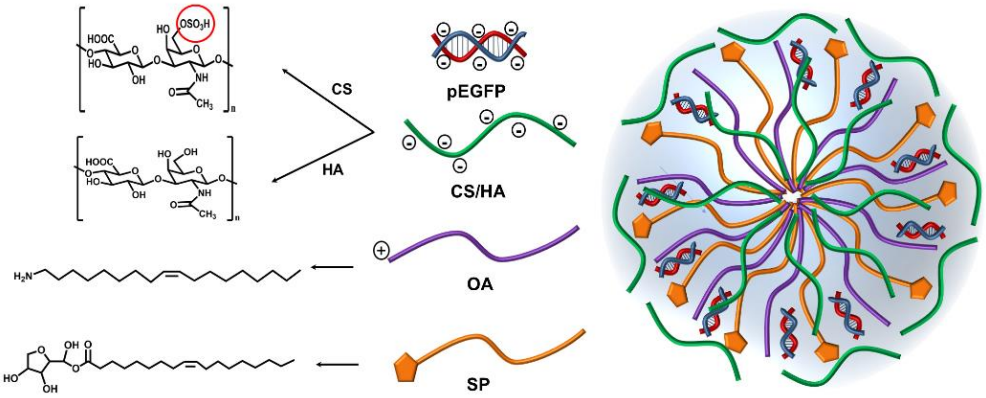

Figure 1. Schematic representation of hybrid nanosystem consisting of sorbitan ester-based nanoparticles decorated with chondroitin sulfate (CS) or hyaluronic acid (HA) and with associated pEGFP.

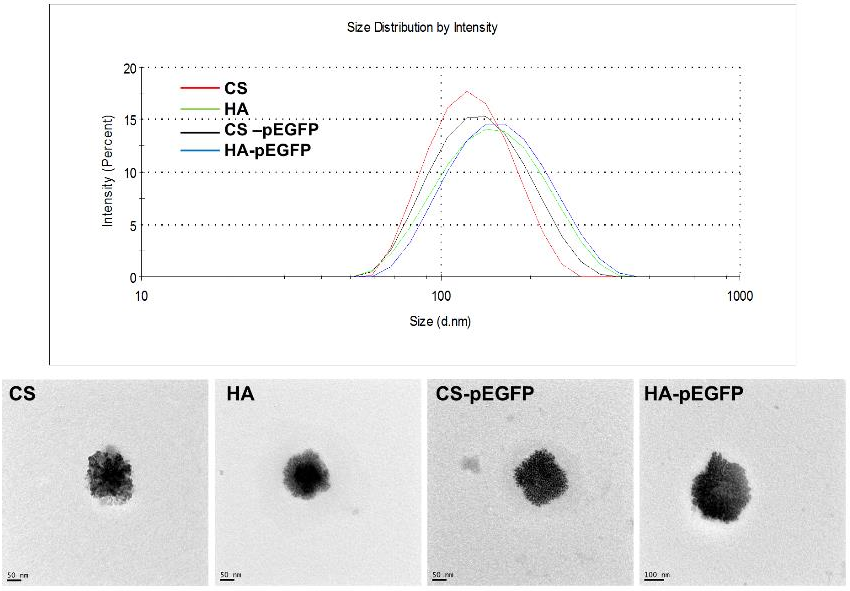

Figure 2. Particle size distribution measured with DLS, and TEM images of blank and pEGFP-loaded nanoparticles.

2.2. DNA binding efficacy

Agarose gel electrophoresis (Figure 3) shows that CS- and HA-decorated formulations have the ability to completely bind pEGFP, as evidenced by the absence of a free DNA band.

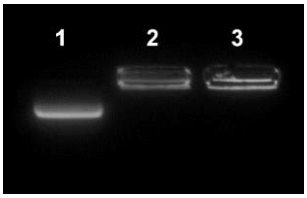

Figure 3. Agarose gel electrophoresis of (1) 200 μg/ml free pEGFP; (2) HA NPs associated with 200 μg/ml pEGFP; and (3) CS NPs associated with 200 μg/ml pEGFP.

2.3. Lyophilisation and stability

HA- and CS-decorated formulations loaded with pEGFP were stored at different temperatures, and their physicochemical properties were analysed after 3 and 12 months. As shown in Figure 4, the size and zeta potential of CS NPs were not significantly modified at any of the temperatures and times studied ($p>0.05$). In the case of HA nanoparticles, the zeta potential remained stable over time and temperature ($p>0.05$), but the size increased considerably from 120 nm to more than 300 and 700 nm after 3 and 12 months of storage at 37°C ($p<0.01$). Gel electrophoresis showed that the NPs were associated with the DNA even after 12 months of storage, although DNA degradation was observed for CS nanoparticles stored at 37°C (Figure 5).

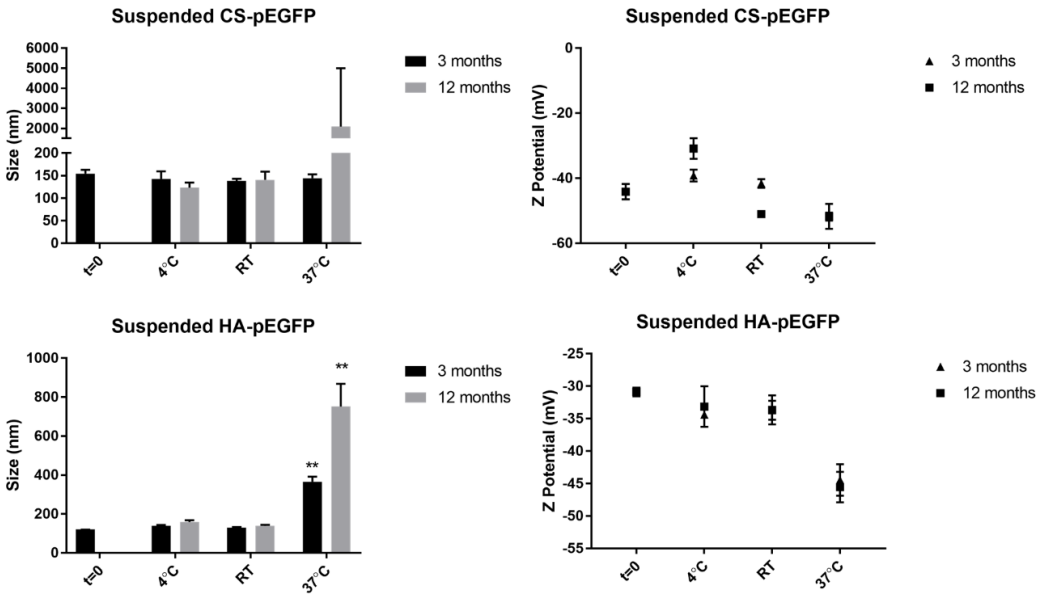

Figure 4. Size and zeta potential of pEGFP-loaded CS and HA NPs stored in suspension at different temperatures for 3 and 12 months. Error bars represents SD (n=3). **p<0.01 vs. samples at the initial time (t=0).

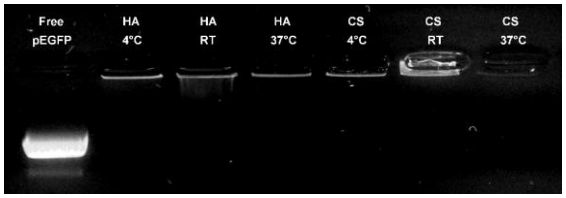

Figure 5. Agarose gel electrophoresis of free pEGFP and pEGFP-loaded HA and CS nanoparticles stored at 4°C, room temperature (RT) and 37°C.

After a preliminary screening of different sugars and their concentrations, 10% glucose and 10% sucrose were applied for lyophilisation of CS and HA nanoparticles, respectively. As shown in Figure 6A, the size of pEGFP-loaded NPs was slightly but significantly ($p<0.01$) increased from approximately 120 nm to 150 nm for both formulations after lyophilisation, while no significant difference in zeta potential was observed. Similar results were obtained for blank NPs, with small increases in size (120 nm to 130 for CS and 135 nm to 160 nm for HA) and zeta potential (-40 mV to -37 mV for CS and -32 mV for HA) for both formulations. Agarose gel electrophoresis was performed to evaluate the association with the plasmid after the freeze-drying process. As indicated by the free DNA bands observed in Figure 6B, lyophilisation decreased the ability of CS NPs to bind pEGFP, whereas the DNA binding property of the HA NPs was not modified.

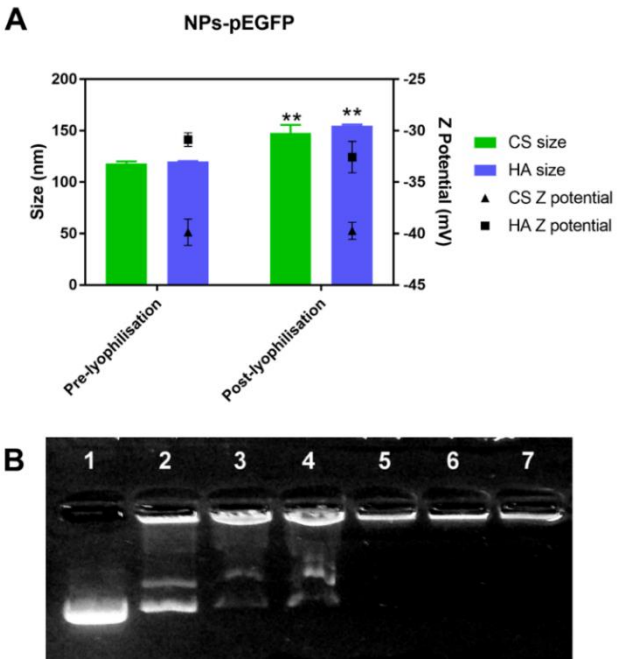

Figure 6A. Size and zeta potential of pEGFP-loaded NPs before and after lyophilisation. Error bars represents SD (n=3). **$p<0.01$ vs. pre-lyophilisation samples. **Fig. 6B**. Agarose gel electrophoresis of free pEGFP (1) and pEGFP-loaded

CS (2, 3, 4) and HA (5, 6, 7) NPs after lyophilisation. Some free DNA bands are observed for CS nanoparticles.

NPs were lyophilised and stored at different temperatures to determine the stability of the NPs in the absence of water. After 12 months of storage, the largest difference in the size of the lyophilised NPs was observed when stored at 37°C, increasing from approximately 140 nm to 180 nm for CS and from 150 nm to 180 nm for HA NPs ($p<0.01$) (Figure 7). The same pattern was observed for zeta potential, which decreased from -34 mV to -49 mV for both formulations.

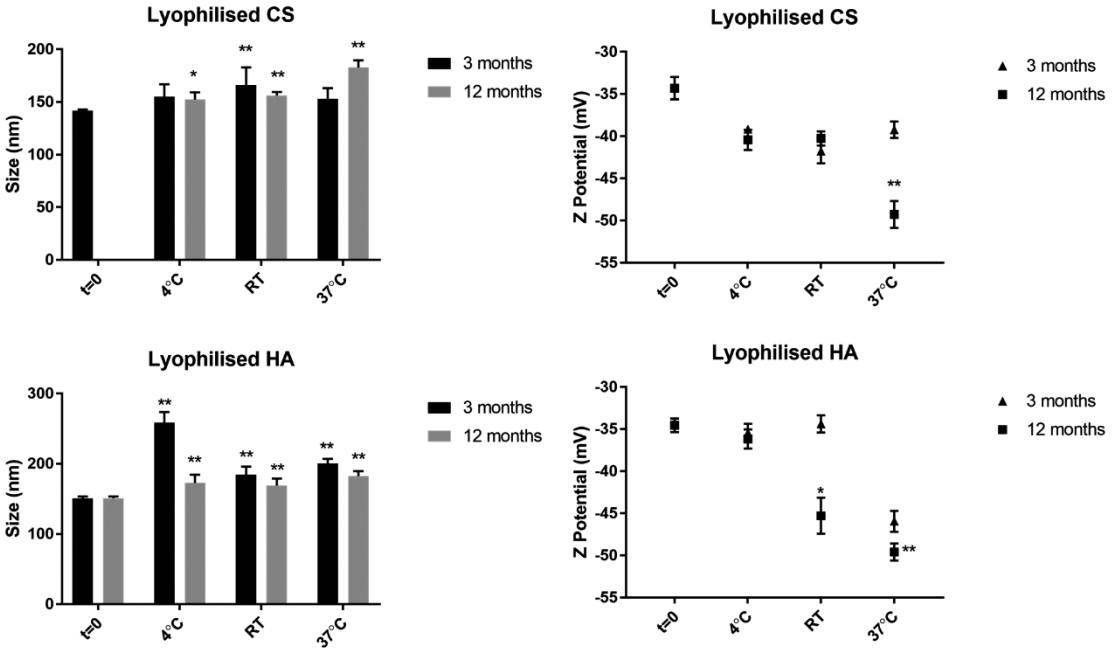

Figure 7. Size and zeta potential of resuspended CS and HA NPs after lyophilisation and storage for 3 and 12 months at 4°C, room temperature (RT) and 37°C. Error bars represent SD (n=3). *$p<0.05$ and **$p<0.01$ vs. samples at the initial time (t=0).

2.4. DNase protection assay

To demonstrate that the NPs protect DNA from endonucleases, DNase I was incubated with free DNA and NP-associated DNA, and DNA was subsequently released from the NPs using SDS. Figure 8 demonstrates the presence of DNA bands corresponding with DNA associated with CS and HA NPs (lanes 3 and 4, respectively) after incubation with DNase I, evidencing the absence of degradation. In contrast, the absence of any band in lane 2 demonstrates the ability of DNase I to degrade free DNA. SDS, which is a surfactant used for

DNA-NP disassembly, was responsible for the smeared DNA bands because it interferes with the electrophoretic mobility of DNA.

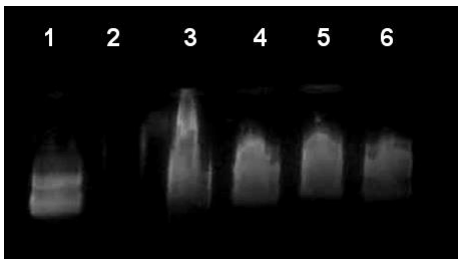

Figure 8. Agarose gel electrophoresis of free pEGFP and pEGFP released from nanoparticles after 1 hour of incubation with DNase I and subsequent pEGFP-NP disassembly mediated by SDS: Free pEGFP (2) and pEGFP-loaded CS (3) and HA (4) nanoparticles in the presence of DNase I. The controls include free pEGFP (1) and pEGFP-loaded CS (5) and HA (6) nanoparticles in the absence of DNase I.

2.5. Cell viability

Figure 9 shows A549 cell viability after incubation with CS and HA NPs at increasing concentrations determined with an XTT assay. Accordingly, the XTT assay results do not show a significant decrease in cell viability until the highest nanoparticle concentration tested (768 μg/ml; 58.63% for CS and 83.63% for HA). There is almost no difference in the effect of both formulations on cell viability, with a slightly higher decrease in cell viability observed with CS at 768 μg/ml being the only significant difference.

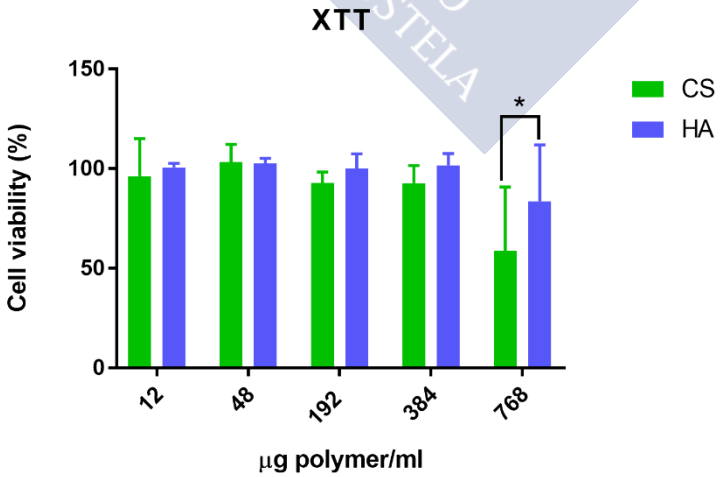

Figure 9. A549 cell viability determined with an XTT assay after incubation with increasing concentrations of CS and HA nanoparticles. Error bars represent SD (n=3). *p<0.05.

2.6. *In vitro* transfection

A549 cells were transfected with different doses of pEGFP-loaded NPs, and GFP expression was observed after 24 hours using fluorescence microscopy. As a positive control, Lipofectamine was used with 1 µg of pEGFP. As shown in Figure 10, efficient transfection can be achieved with both formulations.

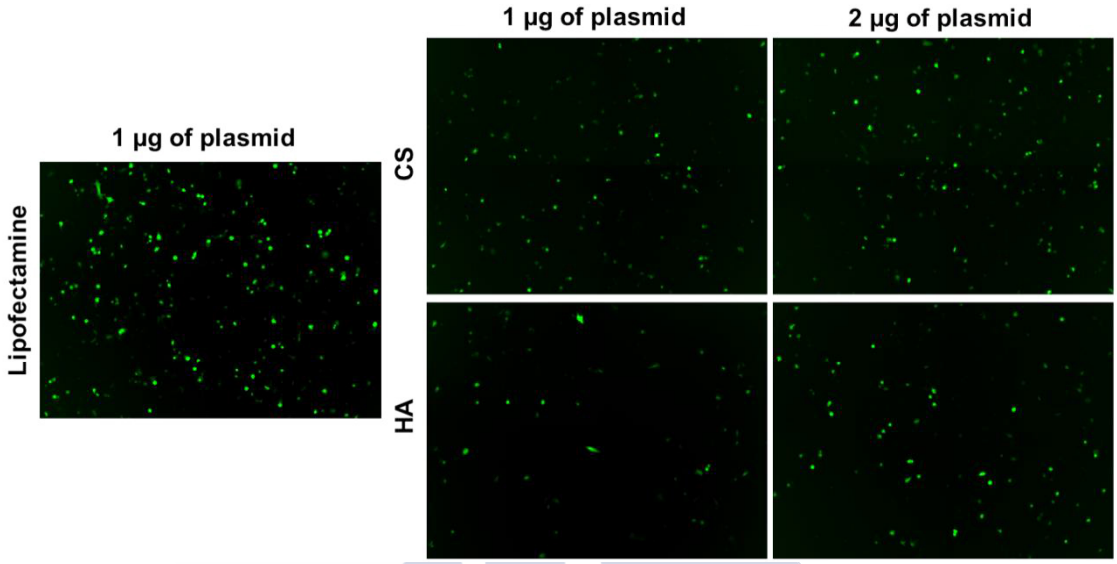

Figure 10. A549 cells expressing GFP 24 hours after transfection with pEGFP-loaded CS and HA nanoparticles at two different plasmid doses and NP concentrations. Lipofectamine was used as the positive control.

2.7. *In vivo* toxicity

The *in vivo* toxicity of pEGFP-loaded NPs was assessed after *iv* administration to mice by monitoring hepatic function through analysis of aspartate aminotransferase (AST) levels. As shown in Figure 11, comparable AST serum levels were found for CS NP-, HA NP- and non-treated animals, suggesting the absence of undesirable effects attributed to the developed nanosystems. To further corroborate the safety of the systems, their cytotoxic effects in the major mouse organs, including the kidney, liver, lung and spleen, were evaluated by performing histopathological studies. No obvious damage was observed in the samples analysed, indicating that the NPs are not toxic to major organs. These results indicate that CS and HA NPs are well tolerated delivery systems with non-immunogenic and biocompatible properties.

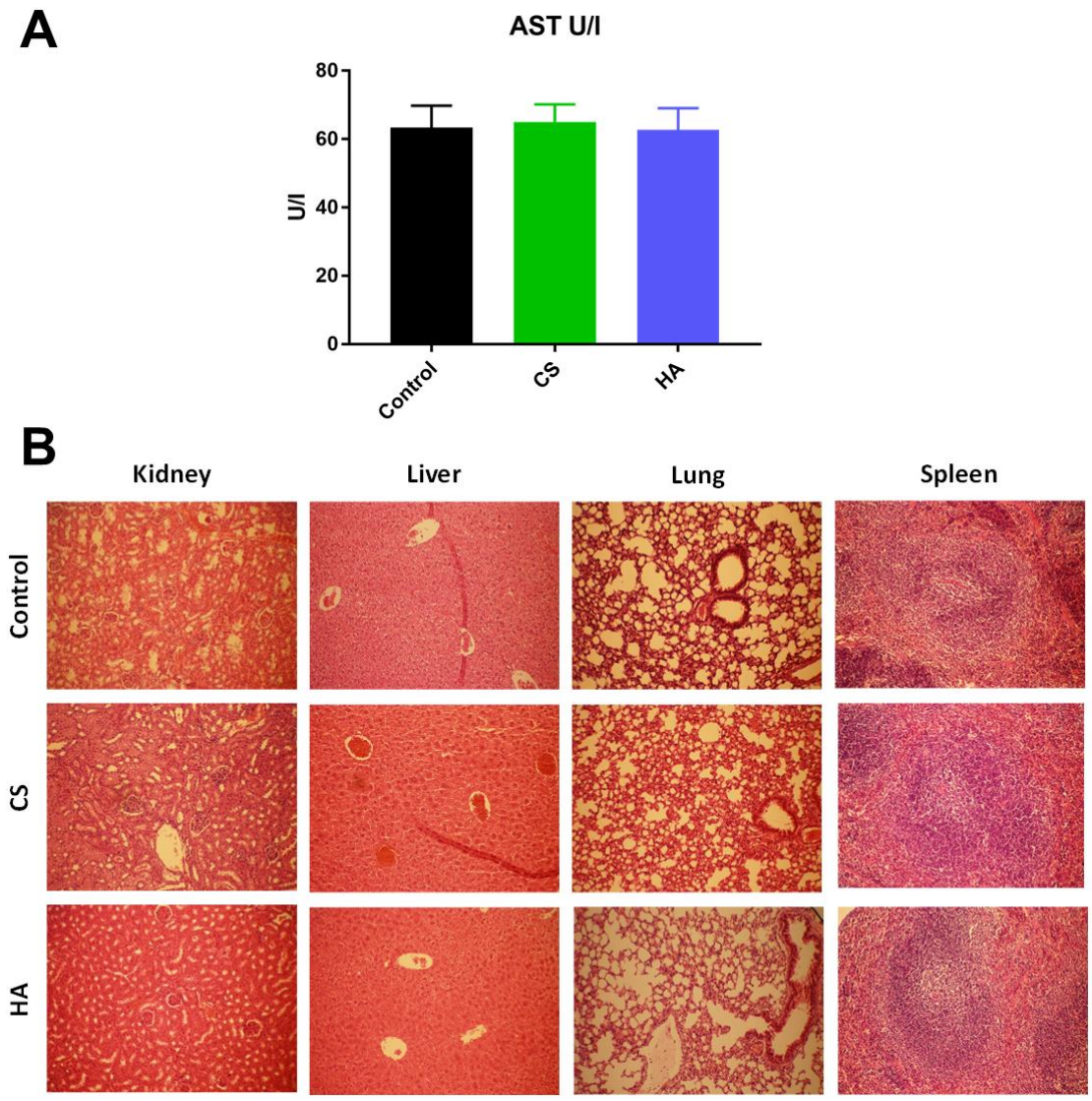

Figure 11A. Aspartate aminotransferase (AST) serum levels in mice 24 hours after iv injection with pEGFP-loaded CS and HA nanoparticles. **Fig. 11B**. Histopathological studies using H&E staining of kidney, liver, lung and spleen sections from mice systemically treated with pEGFP-loaded CS and HA nanoparticles.

3. Discussion

This study was designed to explore the potential of the natural polymers HA and CS to optimise the properties of our previously developed prototype of sorbitan ester-based nanoparticles. These polysaccharides possess properties that make them suitable for gene delivery systems, such as biodegradability, stability, low toxicity and low immunogenicity, and they can be easily modified. In addition, it has been described that CS and HA can enhance

gene transfection efficiency and improve the stability of NP systems (23, 27). However, incorporation of such components is not an easy task because they are hydrophilic macromolecules (carbohydrates with repeating units of saccharides joined by glycosidic linkages) that possess properties that are very different from those of the selected sorbitan ester, sorbitan monooleate. Consequently, our procedure to develop these polymer-lipid hybrid systems required a specific ´bridge´ among the different moieties and therefore a strategy to develop such a bridge. In this study, we resorted to incorporation of a hydrophobic cationic moiety able to satisfy three conditions: i) easily incorporated with the lipophilic sorbitan monooleate component; ii) developed electrostatic interactions with HA and CS polyanions to incorporate them into the final nanosystem; and iii) effectively associated with DNA as the bioactive molecule through electrostatic interactions. After a judicious selection of components, the selected material to build such a bridge was oleylamine (OA).

In our previous work, we demonstrated the solid structure of the sorbitan ester-based nanoparticles, in which there is a gradient of flexibility from a lipophilic rigid core to a hydrophilic flexible surface (28). In the case of the above-described self-assembled nanosystems associated with DNA we can assume that, once developed, the anionic polymers HA and CS tend to localise in the external and hydrophilic region of the nanoparticles, thus decorating the nanosystems (Figure 1). This would explain the change in the nanoparticle surface charge from positive (29) to negative after the polyanion incorporation. In addition, the size of the nanoparticles decreased with CS and HA incorporation (from 200 nm to 130-150 nm), which could be explained by an increase in the polymer packing due to electrostatic interactions and crosslinking of the different components. In addition, we observed that incorporation of pDNA into the systems did not interfere with the size and surface charge (Table 1). Taking into account that such DNA compaction could also be helpful for providing desired properties as gene delivery carriers, such as DNA protection against enzymatic degradation, we decided to evaluate this stabilising effect. As we have demonstrated, the developed nanosystems offer efficient protection of pDNA from DNAse I degradation (Figure 8).

The above-described effect of the incorporation of HA and CS could also be of interest in terms of stability. In this respect, it should be considered that delivery systems based on lipid components are characterised by their low stability in aqueous suspension, a property that limits their use and clinical success. However, we provide evidence that the developed nanosystems have considerable time and temperature stability in aqueous suspension (Figure 4). This

behaviour could be explained by structural differences compared with other lipid-based nanosystems, such as vesicular systems (i.e., liposomes), which are known for their stability limitations. We only observed increases in size and zeta potential after storage at 37°C, a result that could be explained by hydrolysis of the sorbitan monooleate molecules, resulting in free fatty acids that can partially neutralise the positive charge of OA, leading to a decrease in the superficial charge and to an increase in the size. This effect could also be a consequence of Ostwald ripening, with growth of the largest particles at the expense of the smallest ones (30).

Concerning stability against the lyophilisation process, we demonstrated the ability of the developed nanosystems to resist the lyophilisation process and maintain their physical properties (Figure 6), an ability of great value for shipping and long-term storage. Sugars are known to maintain lipid nanosystem stability during freeze-drying, and two different theories to explain this behaviour have been proposed. One of them is the water replacement theory, in which the sugars replace water between the polar head groups of the lipids. The second theory is known as the vitrification model and it assumes that the sugars form a glass matrix during freezing, with high viscosity and low mobility, which prevents lipid systems from aggregation and protects them from damage by ice crystals (31). Taking this into consideration, we hypothesise that the differences observed in DNA leakage among CS and HA NPs after lyophilisation could be explained by the different sugars used as lyoprotectants (glucose versus sucrose) (Figure 6A). In addition, it is possible that differences in the NP packing could interfere with the sugar disposition among the NP components.

From previous work (29) and previous studies, we know that non-functionalised sorbitan monooleate-oleylamine nanoparticles do not interfere with cell viability, even when higher concentrations were tested on the same cell line. Different studies have shown that incorporation of HA and CS into delivery systems did not increase toxicity *in vitro* (32, 33) or even decreased the toxicity of the systems (13, 14, 16, 34). Another study showed an increase in the cytotoxicity of gemcitabine-loaded liposomes when HA was incorporated into the system and explained that this effect was due to an increase in the cellular uptake of the liposomes mediated by the CD44 receptor (35). Considering this, we hypothesise that the higher cytotoxicity observed with the developed nanosystems after incorporation of HA and CS (Figure 9) in comparison with the non-functionalised NPs is a simple consequence of the higher uptake rate of the former. In any case, high transfection efficiencies were achieved at low nanosystem doses without compromising cell viability (Figure 10), which allowed us to

conclude that the developed nanosystems are characterised by an appropriate efficacy-toxicity balance *in vitro.* On the basis of these data, we decided to test the *in vivo* toxicity of the developed nanosystems (Figure 11). No signs of toxicity or inflammation were observed after systemic administration of the developed nanosystems to mice, therefore also demonstrating their innocuity *in vivo,* which further supports the high clinical potential of the developed nanosystems.

4. Conclusions

Herein, we confirm that molecules with high biological value and targeting potential, such as HA and CS, can be successfully incorporated into our recently developed sorbitan ester-based nanoparticles and that such incorporation leads to effective stabilisation of both nanosystems and protection of a delicate bioactive molecule associated with them, such as DNA. Concretely, we have demonstrated that the aforementioned incorporation of HA and CS supports long-term stability of the nanosystems in both liquid and lyophilised states, which is a remarkable property that may aid their transfer to industry. The ability of these functionalised nanosystems to transfect the A549 cell line without compromising cell viability was also shown, as well as their innocuous safety profile *in vivo*. Thus, we provide valuable evidence of the suitable properties and potential of these hybrid nanoparticles as gene delivery systems.

References

1. Naldini L. Gene therapy returns to centre stage. Nature. 2015 Oct 15;526(7573):351-60.

2. Collins M, Thrasher A. Gene therapy: progress and predictions. Proceedings of the Royal Society B: Biological Sciences. 2015 04/21;282(1821):20143003.

3. Pahle J, Walther W. Vectors and strategies for nonviral cancer gene therapy. Expert Opin Biol Ther. 2016;16(4):443-61.

4. Zaimy MA, Saffarzadeh N, Mohammadi A, Pourghadamyari H, Izadi P, Sarli A, et al. New methods in the diagnosis of cancer and gene therapy of cancer based on nanoparticles. Cancer Gene Ther. 2017 Jun;24(6):233-43.

5. Swami R, Singh I, Khan W, Ramakrishna S. Diseases originate and terminate by genes: unraveling nonviral gene delivery. Drug Deliv Transl Res. 2013 Dec;3(6):593-610.

6. Yin H, Kanasty RL, Eltoukhy AA, Vegas AJ, Dorkin JR, Anderson DG. Non-viral vectors for gene-based therapy. Nat Rev Genet. 2014 Aug;15(8):541-55.

7. Ding W, Wang F, Zhang J, Guo Y, Ju S, Wang H. A novel local anti-colorectal cancer drug delivery system: negative lipidoid nanoparticles with a passive target via a size-dependent pattern. Nanotechnology. 2013 Sep 20;24(37):375101,4484/24/37/375101. Epub 2013 Aug 21.

8. Schlenk F, Grund S, Fischer D. Recent developments and perspectives on gene therapy using synthetic vectors. Ther Deliv. 2013 Jan;4(1):95-113.

9. Li L, Song L, Yang X, Li X, Wu Y, He T, et al. Multifunctional "core-shell" nanoparticles-based gene delivery for treatment of aggressive melanoma. Biomaterials. 2016 Dec;111:124-37.

10. Harris TJ, Green JJ, Fung PW, Langer R, Anderson DG, Bhatia SN. Tissue-specific gene delivery via nanoparticle coating. Biomaterials. 2010 Feb;31(5):998-1006.

11. Almalik A, Day PJ, Tirelli N. HA-coated chitosan nanoparticles for CD44-mediated nucleic acid delivery. Macromol Biosci. 2013 Dec;13(12):1671-80.

12. Raemdonck K, Martens TF, Braeckmans K, Demeester J, De Smedt SC. Polysaccharide-based nucleic acid nanoformulations. Adv Drug Deliv Rev. 2013 Aug;65(9):1123-47.

13. Yin H, Zhao F, Zhang D, Li J. Hyaluronic acid conjugated beta-cyclodextrin-oligoethylenimine star polymer for CD44-targeted gene delivery. Int J Pharm. 2015 Apr 10;483(1-2):169-79.

14. Urbiola K, Sanmartin C, Blanco-Fernandez L, Tros de Ilarduya C. Efficient targeted gene delivery by a novel PAMAM/DNA dendriplex coated with hyaluronic acid. Nanomedicine (Lond). 2014 Dec;9(18):2787-801.

15. Ran R, Liu Y, Gao H, Kuang Q, Zhang Q, Tang J, et al. Enhanced gene delivery efficiency of cationic liposomes coated with PEGylated hyaluronic acid for anti P-glycoprotein siRNA: a potential candidate for overcoming multi-drug resistance. Int J Pharm. 2014 Dec 30;477(1-2):590-600.

16. Imamura M, Kodama Y, Higuchi N, Kanda K, Nakagawa H, Muro T, et al. Ternary complex of plasmid DNA electrostatically assembled with polyamidoamine dendrimer and chondroitin sulfate for effective and secure gene delivery. Biol Pharm Bull. 2014;37(4):552-9.

17. He Y, Cheng G, Xie L, Nie Y, He B, Gu Z. Polyethyleneimine/DNA polyplexes with reduction-sensitive hyaluronic acid derivatives shielding for targeted gene delivery. Biomaterials. 2013 January 2013;34(4):1235-45.

18. Kim EJ, Cho HJ, Park D, Kim JY, Kim YB, Park TG, et al. Antifibrotic effect of MMP13-encoding plasmid DNA delivered using polyethylenimine shielded with hyaluronic acid. Mol Ther. 2011 Feb;19(2):355-61.

19. Naik RJ, Sharma R, Nisakar D, Purohit G, Ganguli M. Exogenous chondroitin sulfate glycosaminoglycan associate with arginine-rich peptide-DNA complexes to alter their intracellular processing and gene delivery efficiency. Biochim Biophys Acta. 2015 Apr;1848(4):1053-64.

20. Ohya Y, Takeda S, Shibata Y, Ouchi T, Maruyama A. Preparation of Highly Stable Biodegradable Polymer Micelles by Coating with Polyion Complex. Macromolecular Chemistry and Physics. 2010;211(16):1750-6.

21. Ohya Y, Takeda S, Shibata Y, Ouchi T, Kano A, Iwata T, et al. Evaluation of polyanion-coated biodegradable polymeric micelles as drug delivery vehicles. J Control Release. 2011 Oct 10;155(1):104-10.

22. Ran R, Liu Y, Gao H, Kuang Q, Zhang Q, Tang J, et al. Enhanced gene delivery efficiency of cationic liposomes coated with PEGylated hyaluronic acid for anti P-glycoprotein siRNA: A potential candidate for overcoming multi-drug resistance. International Journal of Pharmaceutics. 2014 30 December 2014;477(1):590-600.

23. Zhao L, Liu M, Wang J, Zhai G. Chondroitin sulfate-based nanocarriers for drug/gene delivery. Carbohydr Polym. 2015 Nov 20;133:391-9.

24. Ulery BD, Nair LS, Laurencin CT. Biomedical Applications of Biodegradable Polymers. J Polym Sci B Polym Phys. 2011 Jun 15;49(12):832-64.

25. Frohlich E. The role of surface charge in cellular uptake and cytotoxicity of medical nanoparticles. Int J Nanomedicine. 2012;7:5577-91.

26. del Pozo-Rodriguez A, Solinis MA, Gascon AR, Pedraz JL. Short- and long-term stability study of lyophilized solid lipid nanoparticles for gene therapy. Eur J Pharm Biopharm. 2009 Feb;71(2):181-9.

27. Mokhtarzadeh A, Alibakhshi A, Yaghoobi H, Hashemi M, Hejazi M, Ramezani M. Recent advances on biocompatible and biodegradable nanoparticles as gene carriers. Expert Opin Biol Ther. 2016 Jun;16(6):771-85.

28. Pensado A, Martin-Pastor M, Zorzi GK, Carvalho ES, Sanchez A. Structural analysis of nanosystems: Solid Sorbitan esters Nanoparticles (SSN) as a case study. Eur J Pharm Biopharm. 2016 Jul;104:189-99.

29. Pensado A, Fernandez-Pineiro I, Seijo B, Sanchez A. Anionic nanoparticles based on Span 80 as low-cost, simple and efficient non-viral gene-transfection systems. Int J Pharm. 2014 Dec 10;476(1-2):23-30.

30. Delmas T, Couffin AC, Bayle PA, de Crecy F, Neumann E, Vinet F, et al. Preparation and characterization of highly stable lipid nanoparticles with amorphous core of tuneable viscosity. J Colloid Interface Sci. 2011 Aug 15;360(2):471-81.

31. Chen C, Han D, Cai C, Tang X. An overview of liposome lyophilization and its future potential. J Control Release. 2010 Mar 19;142(3):299-311.

32. Leite Nascimento T, Hillaireau H, Vergnaud J, Rivano M, Delomenie C, Courilleau D, et al. Hyaluronic acid-conjugated lipoplexes for targeted delivery of siRNA in a murine metastatic lung cancer model. Int J Pharm. 2016 Nov 30;514(1):103-11.

33. Mizrahy S, Raz SR, Hasgaard M, Liu H, Soffer-Tsur N, Cohen K, et al. Hyaluronan-coated nanoparticles: the influence of the molecular weight on CD44-hyaluronan interactions and on the immune response. J Control Release. 2011 Dec 10;156(2):231-8.

34. Park JH, Cho HJ, Yoon HY, Yoon IS, Ko SH, Shim JS, et al. Hyaluronic acid derivative-coated nanohybrid liposomes for cancer imaging and drug delivery. J Control Release. 2014 Jan 28;174:98-108.

35. Arpicco S, Lerda C, Dalla Pozza E, Costanzo C, Tsapis N, Stella B, et al. Hyaluronic acid-coated liposomes for active targeting of gemcitabine. Eur J Pharm Biopharm. 2013 Nov;85(3 Pt A):373-80.

USC
UNIVERSIDADE
DE SANTIAGO
DE COMPOSTELA

Chapter III

MicroRNA-20a-loaded sorbitan ester nanoparticles reduces murine colorectal cancer metastasis to the liver

USC
UNIVERSIDADE
DE SANTIAGO
DE COMPOSTELA

Abstract

Phenotypic transformation of liver sinusoidal endothelial cells is one of the most important stages of liver metastasis progression. The miRNA effects on liver sinusoidal endothelial cells during liver metastasis have not yet been analysed. Herein, analysis of miRNA expression in these cells during colorectal liver metastasis revealed repressed expression of microRNA-20a. Importantly, downregulation of miR-20a occurs in parallel with upregulation of its known protein targets. To restore normal miR-20a levels in liver sinusoidal endothelial cells, we developed chondroitin sulfate-sorbitan ester nanoparticles conjugated with miR-20a in a delivery system that specifically targets liver sinusoidal endothelial cells. The restoration of normal mir-20a levels in these cells induced downregulation of the expression of its protein targets, and this also resulted in a reduction of *in vitro* LSEC migration and a reduction of *in vivo* activation and tumour-infiltrating capacity and ability of the tumour decreased by approximately 80% in a murine liver metastasis model.

1. Introduction

Colorectal cancer is the third most frequently occurring cancer and a common cause of cancer-related death worldwide (1). The origin of colorectal cancer is usually a malignant polyp developed in the mucosa of the intestine (2). Once the cells of the polyp acquire malignant properties they can detach from the primary tumour and spread throughout the body, invading other organs(3). One of the most common metastatic target organs is the liver (4). Because of its anatomic position and special histologic architecture, the liver is frequently metastasized by different cancer types. Special fenestrated capillaries called sinusoids irrigate the liver tissue, and these blood vessels facilitate the infiltration of tumour cells (5). Once the tumour cells are trapped in the sinusoids, they migrate into the tissue parenchyma and grow, thus initiating metastasis. Then, liver cells that are in proximity of tumour undergo deep phenotype changes (6), which include phenotypic transformation of liver sinusoidal endothelial cells (LSECs), one of the most important events in liver metastasis (7). LSECs from the fenestrated capillaries of hepatic sinusoids are the first hepatic cell line that interacts with metastatic cells. Upon such interaction, LSECs activate the production of proinflammatory chemokines that generate a favourable environment for tumour growth (8).

One unexplored potential mechanism of LSEC activation is an alteration in cellular epigenetic regulators, in particular microRNAs (miRNAs). miRNAs are small double-stranded RNA molecules comprising 18-22 nucleotides that negatively regulate protein expression by targeting complementary messenger RNAs (mRNAs)(9). The importance of miRNAs has been described in a great variety of physiological processes, such as development (10) and derivation of stem cells, including hepatic cells,(11) as well as in diseases such as cancer(12) and neurodegeneration (13). In cancer, miRNAs have been shown to play important roles in malignancy processes, which are sometimes associated with their overexpression (14) and other times with their downregulation (15). Among their broad range of features, there is one feature that makes them especially interesting as therapeutic candidates: their multitarget capacity. As binding to the mRNA does not necessarily require 100% complementarity, a single miRNA can bind to many different mRNAs, thus simultaneously blocking protein translation of multiple targets (16),(17). This also entails the possibility of side effects that could emerge if miRNA were to be delivered indiscriminately throughout the body. Herein, we shed light on the physiological significance of miRNA deregulation in LSECs and on the potential therapeutic applications derived from a careful choice of miRNA delivery system. In this regard, it is of key importance to guide miRNAs to the specific target cells we want to treat. miRNA instability in serum along with its inability to cross biological membranes makes it necessary to incorporate them into delivery systems to enhance protection and specific cell-targeting. In this way, nanocarriers have emerged as a promising miRNA delivery tool (18). Thus, we have recently developed and patented sorbitan ester-based nanoparticles

and provided an *in vivo* proof of concept regarding their safety and efficacy for gene therapy (19, 20). Here, we developed chondroitin sulfate-functionalized nanoparticles (SP-OA-CS), and we tested them by loading them with specific miRNA for delivery to LSECs in an attempt to explore their therapeutic potential against liver metastasis progression.

2. Materials and methods

2.1. Animals

Balb/c mice (6- to 8-week-old males) were obtained from Charles River Laboratories Spain S.A. (Barcelona, Spain). All the procedures were approved by the Ethical Committee for Animal Experimentation (CEEA) of the University of the Basque Country (EHU/UPV) in accordance with institutional, national and international guidelines regarding the protection and care of animal use for scientific purposes (CEBA/237/2012/BADIOLA ETXABURU). Mice were kept in the animal facility of EHU/UPV and had access to standard chow and water ad libitum.

2.2. Colorectal cancer cells

Murine colorectal cancer C26 cells (ATCC, Manassas, VA) syngeneic with Balb/c mice were used. The cells were grown under standard conditions in RPMI medium (Sigma-Aldrich; St. Louis, MO, USA) supplemented with 10% fetal bovine serum (FBS), penicillin (100 U/ml), streptomycin (100 µg/ml) and amphotericin B (0.25 µg/ml), all purchased from Life technologies, Carlsbad, CA.

2.3. Control and tumour-activated LSECs

Balb/c mice were anesthetized with isoflurane, and a small cut was made in their left broadside. Then, 50 µl of C26 colon carcinoma cells at a concentration of 2 x 10^6 cells/ml were inoculated into the spleen of each mouse, and the peritoneum and skin were sutured. The control mice were inoculated with PBS. Fourteen days later, all mice were sacrificed, and the tumour-activated LSECs and control LSECs were isolated by Percoll (Sigma-Aldrich; St. Louis, MO, USA) gradient (25% on top of 50%) differential centrifugation. LSECs were seeded with RPMI 1640 medium containing 10% FBS, and finally, RNA purification was performed following the protocol of a Purelink RNA minikit (Gibco Life Technologies Inc., Gaithersburg, MD).

2.4. miRNA microarray analysis

The purified total RNA was analysed using Agilent mouse miRNA microarrays. Release 18.0, 8x60K (v18) microarray slides (Agilent Technologies, USA), with 1,200 mouse miRNAs represented, were used. Briefly, 100 mg of total RNA was labelled and hybridized following

the standard Agilent Protocol for the miRNA Microarray System with a miRNA Complete Labelling and Hybridization Kit, including Agilent miRNA Spike-ins, and the results were scanned using an Agilent Microarray Scanner G2565CA (Agilent Technologies, USA). The scanned TIFF image files were processed using Agilent Feature Extraction Software vs 10.7.3.1 to extract raw data and obtain QC reports. The microarray raw data were normalized using the quantile method. To find the statistically significant differentially expressed miRNAs (DEMs) between two groups of samples, we calculated the mean of each probe across all the samples of the group. Next, we filtered out all the probes whose absolute value of the difference of mean values between the two groups was less than a selection threshold θ_{DEM} = 4 (that corresponds to a fold change of 2 in $\log_2$ scale), and we applied a Student's t-test with a significance threshold α_{DEM} = 0.05. The PCA and the hierarchical clustering of genes and samples were performed with one minus the correlation metric and the unweighted average distance (UPGMA) linkage method. All the analysis algorithms and graphics were implemented functions in Matlab.

2.5. miRNA microarray data validation with miRNA RT-qPCR

The microarray data of three of the most downregulated miRNAs (miR-20a, miR-29 and miR-93) were validated with real-time PCR (RT-qPCR) using a miRCURY LNA™ Universal RT microRNA PCR system (Exiqon, Denmark), following the manufacturer's instructions. Then, 50 ng of total RNA was used for cDNA synthesis using a Universal cDNA synthesis kit II (Exiqon, Denmark). cDNA was amplified in triplicate in a 7900 HT Fast Real Time System (Life Technologies, USA) using microRNA LNA primer sets for the specified miRNAs (Exiqon, Denmark) and ExiLENT SYBR® Green master mix (Exiqon, Denmark). The expression of miRNAs was normalized to the SNORD68 control gene, and the relative expression was calculated with the 2-ΔΔCt method (21).

2.6. Quantitative mass spectrometric analysis of liver sinusoidal endothelial cells

Isolated tumour-activated LSECs and control LSECs were independently processed for mass spectrometric analysis as previously described (22). Briefly, samples were shortly separated in a polyacrylamide gel, and proteins were reduced with dithiothreitol, alkylated with iodoacetamide, and digested with trypsin. After extraction, the peptides were finally resuspended in 0.1% trifluoroacetic acid. Approximately 500 ng of peptides were subsequently separated on an Ultimate 3000 rapid separation liquid chromatography system (Thermo Fisher Scientific, Dreieich, Germany) and analysed on an Orbitrap Elite (Thermo Fisher Scientific, Dreieich, Germany) hybrid mass spectrometer (supplemental methods).

2.7. Preparation and characterization of control SP-OA-CS, SP-OA-CS associated with pEGFP and SP-OA-CS associated with miRNA

For construction of the nanoparticles, a solution of sorbitan monooleate (Span 80, SP) and oleylamine (OA) (Sigma-Aldrich; St. Louis, MO, USA) was prepared in ethanol at a concentration of 6,6 and 0,33 mg/ml, respectively. Then, this organic phase was added under magnetic stirring to an aqueous phase containing chondroitin sulfate (CS) (Calbiochem, USA) at a concentration of 0,125 mg/ml, in a volume ratio of 1:2, respectively. Ethanol was removed under reduced pressure on a rotary evaporator. For the encapsulation of genetic material, this was included in the aqueous phase during the construction of the nanoparticles at concentrations of 33,3 μg/ml for Enhanced Green Fluorescent Protein plasmid (pEGFP) (Elim Biopharmaceutics, USA) and 8,33 μg/ml and 16,7 μg/ml for miRNA (miR-20 or miR-control) (Exiqon, Denmark). The final formulations obtained were 200 μg/ml pEGFP-loaded NPs, 50 and 100 μg/ml miRNA-loaded NPs. Formulations were administered in a 5% glucose solution for the *in vivo* studies. The efficiency of the association of the plasmid DNA and the miRNAs was determined by agarose gel electrophoresis. The morphology of the nanoparticles was examined with transmission electron microscopy (CM 12 Philips, Eindhoven, The Netherlands) after staining with 2% w/v phosphotungstic acid solution. For this purpose, the samples were placed on copper grids (400 mesh) coated with a Formvar® film.

2.8. In vivo validation of nanoparticle-specific targeting to LSECs

To confirm the specific targeting of the SP-OA-CS nanoparticles associated with pEGFP to LSECs, Balb/c mice were systemically inoculated via the tail vein with nanoparticles, and after 48 h, the mice were sacrificed by cervical dislocation. The livers were collected and frozen, and different sections at different levels of each organ were prepared with a cryostat. Finally, the nanoparticle green fluorescence in the sections was analysed using fluorescence microscopy (Zeiss Axioskope).

2.9. Western blot analysis of LESCs activated with tumour-conditioned medium.

Western blotting analysis was performed with tumour-activated LSECs and tumour-activated LSECs cultured with exogenous miR20a. In brief, LSEC cultures were lysed with RIPA buffer, separated through 8% SDS-PAGE electrophoresis and blotted onto a nitrocellulose membrane (Bio-Rad Laboratories, Hercules, CA). E2 transcription factor 1 (E2F1) (Santa Cruz Biotechnology, Dallas, Texas, USA) and Rho GTPase activating protein (ARHGAP1) (Abcam, Cambridge, UK) (1:1000) were detected using horseradish peroxidase-conjugated protein A (1:5,000) (Sigma-Aldrich; St. Louis, MO, USA). The bands were visualized using a Super Signal Femto Substrate kit (Pierce Chemical Co, Rockford, IL). GAPDH was used as a protein loading control.

2.10. Migration of tumour-activated LSECs

A tumour-activated LSEC migration assay was performed on modified Boyden chambers. Briefly, LSECs were cultured onto an 8 µm-diameter pore membrane (Greiner Bio-One, La Jolla, CA, USA) precoated with collagen type I 10 µg/ml (Sigma-Aldrich; St. Louis, MO, USA) at a concentration of 2×10^5 cells/ml. Then, cells were allowed to migrate for 24 h in the presence of different treatments. Migrated cells were quantified after 4% formalin fixation and crystal violet staining (Sigma-Aldrich, St. Louis, MO, USA). The results were calculated from three independent experiments, and data were expressed as the mean of total migrated cells per membrane.

2.11. *In vivo* colorectal cancer liver metastasis development and histological liver tissue analysis

To develop an experimental colorectal cancer liver metastasis model, Balb/c mice were anesthetized with isoflurane (Esteve, Spain), and a small cut was made in their left side. Then, the spleen was exposed to perform an intrasplenic inoculation of 50 µl of C26 colon carcinoma cells at a concentration of 2 $x10^6$ cells/ml for each mouse. The animals were divided into 5 groups, and the treatments were performed every 3 days from the day of the inoculation of cancer cells. Finally, the livers were embedded in paraffin and frozen for histological analyses. To quantify the occupied tumour area, consecutive 7-µm sections were cut with 500 µm between them in paraffin embedded livers. Then, haematoxylin and eosin staining was performed, and the tumour area was quantified using ImageJ Software. In addition, to analyze the potentially activated infiltrating LSECs in the metastasized area, immunostaining with 1:100 dilution of anti-CD31 monoclonal antibody was performed (BD Pharmingen, USA), followed by the appropriate secondary fluorescent Alexa 594 (1:1000) antibody. Images were quantified using the AnalySIS V3.2 program (Olympus Software Imagine Solutions GMBH, Munster, Germany). The results are expressed as a percentage of specifically coloured tissue area relative to the entire analysed area.

3. Results

3.1. The purity of LSEC primary culture is higher than 95%

LSECs were isolated from mice 15 days after inoculation of colorectal cancer C26 tumor cells (Figure 1A). The isolated control and tumour-activated LSEC purity was confirmed by an immunostaining assay as described in materials and methods. More than 95% of the cells in the LSEC cultures were positive for the CD31 marker (Figure 1B). These cells were used to run a microarray analysis to detect which miRNAs were deregulated in LSECs when livers were colonized by tumour cells compared with control livers.

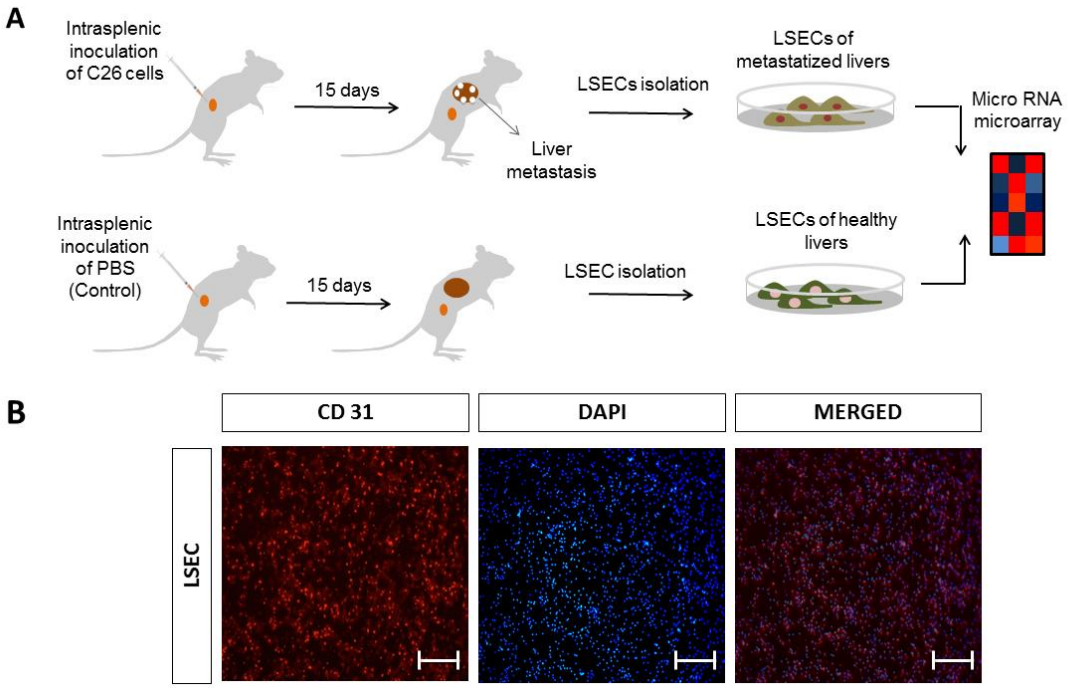

Figure 1. Induction and isolation tumour-activated LSECs. (A) Experimental design: Two groups of mice were inoculated with C26 murine colon cancer cells and with PBS (Control). After 15 days, the mice were perfused and after Percoll ® gradient centrifugation, the LSECs were isolated and miRNA expression microarrays of both cultures were performed. (B) The purity of the LSEC culture was tested by inmunocytochemical analysis. The cells were stained to detect CD31 expression, cell culture purity was analysed using Image J, and the result indicated a purity of up to 95%.

3.2. miRNA microarray assay reveals changes in miRNA expression between tumour activated LSECs and control LSECs.

A 16 k microarray was run to detect changes in miRNA expression in LSECs obtained from tumour-colonized and control livers. The global analysis of the whole genome miRNA expression revealed that tumour-colonized LSECs and healthy LSECs have a very distinct miRNA expression fingerprint, distinct both in the principal component analysis (PCA) shown in Figure 2B and in the hierarchical clustering (Figure 2C). We searched for the most deregulated miRNAs (Figure 2D and Figure 2E) and found 33 miRNAs that were significantly ($p<0,005$) downregulated in tumour-colonized LSEC samples relative to non-colonized samples (Figure 2A). miR-20a, miR-29 and miR-93 were among the most significantly downregulated miRNAs (Figure 2D and Figure 2E). These miRNAs were validated using qPCR. Among these, the most deregulated was miR-20a, with a negative fold change of more than 7 (Figure 2F).

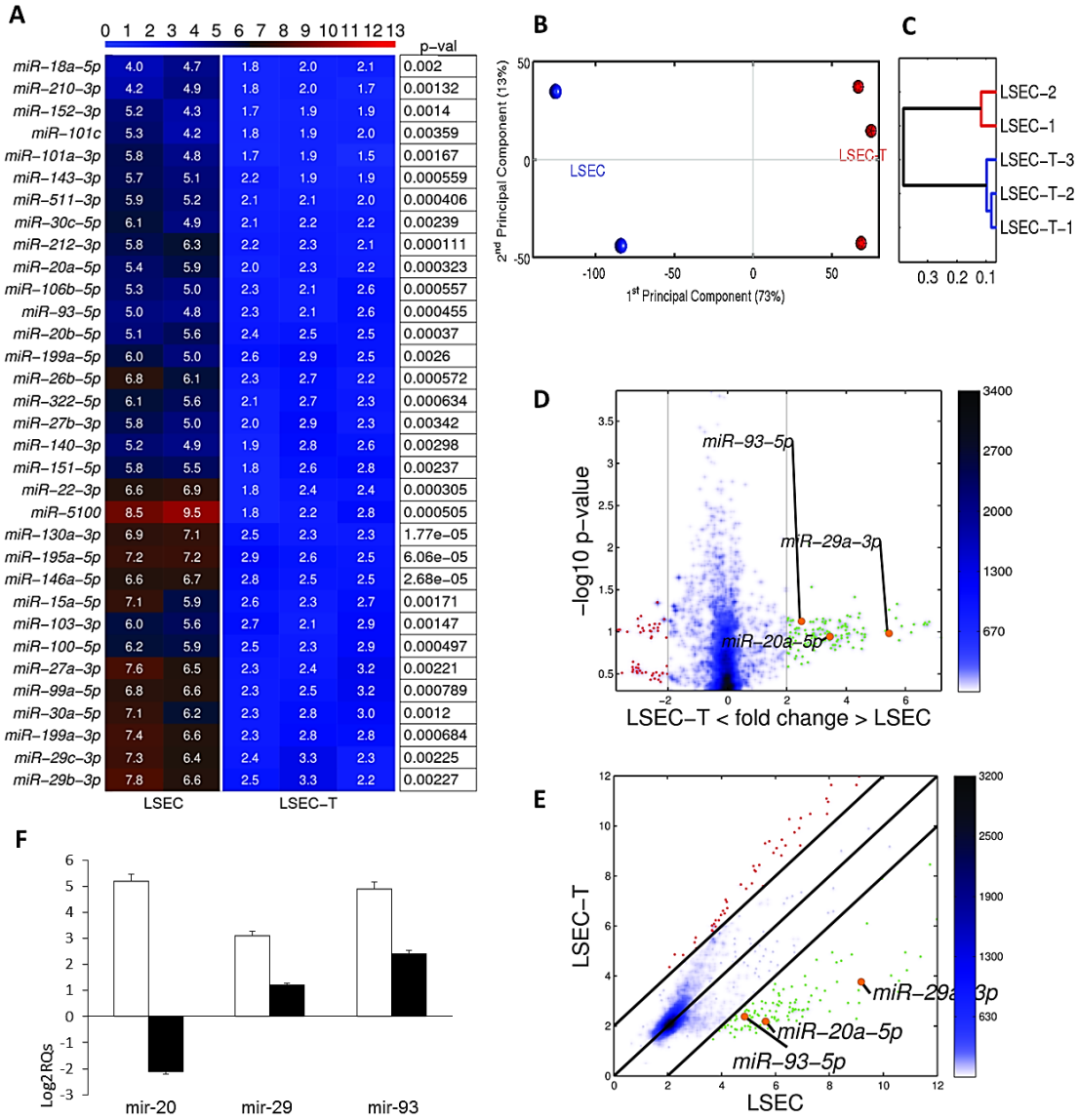

Figure 2. The miRNA expression fingerprint of control and tumour activated LSECs (A) Heat map of the expression of the top 33 most significantly downregulated miRNAs in LSECs colonized by the tumour **(LSEC-T)** relative to healthy **LSECs.** The miRNA expression is represented on a $\log_2$ scale. Higher and lower expression corresponds to a redder and bluer colour, respectively. The colour bar on the top codifies the miRNA expression. The table to the right provides the p-values calculated using a t-test. (B) Principal Component Analysis (PCA) of miRNA expression. (C) Hierarchical clustering of miRNA expression performed with the correlation metric and the average linkage method. (D) Volcano plot of **LSEC** vs **LSEC-T**. The black vertical lines represent the boundaries of the 2-fold changes (in log2 scale) in miRNA expression (E) Pairwise scatter plot of **LSEC** vs **LSEC-T**. The black lines represent the boundaries of the 2-fold changes (in $\log_2$ scale) in miRNA expression levels. Transcripts up- and downregulated in LSEC-T compared with LSECs are shown with red and green dots, respectively. The positions of the three selected miRNAs are shown as orange dots. The colour bar indicates the scattering density. The darker blue colour corresponds to higher scattering

density. The transcript expression levels are log2 scaled. (F) RT-PCR of the three selected miRNAs, where the expression change is compared between healthy LSECs (white) and tumour-activated LSECs (black).

3.3. E2F1 and ARHGAP1 miR-20a target proteins were upregulated in LSECs colonized by the tumour relative to healthy LSECs

We used the miRBASE database (www.mirbase.org) to identify 713 proteins as possible miR-20a targets. In parallel, in a proteomic study, we identified 174 proteins that were upregulated in tumour-activated LSECs compared with control LSECs. When both data sets were compared, 5 coincidentally expressed proteins were found: E2F1, JAK1, ARHGAP1, ACSL4 and DECR1 (Figure 3A).

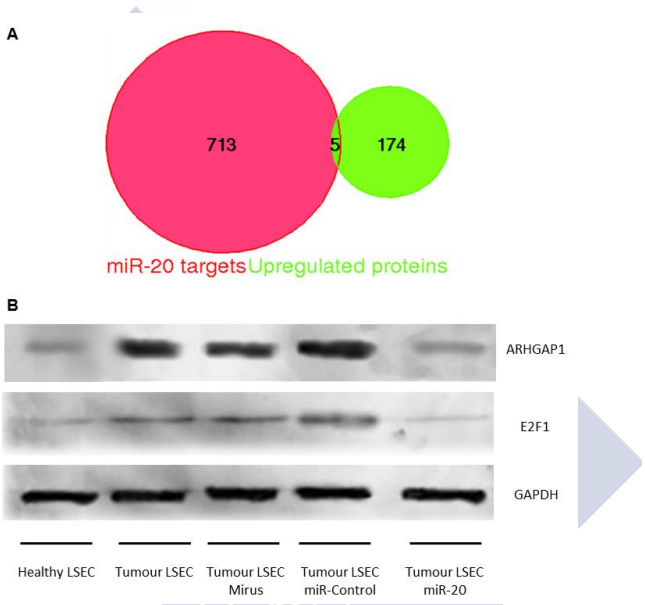

Figure 3. In vitro validation of miR-20a and the effect on the migration capacity of LSECs. (A) Euler-Venn diagram of the number of possible targets of miR-20a predicted by using a list of targets from the miRBASE database (red) and the upregulated proteins by mass spectrometry analysis (green). (B) Western blot analysis of ARHGAP1 and E2F1 validates the miR-20a role in the expression pattern of two of the predicted targets. Analyses were performed under 5 different conditions: i) LSECs from healthy livers, ii) LSECs from livers colonized by the tumour, iii) LSECs from livers colonized by the tumour and treated with the transfection vehicle Mirus, iv) LSECs from livers colonized by the tumour and transfected with control nonspecific miRNA and v) LSECs from livers colonized by the tumour and transfected with miR-20a.

To validate these results, a western blot analysis was performed with LSECs under different treatments. Under control conditions, E2F1 and ARHGAP1 showed low expression. However, after LSEC activation with the tumour, both E2F1 and ARHGAP1 were largely upregulated. Additionally,

when cells were transfected *in vitro* with miR-20a, the protein expression was reduced in both cases to basal levels (Figure 3B).

3.4. Increased migratory capacity of LSECs activated by tumour signals is prevented by miR-20a

To verify whether miR-20a ablation in LSECs from tumour-colonized livers had any consequence on the physiological behavior of these cells, we cultured them in collagen-coated 8-μm pore inserts to measure their migration capacity. Tumour-activated LSECs were treated with miR-20a, with miR-control or with the unloaded transfection vehicle Myrus®. We found that LSEC migration capacity increased approximately two-fold when cells were activated by the tumour, but this was reversed almost to basal levels when cells were transfected with exogenous miR-20a ($p<0,05$). Therefore, restoring cellular miR-20a expression in LSECs was sufficient to prevent the increased migratory capacity associated with tumour-induced activation (Figure 4).

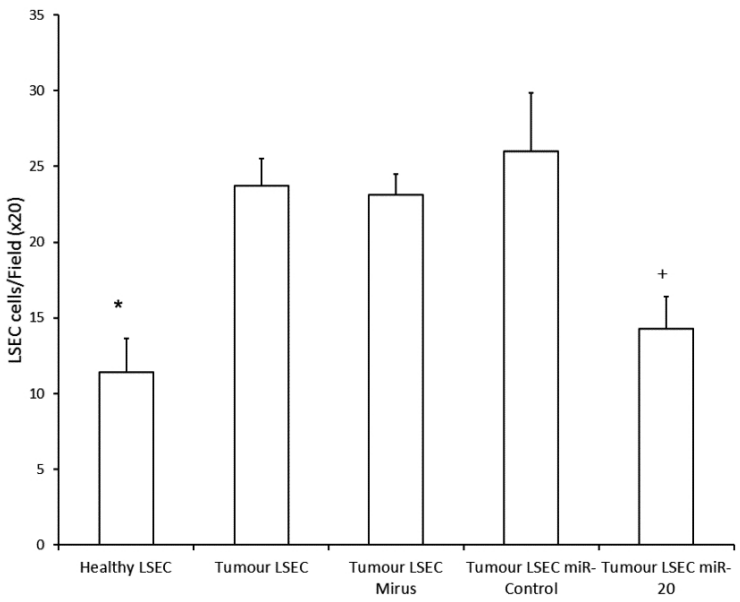

Figure 4. Migration capacity of LSECs analysed under the same conditions used in Figure 3B. * reflects the statistical significance, the difference between healthy LSECs compared with LSECs from liver colonized by the tumour; and + indicates the statistical significance of the difference between LSECs from liver colonized by the tumour and LSECs from liver colonized by the tumour but transfected with miR-20a. In both cases, a $p < 0.05$ threshold was used.

3.5. Sorbitan ester nanoparticles encapsulate both DNA and miRNA forms of nucleic acids

The nanoparticles (SP-OA-CS) were developed through a self-assembly process, as previously described (23) (Figure 5A). The genetic material (plasmid EGFP or miR-20a) inserted into nanoparticles was evaluated using electrophoresis. As shown in Figure 5C, migration of the nucleic acids into the gel was prevented by their association with the nanoparticles in the finally selected formulations (lines 2 and 4), and no free genetic material was observed in these formulations. Blank nanoparticles (with no genetic material incorporated) and those nanoparticles with associated pEGFP and miR-20a had nanometric sizes of 133 nm, 143 nm and 143 nm and negative surface charges of -38 mV, -36 mV and -33 mV, respectively (Table 1 and Figure 5B). The morphology of the nanosystems was observed using transmission electron microscopy (TEM). TEM images confirmed the nanometric size of the formulations (Figure 5D).

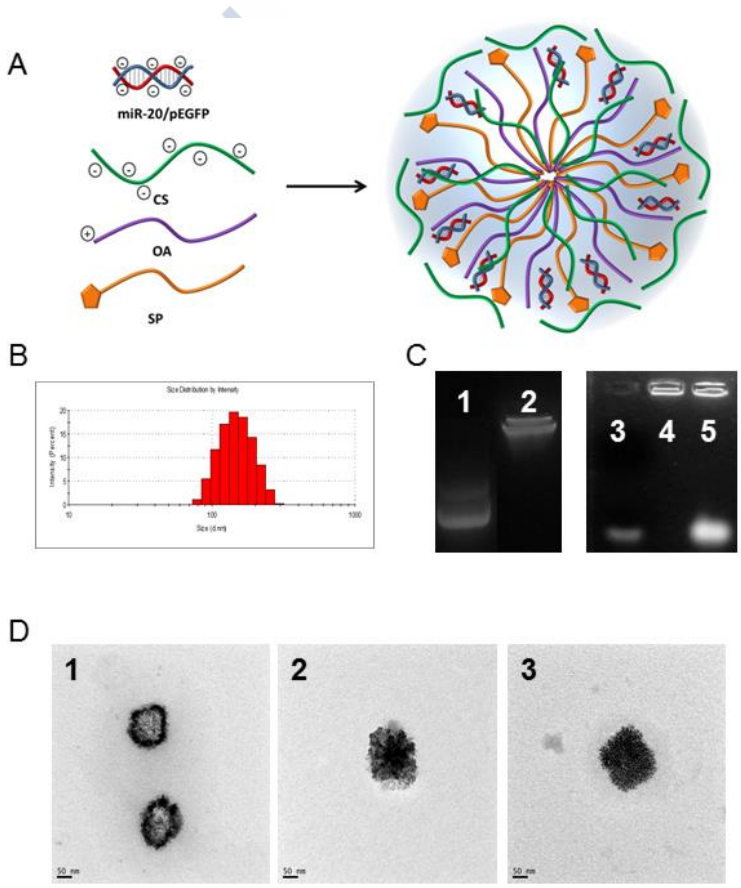

Figure 5. Characteristics of sorbitan ester nanoparticles. (A) Schematic diagram of nanoparticle composition. (B) Size distributions of nanoparticles associated with miR-20a. (C) Characteristics of sorbitan ester nanoparticles coated with chondroitin sulfate. 1) Free pEGFP (200 µg/ml), 2) Nanoparticles + 200 µg/ml pEGFP, 3) Free miR-20a (5 µg/ml), 4) Nanoparticles + 50 µg/ml miR-20a, 5). Nanoparticles + 100 µg/ml miR-20a (D) TEM images of nanoparticles. 1) Blank SP-OA-CS nanoparticles, 2) pEGFP-loaded nanoparticles, 3) miR-20a-loaded nanoparticles.

Table 1. Physicochemical characterisation of blank, pEGFP- and miR-20-loaded CS nanoparticles.

Formulation	Size (nm)	PdI	ζ Potential (mV)
SP-OA-CS	132,9 ± 4,2	0,069	-38,2 ± 1,6
SP-OA-CS-pEGFP	142,7 ± 13,8	0,091	-36,4 ± 8,6
SP-OA-CS-miR-20	142,6 ± 1,4	0,065	-33,3 ± 3,0

To demonstrate the cellular uptake and transfection ability of SP-OA-CS nanoparticles by LSECs a plasmid DNA encoding GFP was incorporated during their preparation. GFP expression was evaluated 24 h post-transfection using fluorescence microscopy. At this experimental time, LSECs expressed GFP, as shown in Figure 6A-B, indicating successful nanoparticle internalization and plasmid delivery. To evaluate whether our nanoparticle-based delivery system could be effective in targeting LSECs *in vivo*, SP-OA-CS containing EGFP plasmid were injected systemically into mice. As shown in Figure 6C, the liver sinusoids expressed GFP, indicating successful plasmid delivery. Moreover, sections were immunostained with anti-mannose receptor (Figure 6E-F) and F4/80 antibodies (Figure 6D). As shown in Figure 6F, the GFP-positive cells were endothelial cells. The miR-20a fluorescence signal was detected in LSECs (Figure 7A-B) when the mice were injected with nanoparticles associated with miRNA. Meanwhile, the fluorescent signal was broader when miR-20a was injected in the naked form (Figure 7C-D).

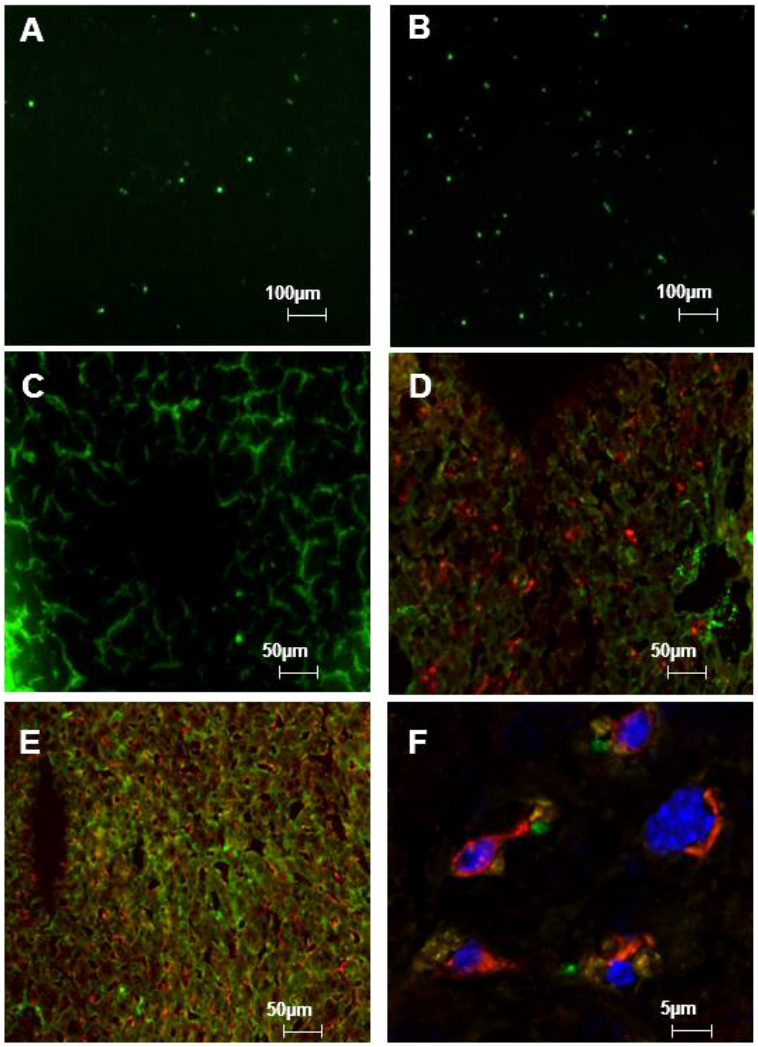

Figure 6. Transfection capacity of chondroitin sulfate-coated sorbitan ester nanoparticles *in vitro* and *in vivo*. The *in vitro* transfection efficiency of SP-OA-CS nanoparticles associated with pEGFP was tested using (A) 1 µg of plasmid, and (B) 2 µg of plasmid. The *in vivo* transfection capacity was measured by injecting the nanoparticles into mice. (C) Liver sinusoids exhibit green fluorescent protein expression at 10X magnification. (D) Samples stained with antibody against F4/80 (red) to detect Kupffer cell uptake of the nanoparticles (10X). (E) To check the origin of GFP expression, the samples were stained with antibody against mannose receptor (red) to detect LSECs and Kupffer cells, and the results show high signal mixing between red and green (10X). (F) The tissue was observed at higher magnification (40x) showing signal mixing (yellow) in LSECs and no mixing (only red) in Kupffer cells.

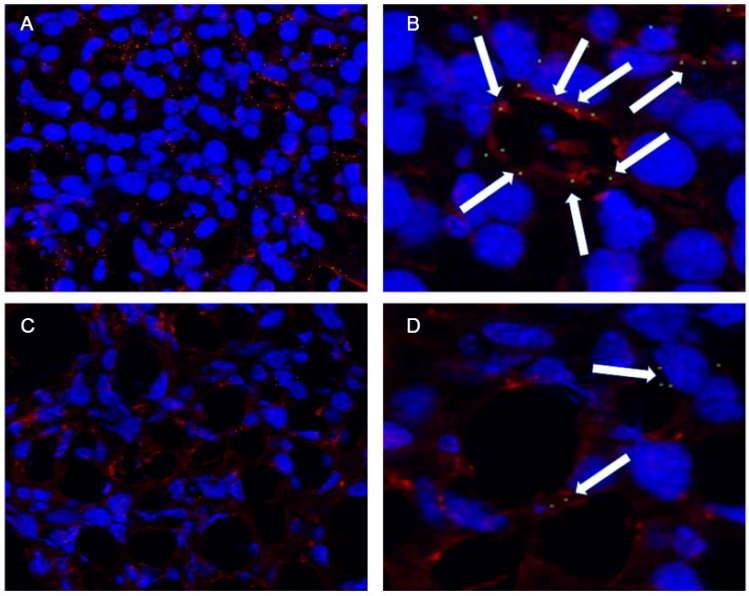

Figure 7. To analyse the *in vivo* nanoparticle miR-20a delivery efficiency to LSECs; fluorescently labelled miR-20a was injected into the mice, either in association with SP-OA-CS nanoparticles (A-B) or naked (C-D). The samples were stained with anti-mannose receptor antibody. The microphotographs (A) at 20x and (B) at 40x show the presence of miR-20a in LSECs. Meanwhile, the microphotographs (I) at 20x and (J) at 40x show miR-20a not only in LSECs but also out of the sinusoids.

3.6. Nanoparticle-mediated delivery of miR-20 to LSECs decreased liver metastasis progression and reduced activated LSEC recruitment into metastatic foci

A murine liver metastasis model was developed to study the potential therapeutic effect of the LSEC-targeted nanoparticles containing miR-20a as previously described (Figure 8). As shown in Figure 9, the tumour-occupied area decreased by approximately 20% when mice were treated with naked miR-20a. Additionally, the tumour-occupied area was decreased by almost 80% when the animals were treated with SP-OA-CS associated with miR-20a. Moreover, quantification of the activated LSECs in the tumour foci by CD31 immunostaining showed a reduction of 70% in tumour-infiltrated LSECs in the livers of mice treated with SP-OA-CS associated with miR-20a compared with control samples (Figure 10).

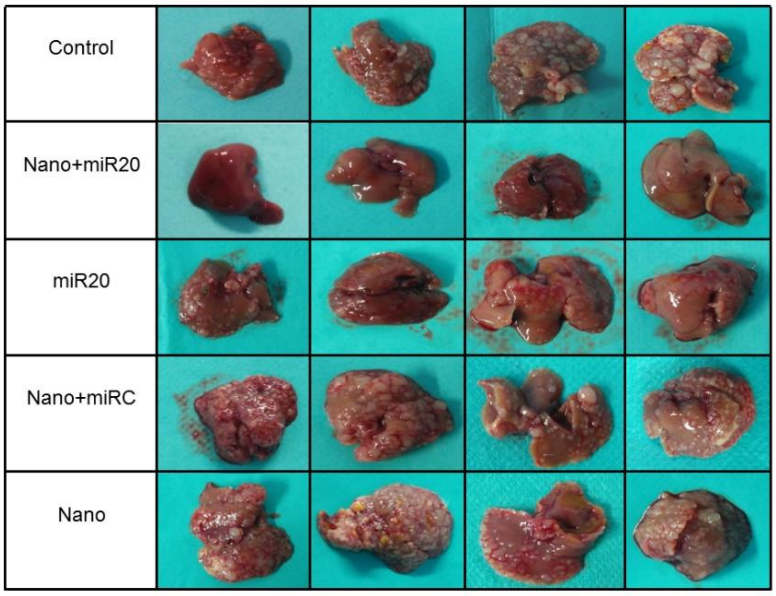

Figure 8. *In vivo* analysis of the effect of treatment with chondroitin sulfate-coated nanoparticles loaded with miR-20a in a murine liver metastasis model. A liver murine metastasis model was developed by intrasplenically injecting C26 murine colon cancer cells into mice. The different treatments were injected into mice every 3 days. Group I mice received PBS as a control treatment; group II mice received miR-20a-loaded nanoparticles; group III mice received miR-20a; group IV mice were treated with nonspecific miRNA (Control)-loaded nanoparticles; and group V mice were treated with empty nanoparticles. After 21 days, the animals were sacrificed, and the livers were removed for histological analysis.

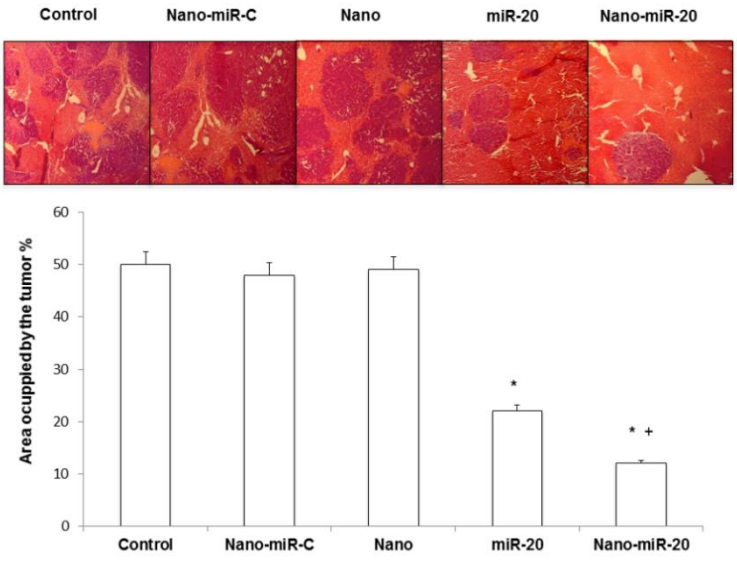

Figure 9. Liver sections were stained with haematoxylin-eosin, and the tumour size was determined as the area of occupied surface relative to the liver surface in a field under the microscope at 4x magnification. Statistically significant ($p < 0.05$) differences between the control group and the group treated with miR-20a without any vehicle and between the control group and the group treated with chondroitin sulfate-coated span nanoparticles loaded with

miR-20a are marked with *. Statistically significant ($p < 0.05$) differences between the group treated with miR-20a without any vehicle and the group treated with chondroitin sulfate-coated span nanoparticle loaded with miR-20a are marked with +.

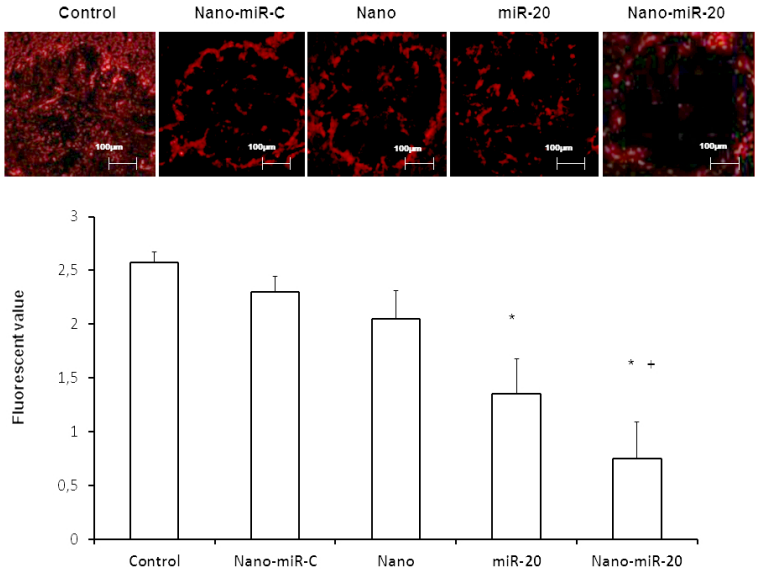

Figure 10. Tumour foci from different groups of metastasis model mice were analysed to determine the number of active LSECs in the tumours to evaluate the tumour supporting role of the cells. Statistically significant ($p < 0.05$) differences between the control group and the group treated with miR-20a without any vehicle and between the control group and the group treated with chondroitin sulfate-coated span nanoparticles loaded with miR-20a are marked with *. Statistically significant ($p < 0.05$) differences between the group treated with miR-20a without any vehicle and the group treated with chondroitin sulfate-coated span nanoparticle loaded with miR-20a are marked with +.

4. Discussion

The importance of miRNAs as key regulators in embryonic development as well as in the maintenance of physiological homeostasis and different diseases has been broadly described (24). In this study, we aimed to analyse the function of miRNAs in LSEC activation during liver metastasis progression.

In an attempt to explore the mechanisms underlying prometastatic LSEC activation, we developed a colorectal cancer liver metastasis model and isolated LSECs to evaluate the deregulation of miRNA expression relative to normal healthy conditions. Microarray data from LSECs colonized by the tumour compared to data from healthy LSECs allowed us to identify 33 upregulated miRNAs. Among the most upregulated miRNAs in terms of fold-expression change, three miRNAs were chosen to be validated by qPCR and, among them, miR-20a was the most altered, with a fold change of up to 7 compared to

healthy LSECs. miR-20a has been previously described as a miRNA that is deregulated in many different tumours, such as lung cancer (25), cervical cancer (26) and thyroid cancer (27), and it has also been described as an essential component of embryonic development and a regulator of Wnt signaling (28).

miRNAs repress protein expression through complementary matching with target mRNA using different mechanisms (29). During liver metastasis progression, the LSEC phenotypic changes to generate a prometastatic cell are the result of a change in the cellular protein expression pattern. We hypothesized that some proteins that facilitate this metastasis-supporting phenotype of LSECs are blocked by miRNA naturally expressed in healthy conditions and that downregulation of these miRNAs during the activation of LSECs leads to prometastatic protein overexpression. Thus, in parallel with the miRNA study, we performed a proteomic study of tumour-colonized and healthy LSECs. In addition, the potential targets of miR-20 were searched using the microRNA database miRBASE, yielding a list of 713 protein target candidates. Specifically, five of them were validated by our proteomic study as overexpressed in tumour-colonized LSECs: JAK1, ARHGAP1, ACSL4, DECR1, and E2F1. In addition, two of them, ARHGAP1 and E2F1, showed direct correlation between tumour-activated expression and miR-20a. ARHGAP1 is a Rho GTPase activating protein that is also related to angiogenic processes in metastasis (30). E2F1 is a transcription factor that can activate different downstream genes involved in many biological processes, such as those involved in the cell cycle during G_1–S-phase transition, DNA synthesis and replication, DNA repair, apoptosis, autophagy, self-renewal, development, and differentiation (31). E2F1 is one of the known key proteins that can modulate cell fate and activation capacity. It has been reported that this protein acts as a crucial protein during mesenchymal cell differentiation to endothelial cells (32) and lymphatic cell differentiation and proliferation (33). E2F1 has not only been described as an endothelial cell differentiation and proliferation element but also as an angiogenesis regulator (34). Thus, E2F1 overexpression could be part of the molecular mechanism involved in LSEC prometastatic activation.

In the present study E2F1 and ARHGAP1 expression levels were upregulated in tumour-activated LSECs. Importantly, the expression of both proteins decreased after exogenous miR-20a administration. In these conditions, *in vitro* LSEC migration decreased, and *in vivo* endothelial cell activation was also reduced. The interaction between miR20a and E2F1 had been previously described in a myoblast differentiation model (35). We show that the number of CD31-positive LSECs was significantly lower in the *in vivo* metastasis model after miR-20a treatment. This indicates that restoration of miR-20a levels in activated LSECs could be sufficient to decrease neoangiogenesis and vascular support to tumours.

Considering the multitarget capacity of miRNAs and the different effects that may be produced depending on the organ they are targeting, it was mandatory to design a system that could specifically

deliver the miR-20a to LSECs. Overall, our previously developed nanoparticle, based on sorbitan esters, met the essential requirements as suitable nucleotide-based bioactive molecules, as previously described (36). In some of our previous patents we collected *in vivo* proofs of concept of the safety and efficacy of such nanosystems for the development of nanomedicines based on delicate bioactive molecules, including gene therapy nanomedicines (37). On the basis of previous data we decided to modify the surface of these nanoparticles with the polysaccharide chondroitin sulfate (CS) as a functional moiety for achieving nanoparticle-mediated miRNA targeted delivery to LSECs, thus producing span, oleylamine and chondroitin sulfate based nanoparticles (SP-OA-CS). This biocompatible and biodegradable material was chosen for its high affinity for hyaluronan receptors and mannose receptors, both of which are expressed on LSECs (38, 39). The hyaluronic acid receptor for endocytosis (HARE, also known as Stabilin-2) is the main scavenger receptor for hyaluronic acid and chondroitin sulfate clearance (40). It is mainly expressed on the sinusoidal endothelial cells of the lymph nodes, liver, and spleen (41). As a first step in the evaluation of the initial nanoparticle prototype, we tried to corroborate the LSEC targeting ability both *in vitro* and *in vivo*. For this purpose, we incorporated the plasmid EGFP into the nanoparticles, as the expression of the GFP protein and subsequent fluorescent labelling will be produced at the targeted cells, thus allowing us to not only corroborate the targeting ability but also the transfection efficacy *in vitro* and *in vivo*. In this respect, we should consider that one of the major limitations of drug delivery nanosystems is their fast uptake by the reticuloendothelial system (RES), which consists of phagocytic cells such as monocytes and macrophages, including liver Kupffer cells, resulting in short circulation half-lives of nanosystems (42-44). However, our anionic nanosystems demonstrated *in vivo* LSEC-specific internalization, avoiding Kupffer cell uptake.

The role of activated LSECs during liver metastasis progression is well known. In this work, we tried to restore the normal healthy LSEC phenotype through miRNA delivery, in an attempt to revert pathological changes in the protein expression pattern of LSECS by affecting multiple prometastatic targets simultaneously. This strategy proved largely successful, because the expression of CD31 in livers collected from the *in vivo* metastasis murine model treated with miR-20a-conjugated nanoparticles revealed a reduction of 70% in CD31-positive LSEC infiltration into tumour foci. Moreover, this correlated well with a metastatic tumour-occupied area reduction of approximately 80% relative to metastasized liver controls, and this reduction was also significantly more than the one induced by naked miR-20a, which merely reduced tumour volume by 20%. In the same way, proteins such as E2F1 and ARHGAP1, which are related to cell cycle, metabolism, migration and differentiation, were found to be depleted *in vitro* after miR-20a injection. It is unknown why early activation of LSECs induces miR-20a depletion, and further research is needed to elucidate the full cascade of events that occur after tumour cell adhesion to LSECs. In any case, in the present report we show that our developed nanosystem is able to specifically deliver miR-20a to LSECs, which could eventually be clinically

exploited as a valuable therapeutic strategy to inhibit the progression of liver metastasis. Accordingly, these results corroborate the implication that miR-20a downregulation plays a prometastatic role in LSEC differentiation, as well as the supporting role of LSECs in the metastatic liver tumour microenvironment.

References

1. Mao H, Pan F, Guo H, Bu F, Xin T, Chen S, et al. Feedback mechanisms between M2 macrophages and Th17 cells in colorectal cancer patients. Tumour Biol. 2016 May 28.

2. Borras E, San Lucas FA, Chang K, Zhou R, Masand G, Fowler J, et al. Genomic Landscape of Colorectal Mucosa and Adenomas. Cancer Prev Res (Phila). 2016 May 24.

3. Li M, Peng F, Li G, Fu Y, Huang Y, Chen Z, et al. Proteomic analysis of stromal proteins in different stages of colorectal cancer establishes Tenascin-C as a stromal biomarker for colorectal cancer metastasis. Oncotarget. 2016 May 14.

4. Fu M, Song Y, Wen Z, Lu X, Cui L. Inositol Hexaphosphate and Inositol Inhibit Colorectal Cancer Metastasis to the Liver in BALB/c Mice. Nutrients. 2016 May 12;8(5):10.3390/nu8050286.

5. Van den Eynden GG, Majeed AW, Illemann M, Vermeulen PB, Bird NC, Hoyer-Hansen G, et al. The multifaceted role of the microenvironment in liver metastasis: biology and clinical implications. Cancer Res. 2013 Apr 1;73(7):2031-43.

6. Olaso E, Salado C, Egilegor E, Gutierrez V, Santisteban A, Sancho-Bru P, et al. Proangiogenic role of tumor-activated hepatic stellate cells in experimental melanoma metastasis. Hepatology. 2003 Mar;37(3):674-85.

7. Arteta B, Lasuen N, Lopategi A, Sveinbjornsson B, Smedsrod B, Vidal-Vanaclocha F. Colon carcinoma cell interaction with liver sinusoidal endothelium inhibits organ-specific antitumor immunity through interleukin-1-induced mannose receptor in mice. Hepatology. 2010 Jun;51(6):2172-82.

8. Salado C, Olaso E, Gallot N, Valcarcel M, Egilegor E, Mendoza L, et al. Resveratrol prevents inflammation-dependent hepatic melanoma metastasis by inhibiting the secretion and effects of interleukin-18. J Transl Med. 2011 May 12;9:59,5876-9-59.

9. Cheng CM, Shiah SG, Huang CC, Hsiao JR, Chang JY. Upregulation of miR-455-5p by the TGF-beta-SMAD signalling axis promotes the proliferation of oral squamous cancer cells by targeting UBE2B. J Pathol. 2016 May 28.

10. Quaranta MT, Spinello I, Paolillo R, Macchia G, Boe A, Ceccarini M, et al. Identification of beta-Dystrobrevin as a Direct Target of miR-143: Involvement in Early Stages of Neural Differentiation. PLoS One. 2016 May 25;11(5):e0156325.

11. Mobus S, Yang D, Yuan Q, Ludtke TH, Balakrishnan A, Sgodda M, et al. MicroRNA-199a-5p inhibition enhances the liver repopulation ability of human embryonic stem cell-derived hepatic cells. J Hepatol. 2015 Jan;62(1):101-10.

12. Hawa Z, Haque I, Ghosh A, Banerjee S, Harris L, Banerjee SK. The miRacle in Pancreatic Cancer by miRNAs: Tiny Angels or Devils in Disease Progression. Int J Mol Sci. 2016 May 26;17(6):E809.

13. Cao DD, Li L, Chan WY. MicroRNAs: Key Regulators in the Central Nervous System and Their Implication in Neurological Diseases. Int J Mol Sci. 2016 May 28;17(6):E842.

14. Langsch S, Baumgartner U, Haemmig S, Schlup C, Schafer SC, Berezowska S, et al. miR-29b mediates NF-kB signaling in KRAS-induced non-small cell lung cancers. Cancer Res. 2016 May 19.

15. Hong L, Pan F, Jiang H, Zhang L, Liu Y, Cai C, et al. miR-125b inhibited epithelial-mesenchymal transition of triple-negative breast cancer by targeting MAP2K7. Onco Targets Ther. 2016 May 4;9:2639-48.

16. Varela MA. Identification of sequences common to more than one therapeutic target to treat complex diseases: simulating the high variance in sequence interactivity evolved to modulate robust phenotypes. BMC Genomics. 2015 Jul 18;16:530,015-1727-6.

17. Fabian MR, Sundermeier TR, Sonenberg N. Understanding how miRNAs post-transcriptionally regulate gene expression. Prog Mol Subcell Biol. 2010;50:1-20.

18. Chen Y, Gao DY, Huang L. In vivo delivery of miRNAs for cancer therapy: challenges and strategies. Adv Drug Deliv Rev. 2015 Jan;81:128-41.

19. Andre EM, Pensado A, Resnier P, Braz L, Rosa da Costa AM, Passirani C, et al. Characterization and comparison of two novel nanosystems associated with siRNA for cellular therapy. Int J Pharm. 2016 Jan 30;497(1-2):255-67.

20. Pensado A, Fernandez-Pineiro I, Seijo B, Sanchez A. Anionic nanoparticles based on Span 80 as low-cost, simple and efficient non-viral gene-transfection systems. Int J Pharm. 2014 Dec 10;476(1-2):23-30.

21. Schmittgen TD, Livak KJ. Analyzing real-time PCR data by the comparative C(T) method. Nat Protoc. 2008;3(6):1101-8.

22. Poschmann G, Seyfarth K, Besong Agbo D, Klafki HW, Rozman J, Wurst W, et al. High-fat diet induced isoform changes of the Parkinson's disease protein DJ-1. J Proteome Res. 2014 May 2;13(5):2339-51.

23. Sanchez A, Fernandez-Piñeiro I, Badiola I, Marquez J, inventors; Nuevos vehículos para la transfección de miRNAs. patent P201630417. 2016 .

24. Ivey KN, Srivastava D. microRNAs as Developmental Regulators. Cold Spring Harb Perspect Biol. 2015 Jul 1;7(7):a008144.

25. Babu KR, Muckenthaler MU. miR-20a regulates expression of the iron exporter ferroportin in lung cancer. J Mol Med (Berl). 2016 Mar;94(3):347-59.

26. Safari A, Seifoleslami M, Yahaghi E, Sedaghati F, Khameneie MK. Upregulation of miR-20a and miR-10a expression levels act as potential biomarkers of aggressive progression and poor prognosis in cervical cancer. Tumour Biol. 2015 Oct 1.

27. Xiong Y, Zhang L, Kebebew E. MiR-20a is upregulated in anaplastic thyroid cancer and targets LIMK1. PLoS One. 2014 May 23;9(5):e96103.

28. Cui Y, Han J, Xiao Z, Chen T, Wang B, Chen B, et al. The miR-20-Rest-Wnt signaling axis regulates neural progenitor cell differentiation. Sci Rep. 2016 Mar 21;6:23300.

29. Bhattacharyya SN, Habermacher R, Martine U, Closs EI, Filipowicz W. Relief of microRNA-mediated translational repression in human cells subjected to stress. Cell. 2006 Jun 16;125(6):1111-24.

30. Zohrabian VM, Nandu H, Gulati N, Khitrov G, Zhao C, Mohan A, et al. Gene expression profiling of metastatic brain cancer. Oncol Rep. 2007 Aug;18(2):321-8.

31. Wang SN, Wang LT, Sun DP, Chai CY, Hsi E, Kuo HT, et al. Intestine-specific homeobox (ISX) upregulates E2F1 expression and related oncogenic activities in HCC. Oncotarget. 2016 May 9.

32. Zhang R, Wang N, Zhang LN, Huang N, Song TF, Li ZZ, et al. Knockdown of DNMT1 and DNMT3a Promotes the Angiogenesis of Human Mesenchymal Stem Cells Leading to Arterial Specific Differentiation. Stem Cells. 2016 May;34(5):1273-83.

33. Baxter SA, Cheung DY, Bocangel P, Kim HK, Herbert K, Douville JM, et al. Regulation of the lymphatic endothelial cell cycle by the PROX1 homeodomain protein. Biochim Biophys Acta. 2011 Jan;1813(1):201-12.

34. Pillai S, Kovacs M, Chellappan S. Regulation of vascular endothelial growth factor receptors by Rb and E2F1: role of acetylation. Cancer Res. 2010 Jun 15;70(12):4931-40.

35. Luo W, Li G, Yi Z, Nie Q, Zhang X. E2F1-miR-20a-5p/20b-5p auto-regulatory feedback loop involved in myoblast proliferation and differentiation. Sci Rep. 2016 Jun 10;6:27904.

36. Sanchez A, Seijo B, Zorzi GK, Carvalho EL, Pensado A, inventors; Nanoparticulate systems prepared from sorbitan esters. patent WO2013068625 A1. 2013 .

37. Diaz-Corrales FJ, Bhattacharya SS, De La Cerda B, Valdés-Sánchez L, Sanchez A, Seijo B, et al., inventors; Nanoparticulate systems for in vivo transfection. patent EP14382221.1. 2014 .

38. Leteux C, Chai W, Loveless RW, Yuen CT, Uhlin-Hansen L, Combarnous Y, et al. The cysteine-rich domain of the macrophage mannose receptor is a multispecific lectin that recognizes chondroitin sulfates A and B and sulfated oligosaccharides of blood group Lewis(a)

and Lewis(x) types in addition to the sulfated N-glycans of lutropin. J Exp Med. 2000 Apr 3;191(7):1117-26.

39. McCourt PA, Smedsrod BH, Melkko J, Johansson S. Characterization of a hyaluronan receptor on rat sinusoidal liver endothelial cells and its functional relationship to scavenger receptors. Hepatology. 1999 Nov;30(5):1276-86.

40. Harris E, Weigel PH. Functional aspects of the hyaluronan and chondroitin sulfate receptors. In: Ahmed H, Vasta GR, editors. Animal Lectins: A Functional View. CRC Press; 2008. p. 171-92.

41. Harris EN, Baggenstoss BA, Weigel PH. Rat and human HARE/stabilin-2 are clearance receptors for high- and low-molecular-weight heparins. Am J Physiol Gastrointest Liver Physiol. 2009 Jun;296(6):G1191-9.

42. Sadauskas E, Wallin H, Stoltenberg M, Vogel U, Doering P, Larsen A, et al. Kupffer cells are central in the removal of nanoparticles from the organism. Part Fibre Toxicol. 2007 Oct 19;4:10.

43. Rinkenauer AC, Press AT, Raasch M, Pietsch C, Schweizer S, Schworer S, et al. Comparison of the uptake of methacrylate-based nanoparticles in static and dynamic in vitro systems as well as in vivo. J Control Release. 2015 Oct 28;216:158-68.

44. Nie S. Understanding and overcoming major barriers in cancer nanomedicine. Nanomedicine (Lond). 2010 Jun;5(4):523-8.

General discussion

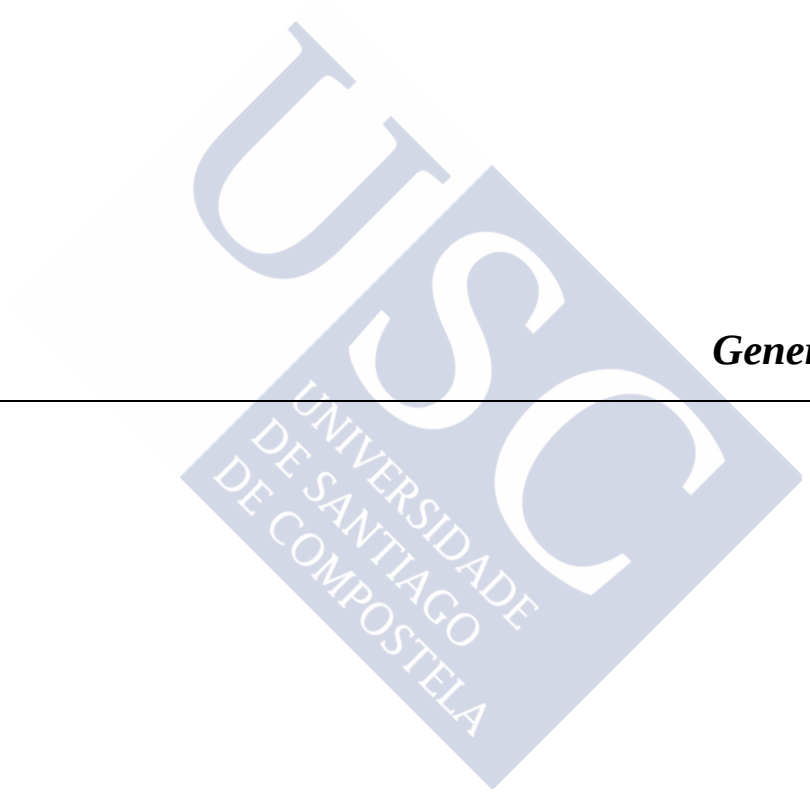

USC
UNIVERSIDADE
DE SANTIAGO
DE COMPOSTELA

The need for new gene delivery systems together with the advantageous properties of nanocarriers have led us to investigate the potential of the herein described polysaccharide-functionalised nanoparticles as carriers for nucleic acids. The rationale behind our therapeutic approach has been based on the current progress in understanding the altered molecular pathways in cancer and the subsequent identification of new targets. Hence, we decided to take advantage of the finding of altered expression of microRNAs in cancer microenviroment and the ideal properties of our nanoparticles to specifically deliver a deregulated microRNA into liver sinusoidal endothelial cells for the treatment of colorectal liver metastasis.

The description of our work has been structured in three chapters. The first two chapters cover the design and development of three different polysaccharide-functionalised nanoparticle formulations, as well as their *in vitro* and *in vivo* evaluation. The last one focuses on the application of the most suitable nanosystem in the treatment of colorectal cancer metastasized to the liver. Below we discuss the aforementioned results.

1. Functionalisation of span nanoparticles with natural polymers.

-Nanoparticle functionalisation and characterisation

Lipid nanocarriers are among the most studied systems for nucleic acid delivery. Herein we have focused on the functionalisation of a lipid nanostructure based on sorbitan monooleate, also known as span 80 (SP). SP is a nonionic surfactant and it is generally recognised as safe (GRAS) by FDA, being widely used in the pharmaceutical industry (1-3). The cationic lipid oleylamine (OA) was added to the system to facilitate the nucleic acid association through electrostatic interactions with the negative charges of nucleic acids. OA is a fatty amine generally used as stabilising agent, being increasingly used for gene delivery due to its high transfection potential (4-7). Physicochemical properties of the basic nanosystems prior functionalisation are listed in Table 1. As shown in this table, SP nanoparticles size increases from 131 nm to 204 nm and zeta potential reverts from negative to positive when OA is incorporated to the system.

Polysaccharides are the most commonly used natural polymers in gene and drug delivery systems due to their optimal properties. They are renewable, biocompatible, biodegradable, and relatively cheap naturally occurring polymers, which can act as targeting moieties, inasmuch

some of them are substrates for cell surface receptors. Alternatively, their presence on nanocarriers surface may also lengthen their circulation time in the bloodstream by reducing mononuclear phagocyte system recognition, due to steric shielding and mitigated complement activation (8, 9). In this work, we have selected the polysaccharides xanthan gum (XG), chondroitin sulfate (CS) and hyaluronic acid (HA) to be incorporated in our previously developed SP-OA nanoparticles in order to modulate their physicochemical properties and biological behaviour. Since the final objective of this project was to develop a novel microRNA-based nanomedicine for colorectal liver metastasis treatment through liver sinusoidal endothelial cells (LSECs) targeting, the potential of these polysaccharides to target endothelial cells and more specifically LSECs has been evaluated.

Table 1. Physicochemical properties of the developed nanoparticles.

Formulation	Size (nm)	PdI	ζ Potential (mV)
SP	131.4 ± 6.9	0.084 ± 0.037	-30.3 ± 2.0
SP-OA	205.4 ± 11.1	0.110 ± 0.015	+46.8 ± 3.3
SP-OA-XG	146.8 ± 7.4	0,150 ± 0.036	-48.0 ± 1.5
SP-OA-CS	122.8 ± 11.9	0.079 ± 0.019	-37.7 ± 2.1
SP-OA-HA	137.0 ± 10.4	0.114 ± 0.024	-28.6 ± 8.4

XG is an exopolysaccharide produced by the bacteria *Xanthomonas campestris*. It is composed of (1, 4)-β-D- glucan with trisaccharide side chains composed of mannose-(1, 4)- β-glucuronic acid-(1, 2)- β-mannose attached to alternate glucose residues in the backbone (10, 11). Considering the presence of mannose residues in XG composition, we initially hypothesized that these residues could be used to target mannose receptor which is known to be overexpressed in LSECs. Mannose receptor acts as a scavenger receptor, recognizing and facilitating uptake of diverse glycoconjugate ligands.

CS and HA are naturally occurring glycosaminoglycans which are main components of the extracellular matrix, considered biocompatible and biodegradable polymers, and are widely used in the biomedical field (12-15). CS and HA are composed of glucuronic acid and N-acetylglucosamine repeats via a β-1-4 linkage, being the sulfate group in at least one of CS side groups the main structural difference among them. These natural polymers were chosen for their high affinity for hyaluronan and mannose receptors, both of which are expressed on LSECs (16, 17). The hyaluronic acid receptor for endocytosis (HARE, also known as Stabilin-

2) is the main scavenger receptor for hyaluronic acid and chondroitin sulfate clearance (18). The mannose receptor, in addition of its role in innate immune response by binding polysaccharides of the surface of pathogenic microorganisms, has a cysteine-rich domain that binds sulfated carbohydrates such as chondroitin sulfate.

The above-described polysaccharides were incorporated to the span system during the nanoparticle preparation, by addition of the polysaccharides to the aqueous phase. As shown in Table 1, this incorporation led to a decrease in the nanoparticle size from 205 nm to 147, 123 and 137 nm for XG, CS and HA functionalised nanoparticles, respectively. In addition, a reversal of the nanoparticle surface charge from positive (+47 mV for SP-OA nanoparticles) to negative (-48, -38 and -29 mV for XG, CS and HA nanoparticles) was observed. According to these results, and considering the lipophilic nature of the span nanoparticle core (19), we can assume that the carboxylic groups of XG, CS and HA, as well as the sulfate groups of CS (Figure 1, 2 and 3) are disposed on the nanoparticle surface, as evidenced by the negative zeta potential of the resulting nanosystems and as schematised in Figure 4. Such negatively charged external shell created around the nanoparticles is an interesting feature to avoid unspecific interactions with serum components and cell membranes after a systemic administration, increasing biological stability of the systems, as well as acting as a targeting moiety. The observed decrease in nanoparticle size after polysaccharide incorporation could be explained by an increase in the polymers packing due to electrostatic interactions and subsequent physical crosslinking of the different components. Moreover, morphological characterisation of the nanosystems was performed by transmission electron microscopy (TEM) and it corroborated the nanometric size and spherical shape of the nanoparticles (Figure 5).

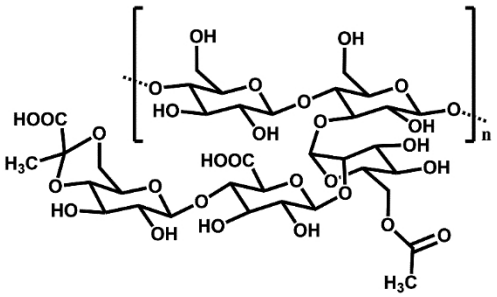

Figure 1. Xanthan gum structure.

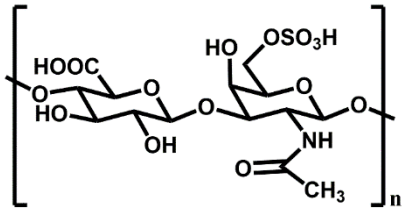

Figure 2. Chondroitin sulfate A structure.

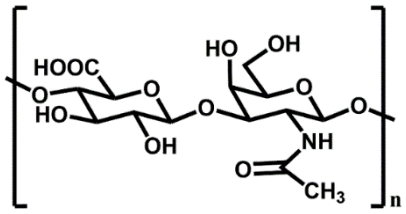

Figure 3. Hyaluronic acid structure.

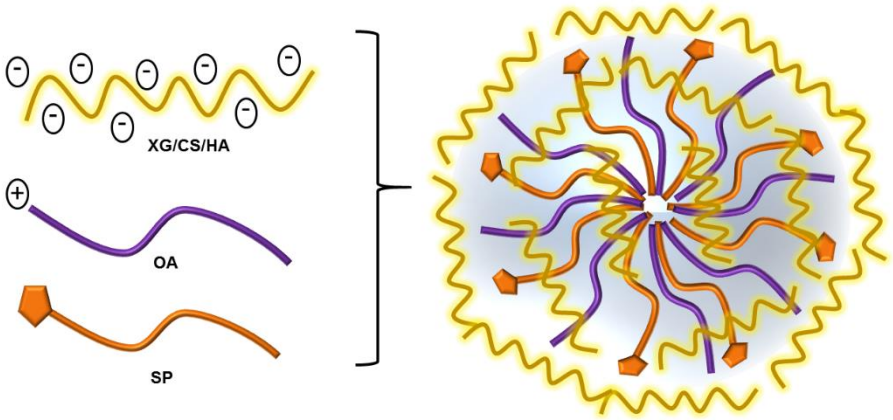

Figure 4. Schematic representation of polysaccharide-functionalised span nanoparticles.

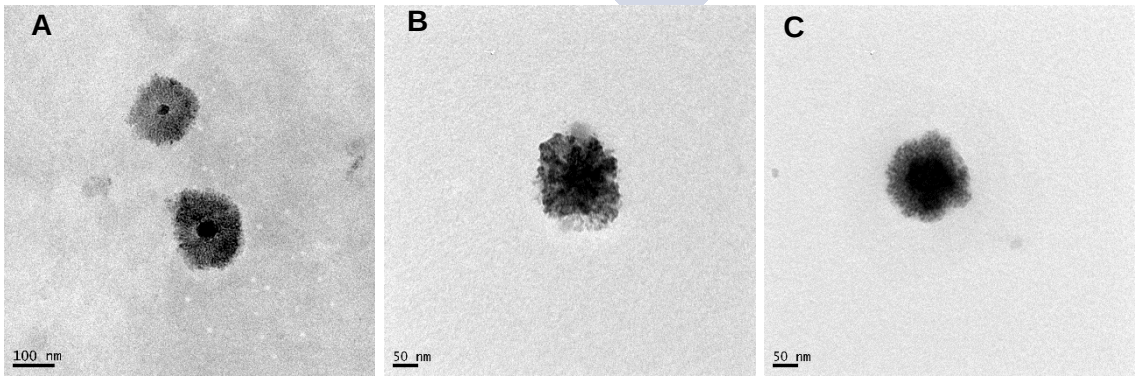

Figure 5. TEM images of XG (A), CS (B) and HA (C) nanoparticles.

-Plasmid association

The potential of the developed nanoparticles to act as gene delivery systems was evaluated using enhanced green fluorescent protein plasmid (pEGFP) as a model molecule. As summarised in Table 2, the incorporation of the plasmid DNA did not significantly interfere in nanoparticles size and surface charge. Once the nanoparticles ability to associate the model plasmid was confirmed, we decided to evaluate the capacity of the systems to protect this plasmid against DNase I degradation (Figure 6). Protection against enzymatic degradation is a prerequisite for ensuring intact delivery of the associated plasmid DNA in its bioactive form into its site of action. In this respect we should consider that when naked nucleic acids are systemically administered they are quickly degraded by DNases, which are enzymes naturally present in tissues and biological fluids. To perform DNase I protection assay, this enzyme was incubated with free DNA and nanoparticle-associated DNA, and DNA was subsequently released from the nanoparticles using the surfactant sodium dodecyl sulfate (SDS). Figure 6 demonstrates the presence of DNA bands corresponding with DNA associated with XG, CS and HA NPs after incubation with DNase I, evidencing the absence of degradation. Therefore, we have demonstrated that the incorporation of plasmid DNA into polysaccharide-functionalised nanoparticles prevents its enzymatic degradation ensuring its intact delivery into its site of action.

Table 2. Physicochemical properties of the developed nanoparticles associating EGFP plasmid (200 μg/ml).

Formulation	Size (nm)	PdI	ζ Potential (mV)
SP-OA-XG-pEGFP	153.5 ± 17.8	0.102 ± 0.036	-40.6 ± 4.6
SP-OA-CS-pEGFP	137.3 ± 13.7	0.091 ± 0.022	-37.1 ± 6.9
SP-OA-HA-pEGFP	134.5 ± 11.4	0.083 ± 0.026	-32.4 ± 2.8

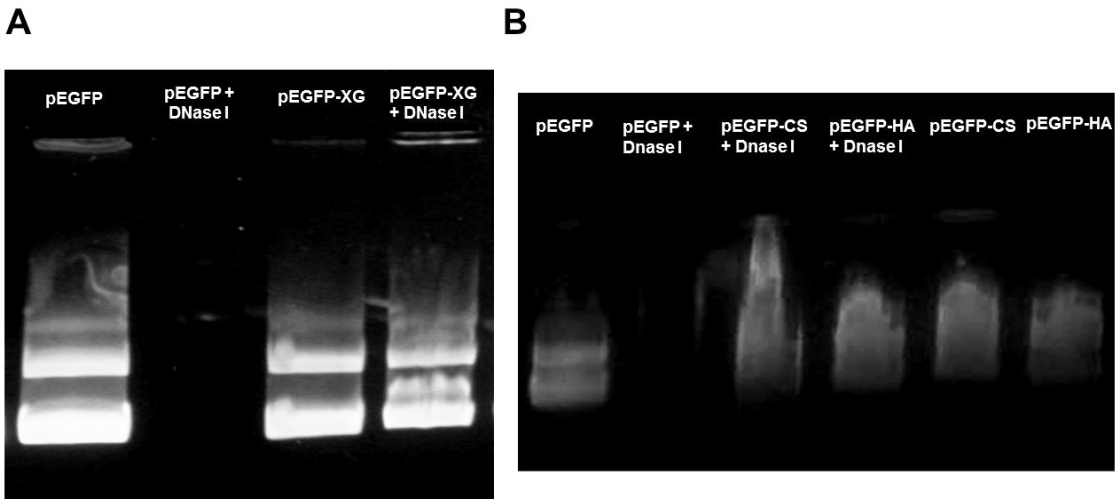

Figure 6. Agarose gel electrophoresis of free pEGFP and pEGFP released from nanoparticles after 1 hour of incubation with DNase I and subsequent pEGFP-NP disassembly mediated by SDS. (A) XG nanoparticles, (B) CS and HA nanoparticles.

-Nanoparticle stability

Another critical issue in the development of nanomedicines is their low stability or tendency to lose their physicochemical properties after storage, which precludes their scalability to pharmaceutical industry. Thus, once the functionalised nanoparticles were developed and characterised, their stability were evaluated after 3 and 12 months of storage at 4°C, room temperature (RT) and 37°C (Figure 7). When nanoparticles were stored in suspension, they resisted even 12 months of storage without major changes in size and Z potential at 4°C and room temperature (RT). Considerable size and Z potential increases were only observed when the nanoparticles were stored at 37°C, a result which could be explained by hydrolysis of the sorbitan monooleate molecules, resulting in free fatty acids that could partially neutralise positive charge of OA, leading to a decrease in the superficial charge and to an increase in the size. This effect could also be consequence of the Ostwald ripening, based on the growth of the largest particles on expenses of the smallest ones (20). Moreover, the developed formulations showed resistance to the lyophilisation process, increasing their long-term stability. In addition, lyophilisation can be used to remove water and protect the loaded bioactive molecule from hydrolysis and degradation. Thus, we have developed lipid systems functionalised with polysaccharides which stand out for their short- and long-term stability both in suspension and as a lyophilised product. This behaviour could be explained by structural

differences with other lipid based nanosystems, such as vesicular ones (i.e., liposomes), known for their stability limitations.

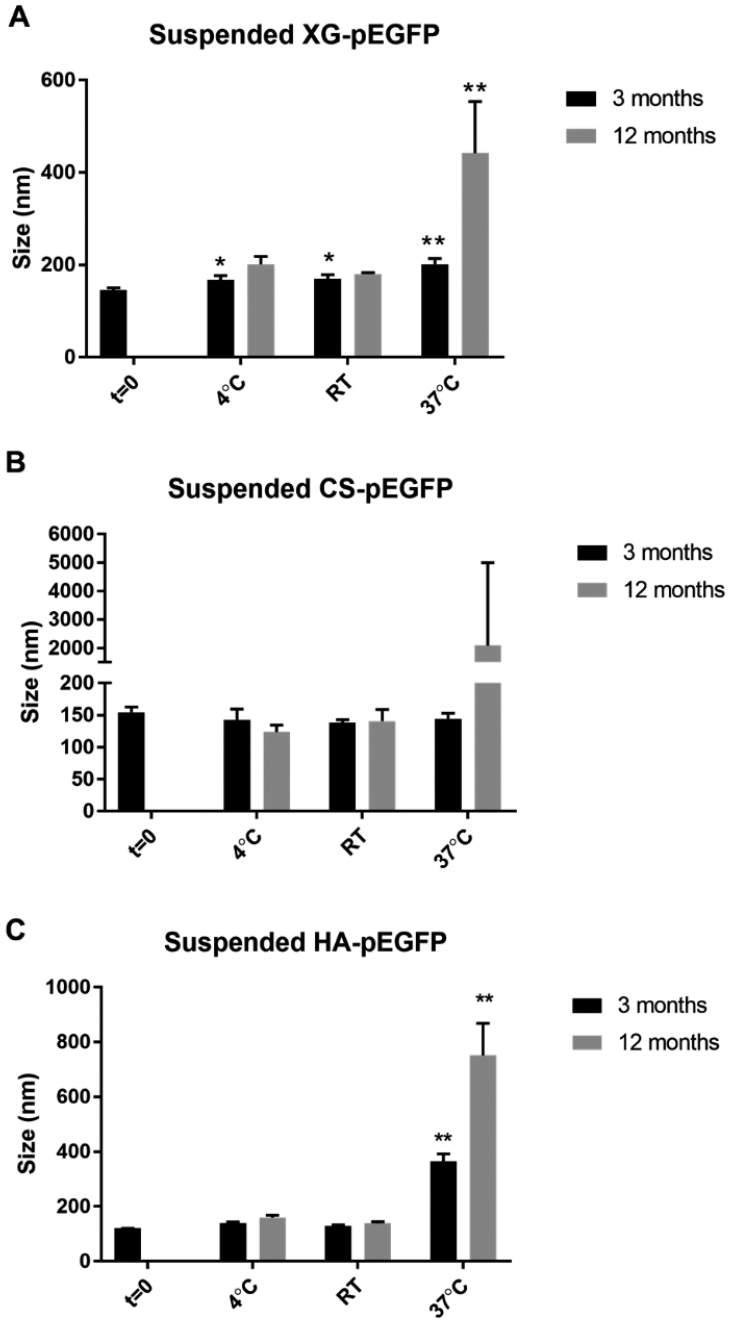

Figure 7. Stability of XG (A), CS (B) and HA (C) nanoparticles stored in suspension at 4°C, room temperature (RT) and 37°C. After 3 and 12 months, size was measured. *p<0.05 and **p<0.01 vs. samples at initial time (t=0).

2. Evaluation of the *in vitro* and *in vivo* toxicity, transfection ability and biodistribution of the developed nanoparticles.

-Nanoparticle influence on cell viability

Once the nanosystems were characterised in terms of physicochemical properties, DNA binding ability and stability, the next step was to determine the biocompatibility of the systems. For this purpose, toxicity of the developed gene delivery systems was evaluated *in vitro* and *in vivo*. Thus, nanoparticles effect on cell viability was assessed in two different cell types using XTT assay: human lung adenocarcinoma cell line (A549) for XG, CS and HA nanoparticles and Human Umbilical Vein Endothelial Cells (HUVEC) for further evaluation of XG nanoparticles. As shown in Figure 8, we have shown that all the CS and HA decrease metabolic activity only at the highest nanoparticle concentration tested of 768 μg/ml. At this concentration, CS and HA functionalised nanoparticles decrease A549 cell viability to 59% and 84% respectively. In the case of XG nanoparticles, this effect on cell viability was not observed in A549 cell line, being just observed when these nanoparticles were incubated with HUVEC (Figure 9), decreasing to 31%. From previous work (21) and from preliminary studies, we know that non-functionalised sorbitan monooleate-oleylamine nanoparticles do not interfere on cell viability even when higher concentrations were tested in different cell lines. However, the effect of polysaccharide functionalised nanoparticles on cell viability can not be explained by the toxicity of the polysaccharides. Diverse studies have described XG, CS and HA biocompatibility and safety (10, 22-25). Accordingly, the cytotoxicity observed for the nanoparticles at the highest tested concentration may be related to a great nanoparticles uptake due to polysaccharide functionalisation, rather than to the toxicity of the polymers themselves. In any case, it should be emphasized that the doses of nanoparticles subsequently used in transfection experiments were much lower than 768 μg/ml.

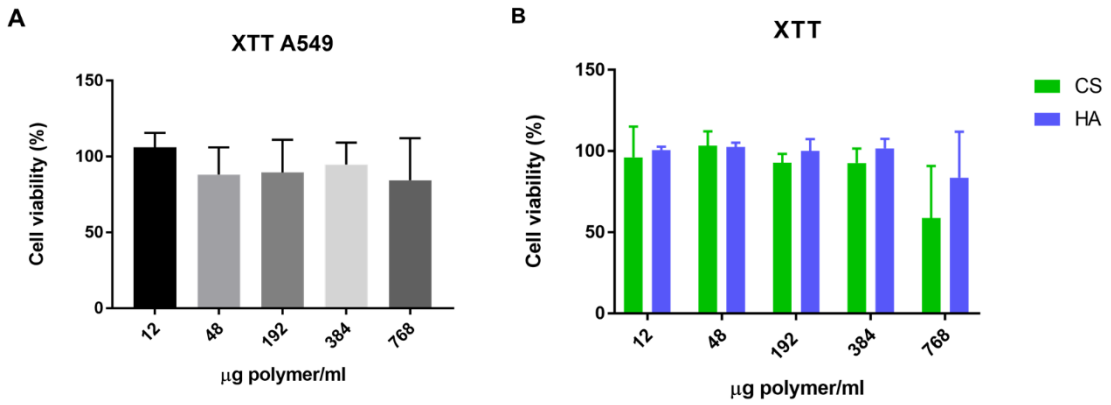

Figure 8. Cell viability of A549 after 4 hour incubation with XG (A), and CS and HA (B).

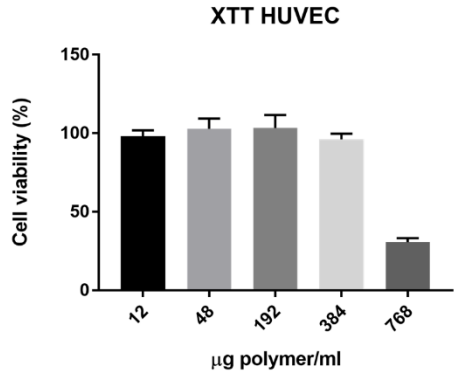

Figure 9. HUVEC cell viability after 2 hour incubation with XG nanoparticles.

-In vitro transfection

Once the nanoparticle cytotoxic profile was determined *in vitro*, the ability of the developed systems to effectively deliver the model plasmid into cells was evaluated. Thus, A549 cells were transfected with different doses of pEGFP loaded in CS and HA nanoparticles whereas that HUVEC were transfected with pEGFP-loaded XG nanoparticles. As shown in Figure 10, efficient transfections were achieved with all formulations. The doses of nanoparticles used were lower than those interfering in cell viability (<300 µg/ml).

Also, it should be considered that HUVEC are primary cells which are isolated directly from tissues and, in contrast with cell lines, are especially sensitive. However, they are more representative of *in vivo* responsiveness and environment. Accordingly, the ability of the system to transfect HUVEC *in vitro* should be noticed, since primary cells resistance to transfection is

widely known. Moreover, in additional studies performed using A549 cell line, XG nanoparticles demonstrated their ability to transfect cells in presence of serum at low doses of the nanosystem (Figure 11). These results demonstrate the protection and stabilising properties of the polysaccharide, avoiding the widely described serum-transfection agent interaction that leads to a decrease in transfection efficacy. Indeed, serum is recognised as one of the most serious barrier for nanocarrier-mediated nucleic acid delivery (26). These results can be considered to predict the system *in vivo* behaviour: XG surface shell could prevent opsonisation of our developed nanoparticles, i.e. the binding of plasma proteins which would make the nanoparticles more visible to phagocytes and, therefore, lead to their removal from the circulation (27). Thereafter, we confirmed that our nanosystems have a specific ability to circumvent one of the main limitations of nanosystems *in vivo*, as they are able to avoid phagocytosis by Kupffer cells (Figure 14A), liver resident macrophages, when systemically administered to mice, lending support to the theory that polysaccharide-functionalisation can help our nanoparticles to avoid reticuloendothelial system (RES) clearance. Moreover, the same RES escape effect was observed for CS nanoparticles (Figure 15), confirming the shielding properties of the polysaccharide external shell on our span nanoparticles.

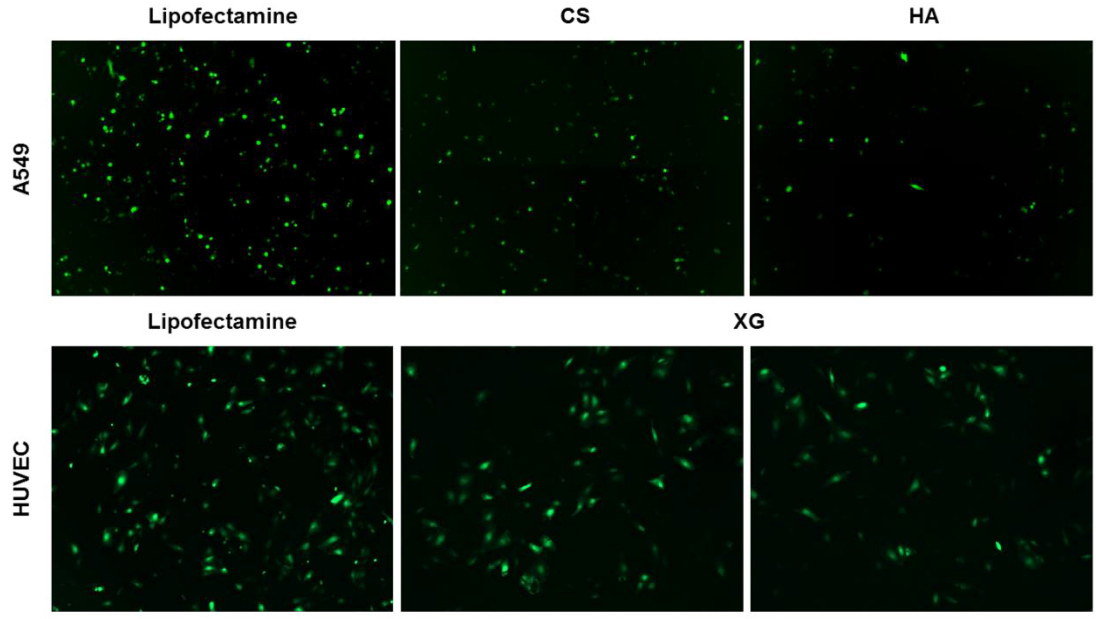

Figure 10. HUVEC and A549 cells were efficiently transfected with pEGFP-loaded NPs using doses of 1 μg of plasmid per well. Lipofectamine was used as positive control.

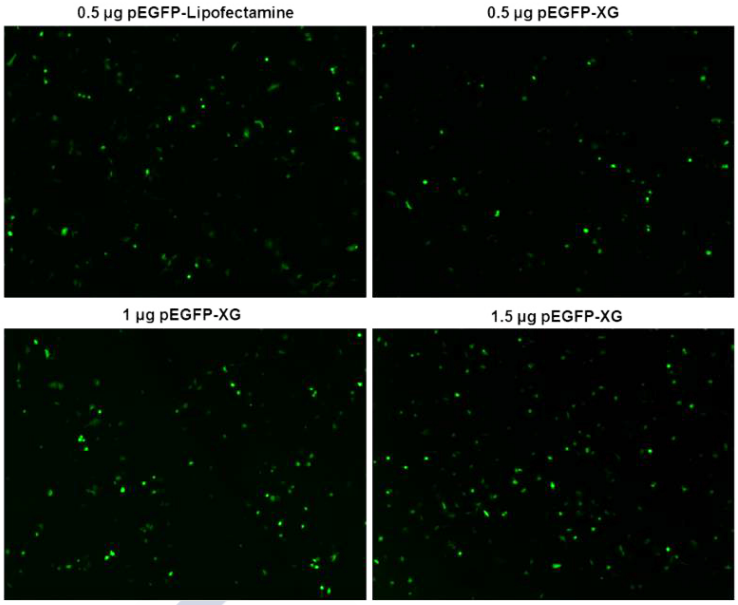

Figure 11. A549 cell line was transfected with increasing doses of pEGFP loaded XG nanoparticles. NPs were incubated during 24 hours with the cells in DMEM containing 10% of foetal bovine serum (FBS). Lipofectamine was used as a positive control.

-In vivo toxicity

To further ensure the biocompatibility of the developed nanosystems, we decided to evaluate their *in vivo* toxicity. For this purpose, pEGFP-loaded nanoparticles were intravenously injected to mice and, after 24 hours, the hepatic function and cytotoxic effects in the major mice organs were evaluated through the analysis of aspartate aminotransferase (AST) serum levels and by means of histopathological examination. No variation of AST levels was observed for any of the assayed formulations, indicating no major liver toxicity caused by the nanoparticles (Figure 12). To further corroborate the safety of the systems, their cytotoxic effects in the major mice organs, including kidney, liver, lung and spleen, were evaluated by performing histopathological studies. No obvious damage was observed on the samples analysed, indicating that the nanoparticles are not toxic to major organs and, therefore, also demonstrating their safety *in vivo* which further supports the high clinical potential of the developed nanosystems (Figure 13).

However, inflammatory cell infiltrates were observed in the liver after XG functionalised nanoparticles systemic administration, which we consider to be a mild inflammatory reaction (Figure 13). We have considered two different possibilities to explain this reaction. On the one

hand, diverse studies have described XG role in immunomodulation, activating polyclonal lymphocytes B in the absence of T-cells (28), as well as inducing humoral response mediated by IgG1 when it was subcutaneously administered as adjuvant associated to ovalbumin (22), through toll-like receptor- (TLR-)-4 recognition (29). On the other hand, we should take into account that the nanoparticles are loaded with pEGFP and that GFP expression has been associated to inflammatory and immune responses (30-34). Accordingly, the mild inflammation observed in the liver could be explained by both the XG immunomodulation activity and/or an immune response to GFP expression or even the synergistic effect of both factors. However, it should be emphasized that AST levels remained unchanged after nanoparticle administration, indicating no major liver toxicity caused by the nanoparticles (Figure 12).

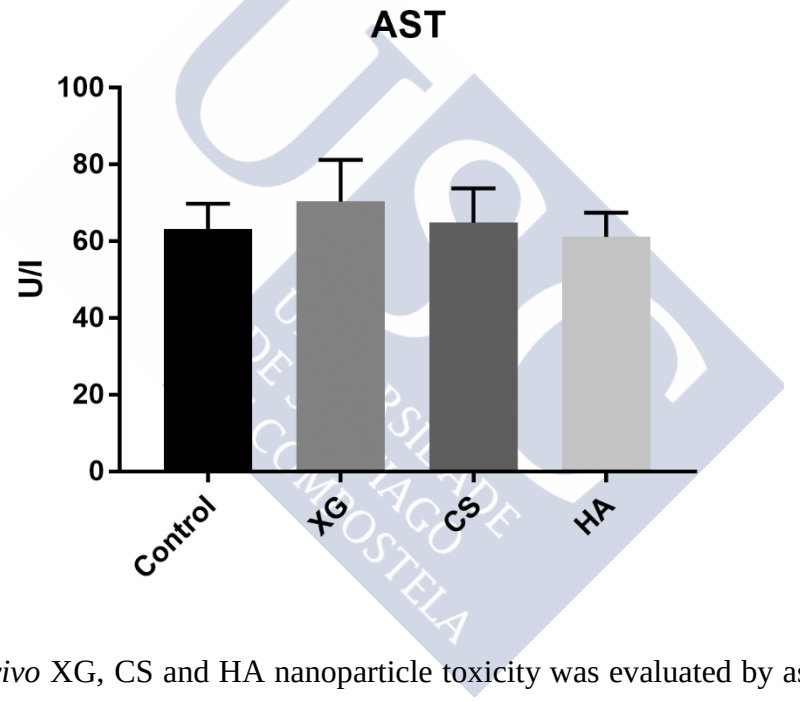

Figure 12. *In vivo* XG, CS and HA nanoparticle toxicity was evaluated by aspartate aminotransferase (AST) serum levels 24 hours after intravenous administration of the nanoparticles to mice.

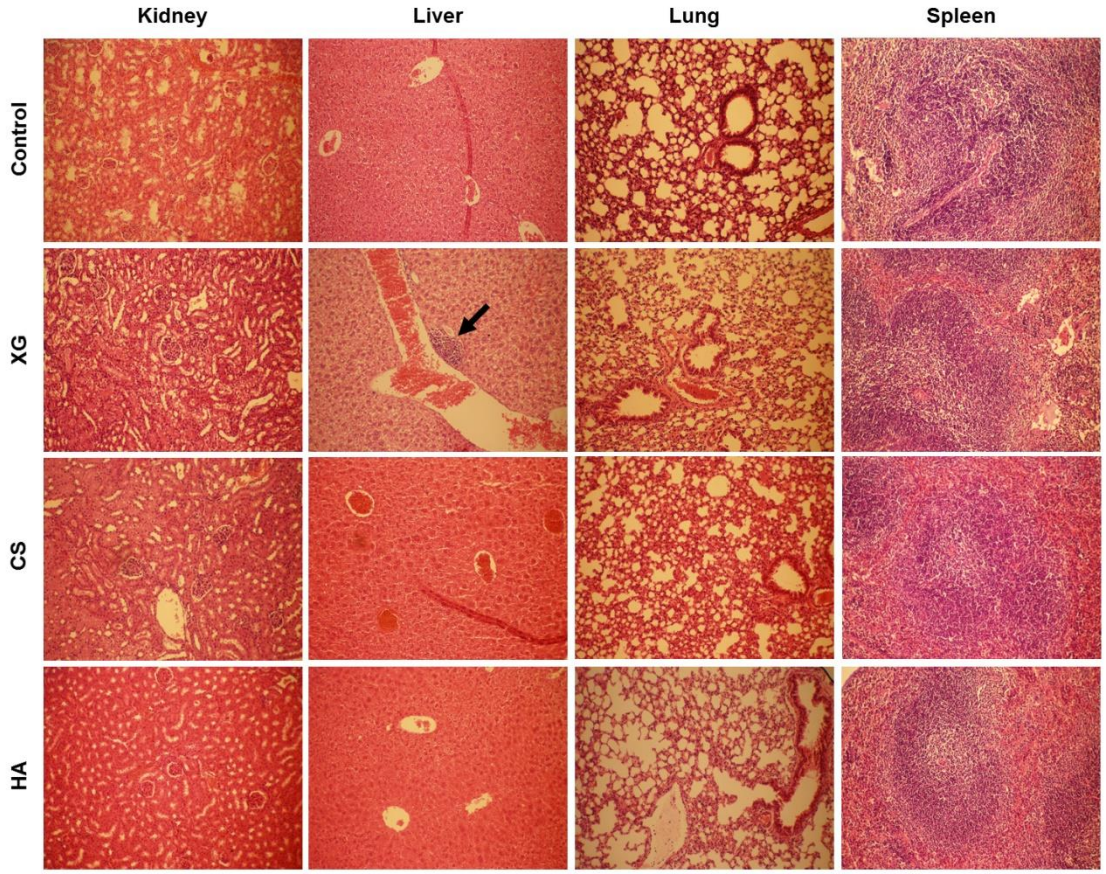

Figure 13. *In vivo* XG, CS and HA nanoparticle toxicity was evaluated by histopathological examination of major organs sections stained with haematoxylin and eosin, after intravenous administration of the nanoparticles to mice. The black arrow shows a small lymphocyte aggregate in the liver of an animal treated with XG nanoparticles.

-In vivo biodistribution

EGFP plasmid enabled not only to analyse nanoparticles potential to act as gene delivery systems but also to study the biodistribution of the nanoparticles after systemic administration to mice. Thus, 24 hours after intravenous pEGFP-loaded XG nanoparticles administration to mice, animals were sacrificed and GFP expression was evaluated in liver, kidney, lung and spleen. As shown in Figure 14, GFP was observed in endothelial cells of liver, lung and kidney blood vessels, as well as in the liver sinusoids, but not in the spleen. In the case of the sinusoids such ability can be mediated by mannose receptor present in LSECs, considering XG mannose residues and expression of this receptor in LSECs. Moreover, the ability of negatively charged

molecules to act as ligands for scavenger receptors in LSECs has been described and exploited for LSECs targeting in numerous works (35-37). However, considering vascular endothelium heterogeneity, as exemplified by the absence of mannose receptors in endothelial cells of blood vessels, further hypothesis should be considered to explain the nanoparticles ability to also target endothelium of blood vessels. Taking this into consideration, we conjecture that sorbitan monooleate nanoparticles can specifically target endothelial cells through the particular surface shell created by the polysaccharide XG without the need of receptor-ligand-type targeting strategies. Thus, we consider that endothelial uptake occurs through the NPs interaction with caveolae lipid rafts or, also, through nonspecific binding and clustering of the particles on cationic sites on the plasma membrane and their subsequent endocytosis (38).

In addition, liver Kupffer cells were immunostained along with GFP, and no colocalization was observed between both stainings (Figure 14), which evidences that the nanoparticles specifically target endothelial cells and escape reticuloendothelial system (RES). Kupffer cells have an important role in the removal of nanoparticles from the organism, being one of the main causes of low stability and efficacy of these systems *in vivo* (39, 40). It has been described that negative surface charge of particles is related to a greater RES uptake (41). Contrary to the literature, we have developed a negatively charged nanosystem that evades the non-specific uptake by RES, achieving a specific targeting of endothelial cells, which can be considered as a paradigm shift.

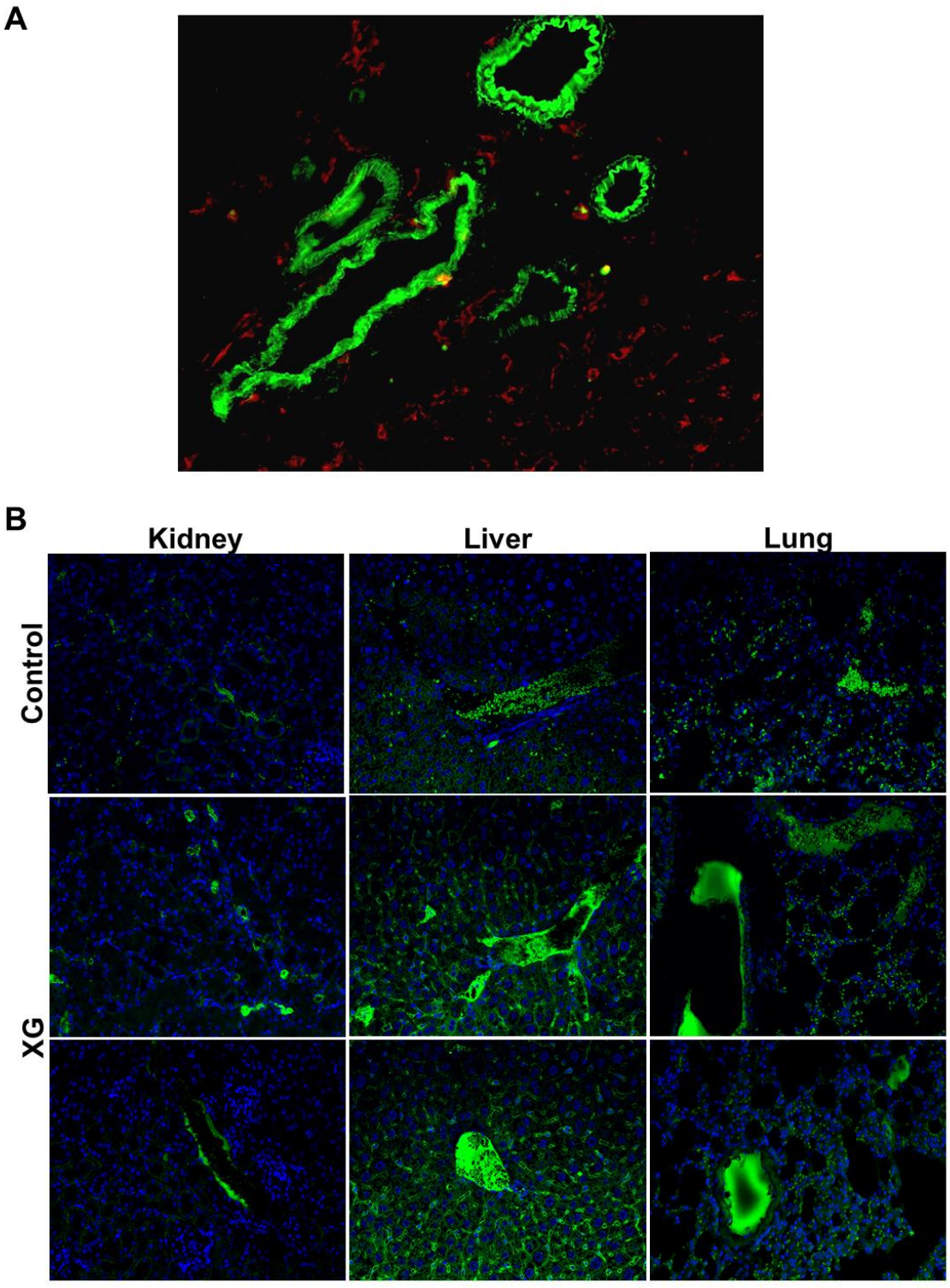

Figure 14. (A) Liver sections showing GFP expression in green and Kupffer cells labelled with F4/80 antibody in red. (B) Immunohistochemistry of major organs sections showing GFP expression (green) in endothelial cells 24 hours after XG-pEGFP intravenous administration to mice. Mice injected with 5% glucose solutions were used as controls. Cell nuclei are stained in blue with DAPI.

In the case of CS and HA nanoparticles, GFP expression was confined to liver sinusoids after intravenous administration to mice. Due to the highest GFP expression observed in the sinusoids with CS nanoparticles, we decided to select these nanoparticles to pass on to the next stage of biological assessment. According to this and to fully characterised CS nanoparticle targeting to LSECs, EGFP plasmid-loaded CS nanoparticles were injected systemically into the tail vein in mice. After 48 hours the mice were sacrificed, and liver sections analysed under confocal microscopy. Liver sinusoids were detected in green under fluorescence conditions (Figure 15A), indicating GFP expression and, therefore, nanoparticle uptake. Then, sections were immunostained with F4/80 antibody (Figure 15B) to detect Kupffer cells (liver resident macrophages) and with CD31 or mannose receptor antibody (Figure 11C-D) to detect LSECs. A merge of signals was detected exclusively in CD31 and GFP positive cells. This result suggests that nanoparticles were specifically internalized by the LSECs while avoiding Kupffer cells uptake.

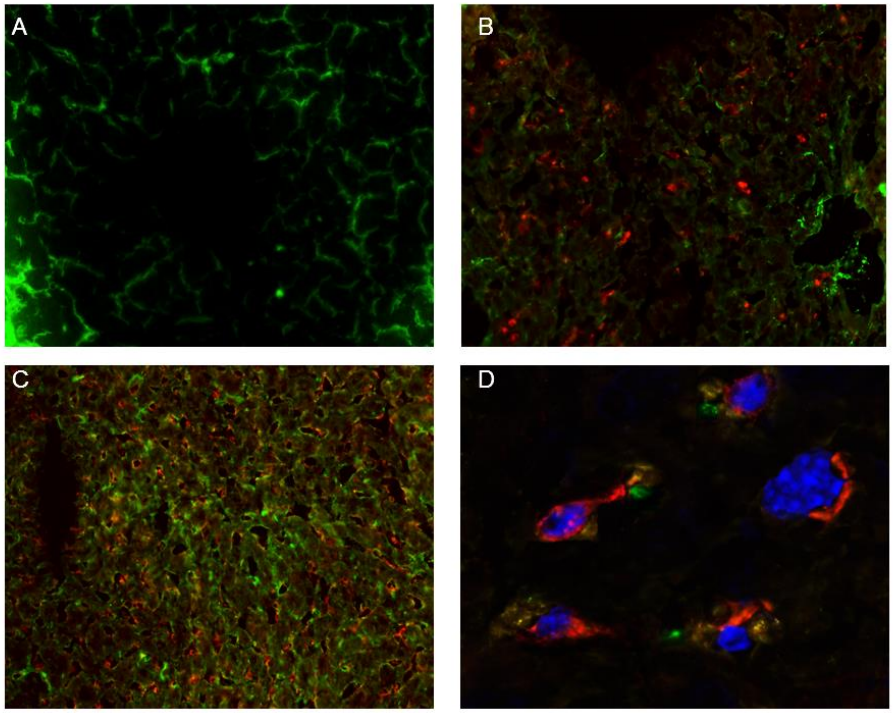

Figure 15. The *in vivo* transfection capacity and targeting ability of CS nanoparticles was measured by injecting the nanoparticles into mice. (A) Liver sinusoids exhibit green fluorescence at 10X magnification. (B) Samples stained with antibody against F4/80 (red) to detect Kupffer cell uptake of the nanoparticles (10X). (C) To check the origin of GFP expression, the samples were stained with antibodies against F4/80 (B) and mannose receptor (C) (red) to detect Kupffer cells and LSECs respectively (10X). The results show high signal mixing between red and green for mannose receptor-

labelled cells. The tissue was observed at higher magnification (40x) showing signal mixing (yellow) in LSECs and no mixing (only red) in Kupffer cells (D).

3. Application of microRNA-loaded CS nanoparticles in the treatment of colorectal cancer metastasis to the liver.

One of the most common metastatic target organs is the liver (42). Because of its anatomic position and special histologic architecture, the liver is frequently metastasized by different cancer types. Phenotypic transformation of liver sinusoidal endothelial cells (LSECs) is one of the most important stages of liver metastasis progression. A murine liver metastasis model was developed through intrasplenic inoculation of mice with colon carcinoma cells (Figure 16). Then, LSECs were isolated and their microRNA expression was compared to that of healthy LSECs. Among all the deregulated miRNA, miR-20a was the most downregulated compared to healthy LSECs. miR-20a has been previously described as a miRNA that is deregulated in many different tumours, such as lung cancer (43), cervical cancer (44) and thyroid cancer (45), and it has also been described as an essential component of embryonic development and a regulator of Wnt signaling (46).

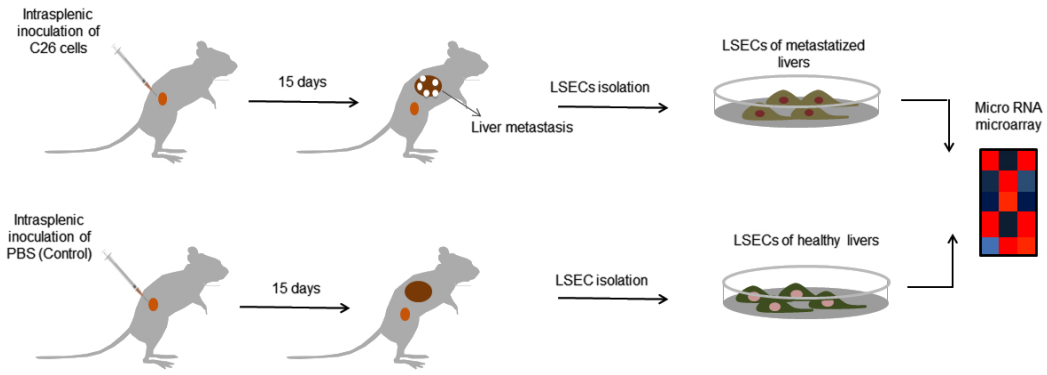

Figure 16. Liver metastasis murine model and liver sinusoidal endothelial cell isolation.

miRNAs repress protein expression through complementary matching with target mRNA using different mechanisms (16). During liver metastasis progression, the LSEC phenotypic changes to generate a prometastatic cell are the result of a change in the cellular protein expression pattern. We hypothesized that some proteins facilitating this metastasis-supporting

phenotype of LSECs are blocked by miRNA naturally expressed in healthy conditions and that downregulation of these miRNAs during the activation of LSECs leads to prometastatic protein overexpression. In the present study E2F1 and ARHGAP1 expression levels were upregulated in tumour-activated LSECs. Importantly, the expression of both proteins decreased after exogenous miR-20a administration. In these conditions, *in vitro* LSEC migration decreased, and *in vivo* endothelial cell activation was also reduced. This indicates that restoration of miR-20a levels in activated LSECs could be sufficient to decrease neoangiogenesis and vascular support to tumours.

Due to miRNA instability and inability to cross biological barriers, it is of key importance to guide miRNAs to the specific target cells we want to treat. Therefore, we decided to apply our chondroitin sulfate-functionalized nanoparticles into miR-20a delivery to LSECs in an attempt to explore their therapeutic potential against colorectal liver metastasis progression.

-Incorporation of miRNA-20a to CS functionalised nanoparticles

Once demonstrated the role of miR-20a in metastasis progress, we decided to incorporate this microRNA in our previously developed CS functionalised nanoparticles in order to achieve a LSEC targeted delivery. Thus, miR-20a was incorporated to the aqueous phase during the nanoparticle preparation. The genetic material association efficiency was evaluated using electrophoresis. As shown in Figure17A, migration of the nucleic acids into the gel was prevented by their association with the nanoparticles, and no free genetic material was observed in the ultimately selected formulation (lane 2). Blank nanoparticles (with no genetic material incorporated) and miR-20a-loaded nanoparticles had nanometric sizes of 133 nm and 143 nm and negative surface charges of -38 mV and -33 mV, respectively (Table 3). The morphology of the nanosystems was observed using transmission electron microscopy (TEM). TEM images confirmed the nanometric size of the miRNA-loaded nanoparticles (Figure 17C).

Table 3. Physicochemical properties of blank and mir-20a loaded CS nanoparticles.

Formulation	Size (nm)	PdI	ζ Potential (mV)
SP-OA-CS	132,9 ± 4,2	0,069	-38,2 ± 1,6
SP-OA-CS-miR-20a	142,6 ± 1,4	0,065	-33,3 ± 3,0

Once the association efficiency of miR-20a to the nanoparticles was determined, the ability of the system to specifically deliver fluorescently labelled miR-20a into LSECs was evaluated. After 24 hours of intravenous administration of miR-20a-loaded CS nanoparticles to mice, the miR-20a fluorescence signal was detected in LSECs (Figure 18A-B). Meanwhile, the fluorescent signal was broader and scarcer when miR-20a was injected in the naked form (Figure 18C-D), indicating that a more specific and efficient miR-20a delivery is achieved when this molecule is incorporated into CS functionalised nanoparticles.

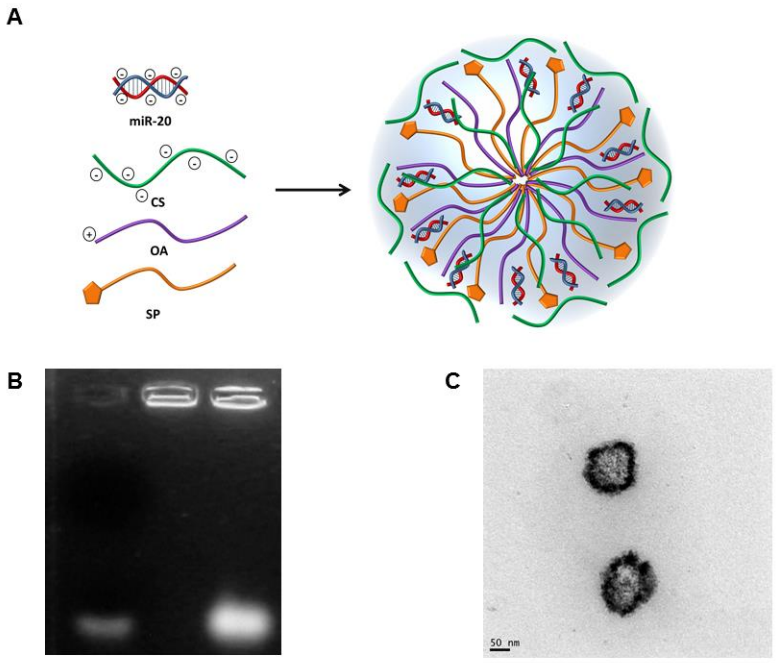

Figure 17. Characterisation of chondroitin sulfate functionalised nanoparticles associating miR-20a. (**A**) Schematic diagram of the nanoparticles. (**B**) Agarose gel showing free miR-20 (5 μg/ml; lane 1), nanoparticles associating 50 μg/ml miR-20 (lane 2), nanoparticles associating 100 μg/ml miR-20 (lane 3) (**C**) TEM image of miR-20a loaded nanoparticles.

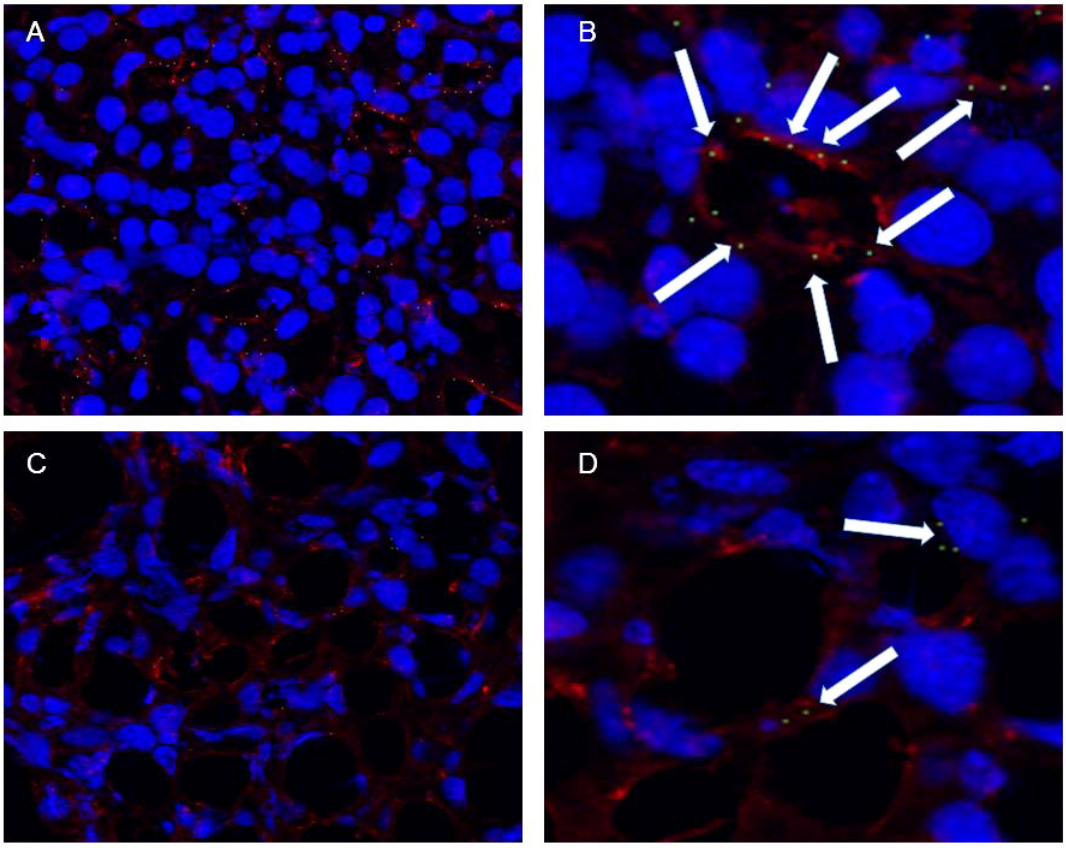

Figure 18. To analyse the *in vivo* nanoparticle miR-20a delivery efficiency to LSECs; miR-20a conjugated with green fluorescence signal was injected into the mice, either in association with CS functionalised nanoparticles (A, B) or naked (C, D). The samples were stained with anti-mannose receptor antibody. The microphotographs (A) at 20x and (B) at 40x show the presence of miR-20a in LSECs. Meanwhile, the microphotographs (C) at 20x and (D) at 40x show miR-20a not only in LSECs but also out of the sinusoids.

-Therapeutic effect of nanoparticle-mediated delivery of miR-20 to LSECs into a mouse model of colorectal liver metastasis.

As previously described, we tried to restore the normal healthy LSEC phenotype through miRNA delivery, in an attempt to revert pathological changes in the protein expression pattern of LSECS by affecting multiple prometastatic targets simultaneously. For this purpose, CS functionalised nanoparticles associating miR-20a were administered to mouse models of colorectal liver metastasis to study the potential therapeutic effect of this system (Figure 19). This strategy has proved to be largely successful, because the expression of CD31, a LSECs

specific marker, in livers collected from the *in vivo* metastasis murine model treated with miR-20a-conjugated nanoparticles revealed a reduction of 70% in CD31-positive LSEC infiltration into tumour foci (Figure 20). This indicates that the nanoparticles efficiently delivered miR-20a into LSECs and the consequently restoration of miR-20a levels could be sufficient to decrease neoangiogenesis and vascular support to tumours. Moreover, miR-20a-loading nanoparticles induced a metastatic tumour-occupied area reduction of approximately 80% relative to metastasized liver controls, and this reduction was also significantly larger than the one induced by naked miR-20a, which merely reduced tumour volume by 20% (Figure 21).

In conclusion, our developed nanosystem was able to specifically deliver miR-20a to LSECs and to offer a new and valuable therapeutic strategy to inhibit the progression of colorectal liver metastasis.

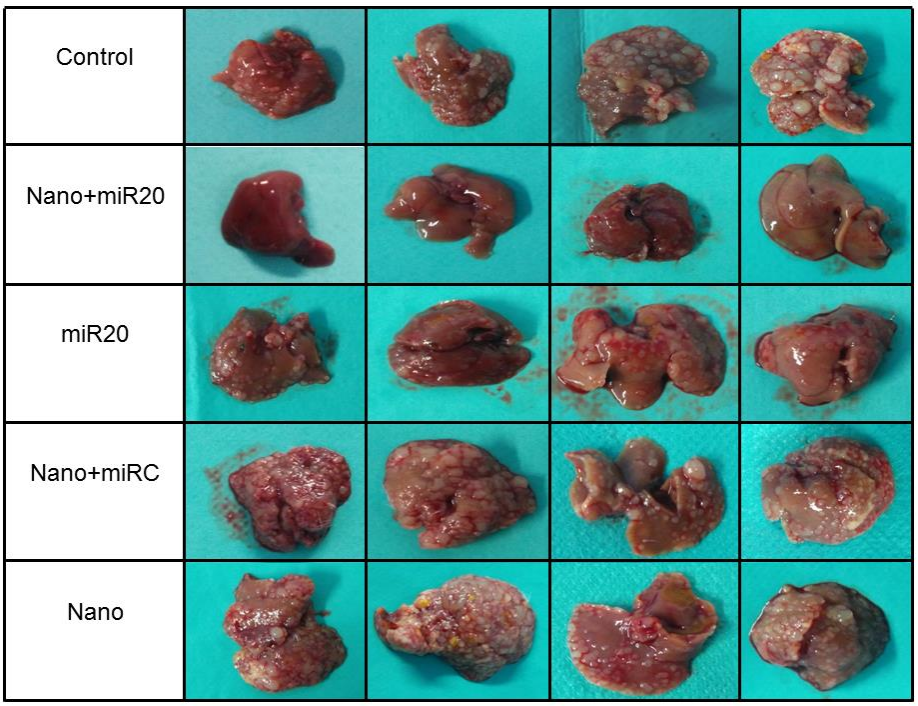

Figure 19. *In vivo* analysis of the effect of treatment with CS functionalised nanoparticles loading miR-20a in a murine liver metastasis model. A liver murine metastasis model was developed by intrasplenically injecting C26 murine colon cancer cells into mice. The different treatments were injected into mice every 3 days. Group I mice received PBS as a control treatment; group II mice received miR-20a-loaded nanoparticles; group III mice received miR-20a; group IV mice were treated with nonspecific miRNA (Control)-loaded nanoparticles; and group V mice were treated with empty nanoparticles. After 21 days, the animals were sacrificed, and the livers were removed for histological analysis.

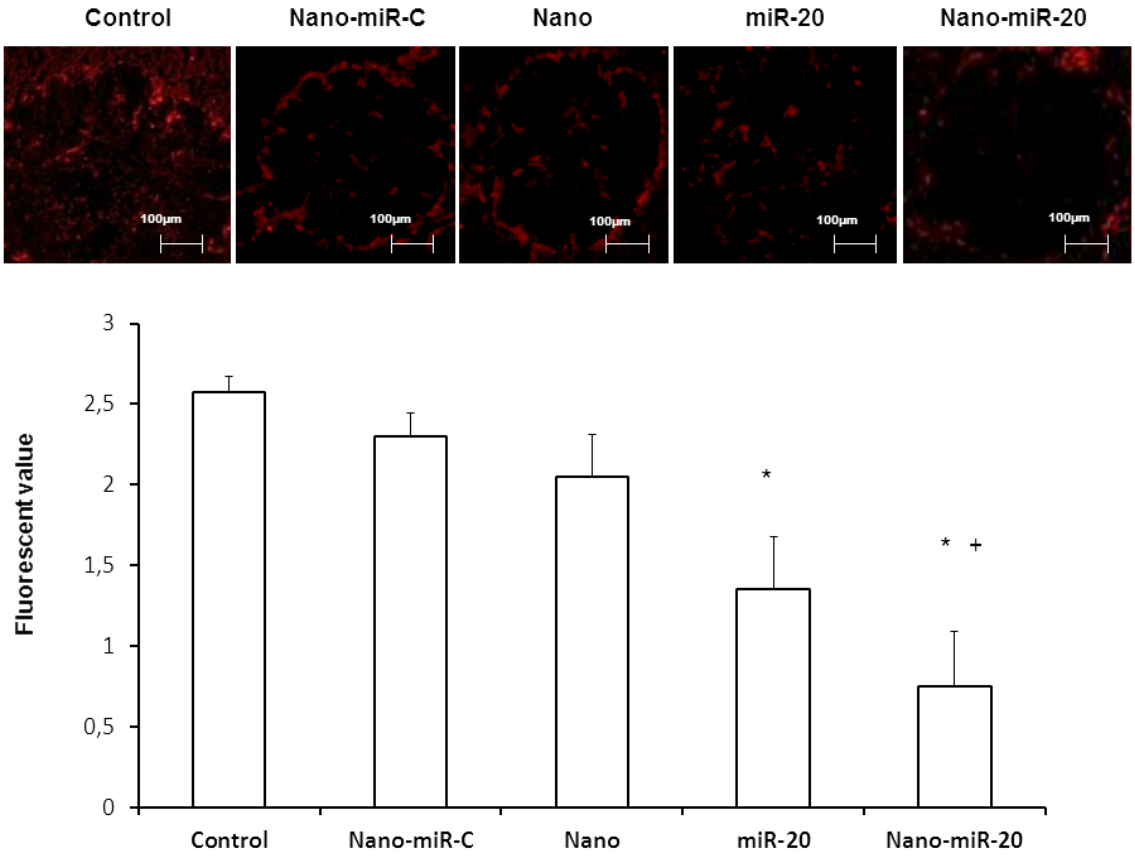

Figure 20. Tumour foci from different groups of metastasis model mice were analysed to determine the number of active LSECs in the tumours to evaluate the tumour supporting role of the cells. Statistically significant ($p < 0.05$) differences between the control group and the group treated with miR-20a without any vehicle and between the control group and the group treated with CS nanoparticles loaded with miR-20a are marked with *. Statistically significant ($p < 0.05$) differences between the group treated with miR-20a without any vehicle and the group treated with CS nanoparticle loaded with miR-20a are marked with +.

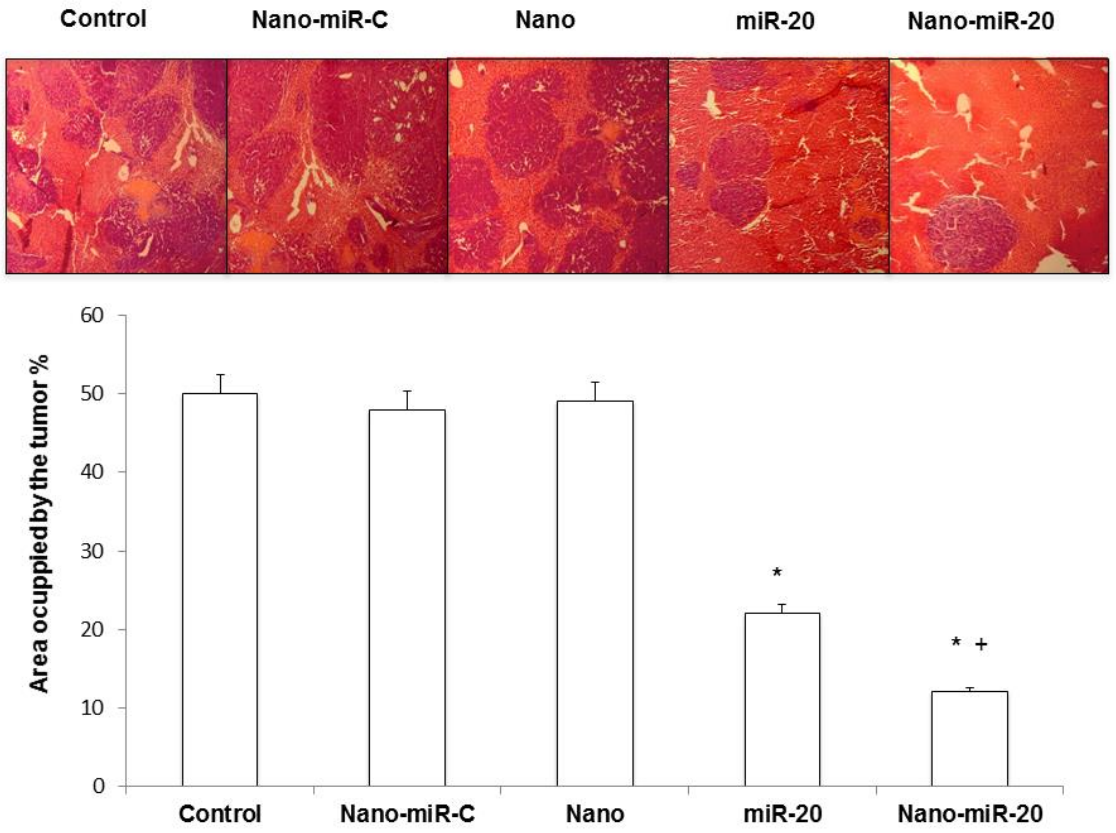

Figure 21. Liver sections were stained with haematoxylin-eosin, and the tumour size was determined as the area of occupied surface relative to the liver surface in a field under the microscope at 4x magnification. Statistically significant ($p < 0.05$) differences between the control group and the group treated with miR-20a without any vehicle and between the control group and the group treated with CS nanoparticles loaded with miR-20a are marked with *. Statistically significant ($p < 0.05$) differences between the group treated with miR-20a without any vehicle and the group treated with CS nanoparticle loaded with miR-20a are marked with +.

References

1. Hayashi K, Tatsui T, Shimanouchi T, Umakoshi H. Enhanced cytotoxicity for colon 26 cells using doxorubicin-loaded sorbitan monooleate (Span 80) vesicles. Int J Biol Sci. 2013;9(2):142-8.

2. Kato K, Walde P, Koine N, Ichikawa S, Ishikawa T, Nagahama R, et al. Temperature-sensitive nonionic vesicles prepared from Span 80 (sorbitan monooleate). Langmuir. 2008 Oct 7;24(19):10762-70.

3. Nakata H, Miyazaki T, Iwasaki T, Nakamura A, Kidani T, Sakayama K, et al. Development of tumor-specific caffeine-potentiated chemotherapy using a novel drug delivery system with Span 80 nano-vesicles. Oncol Rep. 2015 Apr;33(4):1593-8.

4. Bruxel F, Bochot A, Diel D, Wild L, Carvalho EL, Cojean S, et al. Adsorption of antisense oligonucleotides targeting malarial topoisomerase II on cationic nanoemulsions optimized by a full factorial design. Curr Top Med Chem. 2014;14(9):1161-71.

5. Borgheti-Cardoso LN, Depieri LV, Diniz H, Calzzani RA, de Abreu Fantini MC, Iyomasa MM, et al. Self-assembling gelling formulation based on a crystalline-phase liquid as a non-viral vector for siRNA delivery. Eur J Pharm Sci. 2014 Jul 16;58:72-82.

6. Petrilli R, Eloy JO, Praca FS, Del Ciampo JO, Fantini MA, Fonseca MJ, et al. Liquid Crystalline Nanodispersions Functionalized with Cell-Penetrating Peptides for Topical Delivery of Short-Interfering RNAs: A Proposal for Silencing a Pro-Inflammatory Cytokine in Cutaneous Diseases. J Biomed Nanotechnol. 2016 May;12(5):1063-75.

7. Vicentini FT, Depieri LV, Polizello AC, Del Ciampo JO, Spadaro AC, Fantini MC, et al. Liquid crystalline phase nanodispersions enable skin delivery of siRNA. Eur J Pharm Biopharm. 2013 Jan;83(1):16-24.

8. Wen Y, Oh JK. Recent strategies to develop polysaccharide-based nanomaterials for biomedical applications. Macromol Rapid Commun. 2014 Nov;35(21):1819-32.

9. Lalatsa A, Barbu E. Carbohydrate Nanoparticles for Brain Delivery. Int Rev Neurobiol. 2016;130:115-53.

10. Pooja D, Panyaram S, Kulhari H, Rachamalla SS, Sistla R. Xanthan gum stabilized gold nanoparticles: characterization, biocompatibility, stability and cytotoxicity. Carbohydr Polym. 2014 Sep 22;110:1-9.

11. Luo Y, Wang Q. Recent development of chitosan-based polyelectrolyte complexes with natural polysaccharides for drug delivery. Int J Biol Macromol. 2014 Mar;64:353-67.

12. Ohya Y, Takeda S, Shibata Y, Ouchi T, Maruyama A. Preparation of Highly Stable Biodegradable Polymer Micelles by Coating with Polyion Complex. Macromolecular Chemistry and Physics. 2010;211(16):1750-6.

13. Ohya Y, Takeda S, Shibata Y, Ouchi T, Kano A, Iwata T, et al. Evaluation of polyanion-coated biodegradable polymeric micelles as drug delivery vehicles. J Control Release. 2011 Oct 10;155(1):104-10.

14. Ran R, Liu Y, Gao H, Kuang Q, Zhang Q, Tang J, et al. Enhanced gene delivery efficiency of cationic liposomes coated with PEGylated hyaluronic acid for anti P-glycoprotein siRNA: a potential candidate for overcoming multi-drug resistance. Int J Pharm. 2014 Dec 30;477(1-2):590-600.

15. Zhao L, Liu M, Wang J, Zhai G. Chondroitin sulfate-based nanocarriers for drug/gene delivery. Carbohydr Polym. 2015 Nov 20;133:391-9.

16. Leteux C, Chai W, Loveless RW, Yuen CT, Uhlin-Hansen L, Combarnous Y, et al. The cysteine-rich domain of the macrophage mannose receptor is a multispecific lectin that recognizes chondroitin sulfates A and B and sulfated oligosaccharides of blood group Lewis(a) and Lewis(x) types in addition to the sulfated N-glycans of lutropin. J Exp Med. 2000 Apr 3;191(7):1117-26.

17. McCourt PA, Smedsrod BH, Melkko J, Johansson S. Characterization of a hyaluronan receptor on rat sinusoidal liver endothelial cells and its functional relationship to scavenger receptors. Hepatology. 1999 Nov;30(5):1276-86.

18. Harris E, Weigel PH. Functional aspects of the hyaluronan and chondroitin sulfate receptors. In: Ahmed H, Vasta GR, editors. Animal Lectins: A Functional View. CRC Press; 2008. p. 171-92.

19. Pensado A, Martin-Pastor M, Zorzi GK, Carvalho ES, Sanchez A. Structural analysis of nanosystems: Solid Sorbitan esters Nanoparticles (SSN) as a case study. Eur J Pharm Biopharm. 2016 Jul;104:189-99.

20. Delmas T, Couffin AC, Bayle PA, de Crecy F, Neumann E, Vinet F, et al. Preparation and characterization of highly stable lipid nanoparticles with amorphous core of tuneable viscosity. J Colloid Interface Sci. 2011 Aug 15;360(2):471-81.

21. Pensado A, Fernandez-Pineiro I, Seijo B, Sanchez A. Anionic nanoparticles based on Span 80 as low-cost, simple and efficient non-viral gene-transfection systems. Int J Pharm. 2014 Dec 10;476(1-2):23-30.

22. Schuch RA, Oliveira TL, Collares TF, Monte LG, Inda GR, Dellagostin OA, et al. The Use of Xanthan Gum as Vaccine Adjuvant: An Evaluation of Immunostimulatory Potential in BALB/c Mice and Cytotoxicity In Vitro. Biomed Res Int. 2017;2017:3925024.

23. Leite Nascimento T, Hillaireau H, Vergnaud J, Rivano M, Delomenie C, Courilleau D, et al. Hyaluronic acid-conjugated lipoplexes for targeted delivery of siRNA in a murine metastatic lung cancer model. Int J Pharm. 2016 Nov 30;514(1):103-11.

24. Mizrahy S, Raz SR, Hasgaard M, Liu H, Soffer-Tsur N, Cohen K, et al. Hyaluronan-coated nanoparticles: the influence of the molecular weight on CD44-hyaluronan interactions and on the immune response. J Control Release. 2011 Dec 10;156(2):231-8.

25. Park JH, Cho HJ, Yoon HY, Yoon IS, Ko SH, Shim JS, et al. Hyaluronic acid derivative-coated nanohybrid liposomes for cancer imaging and drug delivery. J Control Release. 2014 Jan 28;174:98-108.

26. Rao NM. Cationic lipid-mediated nucleic acid delivery: beyond being cationic. Chem Phys Lipids. 2010 Mar;163(3):245-52.

27. Dobrovolskaia MA, McNeil SE. Understanding the correlation between in vitro and in vivo immunotoxicity tests for nanomedicines. J Control Release. 2013 Dec 10;172(2):456-66.

28. Ishizaka S, Sugawara I, Hasuma T, Morisawa S, Moller G. Immune responses to xanthan gum. I. The characteristics of lymphocyte activation by xanthan gum. Eur J Immunol. 1983 Mar;13(3):225-31.

29. Takeuchi A, Kamiryou Y, Yamada H, Eto M, Shibata K, Haruna K, et al. Oral administration of xanthan gum enhances antitumor activity through Toll-like receptor 4. Int Immunopharmacol. 2009 12;9(13–14):1562-7.

30. Yang C, Hao F, He J, Lu T, Klein RL, Zhao LR, et al. Sequential Adeno-Associated Viral Vector Serotype 9-Green Fluorescent Protein Gene Transfer Causes Massive Inflammation and Intense Immune Response in Rat Striatum. Hum Gene Ther. 2016 Jul;27(7):528-43.

31. Baens M, Noels H, Broeckx V, Hagens S, Fevery S, Billiau AD, et al. The dark side of EGFP: defective polyubiquitination. PLoS One. 2006 Dec 20;1:e54.

32. Zhang F, Hackett NR, Lam G, Cheng J, Pergolizzi R, Luo L, et al. Green fluorescent protein selectively induces HSP70-mediated up-regulation of COX-2 expression in endothelial cells. Blood. 2003 Sep 15;102(6):2115-21.

33. Liu HS, Jan MS, Chou CK, Chen PH, Ke NJ. Is green fluorescent protein toxic to the living cells? Biochem Biophys Res Commun. 1999 Jul 14;260(3):712-7.

34. Goto H, Yang B, Petersen D, Pepper KA, Alfaro PA, Kohn DB, et al. Transduction of green fluorescent protein increased oxidative stress and enhanced sensitivity to cytotoxic drugs in neuroblastoma cell lines. Mol Cancer Ther. 2003 Sep;2(9):911-7.

35. Poelstra K, Prakash J, Beljaars L. Drug targeting to the diseased liver. J Control Release. 2012 Jul 20;161(2):188-97.

36. Melgert BN, Olinga P, Jack VK, Molema G, Meijer DK, Poelstra K. Dexamethasone coupled to albumin is selectively taken up by rat nonparenchymal liver cells and attenuates LPS-induced activation of hepatic cells. J Hepatol. 2000 Apr;32(4):603-11.

37. Kamps JA, Morselt HW, Swart PJ, Meijer DK, Scherphof GL. Massive targeting of liposomes, surface-modified with anionized albumins, to hepatic endothelial cells. Proc Natl Acad Sci U S A. 1997 Oct 14;94(21):11681-5.

38. Verma A, Stellacci F. Effect of surface properties on nanoparticle-cell interactions. Small. 2010 Jan;6(1):12-21.

39. Sadauskas E, Wallin H, Stoltenberg M, Vogel U, Doering P, Larsen A, et al. Kupffer cells are central in the removal of nanoparticles from the organism. Part Fibre Toxicol. 2007 Oct 19;4:10.

40. Rinkenauer AC, Press AT, Raasch M, Pietsch C, Schweizer S, Schworer S, et al. Comparison of the uptake of methacrylate-based nanoparticles in static and dynamic in vitro systems as well as in vivo. J Control Release. 2015 Oct 28;216:158-68.

41. Frohlich E. The role of surface charge in cellular uptake and cytotoxicity of medical nanoparticles. Int J Nanomedicine. 2012;7:5577-91.

42. Fu M, Song Y, Wen Z, Lu X, Cui L. Inositol Hexaphosphate and Inositol Inhibit Colorectal Cancer Metastasis to the Liver in BALB/c Mice. Nutrients. 2016 05/04;8(5):286.

Conclusions

USC
UNIVERSIDADE
DE SANTIAGO
DE COMPOSTELA

Conclusions

This work has been focused on the development of polysaccharide-functionalised nanoparticles as gene delivery systems with potential to act as an alternative therapeutic strategy in the treatment of colorectal cancer metastasized to the liver.

Considering the obtained results we can conclude:

1. It is possible to include diverse natural polysaccharides into sorbitan monooleate-based nanoparticles, modulating the system characteristics and properties.

2. The developed nanoparticles show a remarkable short- and long- term stability at different temperatures both as suspension or lyophilised.

3. These nanoparticles are able to efficiently associate, protect and deliver *in vitro* and *in vivo* plasmid DNA, showing an appropriate toxicological profile.

4. The polysaccharide functionalisation of the nanoparticles allows to modulate their biological behaviour and biodistribution.

5. Treatment of a mouse model of colorectal liver metastasis with selected nanoparticles associating miR-20a allows a decrease of the metastatic tumour-occupied area by approximately 80% and a reduction of 70% in CD31-positive LSEC infiltration into tumour foci. Therefore, these results provide an *in vivo* proof-of-concept of the clinical potential of the developed nanoparticles as a novel microRNA-based therapeutic strategy for cancer treatment.

USC
UNIVERSIDADE
DE SANTIAGO
DE COMPOSTELA

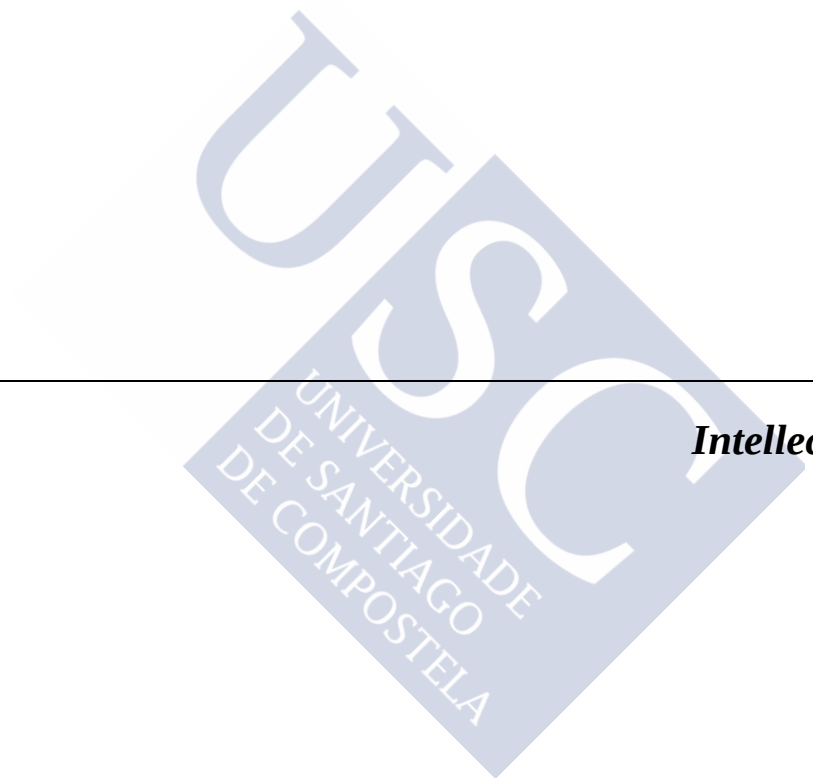

Annex II

Intellectual property

USC
UNIVERSIDADE
DE SANTIAGO
DE COMPOSTELA

Patents derived from this work:

Sanchez, Alejandro; Fernández Piñeiro, Inés; Badiola, Iker; Márquez, Joana. **Novel vehicles for the transfection of miRNAs.** WO2017174847. Universidade de Santiago de Compostela and Universidad del País Vasco, 2017.

(12) SOLICITUD INTERNACIONAL PUBLICADA EN VIRTUD DEL TRATADO DE COOPERACIÓN EN MATERIA DE PATENTES (PCT)

(19) Organización Mundial de la Propiedad Intelectual
Oficina internacional

(43) Fecha de publicación internacional
12 de octubre de 2017 (12.10.2017)

WIPO | PCT

(10) Número de Publicación Internacional
WO 2017/174847 A1

(51) Clasificación Internacional de Patentes:
A61K 31/7105 (2006.01) *A61P 3/00* (2006.01)
B82B 1/00 (2006.01) *A61P 3/10* (2006.01)
B82B 3/00 (2006.01) *A61P 9/00* (2006.01)
B82Y 5/00 (2011.01) *A61P 11/00* (2006.01)
A61P 35/00 (2006.01) *A61P 25/28* (2006.01)
A61P 35/04 (2006.01)

(21) Número de la solicitud internacional:
PCT/ES2017/070205

(22) Fecha de presentación internacional:
4 de abril de 2017 (04.04.2017)

(25) Idioma de presentación: español

(26) Idioma de publicación: español

(30) Datos relativos a la prioridad:
P 201630417 5 de abril de 2016 (05.04.2016) ES

(71) Solicitantes: **UNIVERSIDADE DE SANTIAGO DE COMPOSTELA** [ES/ES]; Edificio Emprendia - Campus Vida, 15782 Santiago de Compostela - La Coruña (ES). **UNIVERSIDAD DEL PAIS VASCO - EUSKAL HERRIKO UNIBERTSITATEA (UPV/EHU)** [ES/ES]; Barrio Sarriena, S/N, 48940 Leioa (ES).

(72) Inventores: **SÁNCHEZ BARREIRO, Alejandro**; Edificio Emprendia - Campus Vida, 15782 Santiago de Compostela - La Coruña (ES). **FERNÁNDEZ PIÑEIRO, Inés**; Edificio Emprendia - Campus Vida, 15782 Santiago de Compostela - LA CORUÑA (ES). **BADIOLA, Iker**; Barrio Sarriena, S/N, 48940 Leioa, Vizcaya (ES). **MÁRQUEZ, Joana**; Barrio Sarriena, S/N, 48940 Leioa, Vizcaya (ES).

(74) Mandatario: **VALLEJO LÓPEZ, Juan Pedro**; Paseo de la Castellana 93, 28046 Madrid (ES).

(81) Estados designados *(a menos que se indique otra cosa, para toda clase de protección nacional admisible)*: AE, AG, AL, AM, AO, AT, AU, AZ, BA, BB, BG, BH, BN, BR, BW, BY, BZ, CA, CH, CL, CN, CO, CR, CU, CZ, DE, DJ, DK, DM, DO, DZ, EC, EE, EG, ES, FI, GB, GD, GE, GH, GM, GT, HN, HR, HU, ID, IL, IN, IR, IS, JP, KE, KG, KH, KN, KP, KR, KW, KZ, LA, LC, LK, LR, LS, LU, LY, MA, MD, ME, MG, MK, MN, MW, MX, MY, MZ, NA, NG, NI, NO, NZ, OM, PA, PE, PG, PH, PL, PT, QA, RO, RS, RU, RW, SA, SC, SD, SE, SG, SK, SL, SM, ST, SV, SY, TH, TJ, TM, TN, TR, TT, TZ, UA, UG, US, UZ, VC, VN, ZA, ZM, ZW.

(84) Estados designados *(a menos que se indique otra cosa, para toda clase de protección regional admisible)*: ARIPO (BW, GH, GM, KE, LR, LS, MW, MZ, NA, RW, SD, SL, ST, SZ, TZ, UG, ZM, ZW), euroasiática (AM, AZ, BY, KG, KZ, RU, TJ, TM), europea (AL, AT, BE, BG, CH, CY, CZ, DE, DK, EE, ES, FI, FR, GB, GR, HR, HU, IE, IS, IT, LT, LU, LV, MC, MK, MT, NL, NO, PL, PT, RO, RS, SE, SI, SK, SM, TR), OAPI (BF, BJ, CF, CG, CI, CM, GA, GN, GQ, GW, KM, ML, MR, NE, SN, TD, TG).

Publicada:
— *con informe de búsqueda internacional (Art. 21(3))*

WO 2017/174847 A1

(54) Title: NOVEL VEHICLES FOR THE TRANSFECTION OF miRNAS

(54) Título : NUEVOS VEHÍCULOS PARA LA TRANSFECCIÓN DE miRNAs

(57) Abstract: The invention relates to a nanoparticle comprising: (i) between 60 wt.-% and 99 wt.-% sorbitan ester, relative to the total weight of the nanoparticle; (ii) a positively charged substance; and (iii) an miRNA. The invention also relates to the methods for producing same and to the uses thereof, particularly for therapeutic uses, such as cancer treatment.

(57) Resumen: La presente invención se refiere a una nanopartícula que comprende (i) entre un 60% y un 99% en peso, con respecto al peso total de la nanopartícula, de un éster de sorbitán; (ii) una sustancia cargada positivamente; y (iii) un miRNA; a sus métodos de fabricación, y sus usos, especialmente en usos terapéuticos, como el tratamiento del cáncer.

https://patentscope.wipo.int/search/en/detail.jsf?docId=WO2017174847

USC
UNIVERSIDADE
DE SANTIAGO
DE COMPOSTELA

The main objective of this work has been the design of a new polysaccharide functionalised nanosystem as a non-viral microRNA vector for the treatment of liver metastasis from colorectal cancer. For this purpose, we modified our previously developed span nanoparticles using polysaccharides with endothelial targeting properties and studied their ability to act as gene delivery systems. Finally, we provide an in vivo proof-of-concept of the clinical potential of these nanoparticles as a novel microRNA-based therapeutic strategy for cancer treatment.